



Centre for Systems Biology
Faculty of Sciences
University of Southern Queensland

**Quantitative PCR and Histopathological Assessment
of Cereal Infection by *Fusarium pseudograminearum*.**

by

Noel Liam Knight, BSc (Hons)

A dissertation submitted in fulfilment of the requirements for the degree of
Doctor of Philosophy

2011

Certificate of Originality

I certify that the experimental work, results, analyses and conclusions reported in this dissertation are entirely my own effort, except where otherwise acknowledged. The text of this thesis contains no material which has been accepted for the award of any other degree or diploma in any University, unless stated. To the best of my knowledge, the text of this thesis is original and contains no material previously published or written by another person, except where due reference is made.

I gratefully acknowledge the financial support of the Grains Research and Development Corporation and the assistance of an Australian Post-graduate Award Scholarship.

Signature of Candidate

Date

ENDORSEMENT:

Signature of Supervisor

Date

Acknowledgments

A PhD is a challenge, an adventure to be embarked upon. It is a test of mental strength, endurance and resolve. In a world of so much, a PhD encompasses relatively little, yet it becomes your life, your world. It represents your sacrifices, your enthusiasm, your highs and lows, your successes and failures, your strengths and weaknesses. A PhD represents work predominantly done alone, however it cannot be achieved alone. For this I must firstly thank my supervisor Professor Mark Sutherland, a source of not only funding, but of guidance, encouragement, wisdom and opportunity. I greatly appreciate the rigorous and thorough thought behind our discussions and the many opportunities I have been given to present my work and interact with other researchers from around the world.

I would also like to thank my associate supervisor Dr. Anke Lehmensiek for advice and discussion during my project. Without such a learned and patient teacher my project would have been a much more daunting challenge. Thanks also go to my associate supervisor Dr. Damian Herde, whose willingness to share experimental material and provide plant materials from field trials is greatly appreciated.

I would also like to thank my colleagues and fellow students at USQ who have at least been a part of this journey. In particular, Bill and Jess Bovill, for encouragement and advice during the uncertain first year of my PhD, Cassandra Percy for advice and discussion on all things crown rot, Philip Davies (University of Sydney) for supplying *Fusarium* isolates and always demonstrating the power of positivity, Garth Marrett for instructing me on use of the fluorescence microscope and Peter Gous for listening to me for so many weeks listing potential problems with my PCR.

To my parents I owe so much, for their financial support through all my studies and particularly for their encouragement, interest and belief in me. Having such role models of hard work and determination has shaped me into the person I am. I cannot put into words my appreciation for all you have given me.

And finally, my best friend, one who is like me in so many ways, who appreciates me for who I am no matter what, my dog Fungis. The amount of talking about my PhD he had to endure is beyond the ability of most people, however a sigh from him would always bring a smile. Thanks.

Abstract

The assessment of crown rot (*F. pseudograminearum*) infections in winter cereals was explored using a quantitative polymerase chain reaction (PCR) approach. A range of cereal genotypes of varying resistance to crown rot were monitored during seedling and adult growth stages. A histopathological investigation of *F. pseudograminearum* (*Fp*) growth during pathogenesis in seedling and adult growth stages was also performed across a range of cereal genotypes. This utilised a novel staining method developed during this project.

Visual assessment of crown rot symptoms in wheat seedlings is commonly conducted in order to rapidly identify resistant genotypes. Ratings rely heavily on discolouration of seedling tissues, predominantly the leaf sheaths. This study is the first to explore the relationship between seedling tissue discolouration and *Fp* DNA content in wheat genotypes of differing resistance. The partially resistant wheat 2-49 exhibited lower visual and qPCR values than the susceptible wheat Puseas. The rate of disease development and *Fp* growth in seedling leaf sheaths was slower in 2-49 than Puseas. The rates of symptom development in intermediate genotypes EGA Wylie and EGA Gregory were not significantly different from that recorded in 2-49. A comparison of visual ratings and qPCR values of *Fp* DNA indicated a strong correlation ($r = 0.89$, $p < 0.01$) between these characters at 14 days after inoculation across all genotypes. The correlation weakened over time. Furthermore, qPCR revealed differences between partially resistant and susceptible genotypes to a much greater extent than possible using visual discolouration.

Crown rot infections of adult cereal stems are typically rated at maturity by recording the amount of discolouration on individual internodes. A comparison was performed between visual ratings and *Fp* DNA content of four cereal genotypes (two bread wheats, one durum wheat and one barley) at anthesis (16 weeks after planting) and maturity (22 weeks after planting). At anthesis a strong correlation ($r = 0.86$, $p < 0.01$) was present between visual and qPCR values. At maturity this relationship was modest ($r = 0.58$, $p < 0.01$). Furthermore, differences between partially resistant and susceptible genotypes were greatest at anthesis.

The strong correlations between visual discolouration and fungal DNA content indicate that visual discolouration is a useful measure of fungal load in

seedling and adult cereal tissues. However, the degree to which these two parameters correlate varies with the time elapsed since tissue infection.

Fluorescence microscopy revealed no major differences between fungal growth patterns or structural characteristics in the host genotypes assessed. Leaf sheaths were most frequently penetrated via stomata, indicated by initial lesions forming at the guard cells. Leaf sheath tissues became extensively colonised in most cell types, except for the vascular bundles and abaxial silica cells. Colonisation of leaf sheaths resulted in the re-emergence of hyphae and occasionally conidiophores from stomata.

Colonisation of culm tissues frequently originated in the parenchymatous hypoderm, which became greatly discoloured, resulting in the visual discolouration used for disease rating. Early infection of pith parenchyma cells was also frequent. Infections typically spread from the culm base upwards through the tissues, typically only to internode three, with a much slower lateral spread of hyphae. Colonisation of sclerified cells occurred later in the infection process. Vascular tissues were frequently colonised by anthesis. This was more rapid in susceptible genotypes. Occlusion of large xylem vessels was rare during moderate infections.

The ability of quantitative PCR to accurately describe the extent of crown rot infection suggests that it could be utilised as a powerful technique for detecting new resistance sources or for identifying quantitative trait loci for resistance. This method, along with further microscopic and biochemical assessments of partially resistant and susceptible genotypes, may provide new information on the pathogenesis of crown rot and the nature of host resistance responses.

Table of Contents

CERTIFICATE OF ORIGINALITY	II
ACKNOWLEDGMENTS	III
ABSTRACT	IV
LIST OF FIGURES	IX
LIST OF TABLES	XI
LIST OF ABBREVIATIONS	XII
CHAPTER 1 : LITERATURE REVIEW	1
1.1 INTRODUCTION	1
1.2 WHEAT	1
1.2.1 Anatomy	3
1.2.2 Growth Cycle	4
1.2.3 Diseases	5
1.2.3.1 Foliar and Head Diseases	5
1.2.3.2 Root and Crown Diseases	5
1.3 CROWN ROT	6
1.3.1 Economic Impact in Australia	6
1.3.2 Crown Rot Distribution	6
1.3.3 History	7
1.4 FUSARIUM GENUS	8
1.4.1 <i>Fusarium pseudograminearum</i>	9
1.4.1.1 Genetic Diversity Studies	9
1.4.1.2 Use of Genetic Information	11
1.5 ASPECTS OF CROWN ROT DISEASE	12
1.5.1 Disease Cycle	12
1.5.2 Host Range	12
1.5.3 Disease Symptoms	13
1.5.3.1 Mycotoxins and Infection	14
1.5.4 Environmental Conditions Affecting Infection	14
1.5.4.1 Temperature	15
1.5.4.2 Water	15
1.5.4.3 Whitehead Formation	17
1.5.5 Management	18
1.6 SCREENING FOR CROWN ROT INFECTION AND YIELD LOSS	19
1.6.1 Adult Screening	20
1.6.2 Seedling Screening	21
1.7 DISEASE REACTIONS	23
1.7.1 Resistance	23
1.7.2 Crown Rot Resistance	24
1.7.2.1 Genetics of Resistance	25
1.8 ESTIMATING FUNGAL LOAD	26
1.8.1 Traditional Quantification Method	27
1.8.2 DNA Based Quantification	27
1.8.2.1 Real-Time Quantitative Polymerase Chain Reaction	28
1.8.2.2 Species-specific qPCR	29
1.9 FUNGAL MICROSCOPY	31
1.9.1 <i>Fusarium</i> Microscopy	32
1.10 PROJECT RATIONALE	33
CHAPTER 2 : SEEDLING INFECTION	37
2.1 INTRODUCTION	37
2.2 METHODS	38

2.2.1	<i>Wheat Genotypes</i>	38
2.2.2	<i>Planting</i>	38
2.2.3	<i>Inoculum Production</i>	39
2.2.4	<i>Inoculation and Harvest</i>	39
2.2.5	<i>Visual Rating</i>	40
2.2.6	<i>Time Course Harvest</i>	40
2.2.7	<i>Seedling Harvest for Sectioning</i>	40
2.2.8	<i>DNA Preparation</i>	41
2.2.9	<i>Primer Selection and Optimisation of PCR Conditions</i>	41
2.2.9.1	Initial PCR Assessment	42
2.2.9.2	Optimisation of the Multiplex Real Time Quantitative PCR Assay	42
2.2.9.3	Confirmation of PCR Products	43
2.2.9.4	Primer Specificity and Sensitivity	45
2.2.10	<i>Multiplex Real Time Quantitative PCR Conditions</i>	45
2.2.10.1	Controls and Standard Curve Production	46
2.2.11	<i>Statistical Methods</i>	46
2.3	RESULTS	47
2.3.1	<i>PCR Optimisation</i>	47
2.3.2	<i>Time Course</i>	50
2.3.2.1	qPCR normalisation using host DNA	56
2.3.2.2	Correlation of visual and qPCR data	58
2.3.3	<i>Comparison of control and infected LS weights</i>	61
2.3.4	<i>Seedling Sectioning</i>	64
2.4	DISCUSSION	67
CHAPTER 3 : ADULT INFECTION		72
3.1	INTRODUCTION	72
3.2	METHODS	73
3.2.1	<i>Cereal Genotypes</i>	74
3.2.2	<i>Inoculum Production</i>	74
3.2.3	<i>Inoculation and Tissue Collection</i>	75
3.2.3.1	Wellcamp	75
3.2.3.2	Leslie Research Centre	75
3.2.4	<i>Visual Rating</i>	76
3.2.5	<i>DNA Preparation</i>	76
3.2.6	<i>Multiplex Real Time Quantitative PCR Conditions</i>	76
3.2.7	<i>Statistical Analyses</i>	76
3.3	RESULTS	77
3.3.1	<i>Wellcamp</i>	77
3.3.1.1	10 WAP	77
3.3.1.2	16 WAP	77
3.3.1.3	22 WAP	78
3.3.1.4	Comparison between 16 and 22 WAP	81
3.3.1.5	Visual versus Normalised qPCR Values	82
3.3.2	<i>LRC</i>	84
3.4	DISCUSSION	85
CHAPTER 4 : HISTOPATHOLOGICAL ASSESSMENT OF INFECTED SEEDLING AND ADULT TISSUES		88
4.1	INTRODUCTION	88
4.2	METHODS	89
4.2.1	<i>Conidial Germination</i>	89
4.2.2	<i>Plant Materials</i>	90
4.2.3	<i>Plant Growth and Tissue Preparation</i>	90
4.2.3.1	Greenhouse Plants	90
4.2.3.1.1	Leaf Sheath Tissues	90
4.2.3.1.2	Culm Tissues	90
4.2.3.2	Field Plants	90
4.2.3.3	Sectioning	91
4.2.4	<i>Clearing and Fixation</i>	91

4.2.5 Staining and Microscopic Observation	91
4.2.5.1 Development of a Fluorescent Staining Technique	91
4.2.5.2 Differential Staining of Hyphae and Plant Tissue.....	92
4.2.5.3 Lesion Microscopy	93
4.2.5.4 Lignin, Suberin and Callose Stain	93
4.2.5.5 Microscopic Observation	93
4.2.5.6 Statistical Methods	93
4.3 RESULTS	94
4.3.1 Legend for Images	94
4.3.2 Development of a Fluorescent Staining Technique.....	94
4.3.3 Initial Conidial Germination.....	95
4.3.4 Initial penetration and growth in the coleoptile.....	95
4.3.5 Initial penetration and growth in LSs.....	99
4.3.5.1 Initial penetration.....	99
4.3.5.2 Lesion formation.....	102
4.3.5.3 Cell Wall Penetration.....	103
4.3.5.4 Hyphal Growth Characteristics	108
4.3.5.4.1 Abaxial surface	109
4.3.5.4.2 Adaxial Surface	116
4.3.5.5 Description of Growth in Different Genotypes.....	118
4.3.6 Initial penetration and growth in culms	119
4.3.6.1 Culm morphology	119
4.3.6.2 Culm Infection	123
4.3.6.2.1 Summary of Observations	130
4.3.6.2.2 Comparison of Fungal Growth in Culms with White (Dead) and Green Heads	146
4.3.7 Staining of Lignin, Suberin and Callose.....	152
4.4 DISCUSSION.....	154
4.4.1 Fluorescent Staining	154
4.4.2 Histopathology of Crown Rot.....	155
4.4.2.1 Initial Plant-Fungi Interactions.....	155
4.4.2.2 Colonisation.....	158
4.4.2.2.1 Colonisation and Visual Symptoms	161
4.4.2.2.2 Inoculation and Hyphal Spread	162
4.4.2.2.3 Vascular Tissue Colonisation	163
4.4.2.2.4 Colonisation of Culms Exhibiting Green and Dead Heads	163
CHAPTER 5: GENERAL DISCUSSION AND CONCLUSIONS.....	165
5.1 FUTURE DIRECTIONS	168
REFERENCES	171
APPENDICES..... provided on CD	
2A - Wheat Pedigrees	
2B - <i>F. pseudograminearum</i> Growth Media	
2C - DNA Extraction Assessment	
2D - Comparison of LS Lengths	
3A - Field Inoculum Production	
3B - Field Trial Plans	

List of Figures

FIGURE 1.1. AREAS AND INTENSITY OF WHEAT PRODUCTION WITHIN AUSTRALIA DURING THE 2000-2001 SEASON.	3
FIGURE 1.2. A, SEEDLING ANATOMY (VESETH, 1987). B, CULM ANATOMY (KNIGHT AND QUIRK, 1994).	4
FIGURE 1.3. QPCR REACTION USING A DUAL-LABELLED PROBE, LABELLED WITH A REPORTER (R) AND A QUENCHER (Q) MOLECULE.	29
FIGURE 2.1. A, NORMALISED FLUORESCENCE CURVES OF FIVE 10 FOLD SERIAL DILUTIONS OF <i>F. PSEUDOGAMINEARUM</i> DNA. B, STANDARD CURVE PRODUCED BY PLOTTING Ct AGAINST QUANTITY OF DNA IN EACH STANDARD DILUTION.	49
FIGURE 2.2. INTRA- AND INTER-ASSAY VARIABILITY OF SAMPLES 38 AND 94.	49
FIGURE 2.3. VISUAL RATINGS OF CROWN ROT INFECTION IN LS1, LS2, LS3 AND LS4 AT (A) 7, (B) 14, (C) 21, (D) 28 AND (E) 35 DAI.	52
FIGURE 2.4. NORMALISED <i>Fp</i> PER WHEAT DNA VALUES OF LS1, LS2, LS3 AND LS4 AT (A) 7 DAI, (B), 14 DAI, (C) 21 DAI, (D) 28 DAI AND (E) 35 DAI.	53
FIGURE 2.5. NORMALISED <i>Fp</i> DNA PER WEIGHT VALUES OF LS1, LS2, LS3 AND LS4 AT (A) 7 DAI, (B), 14 DAI, (C) 21 DAI, (D) 28 DAI AND (E) 35 DAI.	54
FIGURE 2.6. COMBINED LS1, LS2, LS3 AND LS4 VALUES FROM 7 TO 35 DAI USING (A), VISUAL RATINGS OF CROWN ROT SYMPTOMS, (B), <i>Fp</i> PER WHEAT DNA AND (C), <i>Fp</i> DNA PER WEIGHT.	55
FIGURE 2.7. CHANGE IN QUANTITIES OF WHEAT DNA IN CONTROL LS2 TISSUES AND OF BOTH WHEAT AND <i>Fp</i> DNA IN INFECTED LS2 TISSUES OF (A) 2-49, (B) GREGORY, (C) PUSEAS AND (D) WYLIE FROM 7 TO 35 DAI.	58
FIGURE 2.8. RELATIONSHIP BETWEEN COMBINED LS1, LS2, LS3 AND LS4 VISUAL RATINGS OF CROWN ROT SYMPTOMS AND (A), <i>Fp</i> PER WHEAT DNA OR (B), <i>Fp</i> DNA PER WEIGHT VALUES AT 14 DAI OF FOUR WHEAT GENOTYPES. ...	59
FIGURE 2.9. INDIVIDUAL LS1, LS2, LS3 AND LS4 QPCR AND VISUAL SCORES OF CROWN ROT SYMPTOMS AT (A) 7, (B) 14, (C) 21, (D) 28 AND (E) 35 DAI.	60
FIGURE 2.10. WEIGHT DIFFERENCE OF INFECTED LS1, 2, 3, 4 AND 5 FROM CONTROL LSS OF (A) 2-49, (B) GREGORY, (C) PUSEAS AND (D) WYLIE FROM 7 TO 35 DAI. THE WEIGHT OF CONTROL TISSUES IS REPRESENTED BY ZERO ON THE VERTICAL AXIS.	61
FIGURE 2.11. LINEAR RELATIONSHIPS OF THE WEIGHT DIFFERENCE OF <i>Fp</i> INFECTED LS1, 2 AND 3 FROM CONTROL LSS AND ESTIMATED WEIGHT OF <i>Fp</i> TISSUES IN (A) 2-49, (B) GREGORY, (C) PUSEAS AND (D) WYLIE AT 7 TO 35 DAI.	63
FIGURE 2.12. (A) VISUAL RATINGS OF CROWN ROT SYMPTOMS AND (B) <i>Fp</i> DNA PER WEIGHT VALUES OF LSB, LST, LB, SCI AND 1° ROOT TISSUES OF 2-49 AND PUSEAS SEEDLINGS AT 14 DAI.	65
FIGURE 2.13. (A) VISUAL RATINGS OF CROWN ROT SYMPTOMS AND (B) <i>Fp</i> DNA PER WEIGHT VALUES OF LSB, LST AND LB TISSUES OF 2-49 AND PUSEAS SEEDLINGS AT 28 DAI.	66
FIGURE 2.14. (A) VISUAL RATINGS OF CROWN ROT SYMPTOMS AND (B) <i>Fp</i> DNA PER WEIGHT VALUES OF SCI, 1° ROOT AND 2° ROOT TISSUES OF 2-49 AND PUSEAS SEEDLINGS AT 28 DAI.	66
FIGURE 3.1. VISUAL RATINGS OF CROWN ROT SYMPTOMS (A AND C) AND QPCR VALUES (B AND D), OF IN1, IN2 AND IN3 OF FOUR CEREAL GENOTYPES AT 16 WAP (A AND B) AND 22 WAP (C AND D).	79
FIGURE 3.2. COMBINED VISUAL RATINGS OF CROWN ROT SYMPTOMS AND QPCR VALUES, RESPECTIVELY, OF IN1, 2 AND 3 OF FOUR CEREAL GENOTYPES 16 WAP (A AND B) AND 22 WAP (C AND D).	80
FIGURE 3.3. COMBINED VISUAL RATINGS OF CROWN ROT SYMPTOMS OF IN1, 2 AND 3 OF FOUR CEREAL GENOTYPES AT 16 AND 22 WAP.	81
FIGURE 3.4. COMBINED QPCR VALUES OF IN1, 2 AND 3 OF FOUR CEREAL GENOTYPES AT 16 AND 22 WAP.	82
FIGURE 3.5. LINEAR CORRELATION OF CROWN ROT SYMPTOMS OF VISUAL RATINGS AND QPCR VALUES FOR COMBINED TOTALS OF INs 1, 2 AND 3 OF FOUR CEREAL GENOTYPES AT (A) 16 WAP AND (B) 22 WAP.	83
FIGURE 3.6. (A), VISUAL RATINGS OF CROWN ROT SYMPTOMS AND (B), QPCR VALUES OF IN1, 2 AND 3 AT OF THREE CEREAL GENOTYPES AT 16 WAP.	84
FIGURE 4.1. EFFECT OF CLEARING, FIXATION AND STAINING ON 28 DAY OLD BREAD WHEAT LEAF SHEATH TISSUES INFECTED BY <i>Fp</i> . CEREAL CELL AUTOFLUORESCENCE DECREASED AFTER CLEARING AND FIXATION. AFTER STAINING WITH SOLOPHENYL FLAVINE 7GFE, HYPHAE WERE VISIBLE BUT NOT DISTINCT FROM PLANT TISSUES.	97
FIGURE 4.2. INFECTION OF COLEOPTILE TISSUES BY <i>Fp</i> (SV).	98
FIGURE 4.3. PENETRATION OF LEAF SHEATH TISSUES BY <i>Fp</i> (SV).	100
FIGURE 4.4. ASSOCIATION OF <i>Fp</i> HYPHAE WITH TRICHOMES (SV).	101
FIGURE 4.5. INITIAL LESION FORMATION IN LEAF SHEATH TISSUES (SV).	104
FIGURE 4.6. LESION FORMATION AND SPREAD IN LEAF SHEATH TISSUES INFECTED BY <i>Fp</i> (SV).	104
FIGURE 4.7. REACTIONS TO INITIAL INFECTION BY <i>Fp</i> RESULTING IN THE PRODUCTION OF FLUORESCENT MATERIALS (SV). ..	105

FIGURE 4.8. GROWTH OF <i>Fp</i> HYPHAE IN DISCOLOURED STOMATA AND TRICHOMES (SV).....	105
FIGURE 4.9. DENSE COLONISATION OF INDIVIDUAL EPIDERMAL CELLS BY <i>Fp</i> (SV).....	106
FIGURE 4.10. APPRESSORIAL STRUCTURES OF <i>Fp</i> (SV). A, HYPHAL SWELLINGS (HS) DURING CONTACT WITH CELL WALL, 9 DAI (W).....	107
FIGURE 4.11. CEREAL LEAF SHEATH TISSUE ANATOMY.....	108
FIGURE 4.12. RE-EMERGENCE OF <i>Fp</i> HYPHAE FROM STOMATA ON THE ABAXIAL SURFACE OF CEREAL LEAF SHEATH TISSUE (SV).....	110
FIGURE 4.13. HEAVY COLONISATION OF THE ABAXIAL SURFACE OF LEAF SHEATH TISSUE BY <i>Fp</i> (SV).....	111
FIGURE 4.14. MASSES OF <i>Fp</i> CONIDIA FORMING OVER STOMATA ON THE ABAXIAL SURFACE OF LEAF SHEATH 1 TISSUE OF THE WHEAT PUSEAS, 14 DAI (SV).....	112
FIGURE 4.15. GROWTH OF <i>Fp</i> HYPHAE OCCURRED IN TRICHOMES DURING HEAVY INFECTION, WHILE COLONISATION OF SENESCENT TISSUE APPEARED DECREASED (SV).....	113
FIGURE 4.16. RESTRICTION OF <i>Fp</i> HYPHAL GROWTH BY VASCULAR BUNDLES (V) AND ASSOCIATED STEROME TISSUES, 14 DAI (SV).....	114
FIGURE 4.17. SINUOUS SILICA CELLS (SC), PRESENT ONLY ON THE ABAXIAL SURFACE AND WHICH WERE MOST COMMON IN EPIDERMAL TISSUE ADJACENT TO VASCULAR TISSUES, DISPLAYED PROPERTIES ENABLING THEM TO RESIST <i>Fp</i> HYPHAL PENETRATION (SV).....	115
FIGURE 4.18. A AND B, <i>Fp</i> HYPHAE WITHIN EPIDERMAL TISSUE ADJACENT TO VASCULAR BUNDLES ON THE ADAXIAL SURFACE OF A WHEAT LEAF SHEATH FREQUENTLY FORMED THICKENED HYPHAE (SV, P).....	117
FIGURE 4.19. CELL TYPES IN CEREAL CULM INTERNODE TISSUES (TS).....	121
FIGURE 4.20. STOMATA AND VASCULAR BUNDLES IN CEREAL INTERNODE TISSUES (TS).....	121
FIGURE 4.21. GENERAL ANATOMY OF CEREAL NODAL TISSUE.....	122
FIGURE 4.22. INITIAL LESIONS FORMATION OF INTERNODAL TISSUE COULD OCCUR AT STOMATA (SV).....	124
FIGURE 4.23. SUMMARY OF CULM INFECTION BY <i>Fp</i> AT 10 WAP IN FOUR CEREAL GENOTYPES.....	125
FIGURE 4.24. SUMMARY OF CULM INFECTION BY <i>Fp</i> AT 16 WAP IN FOUR CEREAL GENOTYPES.....	126
FIGURE 4.25. SUMMARY OF CULM INFECTION BY <i>Fp</i> AT 22 WAP IN FOUR CEREAL GENOTYPES.....	127
FIGURE 4.26. SUMMARY OF CULM INFECTION BY <i>Fp</i> AT 16 WAP OF 2-49 AND PUSEAS GROWN AT THE LRC.....	128
FIGURE 4.27. SUMMARY OF CULM INFECTION BY <i>Fp</i> AT 16 WAP OF 2-49 AND PUSEAS GROWN IN THE GREENHOUSE.....	129
FIGURE 4.28. <i>Fp</i> HYPHAE INTRACELLULARLY COLONISED EPIDERMAL TISSUES (TS).....	131
FIGURE 4.29. PARENCHYMATOUS HYPODERM WAS COLONISED BY INTRACELLULAR <i>Fp</i> HYPHAE (TS).....	132
FIGURE 4.30. COLONISATION OF THE SCLERENCHYMATOUS HYPODERM BY <i>Fp</i> (TS).....	133
FIGURE 4.31. <i>Fp</i> COLONISATION OF VASCULAR TISSUES OCCURRED IN ALL CELL TYPES (TS).....	136
FIGURE 4.32. COLONISATION OF PHLOEM VESSELS BY <i>Fp</i> IN INTERNODE TISSUE (TS, B).....	137
FIGURE 4.33. INFECTION OF PITH CELLS BY <i>Fp</i> (TS).....	138
FIGURE 4.34. COLONISATION OF THE PITH CAVITY BY <i>Fp</i> (TS).....	139
FIGURE 4.35. COLONISATION OF NODAL TISSUE BY <i>Fp</i> (TS).....	140
FIGURE 4.36. COLONISATION OF CEREAL NODAL TISSUES BY <i>Fp</i>	141
FIGURE 4.37. SERIES OF SECTIONS RISING THROUGH A LIGHTLY INFECTED CEREAL NODE (TS).....	142
FIGURE 4.38. THICK WALLED PITH CELLS (TS).....	143
FIGURE 4.39. A AND B, PENETRATION OF CELL WALLS BY <i>Fp</i> WAS FACILITATED BY APPRESSORIA (A) APPEARING AS SWOLLEN HYPHAL TIPS (TS, P AND SUN, RESPECTIVELY).....	144
FIGURE 4.40. COLONISATION OF LEAF TRACE TISSUES BY <i>Fp</i> (TS).....	145
FIGURE 4.41. SUMMARY OF CULM INFECTION BY <i>Fp</i> OF GREEN CULMS AND DEAD CULMS AT 16 WAP OF THE WHEAT GENOTYPE SUNLAND.....	147
FIGURE 4.42. SUMMARY OF CULM INFECTION BY <i>Fp</i> OF GREEN CULMS AND DEAD CULMS AT 16 WAP OF THE WHEAT GENOTYPE VASCO.....	148
FIGURE 4.43. COLONISATION OF DEAD CULM TISSUES BY <i>Fp</i> (TS).....	149
FIGURE 4.44. COLONISATION OF VASCULAR TISSUES BY <i>Fp</i> IN DEAD CULMS (TS).....	150
FIGURE 4.45. COLONISATION OF GREEN CULM TISSUES BY <i>Fp</i> (TS).....	151
FIGURE 4.46. CONTROL AND INFECTED CULM TISSUES OF 2-49 (A-J) AND PUSEAS (K-T) AT 16 WAP. A-H/K-R, THE FLUORESCENCE OF THE INFECTED TISSUES WAS MUCH LESS THAN THE CONTROL TISSUES.....	153

List of Tables

TABLE 2.1. TISSUE SECTIONS HARVESTED AND ANALYSED BY QPCR.	41
TABLE 2.2. <i>F. PSEUDOGRAMINEARUM</i> PRIMER AND PROBE SEQUENCES ASSESSED FOR HOST SPECIFICITY.	44
TABLE 2.3. WHEAT PRIMER AND PROBE SEQUENCES ASSESSED FOR HOST SPECIFICITY.	44
TABLE 2.4. <i>FUSARIUM</i> AND CEREAL SPECIES ASSESSED USING THE <i>F. PSEUDOGRAMINEARUM</i> AND WHEAT PRIMER/PROBE SETS.	48
TABLE 2.5. COEFFICIENTS OF DETERMINATION (R^2) AND ASSOCIATED GRADIENTS OF THE LOG OF NORMALISED <i>Fp</i> PER WHEAT DNA VALUES OF COMBINED LS1, 2, 3 AND 4 OVER 7-28 DAI.	56
TABLE 2.6. COEFFICIENTS OF DETERMINATION (R^2) AND ASSOCIATED GRADIENTS OF THE LOG OF NORMALISED <i>Fp</i> DNA PER WEIGHT VALUES OF COMBINED LS1, 2, 3 AND 4 OVER 7-35 DAI.	56
TABLE 2.7. CORRELATION COEFFICIENTS (R) FOR LS1, LS2, LS3 AND LS4 SEPARATELY AND COMBINED COMPARING VISUAL RATINGS OF CROWN ROT SYMPTOMS, <i>Fp</i> PER WHEAT DNA AND <i>Fp</i> DNA PER WEIGHT VALUES FROM 7 TO 35 DAI.	57
TABLE 2.8. DIFFERENCE IN MILLIGRAMS OF <i>Fp</i> INFECTED LS TISSUES FROM CONTROL LS TISSUES AT 7 TO 35 DAI FOR (A) 2-49, (B) GREGORY, (C) PUSEAS AND (D) WYLIE.	62
TABLE 3.1. GENOTYPES MONITORED DURING ADULT PLANT ASSESSMENTS AND THEIR CROWN ROT FIELD RATING.	74
TABLE 3.2. CORRELATION COEFFICIENTS (R) FOR VISUAL DISCOLOURATION DUE TO CROWN ROT SYMPTOMS AND QPCR VALUES OF INDIVIDUAL AND COMBINED INs AT 16 AND 22 WAP.	83
TABLE 3.3. CORRELATION COEFFICIENT (R) FOR VISUAL DISCOLOURATION DUE TO CROWN ROT SYMPTOMS AND QPCR VALUES OF COMBINED INs AT 16 WAP.	84
TABLE 4.1. ABBREVIATIONS USED IN FIGURE CAPTIONS.	94
TABLE 4.2. MEAN AND RANGE OF HYPHAL WIDTHS OBSERVED ACROSS LEAF SHEATHS 1 TO 4 OF FOUR WHEAT GENOTYPES AT 14 DAI.	118
TABLE 4.3. NUMBER OF CULMS SECTIONED FOR MICROSCOPIC ASSESSMENT.	123
TABLE 4.4. MINIMUM AND MAXIMUM HYPHAL WIDTHS OBSERVED WITHIN THE CULM TISSUE OF FOUR CEREAL GENOTYPES.	135

List of Abbreviations

1°:	primary
2°:	secondary
Col:	coleoptile
Cro:	crown
Ct:	threshold cycle
dai:	days after inoculation
<i>Fp:</i>	<i>Fusarium pseudograminearum</i>
hai:	hours after inoculation
IN:	internode
LB:	leaf blade
LRC:	Leslie Research Centre
LS:	leaf sheath
LSb:	base 2 cm of leaf sheath
LSt:	top 2 cm of leaf sheath
NA:	not applicable
PCR:	polymerase chain reaction
PH:	parenchymatous hypoderm
PP:	pith parenchyma
qPCR:	quantitative polymerase chain reaction
QTL:	quantitative trait loci
SCI:	sub-crown internode
SH:	sclerenchymatous hypoderm
SNA:	starch nitrate agar
VB:	vascular bundle
Vis:	visual discolouration
VP:	vascular parenchyma
WAP:	weeks after planting
Wh:	wheat

Chapter 1 : Literature Review

1.1 Introduction

Wheat (*Triticum aestivum*), worldwide, is currently grown on more land area (213 million hectares) than any other commercial crop, followed by maize and rice (158 and 155 million hectares respectively) (Cornell and Hoveling, 1998, Curtis *et al.*, 2002, FAOSTAT, 2010). The high dependence of human societies on wheat crops and harvests drives the intense genetic research into *T. aestivum* and related species of grasses, which has continued for over a century, focussing on breeding characteristics for agronomic performance, maximising yields, post harvest grain quality and resistance to disease.

1.2 Wheat

Modern wheat (*Triticum* species) originated from several wild species through hybridisation, mutation and the effects of human selection and cultivation. Wheat has three levels of ploidy (number of sets of the base group of chromosomes): diploid ($2n=2x=14$), tetraploid ($2n=4x=28$) and hexaploid ($2n=6x=42$). Of the three ploidy levels, the tetraploid and hexaploid wheats, being *Triticum turgidum* ssp. *durum* and *Triticum aestivum* respectively, are the most commonly grown in present day cultivation. The earliest evidence of wheat domestication appears ~10 000 years ago in the Fertile Crescent of the Near East (Lev-Yadun *et al.*, 2000). In prehistoric times wheat was cultivated throughout Europe and was one of the most valuable cereals of ancient Persia, Greece and Egypt (Percival, 1921).

Wheat is superior to most other cereals in its nutritive value, particularly due to its protein component. The unique physical and chemical qualities of the wheat grain gluten allow production of more palatable bread than any other cereal. Its cultivation is simple and its adaptability to varying soils and climatic conditions makes it superior to most other crops (Percival, 1921, Zohary and Hopf, 2000).

Wheat is grown in Europe, Asia, Africa, the Americas, Australia and New Zealand. The only parts of the world in which it is less common are hot, low altitude regions of the Tropics. The ten major wheat producing countries in 2007 were China,

India, United States of America, Russian Federation, France, Pakistan, Germany, Canada, Turkey and Argentina, producing 420 million tonnes of wheat in that year (<http://www.fao.org>). Wheat is also the most important crop grown in Australia, the fifteenth highest wheat producer worldwide in 2007. It is the largest single component of the Australian grains industry with a total annual value of between six and seven billion dollars (AWB, 2004).

Within Australia, commercial quantities of wheat are grown in all states (Figure 1.1). New South Wales and Western Australia each contribute approximately one third of the total cropping area and subsequent wheat harvest. Over the period from 2000 to 2009 the average harvest was 18.6 million tonnes from 12.3 million hectares (Australian-Bureau-of-Statistics, 2009). The Australian domestic market consumes around 5.5 million tonnes of wheat annually, evenly divided between human consumption and stockfeed. The remaining 70% of the crop is exported to countries such as China, Egypt, Indonesia, Iraq, Japan and South Korea (Trewin, 2006).

The major limitations to wheat production in Australia are adequate seasonal rainfall and soil fertility. The importance of seasonal rainfall varies between the northern grain growing region (northern New South Wales, southern Queensland and central Queensland) where summer rainfall is predominant and the southern regions (Western Australia, South Australia, Victoria and south-western New South Wales) where winter rainfall is predominant. Yield decreases of nearly 50% compared to the long term average were recorded during the drought years 2003, 2006, 2007 and 2008 (Australian-Bureau-of-Statistics, 2009, Australian-Government-Bureau-of-Meteorology, 2009).

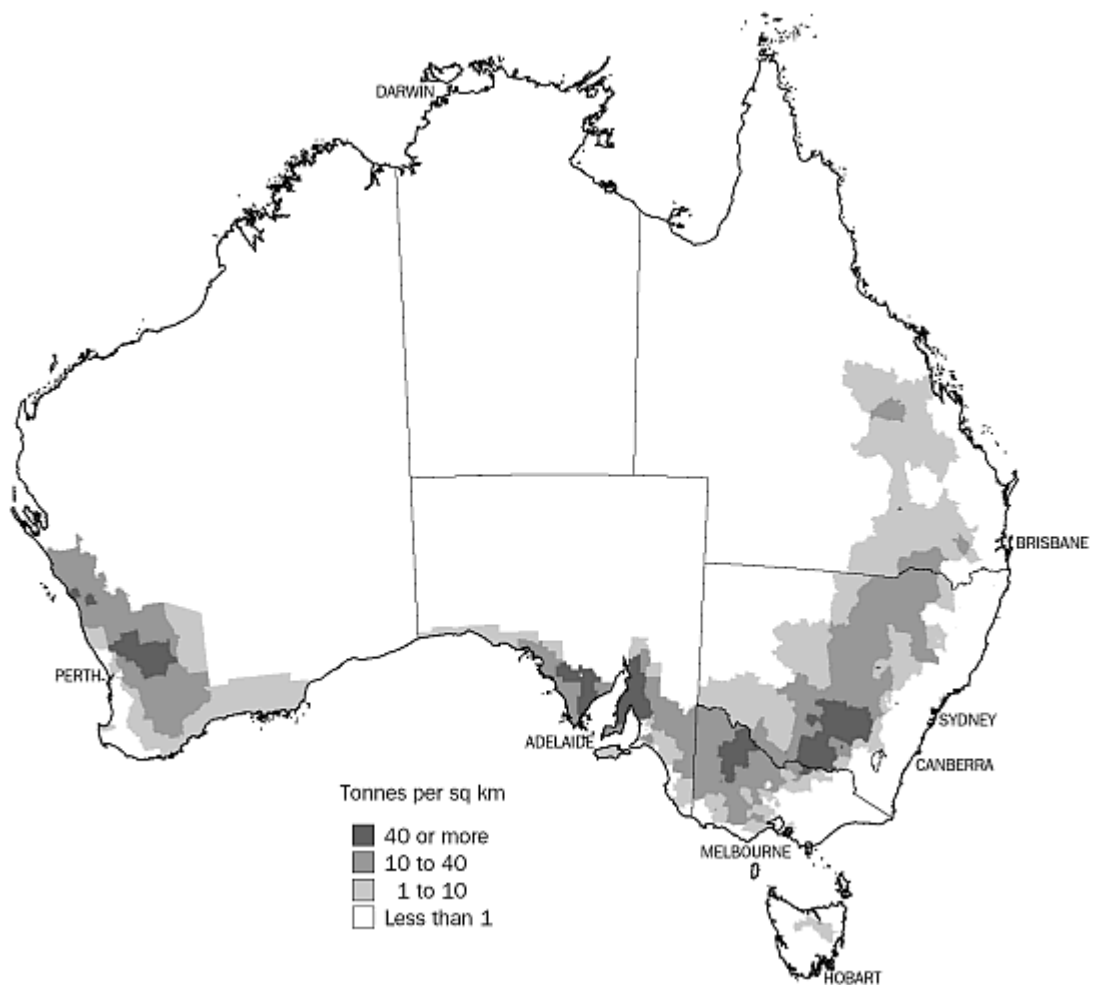


Figure 1.1. Areas and intensity of wheat production within Australia during the 2000-2001 season (Trewin, 2006).

1.2.1 Anatomy

A wheat seedling consists of a crown, coleoptile, sub-crown internode, leaves and seminal (primary) roots (Figure 1.2a). During adult growth the plants produce nodal (secondary) roots and expand into multiple culms (stems) consisting of nodes, internodes and an inflorescence (Figure 1.2b). The culm is composed of subunits called phytomers. The phytomer is composed of the node and the tissues derived from it, being the leaf sheath, leaf blade, internode (above the node) and axillary bud (Briske, 1991, Wilhelm and McMaster, 1995). These phytomers originate at the crown, the region just below the soil surface, and expand during growth of the plant.

Seminal roots and the coleoptile originate from primordia found in the seed (Carver, 2009). The coleoptile encases the sub-crown internode up to the emerging

shoot and functions chiefly as a protective cover to the young leaves during their upward growth through the soil. The crown forms at the top of the sub-crown internode and is located just below the soil surface. Nodal roots are produced from primordia developed at the crown after germination.

The foliage leaves possess a sheath, blade and ligule, with a pair of auricles at the base of each blade (Percival, 1921) (Figure 1.2a). The leaf-sheath, which is split in the upper parts but entire near the base, encircles the culm, protecting the latter from damage by frost, drought and insect attack; it possesses considerable strength and serves as a support for the young growing internode within. The greater portion of the sheath is somewhat thicker and more transparent than the blade, with thin transparent margins. For a distance of 3-5 mm above the point of insertion (node) on the culm it is considerably thickened (about 1 mm thick).

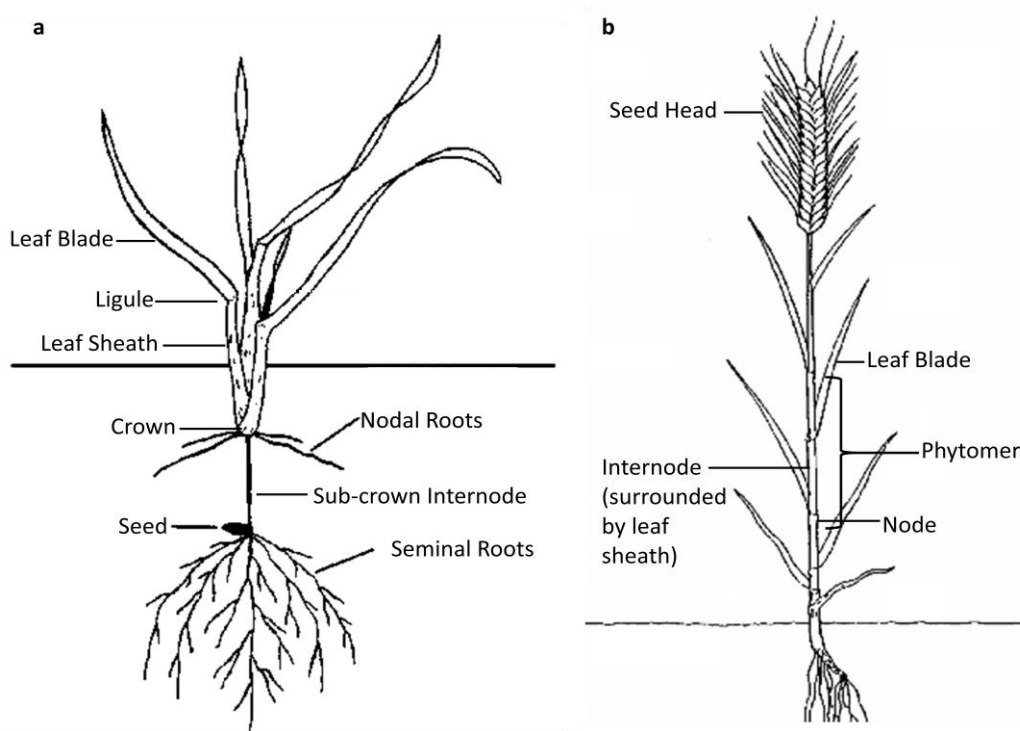


Figure 1.2. a, Seedling anatomy (Veseth, 1987). b, Culm anatomy (Knight and Quirk, 1994).

1.2.2 Growth Cycle

Each culm is able to produce an inflorescence which typically undergoes self pollination. Following pollination the seed head develops and large quantities of starch and protein are stored in the developing seeds. After approximately four weeks

grain filling has been completed, seed moisture levels have fallen below 15% and the crop is ready for harvest (Simmons *et al.*, 1995).

1.2.3 Diseases

Organisms able to cause serious diseases on wheat include fungi, bacteria, viruses and nematodes. It is estimated that losses in Australian wheat yield are as high as \$913 million per year, or approximately 20% of the average annual value of the Australian wheat crop (Murray and Brennan, 2009b). In Australia the major diseases of wheat include yellow spot (*Pyrenophora tritici repentis*), stripe rust (*Puccinia striiformis*), *Septoria nodorum* blotch, crown rot (*Fusarium pseudograminearum* and *F. culmorum*) and root lesion nematode (*Pratylenchus neglectus*), representing \$599 million of the total losses. Without the years of research on breeding for disease resistance and the use of cultural and chemical control measures, such as crop rotations and pesticides, annual losses due to these five diseases would be considerably greater (Murray and Brennan, 2009b).

1.2.3.1 Foliar and Head Diseases

Diseases occurring on the foliage of a wheat plant generally affect the photosynthetic capacity of the plant. This becomes severe when the flag leaf, the major producer of sugars going to the grains, becomes infected. The main effects caused by foliar pathogens are the redirection of nutrients to the pathogen instead of to the host and/or death of host tissue, limiting the photosynthetic capacity of the plant. Diseases of the grain head result in contamination of the grain with the pathogen and may lead to the production of mycotoxins, fungal metabolites which can have serious effects on animal and human health. Foliar diseases commonly result in lower grain yields while diseases of the head may lead to whole crops being discarded due to contamination.

1.2.3.2 Root and Crown Diseases

Diseases of plant roots and crowns are potentially the most debilitating of plant ailments and are harder to monitor and control than leaf diseases. When roots or the crown become infected and either can no longer absorb nutrients and water, or the

nutrients absorbed are diverted by pathogens, growth of the entire plant is restricted. The decrease in nutrient uptake can have highly detrimental effects on plant and crop yields, making these diseases an important focus of modern disease resistance research. In Australia important root and crown diseases of wheat include crown rot (*F. pseudograminearum* and *F. culmorum*), take-all (*Gaeumannomyces graminis* var. *tritici*) root lesion nematode (*Pratylenchus neglectus* and *P. thornei*), cereal cyst nematode (*Heterodera avenae*) and common root rot (*Bipolaris sorokiniana*) (Wallwork, 2000, Murray and Brennan, 2009b).

1.3 Crown Rot

Crown rot is so called because it appears to originate from the crown and spread upwards through the plant during the season, predominantly into leaf sheath and culm tissue where a brown discolouration is observed. Crown rot is generally associated with semi-arid areas where wheat maturation occurs under warm dry conditions (Burgess *et al.*, 2001), however, it has been reported in varying climates ranging from the semi-arid to mediterranean (Backhouse *et al.*, 2004, Gargouri *et al.*, 2006).

1.3.1 Economic Impact in Australia

Yield losses of over 50% due to crown rot have been reported under conditions favourable for this disease (Wallwork, 2000). In 1998 losses due to crown rot were reported to be worth approximately \$50 million in lost yield each year (Brennan and Murray, 1998), with this figure increasing to \$79 million just over a decade later (Murray and Brennan, 2009b).

1.3.2 Crown Rot Distribution

Crown rot is important in the southern and northern regions of the eastern wheat belt of Australia (Burgess *et al.*, 1975, Burgess *et al.*, 1981, Murray and Brown, 1987, Backhouse and Burgess, 2002, Backhouse *et al.*, 2004, Murray and Brennan, 2009b, Hollaway and Exell, 2010). Importance of the disease is increasing in the western

grain growing region of Australia (Murray and Brennan, 2009b). In Queensland and New South Wales crown rot is predominantly caused by the anamorphic fungal pathogen *Fusarium pseudograminearum* (Burgess *et al.*, 1975, Backhouse *et al.*, 2004, Scott *et al.*, 2004). In Victoria and South Australia *F. pseudograminearum* is also the most common species associated with crown rot, however, *F. culmorum* has also frequently been isolated in these states. In the high rainfall areas of Victoria and South Australia *F. culmorum* can be the dominant pathogen in some fields (Backhouse *et al.*, 2004). Other *Fusarium* species such as *F. avenaceum*, *F. crookwellense* and *F. graminearum* Schwabe have been infrequently isolated from crown rot infections. (Backhouse *et al.*, 2004)

Globally, crown rot has also been reported in New Zealand (Monds *et al.*, 2005, Bentley *et al.*, 2006), North America, particularly in the warmer climates of the Pacific Northwest of the United States (Cook, 1968, Smiley *et al.*, 2005), Argentina (Carranza, 1961), Italy (Balmas, 1994), South Africa (Van Wyk *et al.*, 1987, Klaasen *et al.*, 1991), North Africa (Burgess *et al.*, 2001, Gargouri *et al.*, 2006), Western Asia (Burgess *et al.*, 2001, Saremi *et al.*, 2007, Tunali *et al.*, 2008) and Great Britain (Colhoun and Park, 1964).

1.3.3 History

The most common causal agent of crown rot in Australia is currently named *F. pseudograminearum*. However, in the past this fungus has been known under the names *Gibberella saubineti*, *Fusarium roseum* ‘Graminearum’ and later *F. graminearum* Group 1. Burgess *et al.* (1975) provide the first evidence of two groups within *F. graminearum*, reporting that one set of isolates, Group 1, did not form perithecia in culture and were commonly associated with crown rot, while another set, Group 2, normally formed perithecia in culture and was infrequently associated with crown rot. Cultural and genetic characteristics have provided distinctions between the two groups (Burgess *et al.*, 1975, Aoki and O'Donnell, 1999a, Laday *et al.*, 2000). During 1999 *F. graminearum* Group 1 was formally described as a distinct species, *Fusarium pseudograminearum* (Aoki and O'Donnell, 1999a). Aoki and O'Donnell demonstrated that *F. pseudograminearum* is a phylogenetically distinct species using β -tubulin and translation elongation factor gene sequences, coupled with careful measurements of the spores produced. Numerous studies have

confirmed this result (Benyon *et al.*, 2000, Tan and Niessen, 2003, Monds *et al.*, 2005, Scott and Chakraborty, 2006).

Possible documentation of the crown rot fungus in Australia dates back to 1892 where a fungus was observed on herb stems in Victoria and Tasmania and later described using perithecial and conidial form as *Gibberella saubinetti* (Cooke, 1892). In 1896, in Australia, a species of fungi displaying “salmon-coloured patches” of growth on nodal and head tissue was designated as *Fusarium culmorum* based on morphological comparisons to *Fusisporium culmorum* (McAlpine, 1896). This is similar to the report by Hynes (1924) who found what was described as *Gibberella saubinetti* on foot-rot of oats. Hynes stated the belief that due to the frequency of isolation of *Fusarium* from tissues showing foot-rot and nodal symptoms, *Fusarium* may be an important cause of cereal foot-rot in New South Wales. Both Atanasoff (1920) and Bentley (2007) have suggested that the species referred to in 1896 and 1924 was actually the asexual form of *F. pseudograminearum*, due to the lack of documented perithecial production in culture.

The first official record of crown rot of wheat in Queensland was made in 1951 by Dr. T. McKnight. It is probable that the disease was present much earlier, as McKnight and Hart (1966) stated that symptoms similar to crown rot were reported as early as 1940. Purss (1966) conducted the first significant studies into the effects of crown rot disease and found differences in crown rot disease between wheat varieties. During the last 45 years a significant body of research on crown rot has been performed, however, progress has been challenging.

1.4 *Fusarium* Genus

Plant-associated fungi comprise a wide variety of groups, but few are as harmful to plant and animal health as the genus *Fusarium*, a large and ancient group that has evolved extraordinary diversity (Desjardins, 2006). *Fusarium* species can infect many plant species, including cereal crops such as wheat, barley and maize. They cause serious diseases in these crops, such as crown rot and head blight on wheat and barley and ear rot on maize. These pathogens not only have the capability to significantly decrease grain yields but, during infection and after harvest, *Fusarium* species have the ability to produce a range of secondary metabolites known as

mycotoxins, such as, trichothecenes, zearalenones and fumonisins (Desjardins, 2006). During the last 20 years, *Fusarium* species have been studied extensively because the mycotoxins they produce can be a threat to plant, animal and human health. The phytotoxicity and effects in plant-pathogen interactions of some of these toxins have been demonstrated, but the roles of others are still being elucidated.

1.4.1 *Fusarium pseudograminearum*

F. pseudograminearum Aoki and O'Donnell belongs to the phylum Ascomycota. It produces hyaline, septate macroconidia with a foot-shaped basal cell (Leslie and Summerell, 2006). Reproduction is predominantly by asexual means via the anamorphic stage *F. pseudograminearum*, however a teleomorph (sexual stage) *Gibberella coronicola* can be produced. *G. coronicola* is heterothallic (sexes reside in different individuals) and as a result it does not commonly produce perithecia (Aoki and O'Donnell, 1999a). The sexual stage *Gibberella* belongs to the phylum Ascomycota, characterised by formation of asci which are sac-like cells typically containing 8 ascospores (Read and Beckett, 1996). The genus *Gibberella* is within the group of filamentous ascomycetes which form perithecia metallic blue in colour, which enclose the asci (Alexopoulos *et al.*, 1996). Hyphae of both stages are well developed, branched and septate. *F. pseudograminearum* colony colour on Potato Dextrose Agar (PDA) is typically red to light pink, sometimes with yellowish aerial hyphae.

1.4.1.1 Genetic Diversity Studies

Multiple studies have assessed the genotypic diversity present in populations of *F. pseudograminearum* in Australia (Akinsanmi *et al.*, 2006, Bentley *et al.*, 2008, Bentley *et al.*, 2009) and other countries (Monds *et al.*, 2005, Bentley *et al.*, 2006, Mishra *et al.*, 2006, Scott and Chakraborty, 2006). *F. pseudograminearum* populations in Tunisia and Canada have been described as having substantially high genetic diversity with no spatial clustering. This indicates frequent gene flow occurs over a wide geographic area, resulting in a recombining structure corresponding to a single population (Gargouri *et al.*, 2006, Mishra *et al.*, 2006). Other studies using *Fusarium* species have found a similar lack of correlation between genetic clusters

and geographic origin (Ouellet and Seifert, 1993, Benyon *et al.*, 2000, Scott and Chakraborty, 2006).

In an assessment of genetic variation within Australian isolates of *F. pseudograminearum* Akinsanmi *et al.* (2006) observed a high level of intraspecific diversity, identified by five amplified fragment length polymorphism clusters forming within a population collected from Queensland and New South Wales. Akinsanmi *et al.* found that only 4% of the overall genetic diversity could be attributed to differences between isolates from the adjacent states, indicating high gene flow between isolates from different regions and thus a low level of population subdivision. A strong link between aggressiveness and AFLP clusters was also reported. Bentley *et al.* (2008) performed a similar but more geographically diverse experiment comparing *F. pseudograminearum* isolates from across most of the major wheat growing areas of Australia. An assessment of AFLP similarity separated isolates into two groups, originating from either north-eastern Australia or south-central and south-western Australia. Bentley *et al.* (2008) hypothesise that ‘the *F. pseudograminearum* populations from north-eastern and southern Australia are independent, which could result from different founding events or from geographic isolation and the accumulation of genetic differences due to genetic drift and/or selection’. A high level of gene flow was again reported within each of these populations. Bentley *et al.* (2009) performed further analysis of micro-scale genetic variation within 1 metre rows and compared this to field and regional variation. It was found that the genetic diversity amongst the isolates from the 1 metre row populations accounted for a large proportion of the genetic diversity observed for field and regional populations. Genetic differences due to geographic region have also been reported in New Zealand where isolates of *F. pseudograminearum* from the South Island clustered separately from North Island isolates (Monds *et al.*, 2005, Bentley *et al.*, 2006).

While it is apparent that the species *F. pseudograminearum* has high genetic variation, the process by which this has come about is still unclear. Akinsanmi *et al.* (2006) found that the differences in population structure between the heterothallic *F. pseudograminearum* and the homothallic *F. graminearum* were not as pronounced as expected given their contrasting mating systems. They determined that *F. pseudograminearum* was neither panmictic (random mating within a breeding population) or strictly clonal. It was suggested by Akinsanmi *et al.* (2006) that these

results point to a level of sexual recombination in *F. pseudograminearum*. However, ascospores from the sexual stage of *F. pseudograminearum*, *G. coronicola*, have only occasionally been reported in the field or laboratory (Francis and Burgess, 1977, Aoki and O'Donnell, 1999b, Summerell *et al.*, 2001), and only limited information is available on the importance of this stage. Bentley *et al.* (2008, 2009) confirmed that *F. pseudograminearum* has a dimictic mating system. It was revealed that both mating types and genetic distances had significant spatial aggregation. They suggest that this is consistent with the presence of non-random spatial genetic structure due to clonal aggregation. Other theories related to panmixia, sexual recombination, ascospore/inoculum spread and parasexual recombination have been discussed (Benyon *et al.*, 2000, Akinsanmi *et al.*, 2006, Mishra *et al.*, 2006, Scott and Chakraborty, 2006, Bentley *et al.*, 2008, Bentley *et al.*, 2009) but more work is required to convincingly determine the method/s employed by the fungus to increase or maintain genetic variation.

1.4.1.2 Use of Genetic Information

Specific DNA primers for identification of *Fusarium* species are frequently used for experimentation (Schilling *et al.*, 1996). This primarily relates to identification of individual species and quantification of fungal DNA. The section entitled 'Species-specific qPCR' contains further explanation. The availability of the whole genome sequence of *F. graminearum* and an Affymetrix GeneChip (Guldener *et al.*, 2006) allows for molecular characterisation of fungal genes, which could highlight important responses during growth and plant infection. Scott and Chakraborty (2007) have used this genome sequence to identify polymorphic loci suitable for population studies of *F. pseudograminearum*. Stephens *et al.* (2008) have also applied this information to identify genes which may be of importance during crown rot infection.

1.5 Aspects of Crown Rot Disease

1.5.1 Disease Cycle

F. pseudograminearum is a widely distributed soil-borne pathogen found mainly in association with infested plant debris where it can survive for several years (Wallwork, 2000, Leslie and Summerell, 2006). Wheat crops planted into soil containing this debris appear to be infected via the sub-crown internode or crown/leaf sheath bases as the plant comes into contact with the fungus (Purss, 1966). It is probable that the coleoptile of the seedling is the first tissue to come into contact with *F. pseudograminearum* inoculum as it grows towards the soil surface. However, infection has been reported to occur from seedling emergence through to maturity (Purss, 1966, Burgess *et al.*, 1981, Summerell *et al.*, 1989). The fungus may survive on seed, infected stubble or by using alternative hosts (McKnight and Hart, 1966). However, seed-borne carryover of *F. pseudograminearum* is of little practical significance or importance in Australia (Butler, 1961). *F. pseudograminearum* does have the ability to cause head blight, more typically caused by *F. graminearum*. Despite this, head blight infection by *F. pseudograminearum* is relatively rare, due to poor dispersal of its macroconidia and has only infrequently been reported in the northern wheat belt of New South Wales under wet conditions (Burgess *et al.*, 1987).

1.5.2 Host Range

F. pseudograminearum has been isolated from all major winter cereals. However, wheat (*Triticum aestivum*), barley (*Hordeum vulgare*) and triticale (x *Triticosecale* Wittmack) are symptomatic primary hosts (Simmonds, 1941, Purss, 1966, Quazi *et al.*, 2009). Cereal oats (*Avena sativa*) and the grass weed wild oats (*Avena fatua*) become infected by *F. pseudograminearum* but are considered asymptomatic hosts that are likely to contribute to the maintenance of inoculum (Nelson and Burgess, 1994, Nelson and Burgess, 1995, Burgess *et al.*, 2001). *F. pseudograminearum* has been isolated from many other grass genera including *Agropyron*, *Austrostipa*, *Avena*, *Bromus*, *Danthonia*, *Dicanthium*, *Hordeum*, *Panicum*, *Phalaris* and the species *Zea mays* (Simmonds, 1966, Burgess, 1967, Purss, 1969, Bentley, 2007). This large host range, which includes grass weeds, allows *F. pseudograminearum* to survive in many environments and produce further inoculum even when host crops

have been removed. This ability has major implications for cropping, particularly when planning crop rotations, weed control and disease management.

1.5.3 Disease Symptoms

Infection can lead to a variety of outcomes, ranging from the death of seedlings or older plants, through varying degrees of basal tissue discoloration (Purss, 1966, Burgess *et al.*, 1981, Wallwork, 2000). In a wheat crop, crown rot effects are usually first observed after flowering when scattered white (dead) heads develop. These whiteheads have either shrivelled or no grain. Crown rot may be detected before whitehead formation by examining basal leaf sheaths or culm internodes for tissue browning. Infection frequently results in a dark brown discoloration of leaf sheaths and a honey-brown discoloration of culms. Discolouration may also be present on the coleoptile, sub-crown internode and nodal roots. In adult wheat plants the fungus has been found as high as the internode below the head but is more commonly restricted to the first three internodes above the crown (Purss, 1966, Malligan, 2008). Severely infected internodes typically contain pink mycelium characteristic of *F. pseudograminearum*, in noticeably greater abundance in the pith cavity. Under moist conditions sporodochia may be produced on infected tissue and these appear as pink patches near the base of plants.

In warm, moist conditions and in the presence of sufficient *F. pseudograminearum* inoculum, wheat seedlings may suffer seedling blight, where disease results in severe stunting or death. In these early stages brown discoloration/lesioning typically occurs on the seedling leaf sheaths but can also appear on the sub-crown internode, depending on where the plant comes into contact with the fungal inoculum. Curiously, the discoloration of the leaves appears to be confined to the sheath as discoloration stops at the base of the lamina (Liddell, 1985). Infection via the roots is not common, with any fungal growth into the roots appearing to originate from colonised culm or crown tissue (Purss, 1966, Taylor, 1983, Liddell, 1985).

The whitehead symptom of crown rot poses one of the most intriguing questions concerning this disease complex: What causes whitehead formation? Purss (1966) found that while culms with heads classified as whiteheads had a greater level of infection in the third and fourth internodes, culms with heads classified as healthy

also had a remarkably high percentage of infection in the third internode. Water stress increases the frequency of whitehead formation and it has been hypothesised that the fungus may block vascular tissue in the culm, resulting in death of the developing grain; however no strong evidence demonstrating this effect has been produced. The nature of this host-pathogen interaction requires further elucidation.

1.5.3.1 Mycotoxins and Infection

Current knowledge concerning the role of mycotoxins in crown rot infection is limited. Production of the trichothecene mycotoxin deoxynivalenol (DON) has been monitored during crown infections by *F. pseudograminearum* and *F. graminearum*, however its role during infection has not been determined (Mudge *et al.*, 2006). Host cell death due to release of DON has been reported, however the effect of the interactions is not clear as DON may also contribute to the induction of antimicrobial host defences (Desmond *et al.*, 2008). Studies on the numerous other toxins produced by *Fusarium* species have not been performed for *F. pseudograminearum*.

1.5.4 Environmental Conditions Affecting Infection

Environmental conditions have long been known to be important during infection and disease development of plants (Colhoun, 1973). Crown rot incidence and severity are affected by soil moisture, soil type, topography, time of planting and temperature (McKnight and Hart, 1966, Purss, 1966, Purss, 1971, Burgess *et al.*, 1975, Klein *et al.*, 1985). Initial fungal infection of seedlings is favoured by moist soil environments (Liddell and Burgess, 1985, Liddell and Burgess, 1988, Swan *et al.*, 2000) but crown rot can still develop at later growing periods. The disease is usually not severe in crops grown under optimum soil moisture over the entire season, however in low moisture environments the effects of crown rot are enhanced with significant damage being inflicted as plants approach maturation (McKnight and Hart, 1966, Burgess *et al.*, 1975, Klein *et al.*, 1990, Hollaway and Exell, 2010). It also appears that the fungus is able to grow more rapidly through the plant tissues when plants are moisture stressed. Crown rot has been recorded on all major soil types, however it principally occurs on soils of heavy texture or on light-textured soils with an impervious layer in the profile (McKnight and Hart, 1966, Burgess *et*

al., 1975, Burgess *et al.*, 1981). The disease appears to be affected by soil topography, where it is more prevalent on the flatter plains than on undulating terrain. In addition, crown rot is more common in low lying areas within a field, where it can form distinct patches in gilgais (localised depressions) (McKnight and Hart, 1966). Burgess *et al.* (1981) suggest that soil type and topography affect the incidence and severity of crown rot indirectly by their effect on the water relations of the plant. The two main environmental conditions affecting *F. pseudograminearum* growth are temperature and water, with interactions between these factors impacting on fungal and plant growth.

1.5.4.1 Temperature

Temperature is known to effect geographic infection patterns of *Fusarium* species in cereals, with *Fusarium* crown rot being most common in warm, dry areas throughout the world (Cook and Christen, 1976). The temperature of the soil is an important factor determining the extent of seedling infection (Dickson, 1923). Klein *et al.* (1985), Wildermuth and McNamara (1994) and Smiley (2009) found that high soil temperature favours infection of wheat by *F. pseudograminearum* and allows a clearer differentiation of disease responses. Lower temperatures (~ 13°C) typically resulted in indistinguishable differences in crown rot severity between susceptible and partially resistant seedlings, whereas at a temperature of 25°C, visual rating grouped seedlings into distinct groups and correlated with field test ratings (Wildermuth and McNamara, 1994).

Temperature also has significant effects on the early growth patterns and metabolism of wheat seedlings, which may in turn affect the growth of the fungus (Dickson, 1923, Dickson *et al.*, 1923, Gäumann, 1950). In particular, at lower temperatures (~12°C) wheat seedlings have a high content of available carbohydrates, which results in thickened cellulose walls that may offer resistance to fungal penetration.

1.5.4.2 Water

Water is required for germination and growth of *F. pseudograminearum* but optimal water potentials for infection and subsequent *in planta* growth have been identified

as important conditions in respect to crown rot severity. Maximal *in vitro* growth of *F. pseudograminearum* on agar plates, and similar fungi such as *F. roseum* ‘Graminearum’, *F. roseum* ‘Culmorum’ and *G. saubinetti*, has been found to require progressively drier conditions, with similar trends being observed in the field (Dickson, 1923, Cook and Christen, 1976, Wearing and Burgess, 1979). Moisture content of surface soil in particular has a major influence on the incidence of infection of wheat plants by *F. pseudograminearum* (Liddell and Burgess, 1985, Liddell and Burgess, 1988, Swan *et al.*, 2000). It has been determined that a critical threshold level of -1.5 MPa or equivalent surface moisture is needed to initiate infection (Liddell and Burgess, 1985, Liddell and Burgess, 1988). This has been reported for both pot experiments and field experiments.

It has been demonstrated that plant water stress, for example low seedling water potential, predisposes wheat seedlings to colonisation and further damage by *F. pseudograminearum* and also that crown rot incidence and severity, particularly during early head ripening, is greater where adult plants have been affected by low soil moisture (Cook, 1973, Burgess *et al.*, 1975, Beddis and Burgess, 1992, Felton *et al.*, 1998, Li *et al.*, 2008). The rate of infection is most likely influenced by interactions occurring between soil moisture, temperature and other variables (Dickson *et al.*, 1923, Swan *et al.*, 2000). *In vitro* testing has demonstrated that at higher temperatures a lower water potential was generally required for maximal growth. This response has been suggested to be an adaptive mechanism in the fungus to respond to the common situation of a dry environment when temperatures are high (Cook and Christen, 1976). A fitting description of this disease process was reported by Papendick and Cook (1974), who suggest that *Fusarium* is a slow-decay organism in wheat that has optimum water potential leading up to plant maturity but it can kill its host by aggressive attack if the plant water potential decreases (past a specific value) during maturation.

Other potential variables were investigated by Cook and Papendick (1970), who suggested that the frequent occurrence of *F. culmorum* foot rot in dry soils was a result of the germ tubes being much less liable to lysis by bacteria in dry than in wet soils. Malalasekera and Calhoun (1968) suggested that a further factor contributing to the more frequent occurrence of this disease in dry soil is that wheat seedlings take longer to emerge above soil level in dry soil, which increases the time that the highly susceptible seedling coleoptiles are exposed to the pathogen.

Work in the United States of America by Dickson *et al.* (1923) demonstrated interesting interactions between temperature and soil water during seedling development in relation to seedling blight of maize and wheat caused by *Gibberella saubinetii*. Dickson *et al.* reported that at low temperatures (~8°C) wheat seedlings do not blight but as the temperature increases above 10°C blight symptoms appear. The symptoms continued to increase with temperatures up to ~24°C. The authors argued that if the temperature was affecting the fungal growth then blighting of wheat and maize should occur in a similar manner. However, if temperature was causing an effect in plant growth/metabolism the wheat and maize (being cold and warm environment plants respectively) would blight differently. This difference in blighting between the two species was observed, with maize blighting at 8°C while wheat did not and vice-versa at 24°C. In addition to this, when soil moisture was lowered to the point where normal metabolism of the seedling is inhibited (30% of the moisture holding capacity), maize and wheat seedlings became blighted at all temperatures, a finding also reported by Beddis and Burgess (1992). The ability of temperature and water conditions to alter the normal metabolic processes of wheat plants and in turn affect the susceptibility of the plants to infection, rather than directly affecting growth of the fungus, needs close examination.

1.5.4.3 Whitehead Formation

Whitehead formation is described as a 'premature bleaching of the ears and straw, with the resultant production of shrivelled grain' (Butler, 1961). It has frequently been reported as a symptom of crown rot (McKnight and Hart, 1966, Purss, 1966, Wildermuth *et al.*, 1997). It is commonly believed that whitehead formation is due to restriction of water uptake within the vascular tissue caused by blockage of xylem by *F. pseudograminearum*. This leads to premature ripening of heads and poor grain fill. To date, however, very little histopathological evidence to support this theory has been reported. It is noted however that Smiley (2009), Klein *et al.* (1991), Kirkegaard *et al.* (2004) and Bentley (2007) all refer to translocation disruption or vascular blockage resulting in deadhead development. In the cases where references are given for these statements the references do not provide direct evidence for this claim, which must be considered as yet an unproven hypothesis.

Whitehead development in plants affected by crown rot is reportedly favoured by dry conditions (McKnight and Hart, 1966, Burgess *et al.*, 1975, Burgess *et al.*, 1981, Wildermuth *et al.*, 1997, Hollaway and Exell, 2010). In a study observing tillage treatments Wildermuth *et al.* (1997) reported the percentage of whiteheads to be lower in no tillage treatments compared to conventional disc tillage treatments. They hypothesised that high levels of whiteheads in the tillage treatments were due to moderate to high levels of disease and low available soil water at planting and anthesis. The no tillage treatment had a high incidence of crown rot, however, there was a higher availability of soil water (due to no tillage) resulting in a lower disease severity as indicated by percentage of whiteheads. This demonstrates that while water availability is important in relation to crown rot severity (whiteheads), water availability may not greatly affect crown rot incidence, i.e. percentage of plants infected.

1.5.5 Management

Current recommended practices for controlling crown rot are use of resistant (and/or tolerant) cultivars, control of alternative hosts and, probably the most important currently, use of crop rotations with at least two years out of susceptible cereals (Burgess *et al.*, 2001). McKnight and Hart (1966) reported a severe incidence of the disease on previously uncropped soil, suggesting the possibility of seed-borne inoculum or the presence of alternative host grasses. Chemical treatments of seeds and chemical sprays have not proved effective in controlling crown rot (McKnight and Hart, 1966, Lamprecht *et al.*, 1990) and thus are not part of the current recommended practices guide for crown rot control (GRDC, 2009). However, controlling alternative hosts and using crop rotations has proven effective in minimising the effect of crown rot. The integration of non-cereal break crops, such as grain sorghum (*Sorghum bicolor*), chickpeas (*Cicer arietinum*), faba beans (*Vicia faba*), canola (*Brassica napus*) or mustard (*Brassica juncea*), into crop rotations with wheat produces an environment beneficial for the decomposition of cereal stubble, leading to a reduction in inoculum levels before the planting of the next crop of wheat (Felton *et al.*, 1998, Kirkegaard *et al.*, 2003, Kirkegaard *et al.*, 2004, Quazi *et al.*, 2009, Evans *et al.*, 2010).

Tillage practices also influence the severity of crown rot. Conservation tillage, where crops are grown with minimal cultivation of the soil and frequently have a cover of standing stubble, results in soil moisture retention, reducing the risk of late season moisture stress which can enhance symptoms of crown rot (Burgess *et al.*, 2001). Due to the typically dry environment in the northern wheat belt of eastern Australia, conservation tillage has been widely adopted in this area (Summerell *et al.*, 1989). Conservation tillage also has extra requirements, primarily the need to use herbicides to control weeds and the need for specialised machinery. These practices result in retention of stubble above or on the soil surface, which reduces the rate of stubble breakdown and maintains higher inoculum levels, in comparison to full incorporation of the stubble by tillage. While a tillage system does not necessarily result in significantly decreased incidences of crown rot, the associated decrease in inoculum levels lowers the potential disease severity (Summerell *et al.*, 1989, Swan *et al.*, 2000). The associated moisture loss in tillage systems may also increase crown rot severity. Stubble burning can also be effective at reducing inoculum but it also reduces soil moisture storage capabilities and organic matter and increases the risk of erosion (Summerell *et al.*, 1989, Burgess *et al.*, 1996, Backhouse *et al.*, 1997).

Of the wheat cultivars grown in Queensland and northern New South Wales, the majority are moderately susceptible to crown rot (McRae *et al.*, 2010). Farmers in areas prone to crown rot infection are encouraged to grow some of the more modern varieties, such as EGA Wylie, which have partial resistance and the ability to out-yield other varieties under similar crown rot infestation (Nicol *et al.*, 2004).

A recently described method of DNA-based soil testing can also assist grain growers in predicting the likely extent of losses from various soil-borne diseases well before a crop is planted, allowing effective control strategies to be implemented (Ophel-Keller *et al.*, 2008). This method has been applied to both *F. pseudograminearum* and *F. culmorum* in order to compare the ability of different rotation crops to reduce *Fusarium* inoculum in the field (Evans *et al.*, 2010).

1.6 Screening for Crown Rot Infection and Yield Loss

While crown rot infection generally has been assessed by scoring the visual discolouration of seedling leaf sheaths and adult internodes, there are significant

differences in the details of the scoring methods used by different research groups (Hill, 1984, Liddell *et al.*, 1986, Wildermuth and McNamara, 1994, Nicol *et al.*, 2004, Wallwork *et al.*, 2004, Mitter *et al.*, 2006). The degree of discolouration will also vary under different environmental conditions. In order to minimise this problem, experiments typically include a set of standard genotypes known to be partially resistant or susceptible. Observed ratings can then be reported as a percentage response of the most susceptible standard genotype, allowing comparisons between different trial environments.

Environmental variation is greatest between field grown experiments but this variation can be limited by growing plants in controlled growth chambers or greenhouses. Growth chambers limit experiment sizes and are not typically suited for adult plant growth, thus confining growth chamber experiments to seedling tests. Seedling tests are commonly used for measuring disease resistance, however the relationships between crown rot seedling resistance, adult resistance and yield are complicated and not yet well-characterised.

1.6.1 Adult Screening

Adult screening is typically based on the percent of culm discolouration caused by the fungus (Wallwork *et al.*, 2004, Hogg *et al.*, 2007). While this may allow resistance to be identified, the relationship between stem discolouration and grain yield is critical.

Yield loss is an important factor for consideration when selecting wheat lines to be grown in crown rot affected areas. Work has been performed correlating yield loss to infection levels, which could allow rating methods based on visual disease levels to predict potential yield without time-consuming yield experiments.

A strong correlation ($r = 0.94$, $P = 0.01$) between percent yield loss and percent diseased culms (i.e. culms showing discolouration) was reported by Dodman and Wildermuth (1987). This method did not have typical control plants as all plants were grown in the same infested soil. At maturity culms were separated based on presence of visible disease symptoms with the yield from non diseased culms being compared to yield of diseased culms. This method does not compare yields between infected and uninfected plants but demonstrates that within single plants infected tillers show a significant yield loss in comparison to apparently uninfected tillers.

Klein *et al.* (1989) performed a comparison between loss in potential yield and incidence of plants with basal browning across two sites (Edgeroi and Bellata, NSW) with two different sowing dates. Edgeroi had correlations between loss in potential yield and incidence of plants with basal browning at the two time points (early, $r = 0.65$, $P = 0.05$ and late, $r = 0.87$, $P = 0.01$). There was no relationship reported between basal browning and loss in potential yield at the Bellata site. Klein *et al.* (1991) reported further results relating potential yield loss to three characters, plants with whiteheads and basal browning ($r = 0.89$), plants with basal browning ($r = 0.59$) and incidence of infection (based on isolation of *F. pseudograminearum* from culms) ($r = 0.58$, $P = <0.01$). Even though whiteheads demonstrated a strong correlation with yield loss, this character is not suitable for predicting yield loss as it is highly dependent on environmental conditions and in some circumstances infected plants may show no whiteheads (Purss, 1966).

Kirkegaard *et al.* (2004) suggested that for susceptible durum wheat the likely yield loss caused by crown rot is around 1% for every 1% increase in the number of culms with basal browning symptoms at harvest, however no consistent trend was reported for crown rot tolerant bread wheat varieties. Overall it would appear that there is a moderate relationship between the number of diseased culms and yield loss. The method employed by Kirkegaard *et al.* (2004) relied on a random group of plants not becoming infected under conditions with natural inoculum. This group was used for yield comparisons against a group of infected plants of the same plot. In an environment with a high incidence of crown rot, this method cannot be applied. A more suitable method, such as paired plots with and without inoculum, should be used when comparing yield and further separation of plants based on the amount of culm discolouration, not just its presence, would be helpful in determining the effect of disease severity on yield loss.

1.6.2 Seedling Screening

Experiments based on field trials are very time-consuming and prone to environmental variation. In order to speed up the process of selecting wheat lines with potential resistance to crown rot, seedling inoculation procedures have been developed. Numerous techniques for wheat seedling inoculation with *F. pseudograminearum* have been described. Purss (1966) reported two methods based

on direct seed inoculation with *F. pseudograminearum* conidia before planting and another method of planting seed into colonised cornmeal/sand media. These techniques were primarily based on seedling blight symptoms rated from 12 to 24 days after planting. It was concluded that seedling blight reaction gives no guide to field tolerance. However, Purss did state that it could be of use if true resistance was found.

In contrast to this, Klein *et al.* (1985) reported a good correlation between disease symptoms in seedlings and adult plants for six out of eight tolerant and susceptible wheat cultivars at 64 days after planting. This paper reports a novel method for crown rot development in the greenhouse. Briefly, seeds are covered with a layer of soil, a layer of inoculum (ground, colonised grain) was placed over this soil and finally a further layer of soil was added. This method allows the seedling to grow through the fungal inoculum layer in a manner similar to that occurring under natural conditions in the field, where there is an opportunity for infection soon after germination. While the results were promising, the rating method is poorly described but appears to rely solely on counting the number of healthy plants, which may record nothing more than disease escapes. Liddell *et al.* (1986) used a similar method to describe differences between two wheat lines in leaf sheath discolouration from as early as 39 days after planting.

These earlier attempts led to the development of the seedling inoculation and rating method designed by Wildermuth and McNamara (1994). This method utilised a similar inoculation technique to that described by Klein *et al.* (1985) but the rating of disease symptoms was optimised. Wildermuth and McNamara rated coleoptiles, sub-crown internodes, leaf sheaths (1 to 3) and whole plants at 21 days after planting. They determined that combined ratings of the percent discolouration of leaf sheaths 1 to 3 gave the most useful indication of resistance. Most importantly, they reported significant correlations between field ratings for crown rot susceptibility and percent leaf sheath discolouration ($r = 0.78$, $P = <0.01$). This gave the first solid evidence that seedling reactions could be used to predict the response of lines in the field.

Recently various other seedling inoculation techniques and rating methods, frequently based on applying a conidial suspension to host tissues, have also been reported (Mitter *et al.*, 2006, Li *et al.*, 2008, Poole *et al.*, 2009). However, no consensus has yet emerged on which methods, in addition to that of Wildermuth and McNamara (1994), are reliable predictors of field performance.

1.7 Disease Reactions

A plant can have either immunity (it is not attacked by the pathogen even under the most favourable conditions), resistance (prevents infection or limits its extent), tolerance (does not reduce or eliminate infection, but instead reduces or offsets its fitness consequences) or a combination of resistance and tolerance to a pathogen (Fineblum and Rausher, 1995, Agrios, 2005, Raberg *et al.*, 2007). The assessment of resistance and tolerance can be extremely valuable to breeding programmes but while resistance and tolerance are related, they do represent distinct concepts. Resistance improves host fitness by reducing infection, whereas tolerance reduces the effects of infection on fitness.

1.7.1 Resistance

Resistant qualities of plants fall into two major categories: preformed and inducible defence mechanisms. Preformed (or passive) defences represent the first barriers to invasion by a pathogen and include anatomical features such as strengthened cell walls reinforced with lignin or suberin and the accumulation and sequestration of antimicrobial secondary plant metabolites in plant tissues, such as cyclic hydroxamic acids of wheat (Frey *et al.*, 1997, Morrissey and Osbourn, 1999, Osbourn, 2001). Local protection against pathogen invasion also appears commonly as inducible defence mechanisms, including responses such as hypersensitive cell death, strengthening of invaded tissue by callose and/or lignin deposition, production of phytoalexins and induction of expression of defence-related genes (Osbourn, 2001). Numerous pathways resulting in expression of defence-related genes have been documented for many plant pathogens (Bent, 1996, Ellis *et al.*, 2000).

Resistance can further be described as either horizontal or vertical. Horizontal resistance is a resistance in which there are no differential reactions between races of the pathogen and varieties of the host (Van der Plank, 1975) and is classed as a multi-gene or quantitative resistance. Vertical resistance refers to specific interactions occurring between the host and pathogen. If a plant variety exhibits a high degree of resistance to a single race of a pathogen, such as reported for spot blotch (*Bipolaris sorokiniana*) (Meldrum *et al.*, 2004, Knight *et al.*, 2010) and leaf rust (*Puccinia recondita*) (Mesterházy *et al.*, 2000), it is said to be vertically

resistant. This type of resistance is controlled by one or a few genes and is described as qualitative resistance. No pathogenic specialisation of *F. pseudograminearum* isolates has been demonstrated (Malligan, 2008), although differences in aggressiveness between isolates infecting wheat crowns has been reported (Akinsanmi *et al.*, 2004, Malligan, 2008). Therefore, resistance to crown rot is horizontal and quantitative (requiring multiple resistance genes of small effect). This indicates that any partial resistance identified in wheat should be effective against all *F. pseudograminearum* isolates.

1.7.2 Crown Rot Resistance

Progress in producing crown rot resistant genotypes has been slow, with only moderately resistant lines identified to date. A difficulty in the current system is that mechanisms of resistance have not been identified and there is a paucity of information on the disease biology. Furthermore, the popular method of visual rating for discolouration has not been thoroughly described for its properties or relationship to resistance.

The following is a conglomerate of information highlighting the major properties of resistance currently identified for crown rot. An initial study performed by Purss (1966) found no true resistance to crown rot, any differences between varieties were ‘considered to be due to a differential rate of development of the disease rather than to any difference in actual infection’. It could be argued that the partial resistance identified in more modern varieties still only acts to slow the disease development (Malligan, 2008) as no resistance mechanism has been identified. While studying the effects of water potential during *F. pseudograminearum* infection using sterile soil, Liddell and Burgess (1988) found infection rates of 100% and surmised that wheat has little or no inherent resistance to infection by *F. pseudograminearum*. Dodman and Wildermuth (1987) reported the possibility that there is resistance to initial penetration by *F. pseudograminearum* since spraying conidia on culms produced less disease in a resistant cultivar than in a susceptible cultivar. When conidia were injected into culms, thus by-passing the penetration phase, no differences were found. This potentially highlights differences between inoculating seedlings (Liddell and Burgess, 1985, Liddell and Burgess, 1988) and inoculating more mature culms, as culms have stronger cell walls.

Resistant reactions to crown rot have been divided into two types based on the wheat line they appear in, namely 2-49 and Sunco. 2-49 displays a resistant response which can be recorded at seedling and adult stages while Sunco has a resistant response only detectable in adult plant material (Wildermuth *et al.*, 1999). Shallow crown formation has been attributed, at least in part, to the resistance found in 2-49. Shallow crown formation may enable escape of infection but this type of resistance most likely does not operate in Sunco, which has deep crown formation. During additional experimentation Wildermuth *et al.* (2001) produced further evidence that crown depth may be partly responsible for the reaction of a wheat genotype to crown rot.

Wheat adaptations to water stress have also been investigated as a potential area of interaction with crown rot disease. An association between the osmoregulation (*or*) gene and crown rot resistance was explored but analysis of the incidence and severity of the disease showed no association with the presence or absence of the *or* gene (Wildermuth and Morgan, 2004).

Zinc has also been attributed to crown rot resistance. In an experiment comparing crown rot infections of wheat plants grown in different zinc environments it was found that the extent of infection above the infection point decreased significantly when the level of available zinc was increased (Sparrow and Graham, 1988). The incidence of infection was not affected by zinc supply. The effect of zinc on crown rot infection was re-investigated by Grewal *et al.* (1996) where a similar effect was found. A zinc-efficient cultivar, Excalibur, produced more shoot and root dry matter and showed less disease infection compared with the zinc-inefficient cultivars Durati and Songlen. In contrast to Sparrow and Graham (1988) the results of Grewal *et al.* (1996) demonstrated that increased levels of zinc may decrease the incidence of infection. The importance of nutrient deficiencies, especially zinc, to crown rot infection has only had minor attention from researchers to date. This field of study, however, may yield important information about plant physiological pathways which act during crown rot resistance.

1.7.2.1 Genetics of Resistance

Resistance in wheat lines to crown rot disease has been extensively surveyed in glasshouse and field trials and has led to the selection of partially resistant lines

(Wildermuth and Purss, 1971, Wildermuth and McNamara, 1994, Wildermuth *et al.*, 2001). Quantitative trait loci (QTL), regions of DNA associated with a particular trait (e.g. resistance), have been identified for crown rot resistance in different wheat populations, with one of the current goals being the pyramiding of these regions within wheat lines to increase resistance (Wallwork *et al.*, 2004, Collard *et al.*, 2005, Bovill *et al.*, 2006, Collard *et al.*, 2006, Bovill *et al.*, 2010).

Using adult plant reactions to crown rot Wallwork *et al.* (2004) described a QTL located on the long (L) arm of chromosome 4B using doubled haploid lines of a Kukri/Janz cross. Multiple studies have been performed looking for seedling QTL for crown rot resistance. Collard *et al.* (2005) identified significant QTL on chromosomes 1DL and 1AL in a doubled haploid 2-49/Janz cross. Collard *et al.* (2006) performed experiments to confirm the QTL identified by Collard *et al.* (2005) using an independent doubled haploid population of a Gluyas Early/Janz cross. The presence of a major QTL on chromosome 1DL and a minor QTL on chromosome 2BS was confirmed. Bovill *et al.* (2006) performed further QTL analysis on a doubled haploid population of W21MMT70/Mendos cross. This resulted in identification of three loci, on chromosomes 2B, 2D and 5D, which were different from those associated with crown rot resistance in other wheat populations.

Pyramiding of these QTL in a wheat line could be of particular use for increasing resistance to crown rot. Bovill *et al.* (2010) used a population derived from a cross between 2-49 and W21MMT70, two partially resistant lines, to determine if pyramiding was an effective method for producing lines with resistant characteristics of both parents. It was observed that a number of lines from this population performed significantly better than each of the parents. This is one of the first demonstrations that pyramiding of genes is an effective tool for producing new resistance combinations. The identification of QTL has the potential to enhance crown rot resistance breeding by allowing the application of molecular screening before time consuming phenotypic screening is performed.

1.8 Estimating Fungal Load

Rating of crown rot disease of wheat is performed by visually examining the plants for their reaction to disease, in particular tissue discolouration (Wildermuth and

McNamara, 1994). Selecting wheat lines with resistance to infection is based on the ability of visual rating to report on fungal loads in infected tissues. The capacity of new technologies, such as real time quantitative polymerase chain reaction, to accurately quantify pathogen DNA in host tissue has proven to be a valuable resource for assessing current rating methods and producing the next generation of disease rating methodologies.

1.8.1 Traditional Quantification Method

The traditional method is based on visually rating diseased tissues, such as leaf sheaths and internodes and then placing these tissues, after surface sterilisation, onto Czapek Dox agar plates. As the fungus grows out of the tissue counts are performed on the colonies emerging from the tissue over a period of a week. Malligan (2008) reported that isolation scores of *F. pseudograminearum* from diseased wheat leaf sheaths and internodes had a strong to modest correlation with visual symptoms (R^2 of 0.65 and 0.31 respectively). This varied between plant tissue type and time after planting. This result demonstrates that generally, at earlier time points, the relationship between disease symptoms and fungal isolation is quite strong. It is also important to note that at least 20% of the variation was still unexplained by these methods, which indicates that other factors are also contributing.

1.8.2 DNA Based Quantification

The invention of the polymerase chain reaction (PCR) in 1984 by Kary Mullis was a major advance in the study of genetics (Mullis, 1987). PCR has changed the face of DNA analysis, leading to mapping and sequencing of entire genomes and a greater understanding of how biological systems work. One of the important developments has been multiplex PCR. This method allows simultaneous detection of multiple DNA products in one sample. Multiplex PCR was first described by Chamberlain *et al.* (1988) and since then has been applied in many areas of DNA testing, including analyses of deletions, mutations and polymorphisms or quantitative assays. Subsequently, real time quantitative PCR was developed (Heid *et al.*, 1996).

1.8.2.1 Real-Time Quantitative Polymerase Chain Reaction

Real time quantitative PCR (qPCR) measures PCR product accumulation using fluorescent molecules (e.g. intercalating dyes or labelled oligonucleotides) and provides very accurate and reproducible quantitation of DNA products (Heid *et al.*, 1996). qPCR is based on the classic PCR reaction, where primers are used as starting points for DNA polymerase to make copies of specific regions of DNA. PCR consists of three major stages: denaturation, annealing and extension. Cycles of these run the amplification reaction to its endpoint, where exponential increases in DNA product can no longer occur due to enzyme denaturation or exhaustion of raw substrates. qPCR uses the same basic procedure, with an extra component, such as an intercalating dye, the fluorescence of which can be measured spectrophotometrically during the reaction, not just at the endpoint. This dye only binds and fluoresces in the presence of double stranded (ds) DNA. Thus after each PCR cycle the dye binds to the new product and greater fluorescence is recorded by the specialised qPCR machine. The point where an increase in fluorescence is first detected is called the threshold cycle (Ct), which is the cycle at which the fluorescence level increases above the background level. This is more accurate than looking at endpoint fluorescence. The fluorescence after each cycle is plotted against the number of cycles completed, showing the rate at which the DNA amplicon is being produced; this can be related back to initial DNA quantities using a standard curve. The drawback of using an intercalating dye is its lack of specificity for the DNA product, i.e., it will bind to any dsDNA, and thus this is termed a non-specific method.

To overcome this problem sequence specific methods have been devised which use probes specific for the sequence being amplified (Schna *et al.*, 2004). These probes are oligonucleotides with specific reagents attached to each end, called reporter (or fluorophore) and quencher (or acceptor) molecules. The reporter molecule can become excited and emit energy (fluoresce) at a predetermined wavelength and this is what is read by the machine. However, when a quencher molecule is in close proximity to the reporter, the emitted energy is absorbed by the quencher, thus quenching the reporter molecule (Didenko, 2001). The sequence of these dual-labelled probes is designed to be specific for the DNA fragment being amplified, so any fluorescence then corresponds directly to the specific product. This method relies on the exonuclease activity of DNA polymerase to cleave the reporter away from the quencher to allow fluorescence (Figure 1.3). Probes also allow the

production of multiplex assays; this means that multiple DNA amplicons can be amplified in the same reaction and monitored separately, e.g. a fungal amplicon and a host plant amplicon. More advanced and sensitive detection systems such as molecular beacons and Scorpion primers are also available but are technically more demanding (Thelwell *et al.*, 2000, Schena *et al.*, 2004).

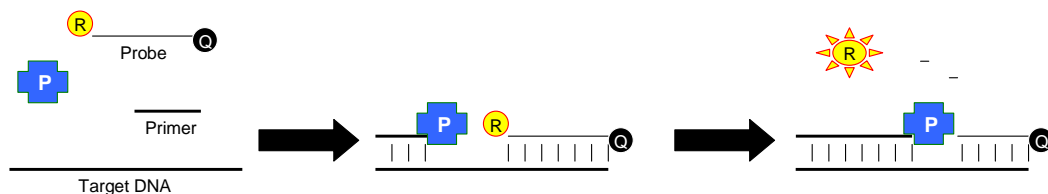


Figure 1.3. qPCR reaction using a dual-labelled probe, labelled with a reporter (R) and a quencher (Q) molecule. The probe binds to a specific sequence within the target DNA at the same time as the primer binds to its complementary sequence. The polymerase enzyme (P) extends the primer along the amplicon; once it meets the probe it progressively cleaves it, releasing the reporter molecule and nucleotides. The reporter molecule now fluoresces as the quencher molecule cannot absorb the released energy.

Real time quantitative PCR has many applications for identification of pathogens and in the study of host–pathogen interactions, including improving the resolution of disease screening programs in selecting highly resistant plants and allowing the infection pathways of pathogens to be tracked (Schaad and Frederick, 2002, Vandemark and Ariss, 2007). Observations of the infection pathways may allow specific regions associated with resistance mechanisms to be identified for future study.

1.8.2.2 Species-specific qPCR

Species specific qPCR assays for detecting pathogen presence in plant material have become relatively common over the last ten years. qPCR assays have been produced for *Mycosphaerella graminicola* during leaf blotch infection of wheat (Guo *et al.*, 2006), verticillium wilt of alfalfa caused by *Verticillium albo-atrum* (Larsen *et al.*, 2006), crown rot (*F. pseudograminearum*, *F. graminearum* and *F. culmorum*) of adult wheat plants (Hogg *et al.*, 2007), crown rust (*Puccinia coronata* f. sp. *avenae*) of oat (Jackson *et al.*, 2006), the interaction of *Aphanomyces euteiches* with legumes

(Vandemark and Ariss, 2007) and crown rot (*F. culmorum*) infection of wheat seedlings (Petrisko and Windes, 2006). Methods and concepts used in these studies can be applied to crown rot disease in Australia, particularly for monitoring fungal proliferation during infection, determining correlations between visible disease or yield loss to fungal DNA content and even for testing fungicide or tillage effects (Waalwijk *et al.*, 2004, Hogg *et al.*, 2007, Stephens *et al.*, 2008, Evans *et al.*, 2010).

PCR-based assays are powerful because they allow specific detection and identification of the target organism. For example, studies have used sequences of particular genes, e.g. the β -tubulin gene, to correctly identify a fungus as *F. venenatum*, instead of the previously reported *F. graminearum* (O'Donnell *et al.*, 1998). This provides strong evidence for the usefulness and accuracy of these PCR-based identification methods. In the case of *F. pseudograminearum*, partial genetic codes for single copy nuclear genes, such as the β -tubulin gene and the translation elongation factor alpha gene, have been sequenced and compared in separate studies (Aoki and O'Donnell, 1999a, Scott and Chakraborty, 2006). Primers designed against these sequences have been found to be specific for *F. pseudograminearum*. The significance of these primers is the ability to use them to determine the presence and extent of *F. pseudograminearum* infection, even in the absence of visible symptoms.

qPCR is not only an important method of monitoring plant resistance, but is also an important technique for classifying how *F. pseudograminearum* causes disease, particularly in relation to its association with necrotic lesions. *F. pseudograminearum* has been shown to produce a range of mycotoxins (e.g. deoxynivalenol and zearalenone) which may diffuse out of the fungal tissue and into the host plant. So while visible ratings cannot distinguish between fungal growth areas and areas affected by mycotoxins, qPCR may help make this distinction.

Some qPCR assessment has been performed for *Fusarium* species and crown rot infections of wheat, particularly comparing visual symptoms and fungal DNA. Hogg *et al.* (2007) developed an assay which amplified DNA of *F. pseudograminearum*, *F. graminearum* and *F. culmorum* during crown rot infection. This study compared disease severity scores, based on discolouration of the first internode, with *Fusarium* DNA content of the crown and found a positive correlation ($R^2 = 0.6$, $P < 0.001$). A similar result was observed for the DNA content of node one. Both the disease severity scores and *Fusarium* DNA content were negatively correlated with yield ($r = -0.64$ and -0.77 , respectively), which indicates that qPCR

can be an effective tool for measuring crown rot severity in wheat. However, these values represent the best correlations. There were large differences between correlations in different years and between cultivars, indicating effects of both genotype and environment on this relationship.

Other studies have used similar qPCR methods and found no or a weak association between classical phenotyping methods and pathogen DNA content (Nicholson *et al.*, 1998, Bateman *et al.*, 2000, Turner *et al.*, 2002). Strausbaugh *et al.* (2005), for example, examined root lesioning, primarily caused by *F. culmorum*, and fungal DNA content of roots and found no correlation. Large quantities of root material were required for accurate quantification of pathogen DNA. Root tissue is commonly associated with soil which can inhibit downstream applications if not removed before DNA extraction and later it was determined that the PCR assay resulted in a lower detection level of *F. culmorum* due to partial inhibition of PCR (Hogg *et al.*, 2007). Other problems occurred due to disease symptoms caused by other pathogens and interactions between pathogen growth and plant age.

1.9 Fungal Microscopy

Bright field microscopy has historically been the major method used to observe plant-pathogen interactions, followed by electron microscopy. While electron microscopy provides high magnification, high resolution images, it is not always readily accessible and involves complicated fixing procedures. Fluorescence microscopy has now become the most common method used to examine biological interactions, mainly due to increased accessibility and easy visualisation of fungal tissues, and has been proven extremely useful for observing plant pathogen interactions (Darken, 1961, Duckett and Read, 1991, Hood and Shew, 1996, Howard *et al.*, 2004, Jansen *et al.*, 2005). This technique relies on exposing samples to particular wavelengths of light which cause the sample to fluoresce. The methods require the use of either fluorescent stains or genetically modified organisms and allow new technologies, such as confocal microscopy, to be harnessed (Spear *et al.*, 1999, Lorang *et al.*, 2001).

Confocal laser scanning microscopy, which enables optical rather than mechanical sectioning of specimens, has been used for studying *Fusarium*

oxysporum f. sp. *radicis-lycopersici*, which causes tomato foot and root rot disease (Lagopodi *et al.*, 2002). This study used genetically transformed fungal isolates expressing the green fluorescent protein, which allows the fungus to be visualised using a fluorescence microscope. This method produces a distinct contrast between plant and fungal cells as they emit different wavelengths of light. The difficult aspect of this method is genetically transforming the fungus without interrupting genes needed for infection and growth. An alternative to genetically modifying fungal isolates is to use differential staining, which involves using a fungal cell wall stain, such as calcofluor, and a separate stain for host cells, thus allowing differentiation between the two cell types. Schäfer *et al.* (2004) used this method to study the wheat and barley pathogen *Bipolaris sorokiniana*, allowing the hemibiotrophic nature and *in planta* growth of the fungus to be observed. The results were not as clear as using the genetically modified fungus but new fungal cell wall binding dyes, such as solophenyl flavine, may allow better contrast compared to calcofluor (Hoch *et al.*, 2005). Either of these methods could be applied to the study of *F. pseudograminearum* crown rot.

1.9.1 *Fusarium* Microscopy

Few studies have been performed on the microscopic assessment of crown rot infection of wheat plants. Taylor (1983) performed the first and only detailed microscopic assessment of *F. pseudograminearum* crown rot. The experiments primarily utilised seedling and adult tissues of the wheat cultivar Timgalen, observed using bright field microscopy and scanning electron microscopy. Taylor reported that the mode of infection was predominantly by the formation of appressoria-like structures on the surface of wheat tissues, particularly of the coleoptile. Further infection involved both intra and intercellular hyphae, particularly in the cortical parenchyma tissues. From the inoculated coleoptile the hyphae appeared to spread into the epidermal cells of the sub-crown internode, progressing down to the crown and scutellum tissues. As the disease progressed xylem tissues were penetrated and became colonised. The invasion of the xylem is described as beginning in the scutellum and then spreading up into the sub-crown internode xylem. No discussion was provided on potential mechanisms or areas displaying resistance to hyphal growth.

Several other microscopic studies have been performed using various *Fusarium* species. Clement and Parry (1998) and Mudge *et al.* (2006) reported on the colonisation of wheat by *F. culmorum* and *F. graminearum*, respectively. Clement and Parry (1998) found that *F. culmorum* colonising wheat culm bases appeared to grow in the pith cavity, with a suggestion that mycelial progression may be delayed by nodes. Mudge *et al.* (2006) used bright field microscopy on stained tissues to observe *F. graminearum* primarily growing in the pith parenchyma with intra- and inter-cellular growing hyphae. Very little colonisation of the vascular tissues in typical plants was observed in either study. *F. graminearum* displays hyphal growth around and up wheat leaf sheath trichomes (Stephens *et al.*, 2008). This study also reported extensive colonisation in the vascular tissue and pith of the wheat crown.

Microscopic studies on other *Fusarium* species may provide ideas on how *F. pseudograminearum* infects and colonises plants. *F. culmorum*, *F. nivale* and *F. solani* f. sp. *phaseoli* have been observed to penetrate host tissues via stomata (Christou and Snyder, 1962, Malalasekera *et al.*, 1973). *F. solani* f. sp. *phaseoli* and *F. lini* have been reported to penetrate host tissues via trichomes (Nair and Kommedahl, 1957, Mulligan *et al.*, 1990). During *F. lini* infection of susceptible flax (*Linum usitatissimum*) tissues hyphae entered through trichomes and became abundant in xylem and phloem (Nair and Kommedahl, 1957). In resistant tissues hyphae were limited to the cortex and were not found in the vascular tissue.

A similar comparison between crown rot susceptible and partially resistant wheat lines would greatly improve current knowledge of the disease processes and would assist both germplasm screening methods and crop management strategies aimed at disease reduction.

1.10 Project Rationale

Since crown rot was first reported in Australia in 1951 (McKnight and Hart, 1966) there has been intense research into establishing the identity of the causal fungus, appropriate management practices and screening varieties for resistance. However, it remains one of the top five diseases of Australian wheat, causing an estimated \$79 million in lost yield annually. The identification of differences in susceptibility to crown rot between wheat lines was first documented in 1966 and since then

numerous studies have reported lines displaying lower susceptibility (Purss, 1966, Wildermuth and Purss, 1971). This susceptibility is most frequently described by observing visual symptoms on the seedling leaf sheaths and adult culms. Malligan (2008) describes the first experiments where fungal quantity was related to visual symptom development. This study used isolation techniques to quantify the fungus and found a strong correlation between fungal quantity and visual disease development. Further studies examining the ability of visual rating methods to describe the extent of infection and examining *F. pseudograminearum* growth habits during pathogenesis will provide a greater understanding of this disease complex.

The four major objectives of this study are outlined below.

1. Produce a specific real time quantitative PCR assay for quantifying *F. pseudograminearum* in plant tissues.

After design and optimisation, the real time quantitative PCR assay has many potential applications within research on *Fusarium* crown rot. A selection of these applications is described in objective 2.

2. Examine cereal tissues affected by *F. pseudograminearum* crown rot using traditional visual rating methods and real time quantitative PCR.

F. pseudograminearum disease symptoms are predominantly classified using traditional visual rating methods. This forms the basis of selection of partially resistant genotypes in wheat breeding programs. The questions this project will seek to answer are:

- a) Is real time quantitative PCR able to accurately determine fungal biomass in infected tissues, potentially providing a more sensitive description of the extent of infection than visual rating? This ability has important consequences as quantitative PCR will be used to assess the ability of visual rating methods to accurately describe infection. Thus the hypothesis examined states that strong correlations exist between visual ratings methods

and real time quantitative PCR in both seedling (Chapter 2) and adult (Chapter 3) tissues.

- b) Is there evidence for host tolerance to *F. pseudograminearum* colonisation? The two rating systems were compared across partially resistant and susceptible cereal genotypes. This allowed investigation of any ability for genotypes to tolerate fungal presence, either without symptom development or with reduced symptom development.
 - c) Do differences in crown rot infection between partially resistant and susceptible genotypes become more apparent when assessed by quantitative PCR than visual rating? This was assessed in seedling and adult tissues across a range of time points.
3. Produce a staining method for microscopic examination of diseased tissue.

Production of a novel, rapid staining technique allowing discrimination between host and pathogen tissues enabled in-depth microscopic examination of plant-pathogen interactions during crown rot infection. While the real time quantitative PCR assay is limited to specific analysis of *F. pseudograminearum*, the tissue staining technique has potential applications in many other plant-pathogen interactions.

4. Microscopically examine the infection and colonisation of partially resistant and susceptible cereal tissues by *F. pseudograminearum* during crown rot disease.

This project has performed the first detailed microscopic examination of crown rot disease in partially resistant and susceptible cereal genotypes. Descriptions of infection structures and behaviours in leaf sheath and internode tissues were particularly targeted (Chapter 4). Leaf sheaths represent the tissues used during visual rating of seedling infections and interactions between the host and pathogen in these tissues demonstrate how infection initiates and progresses. Internode tissues are used to assess disease

in adult plants and are potential tissues where effects of crown rot such as yield loss and whitehead formation may initiate. Due to their nutrient transporting roles vascular bundles were of particular interest for monitoring during infection. It was hypothesised that during culm infection vascular bundles were colonised, with susceptible tissues becoming colonised earlier and to a greater extent than partially resistant tissues. The theory that susceptible tissues become colonised earlier and to a greater extent than partially resistant tissues was investigated using multiple host genotypes. Due to the novelty of detailed microscopic observation of crown rot infection, a general approach to record infection patterns throughout major tissues was applied. This was based on colonisation of partially resistant and susceptible seedling and adult tissues. These findings will greatly extend the currently limited knowledge of *F. pseudograminearum* growth and infection mechanisms during crown rot infection.

Chapter 2 : Seedling Infection

2.1 Introduction

Resistance to crown rot infection has predominantly been described in terms of lesion development or tissue discolouration (Purss, 1966, Wildermuth and McNamara, 1994). Several methods for inoculating seedlings and describing tissue discolouration have been reported to demonstrate differences in resistance between genotypes (Wildermuth and McNamara, 1994, Mitter *et al.*, 2006, Li *et al.*, 2008). Using these methods, only partial resistance has been described in which a reduction of symptoms, rather than absence, is observed.

The relationship between the discolouration of seedling tissues and quantity of fungus has had relatively little attention. Malligan (2008) performed isolation counts on infected cereal tissues by placing them on Czapek Dox Agar and counting the colonies formed after one week. She reported that correlations between disease rating and isolation scores from seedling tissues were all highly significant ($R^2 \approx 0.7$), with younger, less diseased tissues demonstrating the closest relationship. Time after infection, ranging from 14 to 42 days after planting in inoculated medium, did not greatly affect these correlations.

Recently qPCR methodology has been applied to the detection of fungal colonisation in host tissues in a range of interactions (Guo *et al.*, 2006, Petrisko and Windes, 2006, Hogg *et al.*, 2007, Stephens *et al.*, 2008). However, qPCR analysis of *F. pseudograminearum* infection of wheat seedlings has not yet been reported. Stephens *et al.* (2008) used qPCR to describe *F. graminearum* infection of wheat seedlings of the susceptible cultivar Kennedy over a 49 day period. Three phases of infection were reported, i) initial spore germination with formation of a superficial hyphal mat at the inoculation point, ii) colonisation of the adaxial epidermis of the outer leaf sheath and mycelial growth from the inoculation point to the crown, concomitant with a drop in fungal biomass and iii) extensive colonisation of the internal crown tissue.

The primary purpose of this current work was to build on the initial re-isolation studies of Malligan (2008). A qPCR assay was designed to allow accurate quantification of *F. pseudograminearum* in infected tissues and allow comparisons of fungal spread and proliferation between partially resistant and susceptible genotypes.

Visual ratings of diseased tissues were assessed for their correlation with qPCR values.

2.2 Methods

2.2.1 Wheat Genotypes

Four genotypes of bread wheat varying in degree of crown rot resistance were chosen for the seedling study:

- Puseas (Pusa 4//Three Seas) is a variety bred by Richard Soutter in 1939 and was subsequently widely grown in Queensland (Purss, 1966, Skerman, 1990). It is highly susceptible to crown rot (McKnight and Hart, 1966, Purss, 1966, Malligan, 2008).
- 2-49 (Gluyas Early//Gala) is an experimental line selected due to its partial crown rot resistance (Wildermuth and McNamara, 1994, Wildermuth *et al.*, 2001, Malligan, 2008).
- EGA Gregory (Pelsart/2*Batavia doubled haploid line) is a current commercial variety released in 2005 which is described as moderately susceptible/susceptible to crown rot (McRae *et al.*, 2010).
- EGA Wylie (QT2327/Cook//QT2804), released in 2005, is described as moderately resistant to crown rot. It carries one of the highest levels of partial resistance to crown rot among current commercial wheat varieties adapted to the northern grains region (McRae *et al.*, 2010).

A detailed pedigree of these four genotypes is provided in Appendix 2A.

2.2.2 Planting

Wheat seeds were surface sterilised by rinsing for two minutes in a 2% sodium hypochlorite solution followed by three rinses in high purity water (MilliQ system,

Millipore). Each seed was transferred to the surface of a 5 cm x 5 cm x 10 cm pot, filled to 2.5 cm below the rim with Premium Hi-Retention growing medium (Power Blend, Narangba, Qld). Seeds were then covered with a further 2.5 cm of growing medium. The pots were transferred to the greenhouse and watered twice a week.

2.2.3 Inoculum Production

The highly aggressive *F. pseudograminearum* isolate A03#24, collected from Tara, Queensland and characterised by Malligan (2008), was selected for inoculum production. A single conidial culture was grown and maintained on spezieller nährstoffarmer (specific nutrient) agar (Nirenberg, 1976). Sub-cultures of this culture were grown on starch nitrate agar (SNA) (Dodman and Reinke, 1982) in the dark at 25°C for fourteen days. SNA was selected as the growth medium for *F. pseudograminearum* after comparison of conidial production on four different media (Appendix 2B). Conidia were collected by flooding plates with 5 mL of a 6% Tween20 solution before filtering through several layers of cheesecloth with high purity water (MilliQ, Millipore), to a volume of 10 mL. The conidial suspension was quantified using a counting chamber (Weber and Sons, Lancing, United Kingdom) and diluted to a concentration of 10^6 conidia/mL. The final suspension was stored for a maximum of two months at -70°C before inoculation.

2.2.4 Inoculation and Harvest

Inoculation of horizontally laid fourteen day old seedlings was modified from methods reported by Mitter *et al.* (2006). During testing it was found that a 10 µL droplet of the 10^6 conidia/mL inoculum (reported by Mitter *et al.*) frequently rolled off inoculated seedlings. A 6 µL droplet exhibited much greater adherence to the plant tissue. Initially few disease symptoms resulted from this method, however, after very gently rubbing the coleoptile of the seedling with a sterile toothpick before placing the inoculum onto the area 0.5 cm behind the tip of the coleoptile, much greater infection and tissue discolouration resulted. The coleoptile was a useful infection point as it has been found to be highly susceptible across a range of genotypes (Malligan, 2008) and allowed initial growth of the hyphae into enclosed leaf sheath (LS) tissue without any mechanical stress to the LS. Control plants were mock-inoculated with 6 µL of high purity water.

After inoculation seedlings were placed in a growth chamber in the dark for 48 hours with two cycles of 25°C for fourteen hours followed by 15°C for 10 hours at approximately 100% RH. After 48 hours seedlings were placed upright in a growth chamber and maintained under lights at 25°C for fourteen hours followed by a 10 hour dark period at 15°C. Temperature and humidity during all experiments were monitored by a Tinytag Ultra 2 TGU-4500 data logger (Gemini Data Loggers, Chichester, UK). Plants were positioned in a randomised block design.

2.2.5 Visual Rating

At harvest each of the collected tissues was rated based on the percent brown discolouration of the whole tissue and of tissue sections. The method for rating discolouration was described by Wildermuth and McNamara (1994). Briefly, tissues were rated for disease on a 0 to 4 scale. 0 = no visible discolouration, 1 = less than 25% discolouration, 2 = 25 to 50% discolouration, 3 = 51 to 75% discolouration and 4 = greater than 75% discolouration.

2.2.6 Time Course Harvest

Harvest of control and inoculated seedling material of the four wheat genotypes was performed at 0, 1, 3, 5, 7, 14, 21, 28 and 35 days after inoculation (dai). Separately harvested tissues included coleoptiles and separate LSs. The length of each LS was recorded. Each time point was independently replicated. Duplicate samples at each time point consisted of five plants. Tissues were harvested into pre-weighed microfuge tubes. During harvest samples were kept on ice and then stored at -70°C.

2.2.7 Seedling Harvest for Sectioning

Seedlings of Puseas and 2-49 were harvested at 14 and 28 dai. Samples were collected in groups of three plants, with three replicates at each time point. Each of the time points were independently replicated. The seedlings were sectioned as described in Table 2.1. Leaves 1-3 and leaves 1-4 were harvested at 14 and 28 dai respectively. Secondary roots were only available at 28 dai.

Table 2.1. Tissue sections harvested and analysed by qPCR.

Organ	Length (cm)
Leaf Blade (LB) ^a	2
Ligule	0.5
LS Top (LSt) ^a	2
LS Middle	Various ^b
LS Bottom (LSb) ^a	2
Secondary Roots ^a	2
SCI ^a	Various ^c
Primary Roots ^a	2

^a Indicates that tissue underwent qPCR analysis.

^b Length range of 0 – 8.3 cm.

^c Length range of 0 – 4.4 cm.

2.2.8 DNA Preparation

Lyophilised tissues were ground using a TissueLyser (Qiagen, Doncaster, Victoria) and three tungsten-carbide beads. Samples with dry weights greater than 0.01 g were sub-sampled into 0.005 to 0.01 g samples. A Qiagen DNeasy plant mini kit was selected to perform DNA extractions after extensive assessment of several DNA extraction procedures (Appendix 2C). Samples were eluted into 200 µL of Elution buffer and stored at -4°C until required.

2.2.9 Primer Selection and Optimisation of PCR Conditions

Primers and probes were designed from GenBank sequences of *F. pseudograminearum* and wheat (*Triticum aestivum*) using Primer3 (Rozen and Skaletsky, 2000) or were sequences from published literature (Table 2.2 and Table 2.3). The sequences for primer pair Fp TEF1 α .1 were provided by Di Hartley (CSIRO). These sequences were assessed by a BLAST (www.ncbi.nlm.nih.gov/BLAST) search of the GenBank nucleic acid database using the Others (nr etc.) database: Nucleotide Collection (nr/nt). Primer and probe sequences were also assessed for their GC content, potential primer dimer formation and theoretical melting temperature.

2.2.9.1 Initial PCR Assessment

Singleplex PCR conditions were initially optimised for each primer pair, which were tested on *F. pseudograminearum* and wheat DNA separately. Suitable primer pairs for *F. pseudograminearum* and wheat were then combined and assessed in multiplex reactions, using DNA extracted from infected LSs.

PCR was initially performed in 10 μ L reactions (0.5 units Immolase DNA polymerase (Bioline, Alexandria, New South Wales), 100 μ M dNTPs, 1x Immobuffer, autoclaved MilliQ water), with various $MgCl_2$ (5 mM to 1 mM) and primer (1 μ M to 0.0625 μ M) (Invitrogen, Mulgrave, Australia) concentrations, on a TGradient PCR machine (Biometra, Germany). Thermal cycling conditions were 95°C for 7 min, followed by 40 cycles of 94°C for 30 sec, annealing (at temperatures 50 - 70°C) for 30 sec and 72°C for 30 sec, followed by 72°C for 10 min.

Primers were further assessed using a Rotor-Gene 6000 (Corbett Life Sciences, Sydney, Australia). Reactions were performed in 25 μ L reactions, with reagents as previously described, except that 2 μ M of Syto9TM nucleic acid stain (Invitrogen, Mulgrave, Australia) was included. Thermal cycling conditions were 95°C for 7 min, followed by 40 cycles of 94°C for 30 sec, various annealing temperatures (60 - 66°C) for 30 sec and 72°C for 30 sec. Fluorescence was read after each 72°C extension step.

DNA amplicons were observed on a polyacrylamide gel using a Gel-Scan 2000 instrument (Corbett Life Sciences, Sydney, Australia). This assessment resulted in the selection of two pairs of primers, Fp TEF1 α .2 and Wh TEFG.5, which were specific for *F. pseudograminearum* and wheat, respectively, and were compatible in a multiplex reaction.

2.2.9.2 Optimisation of the Multiplex Real Time Quantitative PCR Assay

Multiplex qPCR conditions were optimised for primer pairs Fp TEF1 α .2 and Wh TEFG.5 and their respective dual labelled probes. The 5'-terminal of the *F. pseudograminearum* probe was labelled with the reporter dye CAL Fluor® Gold and the 3'-terminal with quencher BHQ®-1 (Biosearch Technologies, Novato, California). The 5'-terminal of the wheat probe was labelled with the reporter dye FAM and the 3'-terminal with quencher BHQ®-1 (Biosearch Technologies).

These primer/probe sets were tested in singleplex and multiplex reactions using a Rotor-Gene 6000. Negative controls and no template controls (NTCs) were included during qPCR assessment. Primer and probe concentrations were optimised for each set according to the multiplex results. Reactions were performed in 20 μ L volumes (autoclaved MilliQ water, 0.5 units Immolase DNA polymerase, 1x Immobuffer, 2.5mM MgCl₂, 100 μ M dNTPs, 100-150 nM *F. pseudograminearum* CAL Fluor® Gold labelled probe, 100-150 nM wheat FAM labelled probe, 0.0625-0.5 μ M of the *F. pseudograminearum* and wheat primers and 5 μ L of DNA template). Thermal cycling conditions consisted of 10 min at 95°C and 50 cycles of 95°C for 15 s and 60-66°C for 1 min. The final multiplex real time qPCR assay is described below.

2.2.9.3 Confirmation of PCR Products

F. pseudograminearum and wheat fragments from primer sets Fp TEF1 α .2 and Wh TEFG.5 respectively, were cloned using pGEM®-T Easy Vector System II (Promega, Sydney, Australia) and sequenced to confirm that the sequence amplified matched that reported on the GenBank nucleic acid database. Briefly, PCR products were run in a 1.2% agarose gel for 30 min. Fragments were viewed using an ultraviolet transilluminator (Ultra-Lum Electronic UV Transilluminator, California, USA) and the gel containing the fragments was removed using a scalpel. Fragments were cloned into JM109 cells using the recommended kit procedure and sent to the Australian Genome Research Facility, Brisbane, for sequencing.

Table 2.2. *F. pseudograminearum* primer and probe sequences assessed for host specificity.

Primer Name	Forward Primer (5'-3')	Reverse Primer (5'-3')	Fragment Size (bp)	Probe Sequence (5'-3')	GenBank No.
Fp TEF1 α .1	ATCATTCGAATCGCTCGACG	AAAAATTACGACAAAGCCGTAAGAA	82	ACTCGACACGCGCCTGTTACCC	DQ382162
Fp β tubulin	AGCTCACGCGTTTAGGCCTCCGGTA	AGCTGTCCGAAGGGACCAGCACGA	107	-	DQ382227
Fp TEF1 α .2	ATCATTCGAATCGCTCGACG	AAAAATTACGACAAAGCCGTAAGAA	82	ACTCGACACGCGCCTGTTACCC	DQ382162

Table 2.3. Wheat primer and probe sequences assessed for host specificity.

Primer Name	Forward Primer (5'-3')	Reverse Primer (5'-3')	Fragment Size (bp)	Probe Sequence (5'-3')	GenBank No./Reference
Glud	CGTTGGCACCGGAGTTG	TCACCGCTGCATCGACAT	101	-	Terzi <i>et al.</i> (2003)
Wh TEF1 α	GGGTCATGTTCTAATTTGTTAGC	GCGACATATAAATATTCCACACGA	149	TGCAAGCTCGCAATACCGAATCATC	M90077
Puroindoline-b	ATTTTCCATTCACTTGGCCC	TGCTATCTGGCTCAGCTGC	92	-	Li <i>et al.</i> (2004)
Actin	GGAAAAGTGCAGAGAGACACG	TACAGTGTCTGGATCGGTGGT	150	-	Lu <i>et al.</i> (2005)
Wh TEFG.1	CGT GAA GGA TTG AGG AAA GC	ACA TCA CCC AAA TGC TCC TC	89	GGCCCACGACTCCTGGAACCTATAA	DQ247872
Wh TEFG.2	CTTCCGTGAAGGATTGAGGA	CCTCTTCTAGAGTTCAAGTCACCA	120	TGGCCCACGACTCCTGGAACCTATA	DQ247872
Wh TEFG.3	TCCGTGAAGGATTGAGGAA	CCTCTTCTAGAGTTCAAGTCACCA	118	TGGCCCACGACTCCTGGAACCTATA	DQ247872
Wh TEFG.4	TCCGTGAAGGATTGAGGAA	CCTCTTCTAGAGTTCAAGTCACCAA	118	TGGCCCACGACTCCTGGAACCTATA	DQ247872
Wh TEFG.5	TCCGTGAAGGATTGAGGAA	GTCTCTTCTAGAGTTCAAGTCACC	120	TGGCCCACGACTCCTGGAACCTATA	DQ247872

2.2.9.4 Primer Specificity and Sensitivity

The species specificity of the *F. pseudograminearum* primer/probe set was tested on various *Fusarium* species visually identified and supplied by Phillip Davies (University of Sydney) (Table 2.4). *F. pseudograminearum* isolate A03#24 and *F. pseudograminearum* isolates used by DEEDI researchers at the Leslie Research Centre, Toowoomba were also assessed.

Specificity of both primer/probe sets were further tested across pure DNA from multiple bread wheat genotypes (*Triticum aestivum*) as well as single genotypes of durum wheat (*Triticum turgidum durum*) and barley (*Hordeum vulgare*) (Table 2.4).

The sensitivity of the primer/probe sets was tested using DNA quantities in a range from 1000 to 0.0001 ng using either pure *F. pseudograminearum* or wheat DNA or combined DNA extracted from infected LSs. This allowed the optimum quantities for producing precise linear regression models to be determined.

2.2.10 Multiplex Real Time Quantitative PCR Conditions

Reactions were performed in 20 μ L volumes containing autoclaved MilliQ water, 0.5 units Immolase DNA polymerase, 1x Immobuffer, 2.5mM MgCl₂, 100 μ M dNTPs, 150nM *F. pseudograminearum* CAL Fluor® Gold labelled probe, 150nM wheat FAM labelled probe, 0.25 μ M forward and reverse primers for both organisms and 5 μ L of DNA template.

Multiplex real-time qPCR was performed using 50 μ L tubes in a 72 tube rotor of a Rotor-Gene 6000. Thermal cycling was completed in less than 2 h and conditions consisted of 10 min at 95°C and then 35 cycles of 95°C for 15 s and 64°C for 1 min. The Rotor-Gene 6000 series software collected data for both reporter dyes every 0.15 s from each tube, generating a fluorescence profile for each amplification product. The threshold cycle (Ct) was recorded for each dye as the cycle at which fluorescent signal, associated with an exponential growth of PCR product, exceeded background fluorescence.

The wheat primer/probe set was designed to be included in multiplex PCR as both an internal positive control and for normalisation purposes. Normalisation of qPCR results was performed using two methods. After qPCR, normalised estimates of *F. pseudograminearum* colonisation of wheat tissue were obtained by dividing the

quantity of *F. pseudograminearum* DNA by either the quantity of wheat DNA (ng *Fp* / ng wheat) or the original extracted sample dry weight (ng *Fp* / g). These are referred to individually as the *Fp* per wheat DNA and *Fp* DNA per weight methods, respectively, or collectively as qPCR values within this document.

Intra- and inter-assay variability were examined using two experimental DNA samples. This involved each sample being assessed in a qPCR assay as 10 replicates. During further experimentation these two samples were included in at least 10 separate PCR assays. Samples were compared using *Fp* per wheat DNA results.

2.2.10.1 Controls and Standard Curve Production

PCR controls in every assay included no template controls (NTC) and genomic DNA standards (positive/negative) for both *F. pseudograminearum* and wheat. Serial dilutions of pure genomic wheat DNA and pure genomic *F. pseudograminearum* DNA standards were run in duplicate. DNA concentrations of wheat and *F. pseudograminearum* standards were determined spectrophotometrically by measuring optical density at 260 nm using a nanophotometer (Implen, Munich, Germany). Samples were diluted into four 10-fold serial dilutions for *F. pseudograminearum* DNA (10 ng to 1 pg) and three 10-fold serial dilutions for wheat DNA (100 ng to 100 pg). Standard curves for both *F. pseudograminearum* and wheat were generated by plotting known DNA amounts against the Ct calculated by the Rotor-Gene 6000 software in order to produce a regression equation. Unknown samples were quantified by plotting their Ct values on the regression equation.

2.2.11 Statistical Methods

Comparisons between arcsine square root transformed visual and qPCR ratings of individual genotypes were performed using a one-way ANOVA with the Levene Statistic from the Test of Homogeneity of Variance and the multiple comparisons Tukey HSD test in SPSS 17.0. Weights and LS lengths of control and infected tissues were compared using a two-tailed paired sample t-test in SPSS 17.0. All tests used $\alpha = 0.05$. Pearson's Correlation Coefficients (two-tailed) were calculated in SPSS 17.0. The strength of each correlation was reported using the system described by Fowler *et al.* (1998).

2.3 Results

2.3.1 PCR Optimisation

Wheat primer/probe set Wh TEFG.5 and *F. pseudograminearum* primer/probe set Fp TEF1 α .2 were selected as the most compatible combination during multiplex qPCR assessment. These were based on sequences of translation elongation factor G and translation elongation factor α , respectively. Both sets required similar optimum PCR conditions and were specific to their target host (Table 2.4), amplified the expected sequences from their respective target DNA and did not display unwanted interactions between primers.

A maximum of 35 cycles was deemed sufficient for standard curve production, allowing for a rapid qPCR assay. *F. pseudograminearum* was quantifiable from 0.001 to 100 ng and wheat was quantifiable from 0.05 to 500 ng. In singleplex and multiplex reactions both primer/probe sets displayed high precision over a linear range of 4 orders of magnitude (Figure 2.1). The linear regression correlations between Ct and known DNA quantities were high for both *F. pseudograminearum* and wheat ($R^2 > 0.99$).

Normalisation of samples served to adjust the *F. pseudograminearum* DNA estimates of colonisation for differently sized tissue samples and sample-to-sample variation in both DNA extraction and PCR amplification efficiencies (Winton *et al.*, 2002).

Intra- and inter-assay precision in PCR efficiency for this assay was high (Figure 2.2), demonstrating the reproducibility within and between individual qPCR assays. Pipetting accuracy was improved by using “MAXYmum Recovery” pipette tips (Axygen, California, USA).

Table 2.4. *Fusarium* and cereal species assessed using the *F. pseudograminearum* and wheat primer/probe sets.

Species	Number Tested	<i>Fp</i> primers ^c	Wheat primers ^c
<i>F. compactum</i> ^a	2	-	-
<i>F. crookwellense</i> ^a	2	-	-
<i>F. culmorum</i> ^a	2	-	-
<i>F. equiseti</i> ^a	2	-	-
<i>F. poae</i> ^a	2	-	-
<i>F. proliferatum</i> ^a	2	-	-
<i>F. scirpi</i> ^a	2	-	-
<i>F. semitectum</i> ^a	2	-	-
<i>F. pseudograminearum</i> ^b	8	+	-
<i>F. graminearum</i> ^a	5	-	-
<i>Triticum aestivum</i>	5	-	+
<i>Triticum turgidum durum</i>	1	-	+
<i>Hordeum vulgare</i>	1	-	-

^a *Fusarium* species visually identified and supplied by Phillip Davies (University of Sydney).

^b *F. pseudograminearum* included 5 isolates visually identified and supplied by Phillip Davies (University of Sydney) and 3 isolates from the LRC, DEEDI collection.

^c ‘+’ indicates a positive while ‘-’ indicates a negative PCR result for that primer/probe set.

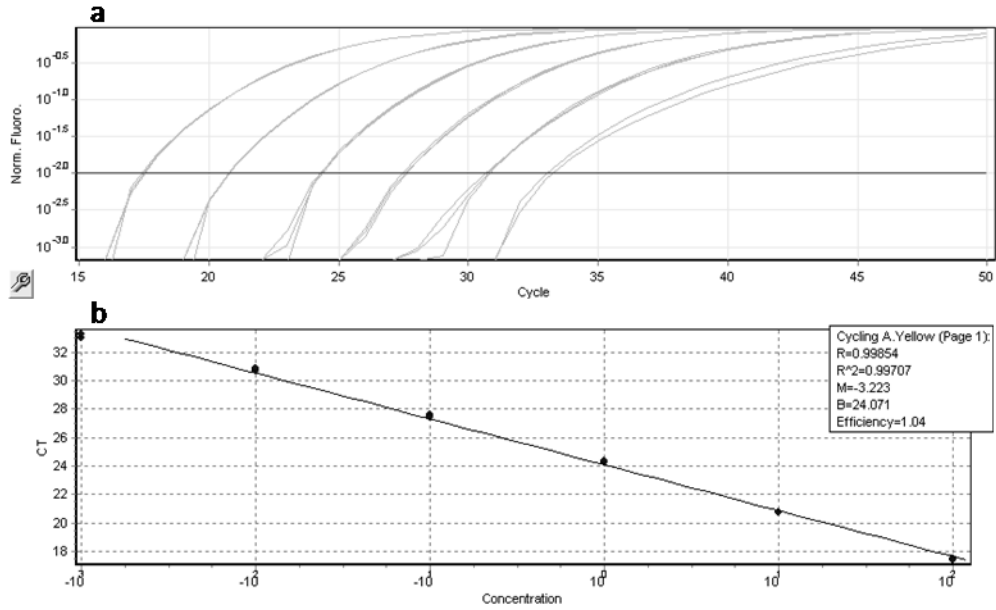


Figure 2.1. a, Normalised fluorescence curves of five 10 fold serial dilutions of *F. pseudograminearum* DNA. b, Standard curve produced by plotting Ct against quantity of DNA in each standard dilution. Calculations and graphs were created using the Rotor-Gene 6000 Series Software 1.7.

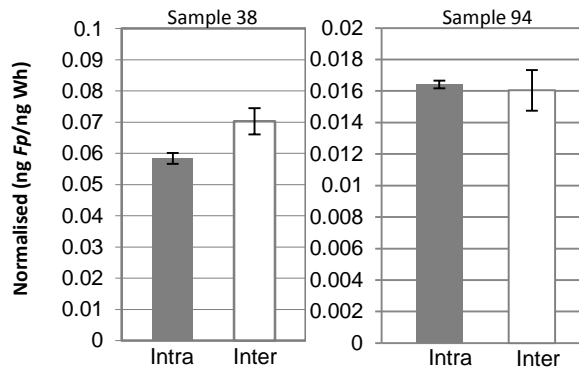


Figure 2.2. Intra- and inter-assay variability of samples 38 and 94. Columns represent the standard error of the mean of ten replicates. Intra-assay variability was assessed across 10 replicates in a single assay. Inter-assay variability was assessed using single reactions across 10 individual assays.

2.3.2 Time Course

The three different rating methods (visual, *Fp* per wheat DNA and *Fp* DNA per weight) varied slightly in their ability to report accurately on colonisation. Tissues of control plants did not become infected.

Visual discolouration of LS tissue was observed from 3 dai, however, consistent ratings could not be assigned until 7 dai. qPCR values for coleoptile or LS1 tissues from one to seven dai were not useful indicators of resistance. Increase in the qPCR values of these tissues was exponential from 1 to 7 dai, however differences between genotypes were inconsistent (data not shown).

Visual ratings and qPCR values indicated significant differences between genotypes from 14 dai (Figure 2.3, Figure 2.4 and Figure 2.5). This proved the most discriminating time to assess resistance using visual ratings. Visual discolouration and qPCR values at 21 and 28 dai did differentiate between partially resistant and susceptible genotypes, however, for visual ratings, differences were less than at 14 dai. At 35 dai only qPCR could discriminate between partially resistant and susceptible genotypes. qPCR values at both 21 and 28 dai indicated a large separation between partially resistant and susceptible genotypes.

Combined values of each LS produced consistent differences between partially resistant and susceptible genotypes from 14 to 28 dai (Figure 2.6). In most cases LS1 and 2 were not useful indicators of resistance. The visual ratings of these tissues rapidly reached the maximum value, inhibiting the ability to discriminate between resistance and susceptibility. LS3 and 4 frequently demonstrated significant differences between Puseas and the other three genotypes. Differences between genotypes were greatest using qPCR. Significant differences between Puseas and 2-49 were more consistent using the *Fp* DNA per weight method than the *Fp* per wheat DNA method.

qPCR values showed exponential growth over a period of time in each LS, however growth reached a plateau phase in heavily infected tissues such as LS1 in Puseas, Wylie and Gregory at 35 dai. A similar trend was observed for LS2 at 35 dai in Puseas. The linear relationships of the log values for the *Fp* per wheat DNA method were very strong, while those of the *Fp* DNA per weight method were strong (Table 2.5 and Table 2.6). The gradients of the linear relationships were greater in the susceptible Puseas than in the partially resistant 2-49.

While 2-49 is considered to have greater resistance than Wylie and Gregory, this was not reflected as a statistically significant difference in fungal DNA content. The mean values for 2-49, however, were predominantly the lowest among the four genotypes for each tissue across the times assessed (Figure 2.6).

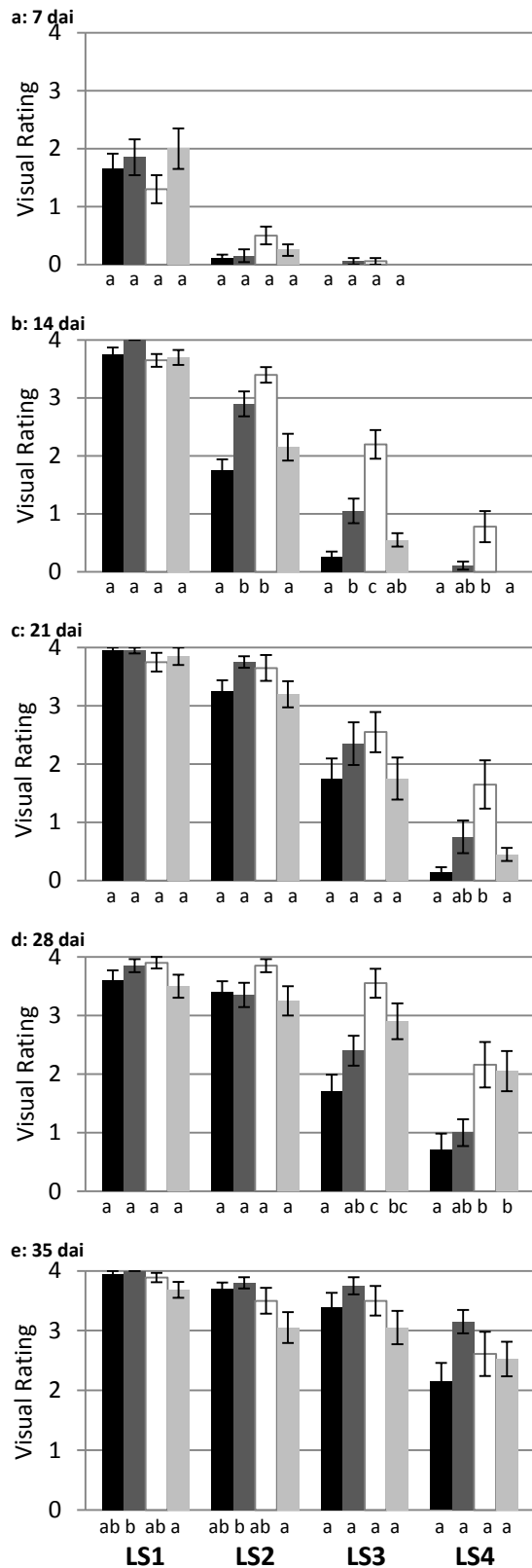


Figure 2.3. Visual ratings of crown rot infection in LS1, LS2, LS3 and LS4 at (a) 7, (b) 14, (c) 21, (d) 28 and (e) 35 dai. Columns represent the standard error of the mean of four replicates. Different letters indicate significant differences ($p < 0.05$) within each LS. ■ 2-49, ■ Gregory, □ Puseas, ■ Wylie.

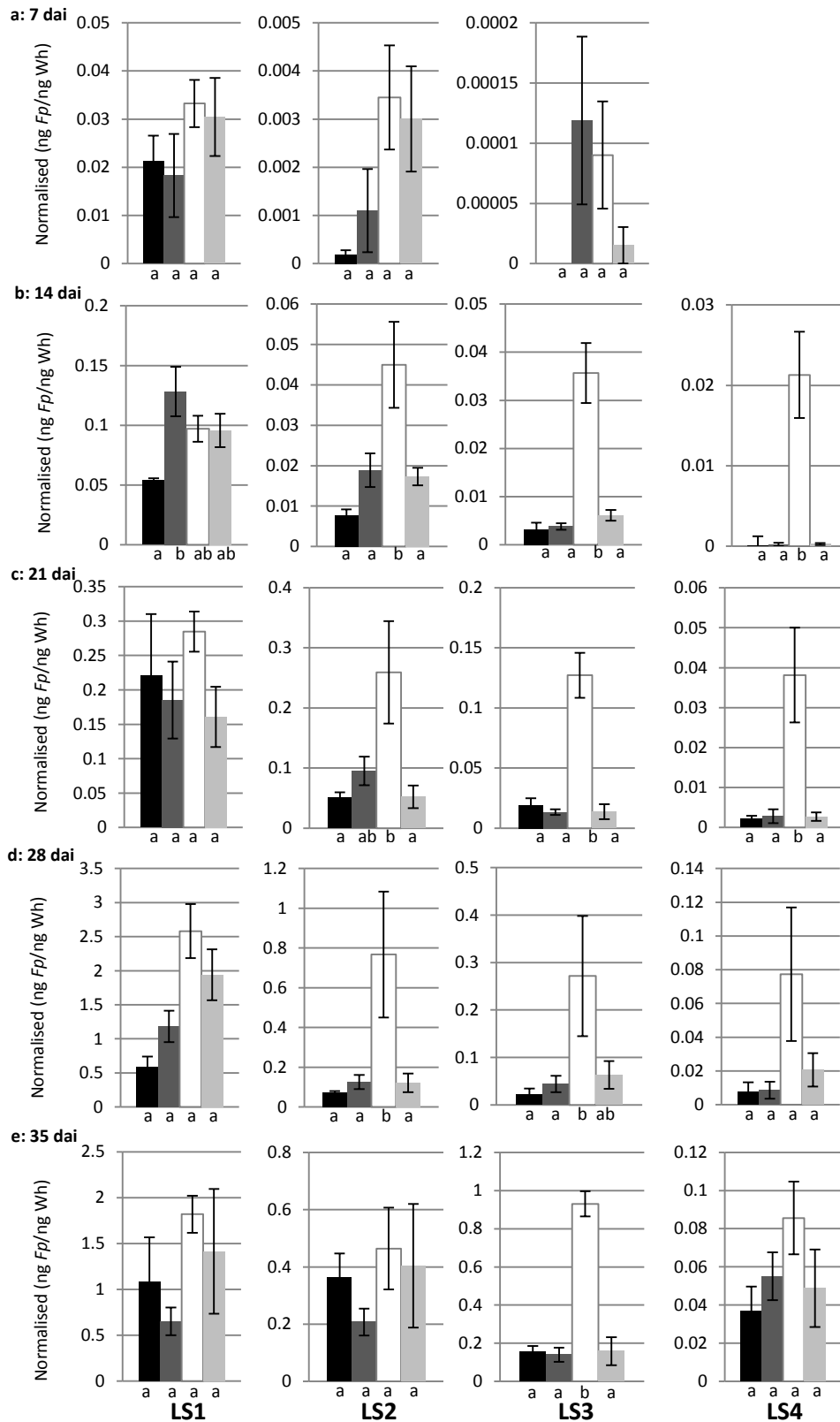


Figure 2.4. Normalised *Fp* per wheat DNA values of LS1, LS2, LS3 and LS4 at (a) 7 dai, (b), 14 dai, (c) 21 dai, (d) 28 dai and (e) 35 dai. Columns represent the standard error of the mean of four replicates. Different letters indicate significant differences ($p < 0.05$) within each LS. ■ 2-49, ■ Gregory, □ Puseas, ■ Wylie.

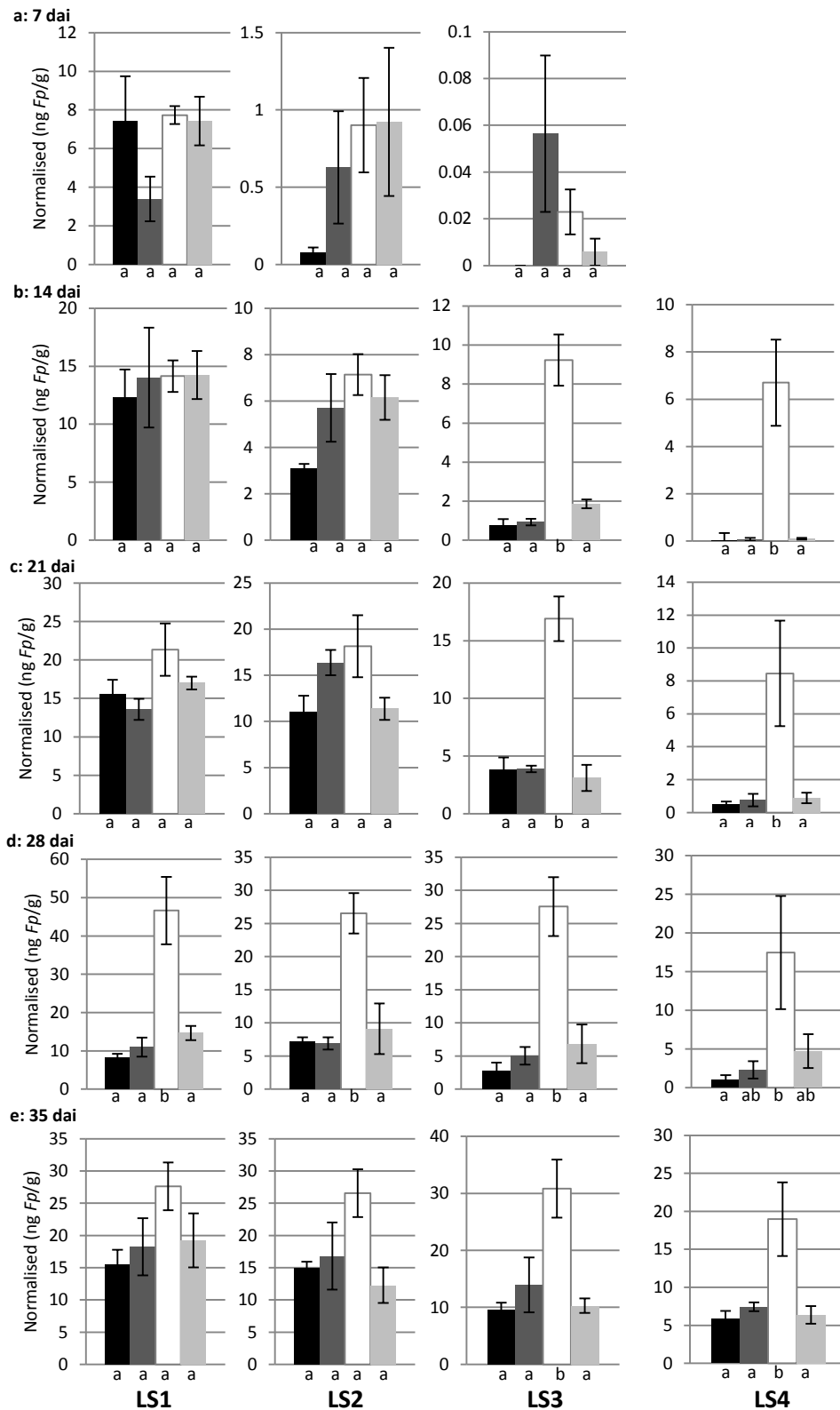


Figure 2.5. Normalised *Fp* DNA per weight values of LS1, LS2, LS3 and LS4 at (a) 7 dai, (b) 14 dai, (c) 21 dai, (d) 28 dai and (e) 35 dai. Columns represent the standard error of the mean of four replicates. Different letters indicate significant differences ($p < 0.05$) within each LS. ■ 2-49, ■ Gregory, □ Puseas, ■ Wylie.

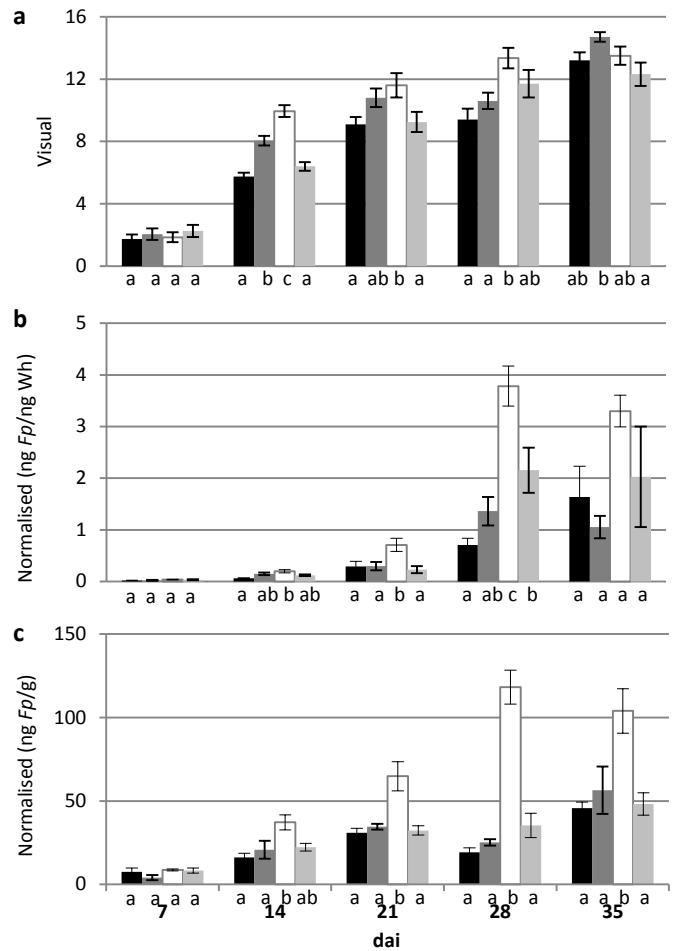


Figure 2.6. Combined LS1, LS2, LS3 and LS4 values from 7 to 35 dai using (a), visual ratings of crown rot symptoms, (b), *Fp* per wheat DNA and (c), *Fp* DNA per weight. Columns represent the standard error of the mean of four replicates. Different letters indicate significant differences ($p < 0.05$) within each time point. ■ 2-49, ■ Gregory, □ Puseas, ■ Wylie.

Table 2.5. Coefficients of determination (R^2) and associated gradients of the log of normalised *Fp* per wheat DNA values of combined LS1, 2, 3 and 4 over 7-28 dai.

7-28 dai	R^2	Gradient
2-49	0.98	0.066
Gregory	0.94	0.092
Puseas	0.99	0.094
Wylie	0.94	0.083

Table 2.6. Coefficients of determination (R^2) and associated gradients of the log of normalised *Fp* DNA per weight values of combined LS1, 2, 3 and 4 over 7-35 dai.

7-35 dai	R^2	Gradient
2-49	0.76	0.165
Gregory	0.75	0.237
Puseas	0.83	0.266
Wylie	0.87	0.172

2.3.2.1 qPCR normalisation using host DNA

During assessment the two methods for normalisation of qPCR results were compared. Both methods were strongly correlated at 7 to 28 dai (**Error! Reference source not found.**) and reported similar results when comparing partially resistant and susceptible genotypes, however, with increasing time periods after inoculation the *Fp* per wheat DNA method became less sensitive at distinguishing partially resistant tissues from susceptible tissues compared to the *Fp* DNA per weight method. The reliance of the *Fp* per wheat DNA method on host DNA quantities was investigated by plotting the quantities of host DNA in control and inoculated wheat tissues from 7 to 35 dai.

A comparison between the wheat DNA present in control and infected LS2 tissues demonstrated that the PCR target wheat DNA decreased over time as tissues began to senesce. The rate of degradation was not greater in infected tissues (Figure 2.7). A visual assessment of DNA quality was performed using gel electrophoresis (data not shown) and no differences in quality, indicated by laddering on the gel, were observed between infected and uninfected tissues.

Table 2.7. Correlation coefficients (r) for LS1, LS2, LS3 and LS4 separately and combined comparing visual ratings of crown rot symptoms, *Fp* per wheat DNA and *Fp* DNA per weight values from 7 to 35 dai.

dai	Tissue	Visual / per DNA	Visual / per weight	per DNA / per weight
		Pearson's r	Pearson's r	Pearson's r
7	LS1	0.68**	0.38	0.67**
	LS2	0.79**	0.74**	0.92**
	LS3	0.39	0.36	0.95**
	Combined	0.76**	0.53*	0.77**
14	LS1	0.41	0.03	0.41
	LS2	0.84**	0.71**	0.75**
	LS3	0.85**	0.86**	0.96**
	LS4	0.95**	0.91**	0.99**
	Combined	0.89**	0.78**	0.85**
21	LS1	0.39	-0.11	-0.13
	LS2	0.51*	0.37	0.68**
	LS3	0.55*	0.26	0.67**
	LS4	0.68**	0.18	0.2
	Combined	0.65**	0.58*	0.81**
28	LS1	0.31	0.12	0.59*
	LS2	0.45	0.44	0.60*
	LS3	0.73**	0.80**	0.88**
	LS4	0.77**	0.81**	0.98**
	Combined	0.76**	0.64**	0.91**
35	LS1	-0.01	0.18	0.3
	LS2	0.18	0.33	0.31
	LS3	0.1	0.14	0.31
	LS4	0.35	0.2	0.66**
	Combined	0.29	0.25	0.5

**Correlation is significant at the 0.01 level (two-tailed).

*Correlation is significant at the 0.05 level (two-tailed).

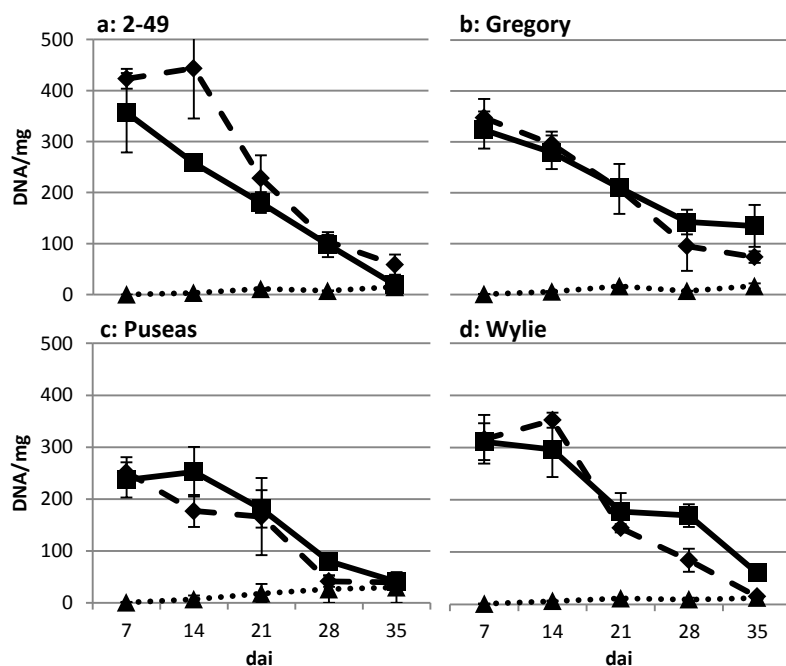


Figure 2.7. Change in quantities of wheat DNA in control LS2 tissues and of both wheat and *Fp* DNA in infected LS2 tissues of (a) 2-49, (b) Gregory, (c) Puseas and (d) Wylie from 7 to 35 dai. Bars represent the standard error of the mean of four replicates. — Control LS wheat DNA, - - · Infected LS wheat DNA, ······ Infected LS *Fp* DNA.

2.3.2.2 Correlation of visual and qPCR data

The infection levels described using qPCR were most strongly correlated to visual ratings at 14 dai, with the *Fp* per wheat DNA method having a slightly stronger correlation than the *Fp* DNA per weight method (Figure 2.8). The strongest combined coefficient of determination was no greater than 0.8. Correlations between qPCR and visual ratings became weaker over time (**Error! Reference source not found.**). This was most obvious in LS1. The strong correlations for LS4 at 14 dai were due to very low infection values, particularly values of zero, at this time. By 35 dai the correlations were very weak. The individual LS correlations between the two qPCR methods and visual ratings were generally similar. Correlations were frequently strongest in younger tissues undergoing initial disease development, with correlations becoming weaker as the period under disease increased.

There were no indications of varietal differences in the relationship between visual discolouration and qPCR values. A consistent trend of increasing visual ratings and qPCR values was observed from 7 to 35 dai (Figure 2.9).

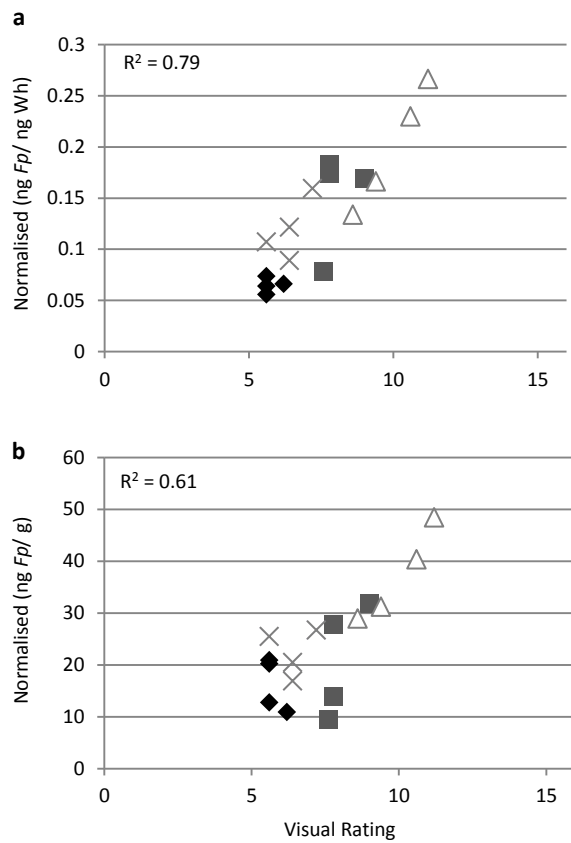


Figure 2.8. Relationship between combined LS1, LS2, LS3 and LS4 visual ratings of crown rot symptoms and (a), *Fp* per wheat DNA or (b), *Fp* DNA per weight values at 14 dai of four wheat genotypes. ♦ 2-49, ■ Gregory, △ Puseas, × Wylie.

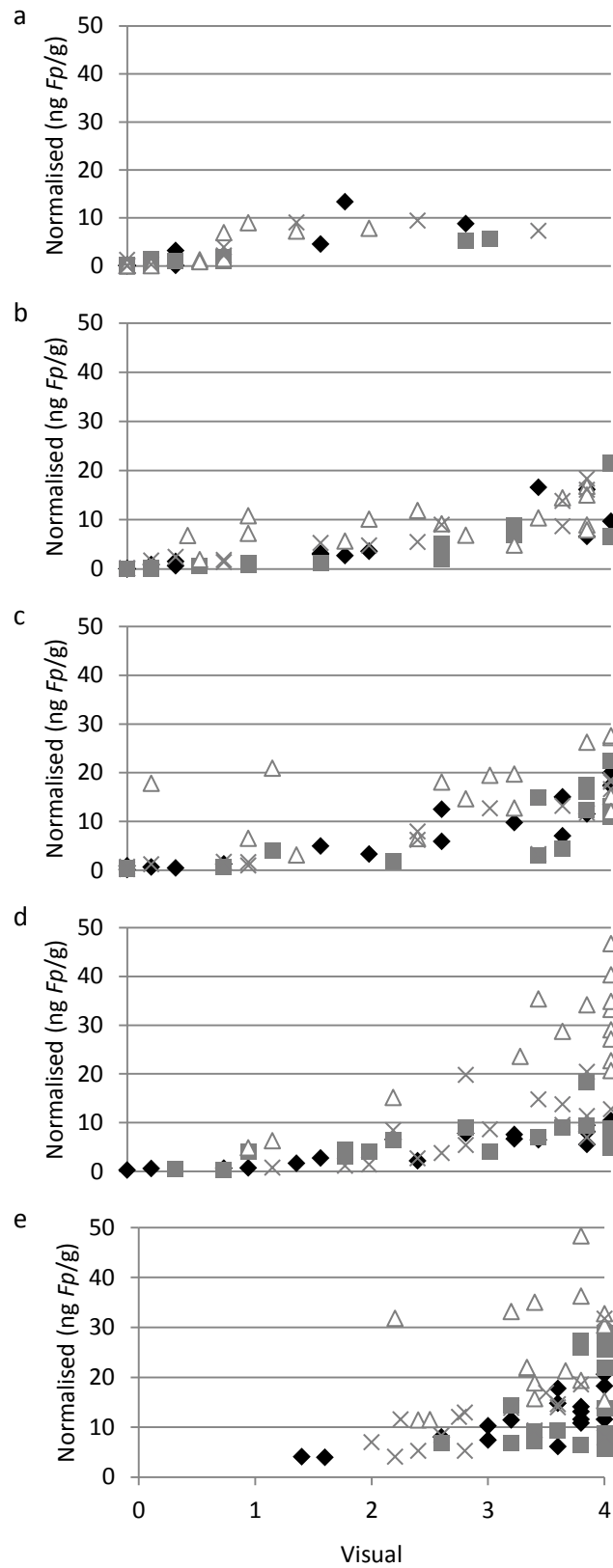


Figure 2.9. Individual LS1, LS2, LS3 and LS4 qPCR and visual scores of crown rot symptoms at (a) 7, (b) 14, (c) 21, (d) 28 and (e) 35 dai. ◆ 2-49, ■ Gregory, △ Puseas, × Wylie.

2.3.3 Comparison of control and infected LS weights

Comparison of dry weights of control and infected LSs revealed that infected LSs were heavier than their control counterparts in all genotypes (Figure 2.10). In some cases this was a significant difference (Table 2.8). Significant increases in weight were most frequent in LS1 and LS2. LS5 in Puseas was the only tissue which recorded a weight significantly less than the control, possibly due to stunting or delayed development in response to disease challenge. The increase in weight did not appear to greatly increase from 7 to 35 dai. The difference in weight was not due to an increase in LS length during infection (Appendix 2D). Estimated weight of *F. pseudograminearum* hyphae in infected tissue was modestly to strongly correlated with the LS weight increase, however, the estimated weight of hyphae was much less than the actual increase in weight of the tissue (Figure 2.11).

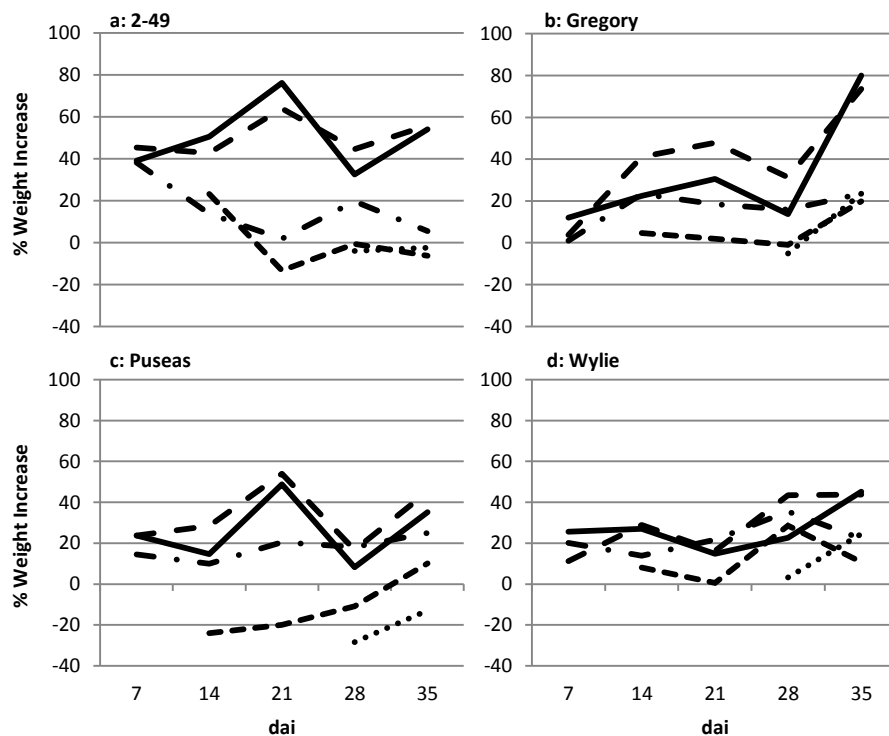


Figure 2.10. Weight difference of infected LS1, 2, 3, 4 and 5 from control LSs of (a) 2-49, (b) Gregory, (c) Puseas and (d) Wylie from 7 to 35 dai. The weight of control tissues is represented by zero on the vertical axis. — LS1, — — LS2, - · - · LS3, - - - LS4, ····· LS5.

Table 2.8. Difference in milligrams of *Fp* infected LS tissues from control LS tissues at 7 to 35 dai for (a) 2-49, (b) Gregory, (c) Puseas and (d) Wylie. Letters indicate significant differences ($p < 0.05$). a = no significant difference, b = significantly higher and c = significantly lower.

a: 2-49	7 dai	14 dai	21 dai	28 dai	35 dai
LS1	3.9b	5.4b	8.9a	3.8a	7.3b
LS2	4.5b	5.4b	10.5b	6.5a	10.2a
LS3	0.8a	2.8a	0.6a	4.4a	1.9a
LS4	-	2.0a	-6.5a	-0.2a	-4.0a
LS5	-	-	-	-1.3a	-2.0a

b: Gregory	7 dai	14 dai	21 dai	28 dai	35 dai
LS1	1.6b	3.1b	4.0b	1.5a	8.1b
LS2	0.8a	7.9b	8.6b	4.9a	12.1b
LS3	0.2a	5.3b	5.4a	3.5a	6.3a
LS4	-	1.3a	0.9a	-0.4a	9.4a
LS5	-	-	-	-2.5a	14.3a

c: Puseas	7 dai	14 dai	21 dai	28 dai	35 dai
LS1	4.3a	2.7a	7.2b	1.7a	6.7a
LS2	7.3b	7.8a	12.2a	5.4a	12.2a
LS3	3.4a	3.7a	8.0a	6.5a	10.1a
LS4	-	-12.1a	-13.1a	-5.7a	6.9a
LS5	-	-	-	-18.7c	-10.8a

d: Wylie	7 dai	14 dai	21 dai	28 dai	35 dai
LS1	2.4a	2.7b	1.6a	2.2a	4.1a
LS2	1.5b	4.3a	2.9a	6.7b	6.4a
LS3	2.1a	2.3a	5.1a	6.4b	4.7a
LS4	-	1.6a	0.2a	8.4a	3.7a
LS5	-	-	-	1.6a	11.0a

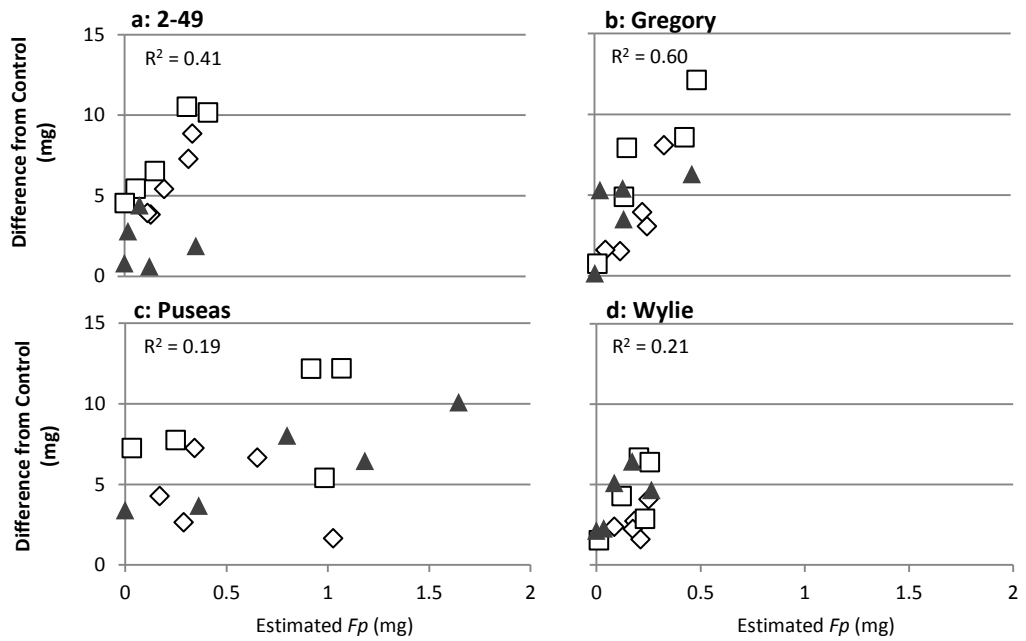


Figure 2.11. Linear relationships of the weight difference of *Fp* infected LS1, 2 and 3 from control LSs and estimated weight of *Fp* tissues in (a) 2-49, (b) Gregory, (c) Puseas and (d) Wylie at 7 to 35 dai. R^2 values are Pearson's coefficients of determination. \square LS1, \blacktriangle LS2, \diamond LS3. *Fp* weights were estimated from a standard curve comparing DNA yields from a range of weights of pure *Fp* mycelium (Appendix 2C).

2.3.4 Seedling Sectioning

Sections of LSs and tissues of sub-crown internodes (SCI), primary roots and secondary roots were compared for visual discolouration and fungal DNA content in 2-49 and Puseas at 14 and 28 dai. Visual discolouration was present in all tissue types for both 2-49 and Puseas at 14 dai (Figure 2.12). qPCR confirmed the presence of *F. pseudograminearum* in these tissues. Significant differences between these two genotypes were few and inconsistent (data not shown), however it appeared that Puseas generally showed higher infection levels than 2-49. Colonisation increased from 14 to 28 dai (Figure 2.13). SCI and root colonisation did not differ between the two genotypes (Figure 2.12 and Figure 2.14). The SCI contained moderate quantities of *F. pseudograminearum*, while the primary roots were very lightly infected. Infection of the LSs was greatest towards the lower (proximal) end of the sheath and minimal towards the top (distal) end of the LS. Discolouration of the LSs was progressively less in the younger LSs. Leaf blade colonisation was generally restricted to the very base of the blade. This was highlighted by qPCR.

At 14 dai LS1 contained similar levels of *F. pseudograminearum* infection between the two genotypes, while growth of *F. pseudograminearum* was more extensive in Puseas in LS2 and LS3. The lack of consistent differences, compared to those reported in the Time Course study, may reflect both experimental variation due to smaller and more numerous samples and differences due to collecting specifically targeted tissue sections.

Infection at 28 dai revealed similar trends to those recorded at 14 dai. Colonisation levels of secondary roots were similar to those in primary roots. The upper LS and the leaf blade all contributed very little to the total values.

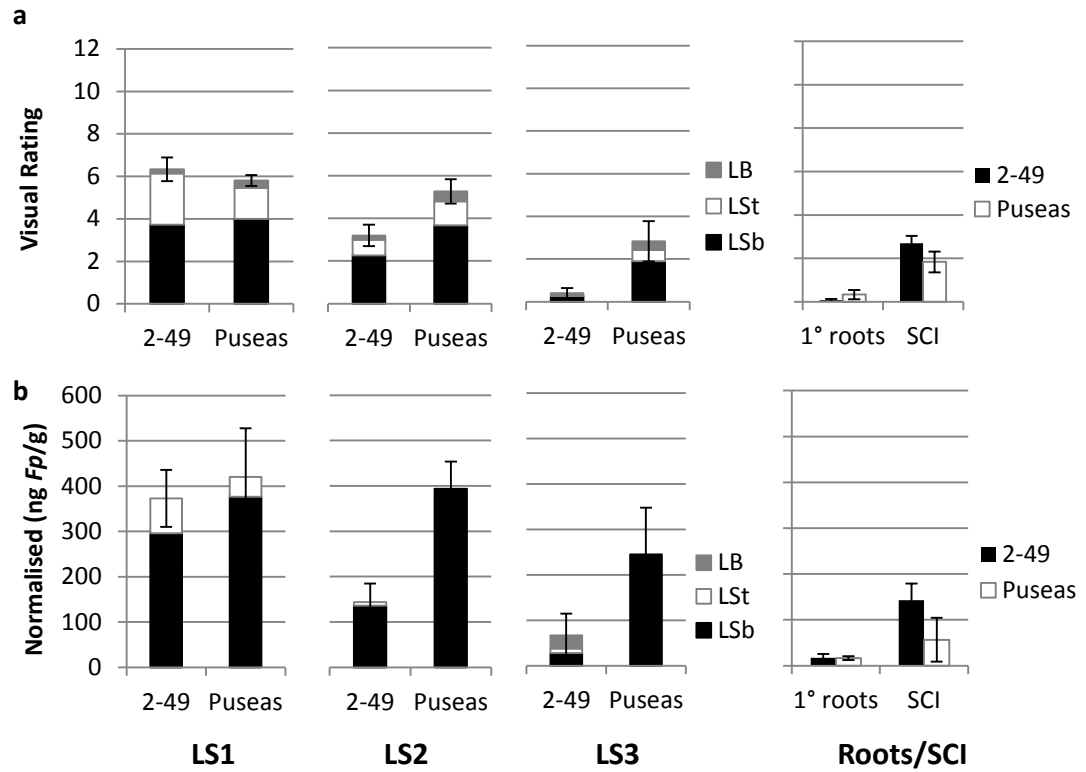


Figure 2.12. (a) Visual ratings of crown rot symptoms and (b) *Fp* DNA per weight values of LSb, LSt, LB, SCI and 1° root tissues of 2-49 and Puseas seedlings at 14 dai. Columns represent the standard error of the mean of six replicates.

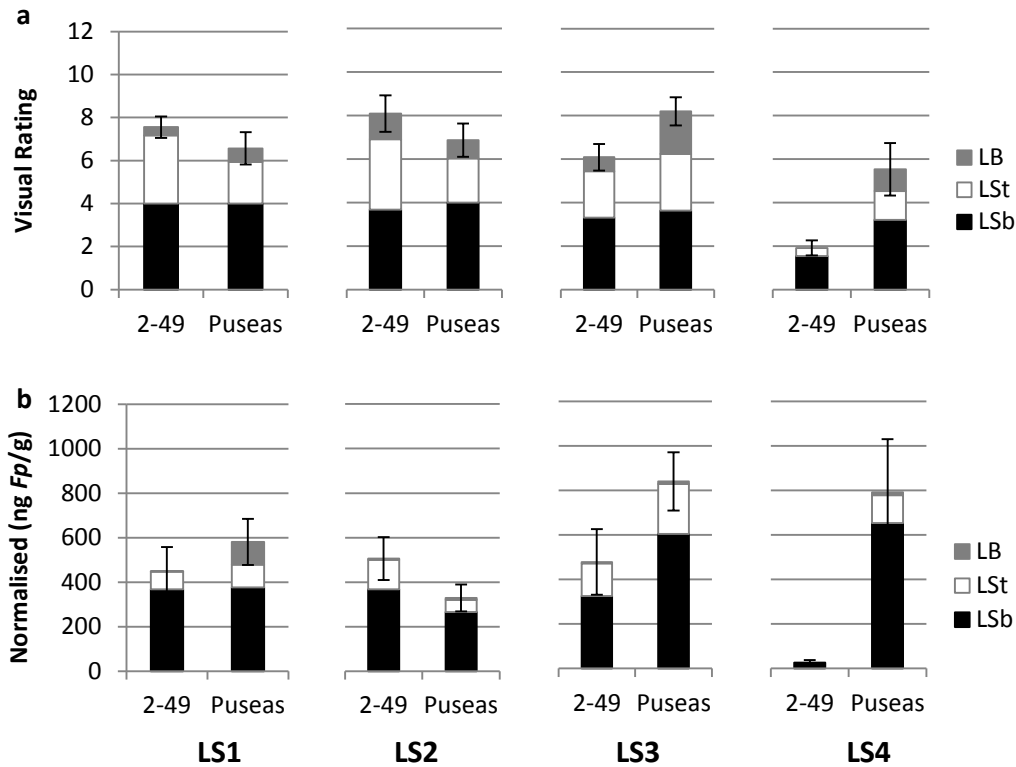


Figure 2.13. (a) Visual ratings of crown rot symptoms and (b) *Fp* DNA per weight values of LSb, LSt and LB tissues of 2-49 and Puseas seedlings at 28 dai. Columns represent the standard error of the mean of six replicates.

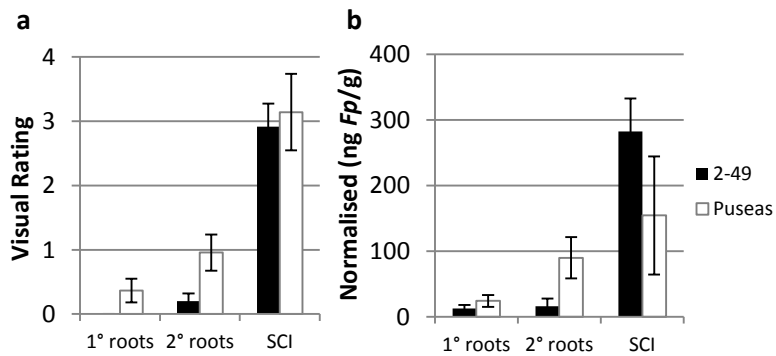


Figure 2.14. (a) Visual ratings of crown rot symptoms and (b) *Fp* DNA per weight values of SCI, 1° root and 2° root tissues of 2-49 and Puseas seedlings at 28 dai. Columns represent the standard error of the mean of six replicates.

2.4 Discussion

Accurate quantification of a pathogen in diseased host tissue is an important aspect of defining the degree of host susceptibility and assessing other characteristics involved during colonisation, such as the extent of disease symptom expression. Compared to traditional quantitative methodologies, which rely on culturing the pathogen from infected tissues, real time qPCR is a more accurate and rapid method, able to quantify pathogens in colonised tissues at very early to late stages of infection. The ability to compare traditional disease rating methods with qPCR measurements provides important information on the relationship between symptom expression and the extent of fungal colonisation in different genotypes.

Visual rating of discolouration due to crown rot is the most common method used to describe resistance (Purss, 1966, Wildermuth and McNamara, 1994, Malligan, 2008). Examination of the relationship between visual discolouration and quantity of fungus has had limited examination. Malligan (2008) reported that the correlation between visual ratings and re-isolations of the pathogen from infected tissues was highly significant. However, this methodology is only semi-quantitative and may be insensitive to both low and very high fungal load. In contrast, the use of qPCR in the current study resulted in accurate quantitation of the amount of fungal DNA in the infected tissue.

The strongest correlation between visual rating and qPCR data occurred at 14 dai; this greatly decreased at later time points, however visual ratings and qPCR values were always positively correlated. This demonstrates that the visual rating method was able to report fungal colonisation in a similar manner to qPCR, however, the timing of visual rating was important as ratings at 14 dai were most indicative of colonisation. No instances were observed where tissues displayed no discolouration but had detectable quantities of fungal DNA, indicating that there is no tolerance to presence of the fungus.

Periods earlier than 7 dai did not reveal differences in resistance and significant differences did not occur until 14 dai. This suggests that resistance mechanisms did not immediately affect growth of *F. pseudograminearum*. From 14 dai onwards differences between genotypes were most obvious during infection of younger LSs, which frequently indicated significant differences between partially resistant and susceptible genotypes. Differences in resistance may have been due to a

combination of resistance mechanisms, such as resistance to spread within and between tissues. It is interesting to note that Wylie and Gregory, considered to be moderately resistant and moderately susceptible respectively, were not significantly different from 2-49 at any time point, demonstrating the continuing difficulty in accurately differentiating moderate resistances and susceptibilities in seedling tissues. A likely contributing factor to reported differences in resistance is the variation in adult resistance, rather than seedling resistance, between these genotypes.

Each of the three rating methods (visual rating; *F. pseudograminearum* DNA content relative to host DNA; and *F. pseudograminearum* DNA content relative to the dry weight of tissue) was able to determine significant differences between partially resistant and susceptible genotypes, however the period most effective for describing differences between partially resistant and susceptible genotypes varied between rating methods. In contrast to visual rating, qPCR differentiated the degree of colonisation between 2-49 and Puseas from 14 to 35 dai. The reason for the difference between rating methods at later time points is that the visual rating method used an ordinal scale (with ratings reaching maximum values at later time points) compared to the continuous scale of the qPCR method. The continuous scale used in qPCR enabled a range of time points after infection to be accurately assessed. This indicates that even after maximum symptoms are expressed the fungus still increases its concentration in the tissues.

The normalised *Fp* DNA per weight method proved to be the most sensitive approach for reporting differences in fungal DNA content between genotypes. This method reported on only one variable, *F. pseudograminearum* DNA, and used dry weights as a known constant between samples. This was more reliable than host DNA, which varied between tissues and with age of plant. While the *Fp* per wheat DNA method produced significant differences between the partially resistant 2-49 and Puseas, the variation in wheat DNA between wheat plants, and particularly between LSs, inhibited its sensitivity for determining differences in resistance. The importance of retaining the wheat primer–probe system was to allow wheat DNA to serve as an internal positive control in each reaction, eliminating the potential for false negatives.

It was interesting that the rate of degradation of the target wheat DNA was not different between the infected and control LS2 tissues. It has been demonstrated

that response to infection may lead to cleavage of nuclear DNA into oligonucleosomal fragments during certain plant-pathogen interactions (Ryerson and Heath, 1996, Hietala *et al.*, 2003), however this was not observed during *F. pseudograminearum* infection of LSs. The target DNA in the current study was only 120 bp, yet it obviously became degraded in both susceptible and partially resistant tissues under control and inoculated conditions. This suggests that the decrease in host target DNA is due to natural senescence.

In contrast to Stephens *et al.* (2008), the current study did not detect the different phases of infection observed for *F. graminearum* infections. Instead a general exponential increase in *F. pseudograminearum* DNA was observed from 1 to 28 dai. A plateau phase was similarly reported by both studies at 35 dai, where it appears fungal increase can no longer be supported in the heavily infected tissues. Malligan (2008) similarly reported that the number of isolations from LSs at later harvest times was often lower than earlier harvests. The exponential phase was present in partially resistant and susceptible genotypes, however, the rate of increase was less in the partially resistant genotype than in the susceptible genotype, indicating a slower rate of colonisation. This is supported by infection data for individual LSs, with 2-49 having less infection in younger tissues than Puseas. This effect has frequently been reported (Purss, 1966, Malligan, 2008).

In further contrast to Stephens *et al.* (2008), who stated that crown rot symptom development occurs slowly, usually taking 4 to 8 weeks to become visible, the current study observed discolouration of LS tissue under inoculated coleoptiles from 3 dai. Readily observable discolouration of at least three LSs was present at 7 dai, with significant differences indicating resistance at 14 dai. Stephens *et al.* (2008) suggests that the delay in visible symptoms observed in their study may be partly explained by the delayed production of DON, a mycotoxin which induces cell death in wheat (Desmond *et al.*, 2008). As both studies used a similar droplet inoculation procedure, the contrast is more likely due to the differing pathogenicities of *F. pseudograminearum* and *F. graminearum*, the latter of which is isolated only infrequently from wheat tissues expressing symptoms of crown rot (Backhouse *et al.*, 2004).

Characterising and monitoring the spread of *F. pseudograminearum* hyphae during seedling infection has clarified which tissues are the important targets during crown rot infection. All seedling tissues could be infected by 14 dai after inoculation

of the coleoptile, indicating that the hyphae are able to spread down the coleoptile to the primary roots, as well as up the LS to the base of the leaf blade (LB). qPCR indicated that the lowest 2 cm of a LS was the area of greatest hyphal proliferation. Using fungal isolation procedures, Malligan (2008) reported a similar result. Colonisation of this area likely plays an important role in infection of culm bases. The top 2 cm of a LS was the next most infected area, most obviously at 28 dai, followed by the SCI. Infection of the primary roots, secondary roots and base of the leaf blade was, by comparison, very limited. Liddell (1985) reported that *F. pseudograminearum* caused severe discolouration of the SCI, the LSs and the culm bases. However, there was no effect on the primary roots or secondary roots. Liddell (1985) also reported that infection (indicated by discolouration) of the LS typically extended only to the very base of the LB, and this has been confirmed by the qPCR results in the current study. Small, isolated, distinct lesions on the LB were occasionally observed on distal regions of the blade, suggesting that they represent infection sites occasionally initiated while the LB was still confined within the newly-infected leaf sheath of the preceding leaf. Following this initial lesion formation the leaf blade emerges rapidly from the subtending sheath and assumes its photosynthetic functions, resulting in a small isolated lesion on the exposed LB. The fact that these lesions fail to develop further, suggests that fully photosynthetic leaf mesophyll is not suitable host tissue for pathogen infection.

The increase in the dry weights of infected LS tissues was an unexpected observation. In contrast, Miedaner (1988) provided evidence that infection of wheat seedlings by *F. culmorum* caused significant reduction of root and shoot dry weights. The increase in dry weight was ubiquitous in infected LS1, 2 and 3. Potential effects of disease such as causing an increase in LS length or the weight of *F. pseudograminearum* hyphae being the cause of the increased weight were excluded. While a modest correlation was observed between amount of *F. pseudograminearum* present and weight increase, the magnitude of the weight difference was much greater than that of potential hyphal mass. Furthermore, the weight difference did not continue to increase at later harvest times, even though hyphae continued to proliferate. Significant differences in weight were more common in 2-49 and Gregory, however, this phenomenon was also observed in Wylie and Puseas, suggesting it may not be a form of resistance but rather a non-specific reaction to infection. The reaction was rapid as significant differences were recorded at 7 dai.

The mechanism and physiology behind this reaction remains unknown. Biochemical tests for substances potentially related to resistance, such as lignin (Vance *et al.*, 1980), cellulose (Dickson *et al.*, 1923) and silicon (Fauteux *et al.*, 2005) are required.

Chapter 3 : Adult Infection

3.1 Introduction

Rating of crown rot disease in seedling tissues has become popular due to its rapid nature and the ability to grow large quantities of seedlings in controlled growth environments (Wildermuth and McNamara, 1994, Mitter *et al.*, 2006, Li *et al.*, 2008). While these assays have been reported to correlate with ratings performed on adult plants in the field, they cannot replace field grown trials. Assessment of crown rot of adult tissues in field trials has varied over time, with the original methods measuring percent deadheads or diseased culms (McKnight and Hart, 1966, Purss, 1966) being replaced by systems recording actual amounts of visual discolouration (Wildermuth and McNamara, 1994, Wallwork *et al.*, 2004).

While visual discolouration is used as a measurement of resistance, this relationship has been poorly described. Malligan (2008) performed the first experiments relating visual symptoms to isolation counts of *F. pseudograminearum* from infected tissue. At the time these field studies were performed (2000-2001) appropriate quantitative PCR (qPCR) methods were not available. Correlations of visual disease rating and isolation counts were strong at approximately 16 weeks after planting ($r \approx 0.7$) in several field trials. Symptoms of crown rot disease were observed in all genotypes with severity of symptoms and re-isolation of *F. pseudograminearum* from infected tissue increasing over time. Genotypic differences were observed in both visual discolouration and in the extent of fungal colonisation, with the development of discolouration on internodes being delayed in partially resistant genotypes. It is interesting that while assessment of crown rot in field trials is usually conducted on mature plants, the weakest correlation between disease rating and isolation data was seen at maturity ($r \approx 0.4$). While genotypic differences were still detected by Malligan (2008) in certain tissues at maturity, the most consistent differences were recorded approximately 16 weeks after planting. She stated that the period between flowering and seed formation was the most appropriate time to test for genotypic differences in crown rot susceptibility.

A less laborious and more accurate method than manual isolation counts of infected tissues, such as qPCR, may enhance the assessment of crown rot resistance. Hogg *et al.* (2007) evaluated field grown spring and durum wheat inoculated with *F.*

pseudograminearum using primers and probes specific for a segment of the trichodiene synthase gene. This amplified DNA of *F. graminearum*, *F. culmorum* and *F. pseudograminearum*. Two weeks prior to harvest, plants were collected and visually assessed for crown rot severity and analysed by qPCR for *Fusarium* DNA quantities. Visual disease and *Fusarium* DNA quantities were positively correlated with each other for all three genotypes assessed in 2004 ($R^2 \approx 0.6$) however, a positive correlation only occurred for the durum wheat in 2005. Hogg *et al.* (2007) further analysed relationships between crown rot infection and grain yield, reporting that yields for two spring wheat genotypes were negatively correlated with *Fusarium* DNA quantities in 2004. Both visual and qPCR measurements were comparable in predicting yield reduction. This was the first published report which indicates that qPCR is effective in measuring crown rot severity in wheat.

It is important to note that variation in the extent of infection between experiments, predominantly due to environmental conditions, greatly altered correlations between visual ratings, fungal biomass and yield. The effect of differing temperatures and moisture levels between field trials and years was highlighted by both Hogg *et al.* (2007) and Malligan (2008) as a major source of variation in infection.

The current experiment was designed to highlight the relationship between visual discolouration and level of fungal colonisation, determined by qPCR, due to crown rot disease in cereal culms. A selection of cereal genotypes of differing resistances was assessed to determine the ability of qPCR to differentiate between resistant and susceptible tissues. A comparison between two times of plant collection, anthesis and maturity, was also performed to confirm when differences between host genotypes were greatest.

3.2 Methods

Field trials were conducted during 2009. One trial was conducted at the Leslie Research Centre (LRC) Experimental Farm at Wellcamp, 9kms west of Toowoomba. The other, a plus and minus inoculum experiment, was performed in field plots at the LRC site in Toowoomba.

3.2.1 Cereal Genotypes

Three genotypes of bread wheat, one durum wheat and one barley were chosen for the adult study based on a range of crown rot resistances (Table 3.1).

Table 3.1. Genotypes monitored during adult plant assessments and their crown rot field rating.

Genotype	APR ¹	Species
2-49 ^{ab}	MR-R	<i>Triticum aestivum</i> (bread wheat)
EGA Wylie ^b	MR	<i>Triticum aestivum</i> (bread wheat)
Grimmett ^a	MS	<i>Hordeum vulgare</i> (barley)
Puseas ^{ab}	S	<i>Triticum aestivum</i> (bread wheat)
EGA Bellaroi ^a	VS	<i>Triticum turgidum durum</i> (durum wheat)

¹Adult Plant Rating = Resistance Rating: VS - Very Susceptible, S - Susceptible, MS-S - Moderately Susceptible-Susceptible, MS - Moderately Susceptible, MR – MS - Moderately Resistant-Moderately Susceptible, MR - Moderately Resistant, MR – R - Moderately Resistant- Resistant, R - Resistant, VR - Very Resistant. Field-based crown rot rankings according to McRae *et al.* (2010) and personal communication from Dr. Damian Herde (DEEDI).

^aGenotypes assessed in the Wellcamp field trial.

^bGenotypes assessed in the LRC field trial.

3.2.2 Inoculum Production

Methods of inoculum production can be found in detail in Appendix 3A. Briefly, mycelium of *F. pseudograminearum* was added to a flask containing saturated, autoclaved millet seed and incubated at 23°C for 11 days. After this initial incubation the colonised grain was placed on a tray in a growth cabinet in the dark at 25°C. After 4 days clumps in grain were broken up with gloved hands and each tray was shaken every second day thereafter for seventeen days. Inoculum was stored in plastic bags in a cold room until required.

3.2.3 Inoculation and Tissue Collection

3.2.3.1 Wellcamp

The Wellcamp field block had been maintained on a three year rotation where year 1 was fallow, year 2 was inoculated durum, which was ploughed into the soil, and year 3 was the experimental site. The Wellcamp trial was tractor planted using a cassette system for seed. The inoculum was delivered to each furrow at planting via a fertiliser applicator. A field plan for Wellcamp detailing the layout of the genotypes is in Appendix 3B. Genotypes were planted as paired 3 m single row plots with 5 g of seed planted per plot. Each paired plot was replicated. Inoculum was delivered at a rate of 2.5 g/m in a band lying above the seed. Inoculum added at planting contained the isolates A03#24, A05#49 and A05#54, provided from the Leslie Research Centre collection. Due to a long history of crown rot in this field it was assumed that numerous other isolates were present.

A selection of the available genotypes underwent examination (Table 3.1). Plants were collected at 10, 16 and 22 weeks after planting (WAP). At 10 WAP leaf sheaths, coleoptiles, SCIs and IN1 tissues were combined into two groups of 5. The 16 and 22 WAP time points approximately coincided with anthesis and maturity, respectively. Typically, five plants from each replicate were collected at each time point. Visual rating and qPCR analysis was performed on the individual IN1, IN2 and IN3 tissues of the main culm of four of these plants at 16 and 22 WAP. The remaining plants and culms were kept for microscopy (Chapter 4).

3.2.3.2 Leslie Research Centre

Three metre paired plots, being either plus or minus inoculum, of 2-49, Puseas and Wylie were hand planted in soil assumed to be free of natural *F. pseudograminearum* inoculum (soil cores not tested). The planting plan is in Appendix 3B. Each inoculated row had inoculum applied above the seed at 2.5 g/m, with a total of 7.5 g of inoculum applied to each plot. Inoculum was produced from the single isolate A03#24.

Five plants of each treatment were collected at 10, 16 and 22 WAP. IN1, IN2 and IN3 of the primary culm of each plant underwent visual and qPCR analysis. Additional plants were collected for the microscopic analysis described in Chapter 4.

3.2.4 Visual Rating

At harvest (10, 16 and 22 WAP) collected culms were rated based on the percent of brown discolouration of each internode (IN). LS, SCI, coleoptile, and crown tissues were also collected and rated at 10 WAP. The method for rating discolouration was described by Wildermuth and McNamara (1994). Briefly, tissues were rated for disease on a 0 to 4 scale. 0 = no visible discolouration, 1 = less than 25% discolouration, 2 = 25 to 50% discolouration, 3 = 51 to 75% discolouration and 4 = greater than 75% discolouration. Separated INs (sectioned from the top of the lower node to the top of the higher node) were placed into microfuge tubes.

3.2.5 DNA Preparation

Lyophilised tissue samples with dry weights of more than 0.02 g were sub-sampled into a new tube containing from 0.015 to 0.02 g of material. A Wizard Genomic DNA Extraction kit (Promega) was used to extract DNA following the plant DNA extraction protocol (Appendix 2C). DNA was eluted in 200 μ L of DNA Rehydration Solution.

3.2.6 Multiplex Real Time Quantitative PCR Conditions

This was as described in Chapter 2, Section 2.2.10.

3.2.7 Statistical Analyses

Comparisons between arcsine square root transformed visual or qPCR values of individual genotypes within time points were performed using a one-way ANOVA with the Levene Statistic from the Test of Homogeneity of Variance and the multiple comparison Tukey HSD test in SPSS 17.0. Comparisons between time points were performed using an independent samples t-test in SPSS 17.0. For comparison tests $\alpha = 0.05$. Pearson's Correlation Coefficients (two-tailed) were calculated in SPSS 17.0. The strength of each correlation was reported using the system described by Fowler *et al.* (1998).

3.3 Results

qPCR results are reported using only the normalised by extracted weight (ng *Fp* / g) method. This is firstly due to the consistency of the *Fp* DNA per weight method in Chapter 2, Section 2.3.2. The other consideration is that the genomic DNA content of hexaploid bread wheat, tetraploid durum wheat and diploid barley differ on a per cell basis. The wheat primer/probe reaction was still included as an internal positive control for the bread and durum wheat samples.

3.3.1 Wellcamp

3.3.1.1 10 WAP

At 10 WAP visual ratings of LS, SCI, coleoptile, crown and IN1 tissues of 2-49, Grimmatt, Puseas and Bellaroi did not reveal consistent differences between genotypes (data not shown). qPCR data of these same tissues revealed a similar result (data not shown). A general trend suggestive of 2-49 having lower values than the other genotypes was observed.

3.3.1.2 16 WAP

Visual rating values at 16 WAP (approximately anthesis) revealed significant differences between the genotypes (Figure 3.1a). 2-49 was the least discoloured in all INs. IN1 of 2-49 was significantly less discoloured than IN1 of Puseas and Bellaroi. IN1 of Grimmatt was not significantly different from any of the other genotypes. Discolouration of IN1 in Puseas and Bellaroi had reached the maximum value by 16 WAP. Discolouration of IN2 indicated that 2-49 was significantly less discoloured than Puseas and Bellaroi. IN3 showed no discoloration in 2-49. As a general assessment IN1 was similarly affected in Puseas and Bellaroi, however the extent of symptoms in IN2 and IN3 was greater in Bellaroi than in Puseas. Grimmatt was less discoloured than Puseas and Bellaroi but more than 2-49. Spread of discolouration had risen beyond IN3 for some culms, particularly Bellaroi, and discolouration was associated with presence of fungal DNA. Due to lack of symptoms on similar tissues of the other genotypes this data was not used for comparison.

qPCR revealed differences between genotypes similar to the visual data (Figure 3.1b). Colonisation of IN1 on 2-49 was significantly less than Puseas and Bellaroi, while colonisation of IN2 on 2-49 was only significantly less than Bellaroi. In general, 2-49 showed the least colonisation in all INs, followed by Grimmatt. While IN1 of both Puseas and Bellaroi had similar levels of colonisation, IN2 of these genotypes revealed Puseas to have much less colonisation than Bellaroi, actually being at a level closer to Grimmatt. IN3 values revealed much greater mean colonisation for both Puseas and Bellaroi than 2-49 and Grimmatt. High levels of variation occurred within genotypes.

Combined values of IN1, 2 and 3 at 16 WAP were the best indicator of differences in discolouration and colonisation between partially resistant and susceptible genotypes (Figure 3.2a, b).

3.3.1.3 22 WAP

Visual ratings of IN1 at 22 WAP (maturity) were significantly less for 2-49 compared to the other three genotypes (Figure 3.1c). At IN2 only 2-49 and Bellaroi were significantly different. Differences between the other three genotypes were absent in both IN1 and IN2. IN3 revealed no differences between any genotypes.

qPCR of IN1 demonstrated that colonisation of this tissue was similar for each genotype (Figure 3.1d). No significant differences between genotypes were reported for IN2 and 3. This is predominantly due to the large degree of variation within genotypes. In general, however, 2-49 had the least colonisation of IN2. Colonisation of IN2 in the other three genotypes was similar. Colonisation of IN3 was highly variable; however Bellaroi did have a greater mean value.

Combined values of IN1, 2 and 3 at 22 WAP were not a strong indicator of differences in discolouration and colonisation between partially resistant, moderately susceptible and susceptible genotypes (Figure 3.2c, d).

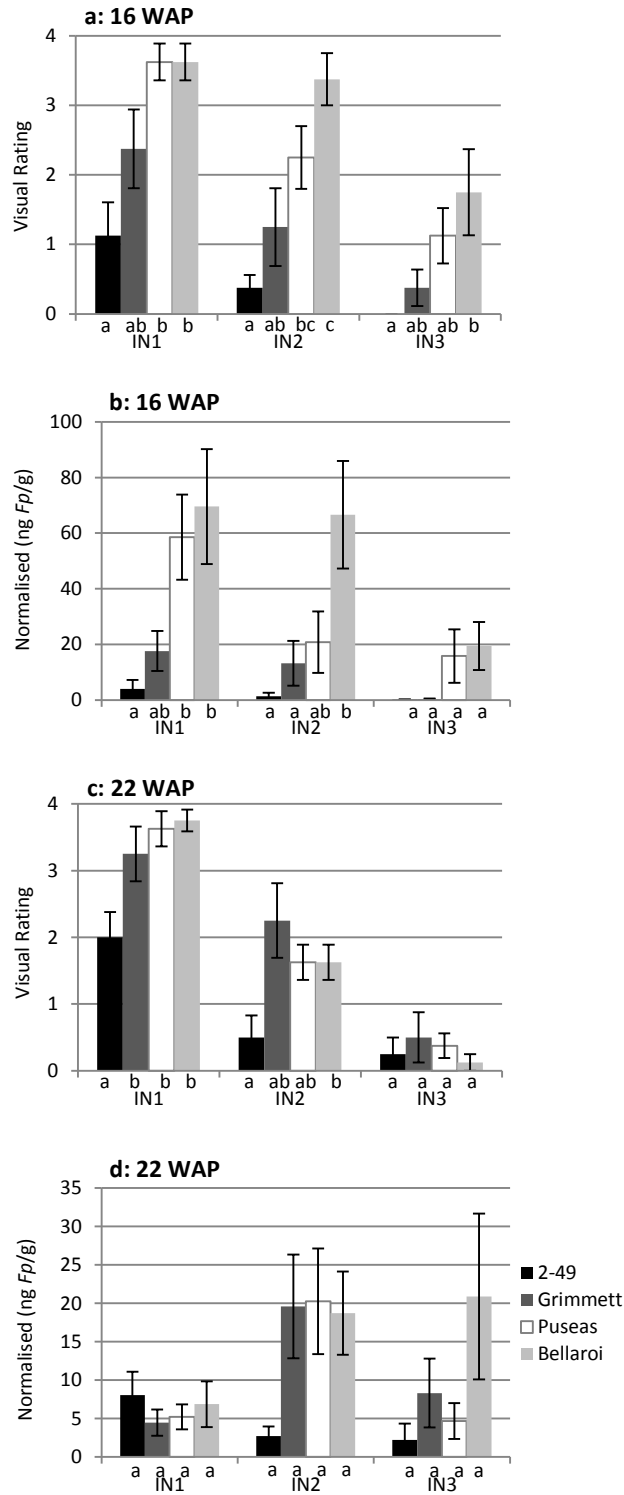


Figure 3.1. Visual ratings of crown rot symptoms (a and c) and qPCR values (b and d), of IN1, IN2 and IN3 of four cereal genotypes at 16 WAP (a and b) and 22 WAP (c and d). Columns represent the standard error of the mean of eight replicates. Different letters indicate significant differences ($p < 0.05$).

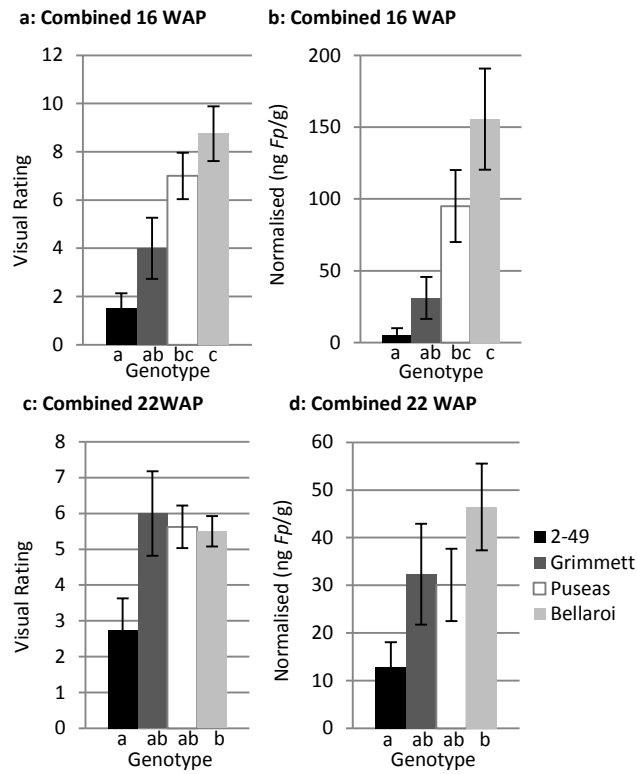


Figure 3.2. Combined visual ratings of crown rot symptoms and qPCR values, respectively, of IN1, 2 and 3 of four cereal genotypes 16 WAP (a and b) and 22 WAP (c and d). Columns represent the standard error of the mean of eight replicates. Different letters indicate significant differences ($p < 0.05$).

3.3.1.4 Comparison between 16 and 22 WAP

Combined visual rating values demonstrated that visual discolouration of 2-49 and Grimmnett slightly, but not significantly, increased from 16 to 22 WAP (Figure 3.3). In contrast, the visual rating values of Puseas slightly, but not significantly, decreased while visual ratings of Bellaroi significantly decreased. The greatest areas of discolouration were related to time exposed to infection, with IN1 being the most affected, followed by IN2 and IN3. The decrease in visual discolouration observed in Puseas and Bellaroi was due to differences in IN2 and IN3. Overall, differences in infection between genotypes were most obvious before maturity, at 16 WAP (Figure 3.2).

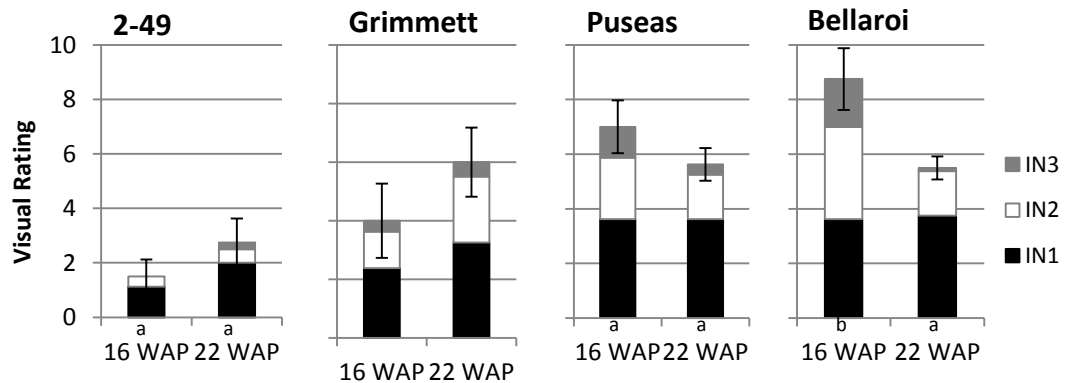


Figure 3.3. Combined visual ratings of crown rot symptoms of IN1, 2 and 3 of four cereal genotypes at 16 and 22 WAP. Columns represent the standard error of the mean of combined IN values of eight replicates. Different letters indicate significant differences ($p < 0.05$).

Combined qPCR values revealed similar overall trends to the visual data (Figure 3.4). Colonisation of 2-49 and Grimmnett did not alter between 16 and 22 WAP, however both Puseas and Bellaroi showed a significant decrease in fungal DNA content. The decrease in Puseas was primarily due to a decrease in fungal content in IN1. The decrease in Bellaroi was due to a decrease in fungal content in both IN1 and IN2.

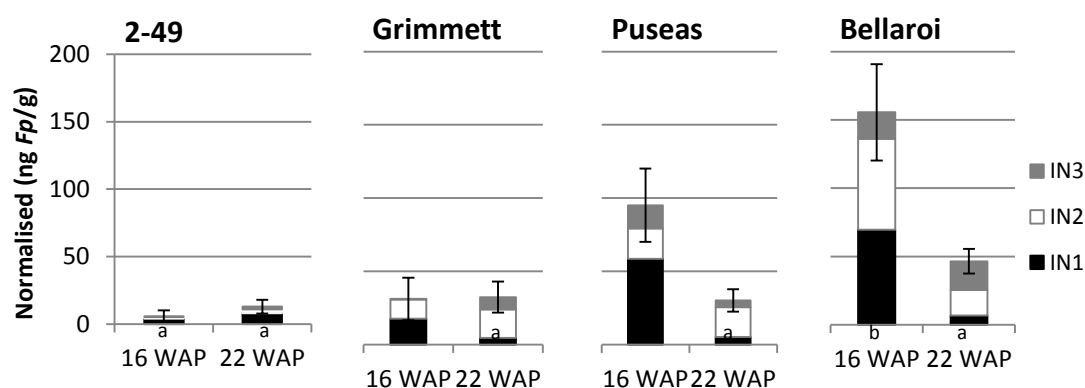


Figure 3.4. Combined qPCR values of IN1, 2 and 3 of four cereal genotypes at 16 and 22 WAP. Columns represent the standard error of the mean of combined IN values of eight replicates. Different letters indicate significant differences ($p < 0.05$).

3.3.1.5 Visual versus Normalised qPCR Values

At 10 WAP infection of IN1 was limited and thus was not included in this analysis. Comparisons between visual and normalised qPCR values were performed on 16 and 22 WAP tissues (Figure 3.5). Separate INs at 16 WAP had modest to strong correlation coefficients but they were each less than the strong combined IN correlation where visual discolouration explained at least 74% of the qPCR data (Table 3.2). Separate INs at 22 WAP had very weak to weak correlation coefficients and they were each less than the modest combined IN correlation where visual discolouration explained 34% of the qPCR data.

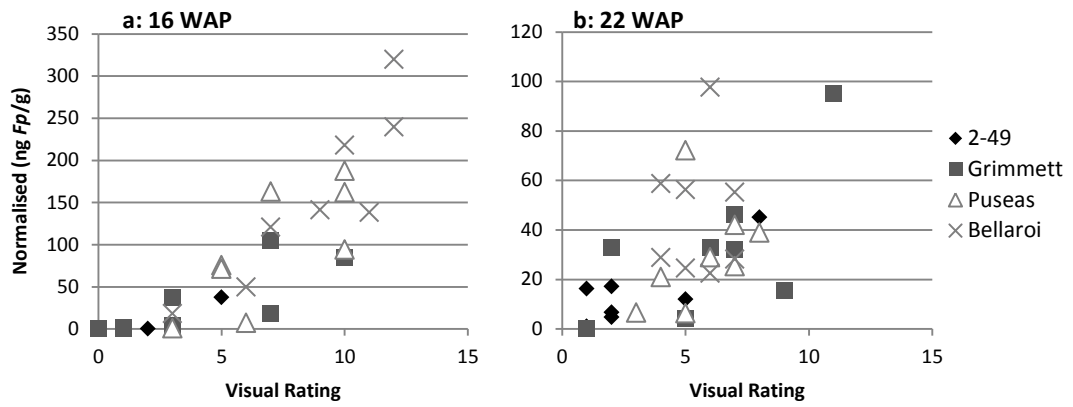


Figure 3.5. Linear correlation of crown rot symptoms of visual ratings and qPCR values for combined totals of INs 1, 2 and 3 of four cereal genotypes at (a) 16 WAP and (b) 22 WAP.

Table 3.2. Correlation coefficients (r) for visual discolouration due to crown rot symptoms and qPCR values of individual and combined INs at 16 and 22 WAP.

	16 WAP	22 WAP
Tissue	Pearson's r	Pearson's r
IN1	0.68**	0.2
IN2	0.67**	0.42*
IN3	0.61**	0.2
Combined	0.86**	0.58**

**Correlation is significant at the 0.01 level (two-tailed).

*Correlation is significant at the 0.05 level (two-tailed).

3.3.2 LRC

Infection of 2-49, Wylie and Puseas at the LRC trial was considerably less than that at the Wellcamp trial due to it relying solely on artificial crown rot inoculum. Infection progressed slowly and at 10 WAP differences between genotypes were not observed (data not shown). By 16 WAP significant differences in the visual discolouration were present between 2-49 and Puseas in IN1 and 2 (Figure 3.6a), however, qPCR data did not reveal significant differences (Figure 3.6b). The mean qPCR values of Puseas were much greater than 2-49 or Wylie.

The correlation coefficient between visual and qPCR data was very strong at 16 WAP, with visual discolouration explaining 84% of the qPCR data (Table 3.3). Due to low disease levels and time constraints tissues of plants collected at 22 WAP were not assessed. Control plants were not infected by *F. pseudograminearum*.

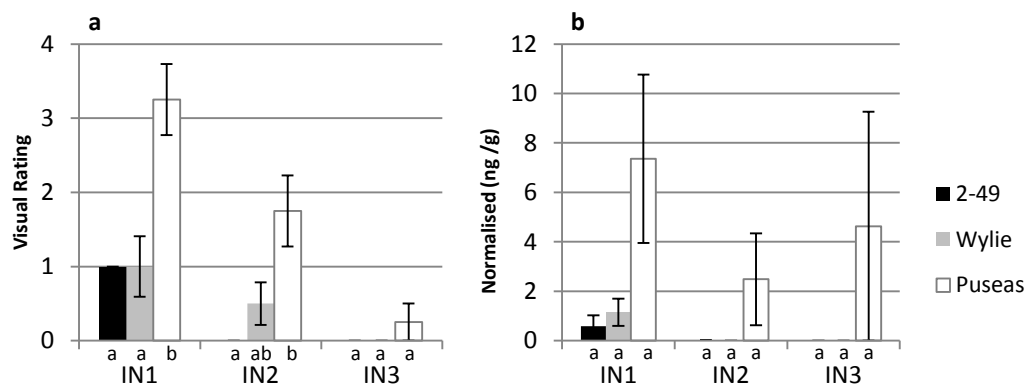


Figure 3.6. (a), Visual ratings of crown rot symptoms and (b), qPCR values of IN1, 2 and 3 at of three cereal genotypes at 16 WAP. Columns represent the standard error of the mean of eight replicates. Different letters indicate significant differences ($p < 0.05$).

Table 3.3. Correlation coefficient (r) for visual discolouration due to crown rot symptoms and qPCR values of combined INs at 16 WAP.

	Pearson's r
Combined	0.92**

**Correlation is significant at the 0.01 level (two-tailed).

3.4 Discussion

The current study is the first detailed assessment of crown rot of adult cereal plants in Australia using qPCR specific for *F. pseudograminearum*. Differences between partially resistant and susceptible genotypes were observed using both visual discolouration and qPCR data. The correlation between these two characters was strong, particularly at anthesis.

Assessment of leaf sheaths, coleoptiles, SCIs and IN1 at 10 WAP did not reveal useful differences between the genotypes assessed. The similarity in infection levels was too great to allow significant differences to be recorded. This is similar to results reported by Wildermuth and McNamara (1994) at 42 dai, Malligan (2008) in seedling tissues at 10 WAP and in seedling tissues at 35 dai (Chapter 2, Section 2.3.2).

The variation in infection within genotypes was most likely due to variation in the time/region of initial infection and the quantity of inoculum encountered in the field. A large difference in infection intensity was observed due to the effect of supplementing natural soil inoculum with artificial inoculum compared to providing artificial inoculum to non-infested soil. This was most obvious for the susceptible Puseas, whereas the partially resistant 2-49 did not show a large difference in infection between the two methods. The Wellcamp trial, utilising natural and artificial inoculum, resulted in greater infection which effectively revealed greater differences in resistance than the LRC trial.

In agreement with Malligan (2008), plants collected at 16 WAP were the most useful for recording differences in resistance, with tissues at this stage demonstrating a strong correlation between visual and qPCR ratings. Purss (1966) reported that the greatest rise in *F. pseudograminearum* isolations was during 67 and 100 days, the 100 days being 15 WAP, similarly indicating that this is a useful stage for assessing infection.

Adult plant resistance to crown rot has most commonly been assessed in plants at maturity (Dodman and Wildermuth, 1987, Wallwork *et al.*, 2004, Malligan, 2008). However, plants collected at 22 WAP did not allow differences in resistance to be distinguished in the same manner as plants at 16 WAP, which was further evidenced by a weak to modest correlation between visual and qPCR ratings at 22

WAP, similar to that reported by Malligan (2008) for visual symptoms and isolation data.

Similar to the current study, Hogg *et al.* (2007) reported visual discolouration and *Fusarium* DNA quantities were positively correlated with each other for three wheat genotypes in a 2004 trial but for only a durum wheat genotype in 2005. As discussed in Chapter 2, the most likely reason for the lack of a very strong relationship is that the visual rating method used an ordinal scale compared to the continuous scale of the qPCR data. Visual rating of IN1 and 2 frequently had maximum visual scores while the qPCR data still demonstrated a range of colonisation levels in these tissues. The qPCR rating method has much greater power to describe colonisation of tissues than the visual rating method and does not suffer from differences in visual scoring between operators. Furthermore, the strong correlation between visual discolouration and qPCR data indicates that no cereal genotype was able to symptomlessly tolerate the presence of *F. pseudograminearum*. Tolerance may be present within some cereal genotypes however it is most likely combined with resistance. The distinction between these two mechanisms in terms of crown rot is still unclear.

Combined values for IN1, IN2 and IN3 gave the best indication of resistance to crown rot. Hogg *et al.* (2007) did not find that *Fusarium* DNA quantities obtained from one culm location were superior to another at predicting visual symptoms or yield losses. Malligan (2008) similarly reported that infection of the whole culm, particularly IN1, 2 and 3, was more useful than individual IN assessment. This is most likely due to variation in extent of infection between genotypes, which does not appear to be affected by INs or nodes, but is a reflection of the spread and proliferation of the fungus within a whole culm.

The proliferation and spread of the fungus within a culm was altered at maturity. qPCR values at 22 WAP indicated, most obviously in the susceptible genotypes, that IN1 colonisation was low, even less than IN2. Purss (1966) reported a similar result in culm tissue where fewer isolations were made from IN1 compared with IN2 in mature wheat plants. It was suggested that due to the advanced stage of disease, the badly decayed lower INs did not offer good material for isolation. Another suggestion was that infection could originate in IN2 via penetration through leaf sheath tissues. Malligan (2008) similarly reported that the number of isolations made from leaf sheaths at later harvest times was often lower than earlier harvests.

The qPCR method was not limited by badly decayed tissues, however similar results were observed. The large drop in levels of infection in Puseas and Bellaroi from 16 to 22 WAP suggests that prolific growth of *F. pseudograminearum* is supported by live tissues. The more resistant 2-49 and Grimmett did not have a large change in *F. pseudograminearum* content from 16 to 22 WAP, demonstrating that resistance limits infection during the anthesis stage. It is possible that the decline of nutrients and water within culm tissue during maturation may result in a reduction of *F. pseudograminearum* hyphal mass.

qPCR proved an effective and accurate method for describing colonisation of tissues by *F. pseudograminearum* during crown rot infection. Various methods of assessing infected plants using qPCR are possible, such as assessing individual INs, taking sections of multiple culms for analysis (Hogg *et al.*, 2007) or comparing similar lengths of culm bases (pers. comm. Margaret Evans, SARDI, SA). Furthermore, the difficulty of correlating crown rot disease with yield may in part be overcome by utilising a method similar to that of Hogg *et al.* (2007), where a representative sample of tissues is collected before maturity and assessed using qPCR, followed by a yield assessment at maturity and subsequent correlation between these two factors.

The disadvantages of qPCR are that it is more time consuming than simply visually rating culm discolouration and it has the associated cost of the equipment and chemicals required to perform routine tests. This must be taken into account against the increased accuracy of describing *F. pseudograminearum* colonisation of infected tissues. The author believes that a combination of visual and qPCR ratings will most effectively yield results leading to the identification of new resistant materials.

Chapter 4 : Histopathological Assessment of Infected Seedling and Adult Tissues

4.1 Introduction

Histopathological examination of plant tissues during infection provides essential information relevant to understanding pathogenesis and mechanisms of resistance. Paul Taylor, during his Master's studies (1983) performed the only prior histopathological examination of crown rot caused by *F. pseudograminearum*, detailing infection and colonisation of the coleoptile, SCI, scutellum and culm tissues from seedling stages (7, 14 and 56 dai) through to maturity. This MSc thesis provides the first description of *F. pseudograminearum* using appressoria to penetrate cell walls, either over the vertical union of cell walls or directly through the epidermis. Unfortunately, none of this work was subsequently published in the literature.

A further assessment of fungal colonisation during crown rot disease in partially resistant and susceptible genotypes is important in order to determine mechanisms of resistance and differences in pathogenesis between genotypes of differing resistance. Furthermore, the development of visual symptoms of crown rot has been studied in detail (McKnight and Hart, 1966, Purss, 1966, Malligan, 2008), however, the physical attributes of this characteristic have not been well described.

This study also addresses the recommendation by Taylor (1983) that further studies are required to determine if the location of the inoculum can modify the site and nature of infection and subsequent colonisation. Methods involving inoculum encountering coleoptile tissue below ground and above ground have been compared.

In order to build on the study of Taylor a selection of wheat of differing crown rot resistance underwent examination. As reported in Chapter 2 and 3 the partially resistant 2-49 frequently had a lower *F. pseudograminearum* biomass in infected tissues than the susceptible Puseas. Differences in colonisation of leaf sheath and culm tissues between these genotypes at early to late stages of infection were targeted during microscopic examination. Furthermore, the first examinations of barley and durum wheat genotypes were performed.

An obvious symptom of crown rot in the field is whitehead formation (Butler, 1961). A popular theory for formation of these whiteheads is that water flow

through xylem vessels is blocked by hyphae. The first microscopic examination of the whitehead phenomenon was performed, comparing the colonisation of whiteheads with that of greenheads from a single plant. This also included extensive observations of colonisation of culm vascular bundles, not only of whiteheads but of each genotype at 10, 16 and 22 weeks after planting.

Of particular interest is resistance to penetration by hyphae, differences in patterns of colonisation in different cell types between genotypes and/or species and comparing the extent of colonisation vertically in the culm.

Many staining techniques have been reported for observing fungi in plant tissues (Johansen, 1940, Meyberg, 1988, Saha *et al.*, 1988), however, studies using fluorescence microscopy to observe *F. pseudograminearum* growth during crown rot of wheat have not been reported. A new procedure for fluorescent hyphal staining was designed to allow a distinct contrast between wheat cells and *Fusarium pseudograminearum* hyphae.

Epifluorescence, rather than bright field microscopy, was the method pursued due to the potential for optimised visualisation of fluorescent structures. In consideration of harnessing the ability to clearly observe fungal hyphae and produce a strong contrast between host and hyphae, several dyes and methods were assessed.

4.2 Methods

4.2.1 Conidial Germination

Examinations of conidial germination and infection structure formation on glass slides were performed similarly to Apoga and Jansson (2001) (*Bipolaris sorokiniana*) and Li *et al.* (2005) (*Erysiphe pulchra*). A brief examination of the initial germination of *F. pseudograminearum* conidia on a glass surface was performed. This involved placing 100 μL of a conidial suspension (10^4 conidia/mL) of isolate A03#24 onto a glass slide and observing the germination and growth after 3 to 72 hours. Slides were placed in a Parafilm® sealed Petri dish and incubated at 25°C. Before observation using light microscopy, MilliQ water and a coverslip were placed over the germinating conidia. Each slide was only observed at a single time point.

4.2.2 Plant Materials

A range of cereals including bread wheat (2-49, Puseas, Wylie, Gregory, Vasco and Sunland), durum wheat (Bellaroi), barley (Lindwall and Grimmett) and oats (Riverina Racehorse Oats) underwent examination.

4.2.3 Plant Growth and Tissue Preparation

4.2.3.1 Greenhouse Plants

4.2.3.1.1 Leaf Sheath Tissues

Seedlings were grown and inoculated as described in Chapter 2, Section 2.2. Briefly, 14 day old seedlings were inoculated with a droplet of inoculum and maintained in an environmentally controlled greenhouse. Some experiments were coupled to those performed for PCR analysis while others, consisting of ten plants of the genotypes 2-49, Puseas, Wylie and Gregory, were performed separately. Seedlings of oats and barley (Lindwall) also underwent a brief examination. LS tissue was the main focus for microscopic examination; coleoptiles were initially assessed. Tissues were harvested from 24 hours to 35 days after inoculation.

4.2.3.1.2 Culm Tissues

Infected adult wheat plants were produced in the greenhouse by planting seeds into 5 litre pots (five seeds per pot). Six pots of 2-49 and Puseas were planted. Fourteen day old seedlings were inoculated using the modified droplet method described in Chapter 2, Section 2.2.4. Plants were harvested at anthesis (approximately 16 weeks after planting (WAP)) and tissues were microscopically examined.

4.2.3.2 Field Plants

Genotypes of bread wheat (2-49, Puseas, Sunland and Vasco), durum wheat (Bellaroi) and barley (Grimmett) were collected from the field trials grown at Wellcamp and the LRC. These trials are described in Chapter 3, Section 3.2. The plants were collected 10, 16 and 22 WAP. The 16 and 22 WAP time points approximately coincided with anthesis and maturity, respectively. Sunland and Vasco were only opportunistically collected at 16 WAP due to a great number of

whiteheads being available in neighbouring plots, which allowed a close examination of this phenomenon. Plants were stored at -70°C before processing for microscopy.

4.2.3.3 Sectioning

Transverse sections were produced by hand-sectioning using a microtome blade (Feather, Japan). Fragile tissues such as heavily infected culms or LSs were hand-sectioned while between two pieces of Parafilm®, as described by Frohlich (1984). On average a total of 6 sections were observed from each tissue segment sectioned. During observations of LS surfaces the tissues were left whole.

4.2.4 Clearing and Fixation

During method optimisation it was determined that culm sections did not require clearing and fixing in order to produce adequate staining, in contrast to LSs. This significantly reduced the preparation time for culm sections. Tissues were cleared and fixed as described by Hückelhoven and Kogel (1998) and Schäfer *et al.* (2004). Briefly, the LSs were placed in a clearance solution (0.15% trichloroacetic acid [wt/vol] in ethylalcohol: chloroform [4:1; vol/vol]) for 48 hours, with the solution being changed once during this time. The samples were then washed 2×15 min with 50% ethanol, 2×15 min with 50 mM NaOH and 3×10 min with MilliQ H₂O, subsequently followed by 30 min of incubation in 0.1 M Tris/HCl (pH 8.5). Samples were either immediately stained or stored in 50% (v/v) glycerol.

4.2.5 Staining and Microscopic Observation

4.2.5.1 Development of a Fluorescent Staining Technique

A range of epifluorescence-based staining procedures was trialled. Initially, fluorescent dyes were assessed for their ability to distinctively stain hyphae of *F. pseudograminearum* in infected wheat tissues. These dyes included Uvitex 2B (Polysciences, Inc.) (Moldenhauer *et al.*, 2008), 3,3'-dihexyloxycarbocyanine iodide (Invitrogen) (Duckett and Read, 1991), pontamine fast scarlet 4B (Kemira Pigments) (Hoch *et al.*, 2005) and solophenyl flavine 7GFE (Ciba Specialty Chemicals) (Hoch *et al.*, 2005). The non-fluorescent dyes aniline blue, toluidine blue and safranin were

investigated for their ability to specifically stain plant tissue and at the same time quench autofluorescence. Each non-fluorescent dye was tested in combination with each fluorescent dye to evaluate the degree of staining contrast between host and pathogen.

Initial experiments involved staining tissues for 5 min with one of each of the four fluorescent dyes. High purity water (MilliQ system, Millipore) was used to make each dye solution and for each rinsing step, unless otherwise stated. The stain solutions were Uvitex 2B (0.1% w/v), 3,3'-dihexyloxycarbocyanine iodide (50 µg/mL in ethanol), pontamine fast scarlet 4B (0.1% v/v) and solophenyl flavine 7GFE (0.1% w/v). After several rinses with water, tissues underwent microscopic assessment.

Further experiments involved initially staining tissues with the non-fluorescent dyes, either aniline blue (0.1% w/v), toluidine blue (0.05% w/v) or safranin (0.2 g safranin, 100 mL 10% v/v ethanol) for 5 min. Tissues were then passed through several changes of water and stained with one of the four fluorescent dyes for 5 min. After several rinses with water, tissues underwent microscopic assessment.

While some combinations of stains gave satisfactory results, the best results, giving a strong contrast between plant and fungal cells, were produced by staining tissues with safranin followed by staining in solophenyl flavine 7GFE. This resulted in hyphae fluorescing when exposed to ultraviolet light. For details of the procedure see below.

4.2.5.2 Differential Staining of Hyphae and Plant Tissue

Tissue samples were stained for 5 min in safranin O solution (0.2 g safranin O alcoholic (Mochrome, Edward Gurr Ltd, London, England), 10 mL ethanol and 90 mL water) and then washed three times in water. The samples were then stained for 10 min in solophenyl flavine 7GFE (Ciba Specialty Chemicals, USA) (0.1% w/v with 0.1 M Tris/HCl [pH 8.5]) and finally washed 4 × 10 min with water. Samples were mounted in 50% (v/v) glycerol.

4.2.5.3 Lesion Microscopy

Tissues which displayed the initial formation of lesions were selected for microscopic examination using bright field and fluorescence microscopy. Tissues underwent clearing and fixation but were not stained until after bright field observations. These tissues were most frequently LSs.

4.2.5.4 Lignin, Suberin and Callose Stain

A slightly modified staining procedure for lignin, suberin and callose, described by Brundrett *et al.* (1988), was performed on inoculated and uninoculated adult plant sections from the LRC field trial. Briefly, sections were initially stained in 0.1% (w/v) berberine hemi-sulphate (Sigma-Aldrich, Sydney, Australia) for 1 hour. The sections were then rinsed by passing through several changes of water, before staining in 0.5% (w/v) aniline blue WS (Gurr Microscopy Materials, BDH Chemicals Ltd, Poole, England) for 30 minutes. Sections were again rinsed in water and then mounted on slides in 50% (v/v) glycerol. Sections were observed immediately, obviating the need for Fe Cl₃ treatment (Brundrett *et al.*, 1988).

4.2.5.5 Microscopic Observation

Tissues were observed using a Nikon Eclipse E600 fluorescence microscope. Unstained tissues were observed using both bright field microscopy and fluorescence filter B-2A (excitation filter, 450-490 nm; dichroic mirror, 500 nm; barrier filter, 515 nm). Stained tissues were viewed under fluorescence filter UV-2A (excitation filter, 330–380 nm; dichroic mirror, 400 nm; barrier filter, 420 nm). Images were captured using a MicroPublishing 5.0 RTV digital camera (QImaging, Canada) and analySIS software (Soft Imaging System).

4.2.5.6 Statistical Methods

Comparisons of hyphal widths between individual genotypes were performed using a one-way ANOVA and the multiple comparisons Tukey HSD test in SPSS 17.0. Tests used $\alpha = 0.05$.

4.3 Results

4.3.1 Legend for Images

Images are labelled according to the genotype and section type (Table 4.1). No differences in cell structure or areas of colonisation were observed between the genotypes.

Furthermore, unless otherwise indicated, coleoptile and leaf sheath tissues were cleared, fixed and stained with safranin and solophenyl flavine 7GFE and viewed under fluorescence using filter UV-2A. Adult tissues underwent a similar procedure, omitting the clearing and fixation steps.

Table 4.1. Abbreviations used in Figure captions.

Description	Abbreviation
2-49	2-49
Bellaroi	B
Gregory	G
Grimmett	Gr
Lindwall	L
Puseas	P
Sunland	Sun
Vasco	V
Wylie	W
Surface View	SV
Transverse Section	TS
Longitudinal Section	LSn

4.3.2 Development of a Fluorescent Staining Technique

While each individual fluorescent dye stained the fungal hyphae, a strong distinction between host and fungal tissue was not achieved due to both autofluorescence and staining of host tissues (Figure 4.1a, b and c). When the fluorescent dyes were used in combination with either aniline blue or safranin, the most informative visual images, giving a strong contrast between plant and fungal structures, were produced using solophenyl flavine 7GFE and safranin (Figure 4.1d). This combination of stains has not previously been reported.

The solophenyl flavine 7GFE bound to the cell walls of the hyphae and allowed clear distinction of hyphal septa (Figure 4.1e) and a strong contrast with plant cell walls (Figure 4.1f). Transverse sections of wheat tissues allowed both intra- and inter-cellular hyphae to be visualised (Figure 4.1g, h). The safranin stain

sufficiently quenched plant cell autofluorescence yet still allowed sufficient red safranin staining to differentiate plant cell walls from the green/blue fluorescence of the fungal hyphae. Host cell wall fluorescence varied in relation to degree of infection and cell type. It was observed that younger plant tissues do not as readily take up the safranin stain, most likely because very little lignin had yet been deposited. The staining, however, was still adequate for viewing of hyphae. Bread wheat, durum wheat, barley and oat tissues produced similar results. Stained specimens retained significant fluorescence for a period of at least two months.

4.3.3 Initial Conidial Germination

Three hours after placing the conidial suspension onto a glass surface, tips of conidia were slightly swollen. After 6 hours obvious germ tube formation occurred from the tips of the conidia (Figure 4.2a, b), sometimes in a bipolar fashion, but germ tubes also occasionally originated from the middle of the conidia. In some cases germ tubes grew from each end of a conidium and from a middle point. After 22 hours hyphae had grown along the glass surface, typically as a single strand. After 72 hours branching of the hyphae was frequent, however, no infection structures were observed.

4.3.4 Initial penetration and growth in the coleoptile

Inoculum was initially placed on the coleoptile of the four bread wheat genotypes and as such this tissue was examined as the first potential site of hyphal growth and penetration. Properties of the coleoptile made staining and observation difficult. As the coleoptile had only two vascular bundles occurring near either edge of the tissue, this resulted in two raised ridges which made clear visualisation of the tissue in between difficult. In addition strong fluorescence, most commonly at the coleoptile tip and not associated with hyphae or disease, occurred sporadically. Germination of the conidial inoculum was not observed until 48 hours after inoculation, most likely because at earlier times the fixing and clearing procedures washed the conidia off the tissue surface. At 48 hours after inoculation small amounts of thin hyphae, originating from conidia, were growing on the surface of the coleoptile tissue. Surface hyphae frequently grew appressed to the host cell exterior. Direct penetration

of the epidermal cells was facilitated by slightly thickened hyphal tips, underneath which small, brown, halo-like lesions appeared (Figure 4.2c, d). Penetration events into the coleoptile were infrequently observed, however, penetration was most commonly observed to occur directly through epidermal cell walls and also over the union of vertical cell walls.

The high humidity environment created during the first 48 hours after inoculation may have encouraged growth of hyphae across the coleoptile surface, with some hyphae growing onto the surface of LS1. Following penetration of the coleoptile cuticle, hyphae were observed to grow in cells of the epidermis, cortical parenchyma and less frequently in cells of the vascular bundles. Associations with stomata were infrequent and trichomes were not present on the coleoptile. When hyphae grew through the epidermal and cortical parenchyma cells thickened hyphae were sometimes observed, producing appressorial-like swellings to facilitate cell wall crossings (Figure 4.2e). This feature of *F. pseudograminearum* growth was more frequently observed for LS tissue. At 10 days after inoculation conidia sporadically began to form on coleoptiles of Puseas, with hyphae erupting through the epidermal cells to form masses of conidia (Figure 4.2f). While coleoptiles of 2-49, Wylie and Gregory were also heavily infected with hyphae, the formation of conidial masses was not observed.

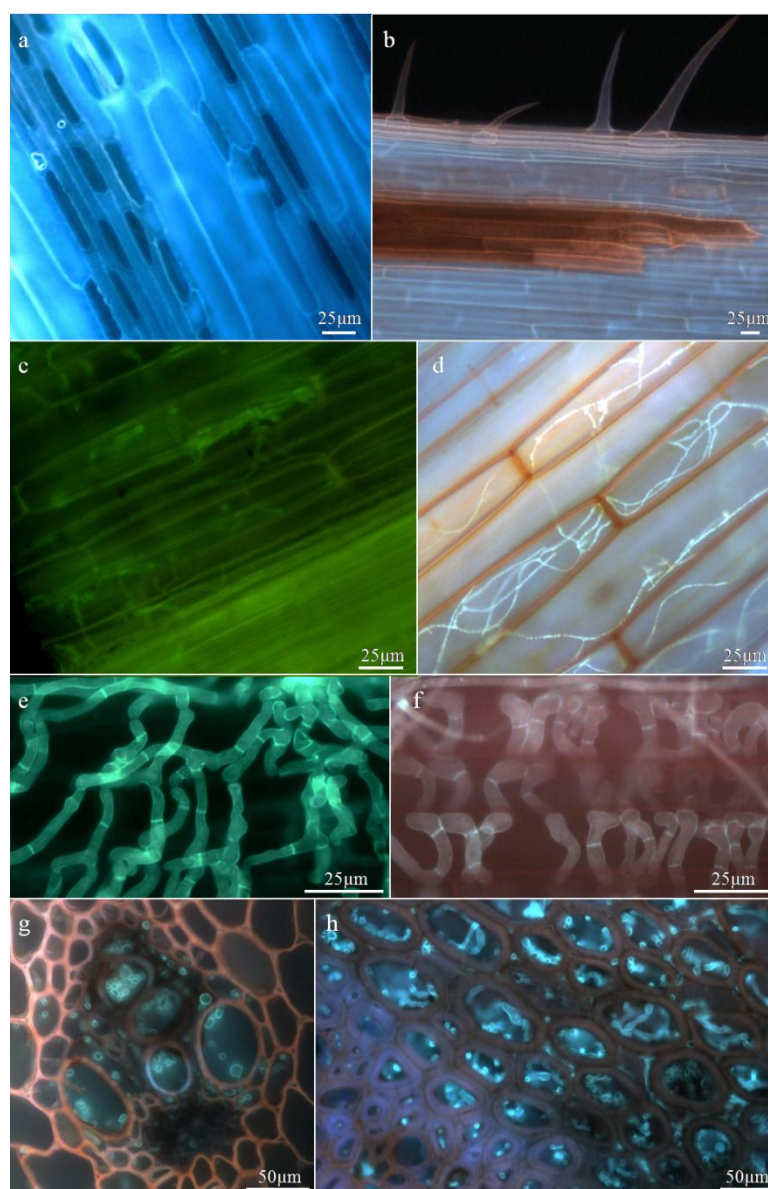


Figure 4.1. Effect of clearing, fixation and staining on 28 day old bread wheat leaf sheath tissues infected by *Fp*. Cereal cell autofluorescence decreased after clearing and fixation. After staining with solophenyl flavine 7GFE, hyphae were visible but not distinct from plant tissues. a, Tissue fluorescence before clearing and fixation. b, Tissue fluorescence after clearing and fixation. Brown discolouration is a lesion caused by fungal infection. c, Fixed and cleared tissue after staining with solophenyl flavine 7GFE only. Hyphae are visible but have similar emission spectra to the host tissues. d, Fixed and cleared tissue after staining with safranin and solophenyl flavine 7GFE. Hyphae are visibly distinct from the host tissues. e and f, Cleared and fixed 28 day old bread wheat leaf sheath tissues stained with safranin and solophenyl flavine. After staining hyphal cell walls and septa are very distinct. Autofluorescence of plant cells has been quenched by the safranin. e, Hyphae growing through heavily infected tissue. Hyphal wall fluorescence is more intense than plant wall fluorescence and adjustment of the camera exposure time in order to produce a clear image of fungal hyphae at high magnification resulted in plant walls not being visible. f, Hyphae growing within and across epidermal cells. This tissue was less diseased and viewed under lower magnification than (e), resulting in plant cell walls being visible. (g and h) Uncleared transverse sections showing distinct differentiation between bread wheat cells and hyphae in 16 week old plants. g, *Fp* hyphae growing within vascular tissue of a wheat internode. h, *Fp* hyphae growing within non-vascular nodal tissue.

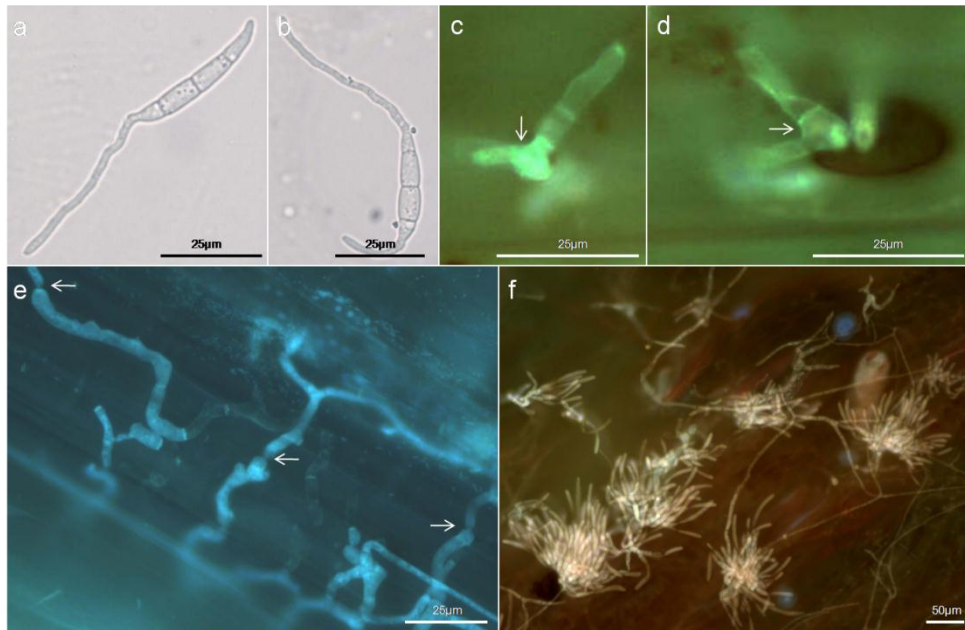


Figure 4.2. Infection of coleoptile tissues by *Fp* (SV). a and b, Formation of a germ tube from a conidium after 6 hrs. Conidia were viewed under bright field microscopy. c, Slightly thickened hyphae forming over an epidermal cell (arrow) (2-49), 5 dai. d, Swelling at a hyphal tip occurring over an initial lesion in an epidermal cell (arrow), 5 dai (2-49). e, Slightly thickened hyphae within epidermal cells crossing walls by appressoria-like structures (arrows), 9 dai (W). f, Conidial formation after hyphal eruption through epidermal cells, 10 dai (P). This was only observed in Puseas.

4.3.5 Initial penetration and growth in LSs

4.3.5.1 Initial penetration

Hyphal growth on the LS adjacent to the coleoptile involved either penetration of hyphae directly from the coleoptile into the LS or growth across the LS surface. Penetration of hyphae through stomatal apertures was frequently observed (Figure 4.3a, b, c). Penetration via stomata and the base of trichomes was facilitated by appressoria-like structures, typically occurring as simple swellings at the end of hyphal tips but also as ‘hooks’ around trichomes or into stomata (Figure 4.3d, e, f).

During several weeks after germination the coleoptile remained tightly wrapped around the outside of LS1. This allowed hyphae which penetrated through the coleoptile to grow in the small space between the coleoptile and LS1. It was observed that these hyphae grew in a coralliform mass on the LS surface, forming adjacent to a stomate and penetrating through the stomatal aperture (Figure 4.3g, h, i).

Initial surface growth of hyphae was also a frequent feature on LSs. Hyphae were observed to grow from the coleoptile onto the surface of the LS. These hyphae grew aerially across the LS surface between trichomes. While patterns of growth were difficult to discern, growth of hyphae around trichomes (Figure 4.4a, b, c, d, e and f) and penetration into stomata was frequently observed. Hyphal growth around trichomes occurred from 48 hours after inoculation. This frequently involved multiple hyphae growing to and around an individual trichome. All wheat genotypes displayed this growth pattern. An attempt to count trichomes was made however within the wheat genotypes the density of trichomes varied between individuals. Trends in trichome density between genotypes were not obvious.

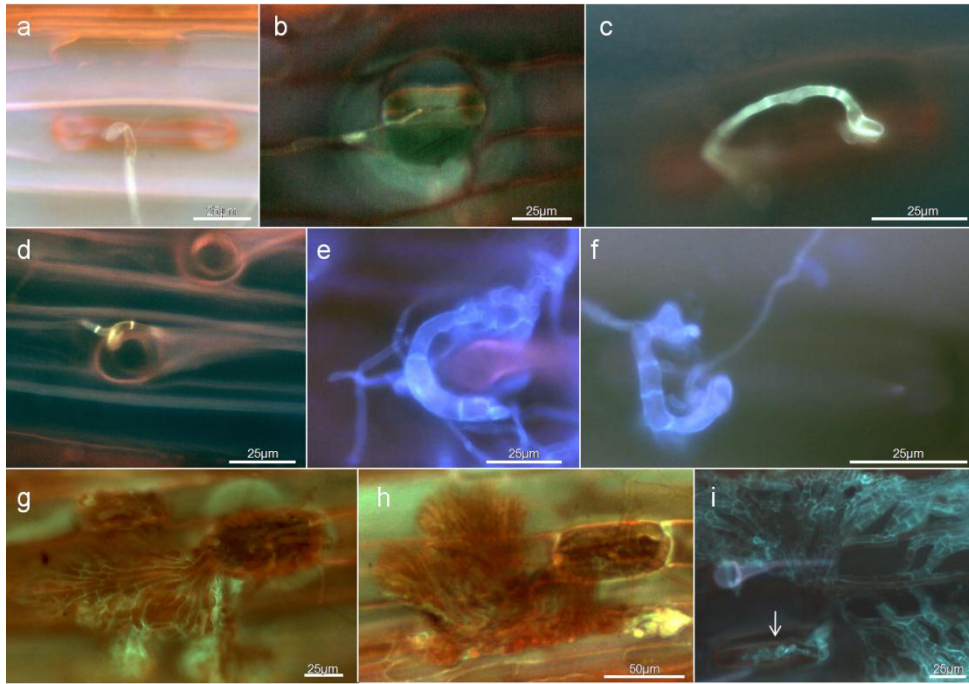


Figure 4.3. Penetration of leaf sheath tissues by *Fp* (SV). a, Surface hyphae growing into a stoma, 5dai (2-49). b, penetration of a stoma by a single hyphae resulting in a halo-effect around the guard cells, 14 dai (2-49). c, Swollen hyphal tip forming over a stoma, 14 dai (P). d, surface hyphae growing appressed to the base of a trichome, 14 dai (P). Discolouration was observed under the trichome base. e, Thickened 'hook-shaped' hyphal structure forming around a trichome base, 21 dai (P). f, Thickened 'hook-shaped' hyphal structure forming over a stoma, 21 dai (2-49). g and h, Coralliform hyphae formed adjacent to a stomate and also penetrating the stoma. The hyphae grew between the coleoptile and leaf sheath 1 tissues, 5 dai (2-49). i, Large growth of coralliform hyphae across the leaf sheath surface, also penetrating the stoma (arrow), 9 dai (G).



Figure 4.4. Association of *Fp* hyphae with trichomes (SV). a, Surface growth of hyphae was frequently observed to pass around trichomes (arrow), 48 hai (2-49). b, Growth of multiple hyphae to a single trichome, 48 hai (2-49). c, Hyphal wrapping around trichomes bases (arrows), 14 dai (P). d, Hyphal wrapping around the midpoint of a trichome (arrow), 14 dai (P). e, Hyphal growth around trichome bases (arrows) and within epidermal cells, 26 dai (W). f, Hyphae wrapping around a trichome and also penetrating a stoma, 14 dai (P).

4.3.5.2 Lesion formation

Stomatal penetration was the method by which *F. pseudograminearum* was most frequently observed to gain access into LS tissue. Other sites of penetration included trichomes, wounds and, infrequently, direct penetration of the epidermis. Evidence for stomata being the initial entry points for the fungus arose from observations of the initial brown lesions associated with crown rot disease. Tissues displaying initial lesions were collected from 5 to 26 days after inoculation and ranged from LS2 to LS5 of Puseas, 2-49, Wylie and Gregory. Under bright field microscopy, initial lesion formation was frequently observed at the guard cells, which became light to dark brown (Figure 4.5a, b, c, d). Bases of penetrated trichome cells displayed a similar discolouration (Figure 4.5d, e, f, g, h). Discolouration of guard cells frequently occurred along rows of stomata, with individual lesions forming at similar times but separately at each stoma (Figure 4.6a). Lesions forming at trichomes appeared in a random fashion. Lesion formation progressed into adjacent epidermal cells, where the entire cell became discoloured (Figure 4.5c, h). Within these cells the brown discolouration appeared to be associated with cytoplasmic granulation. Discoloured guard and epidermal cell walls also appeared to become rough and granular. The lesioning continued to spread into adjoining epidermal cells (Figure 4.6b). In some cases the discolouration appeared to spread into the parenchyma cells directly below these epidermal cells.

Observation of areas with small lesions under fluorescence filter B-2A resulted in halos of yellow fluorescence along cell walls of cells either displaying discolouration or adjacent to cells with discolouration. This was observed in both partially resistant and susceptible genotypes. The fluorescence was most visible around lesions which were just forming at the stomata (Figure 4.7a, b, c). Halo effects around penetration sites were also observed after staining with solophenyl flavine 7GFE and safranin.

After staining tissues with initial lesions, hyphae were observed penetrating the stoma and trichomes which displayed discolouration (Figure 4.8a, b, c, d, e). Guard cells were also frequently colonised (Figure 4.8f). In some cases no hyphae were seen at the lesion point, but this may have been caused by hyphae being removed when the outer LS was detached. Where LSs had been tightly wrapped the hyphae frequently had coralliform surface growth adjacent to stomata. Hyphal growth was not predictable. It occurred on the surface along cell wall boundaries

(Figure 4.8f) but hyphae not closely appressed to the epidermal surface were also common.

Discoloured epidermal cells adjacent to penetrated stomata were frequently observed to be filled with hyphae (Figure 4.9a, b, c, d and f). These cells initially appeared to inhibit further penetration of the hyphae into adjacent epidermal cells. Hyphae within such cells frequently appeared to grow towards a corner of the cell *en masse* (Figure 4.9g). This concentration of hyphae within individual epidermal cells was observed in Puseas, 2-49, Wylie and Gregory.

4.3.5.3 Cell Wall Penetration

Penetration of cell walls was facilitated by small swellings, believed to be appressoria, at the hyphal tips. The appressoria ranged from small swellings of hyphal tips or strands to large septated foot shaped cells (Figure 4.10a, b, c, d, e, f, g). During direct penetration the hyphae became constricted as they passed through the cell wall, returning to normal diameter once through the wall.

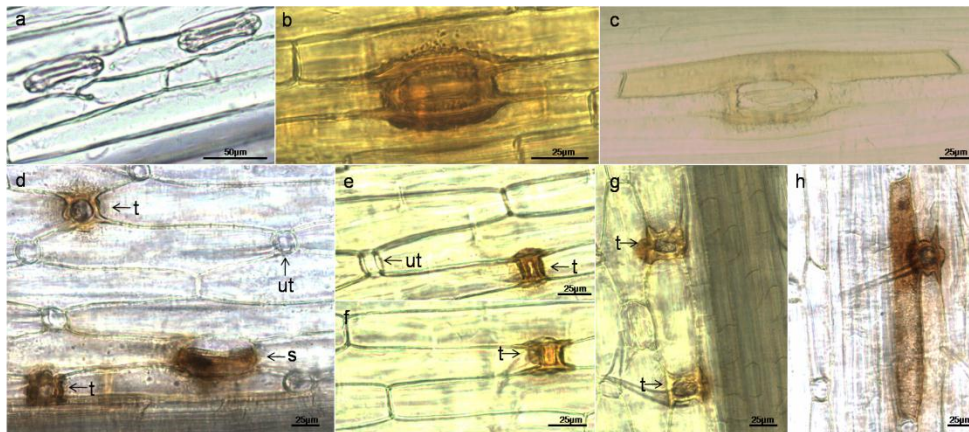


Figure 4.5. Initial lesion formation in leaf sheath tissues (SV). a, Stomata in control tissues unaffected by *Fp*, 28 dai (2-49). b, Initial lesion forming at a stomate, 28 dai (2-49). Along with the brown discolouration around the stomate, the cell walls appear granulated. c, Initial lesion forming at a stomate with an adjoining epidermal cell also exhibiting brown discolouration, 7 dai (P). d, Initial lesion formation at trichome bases (t) and at a stomate (s), 26 dai (W). Unaffected trichomes (ut) do not display discolouration. e, f and g, Discoloured (t) and unaffected trichome bases (ut), 28 dai (2-49). h, Initial lesion formation at a trichome base with an adjoining epidermal cell also exhibiting brown discolouration, 26 dai (W). Leaf sheath tissues were cleared, fixed and viewed under bright field microscopy.

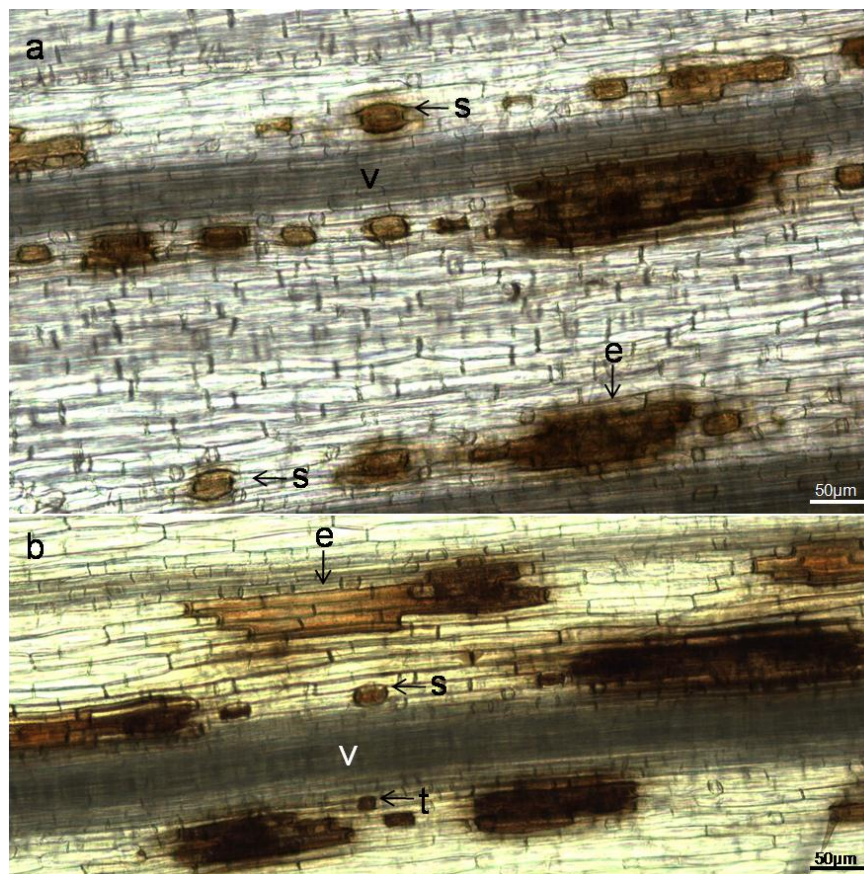


Figure 4.6. Lesion formation and spread in leaf sheath tissues infected by *Fp* (SV). a and b, Initial lesion formation frequently occurred at multiple individual stomata (s) and occasionally at trichome bases (t), 28 dai (2-49). The lesions spread into adjoining epidermal cells (e), eventually coalescing to form one large area of discoloured tissue. Lesion formation in epidermal cells adjacent to vascular tissue (v) was infrequent. Leaf sheath tissues were cleared, fixed and viewed under bright field microscopy.

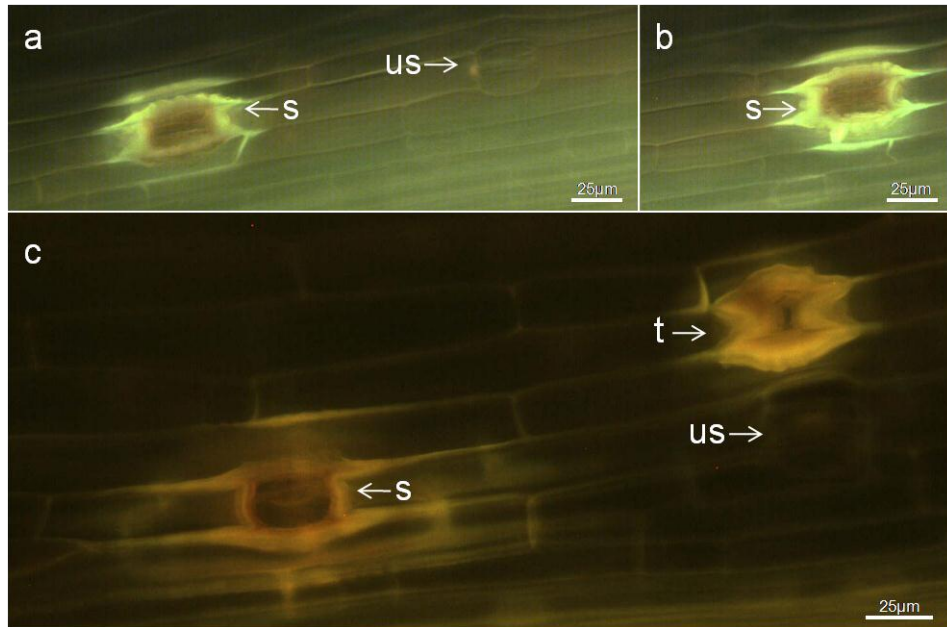


Figure 4.7. Reactions to initial infection by *Fp* resulting in the production of fluorescent materials (SV). a, b and c, Fluorescence occurring around stomata (s) and trichomes (t) during initial infection, 28 dai (2-49). Unaffected stomata (us) did not fluorescence. Leaf sheath tissues were cleared, fixed and viewed under fluorescence using filter B-2A.

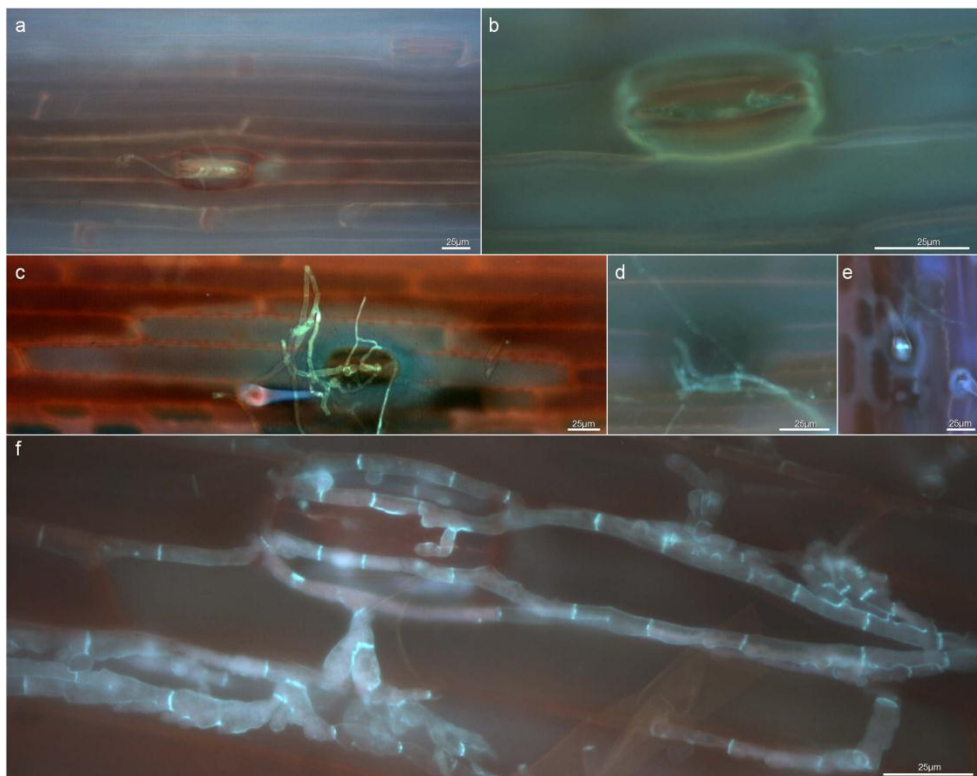


Figure 4.8. Growth of *Fp* hyphae in discoloured stomata and trichomes (SV). a and b, Initial penetration of hyphae into stoma, 7 and 5 dai, respectively (P and 2-49, respectively). c, Initial penetration of hyphae into a stoma, 14 dai (2-49). The adjoining epidermal cells have become lighter in colour. d, Hyphae wrapped around the base of a discoloured trichome, 26 dai (W). e, Hyphae inside the base of a discoloured trichome, 26 dai (G). f, Guard cell colonisation and penetration of the stoma, 26 dai (G). Surface growth of the hyphae is frequently along the grooves at adjoining cell walls.

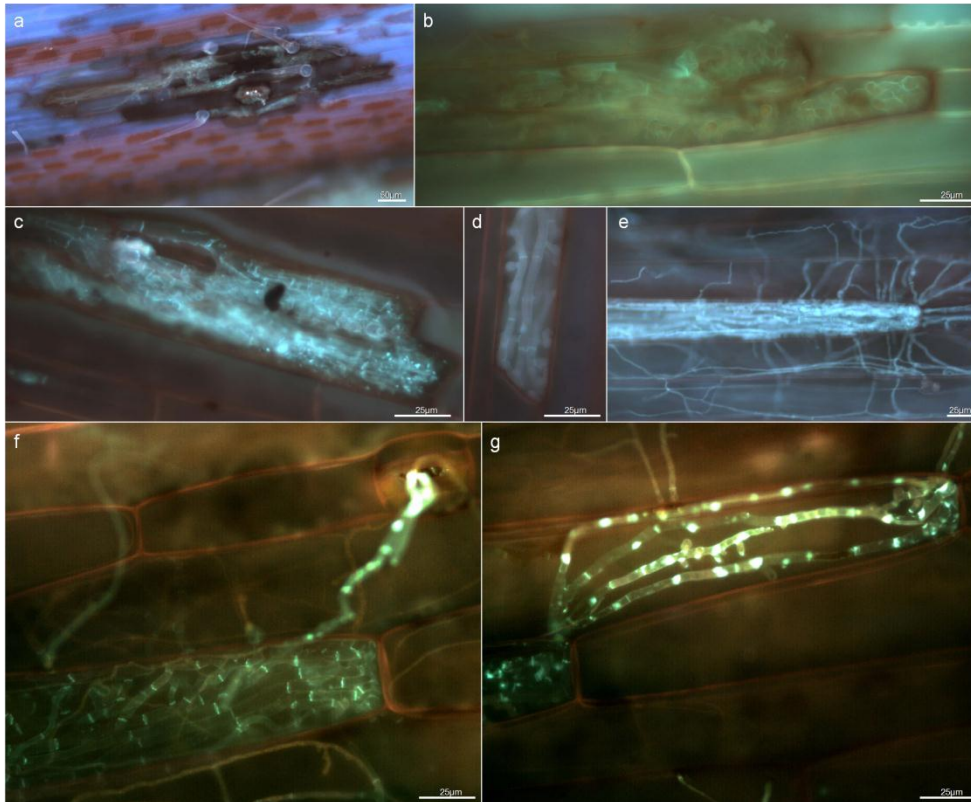


Figure 4.9. Dense colonisation of individual epidermal cells by *Fp* (SV). a, Penetrated stoma surrounded by discoloured epidermal cells containing large quantities of hyphae, 26 dai (G). b, Epidermal cell adjoining stomata, 5 dai (2-49). c and d, Epidermal cells adjoining stomata, 26 dai (G). These epidermal cells appear to resist penetration of the hyphae, with multiple hyphae forming to fill the entire cell. e, Epidermal cell adjoining stomate, 26 dai (G). This cell initially resisted penetration, however, the hyphae were eventually able to break through the cell wall and spread through the tissue. f, Epidermal cell adjoining stomata and initial penetration of a stoma, 14 dai (2-49). The epidermal cell wall appeared to have resisted penetration. g, Hyphal penetration through epidermal cells occurring through the corner of cell walls, 14 dai (2-49).

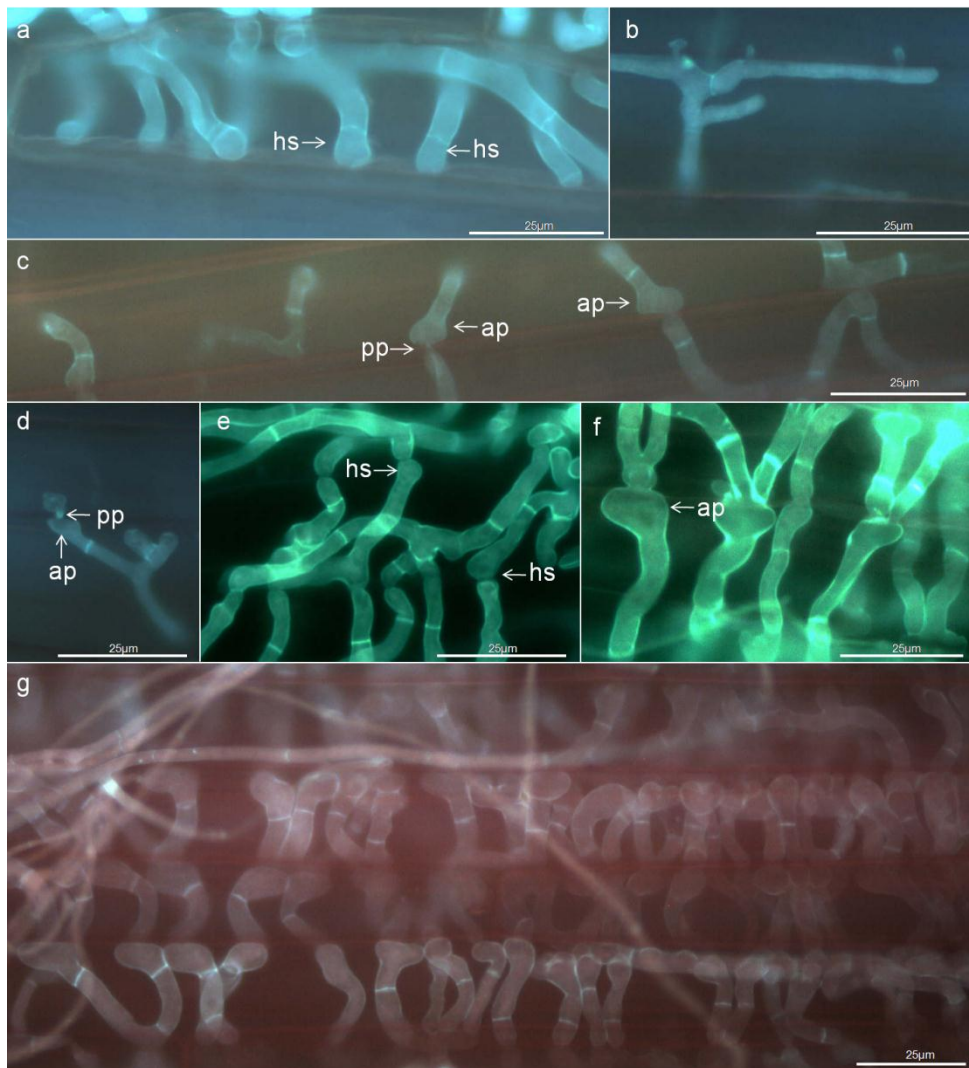


Figure 4.10. Appressorial structures of *Fp* (SV). a, Hyphal swellings (hs) during contact with cell wall, 9 dai (W). Indentations of the cell wall are present under the hyphal tips. b, Penetration of the cell wall directly via hyphae, 9 dai (G). c, Formation of septated foot-shaped appressoria (ap) , 9 dai (W). Penetration peg (pp) formation occurs during penetration. d, Foot-shaped appressoria forming a penetration peg, 9 dai (G). After penetration the hyphae resumes its initial diameter. e, Simple hyphal swellings facilitating crossing of cell walls, 14 dai (P). Cell walls are not visible as the hyphal fluorescence was too intense. f, Foot-shaped appressoria facilitating cell wall crossing, 14 dai (P). After crossing the hyphae frequently split into two. g, Multiple foot-shaped appressoria and simple hyphal swellings penetrating through cell walls, 9 dai (W). Hyphal curvature within cells is obvious.

4.3.5.4 Hyphal Growth Characteristics

Differences in hyphal growth patterns were observed between the abaxial and adaxial surfaces of LS tissues. An outline of the anatomy of LS tissue is provided in Figure 4.11 a, b, c, d and e. The epidermal cells of both LS surfaces were the site of greatest hyphal proliferation. The hyphal infection edge was typically located in the epidermal cells. Hyphae were also able to penetrate into the cortical parenchyma cells. Vascular tissues of the LS were infrequently observed to have been colonised.

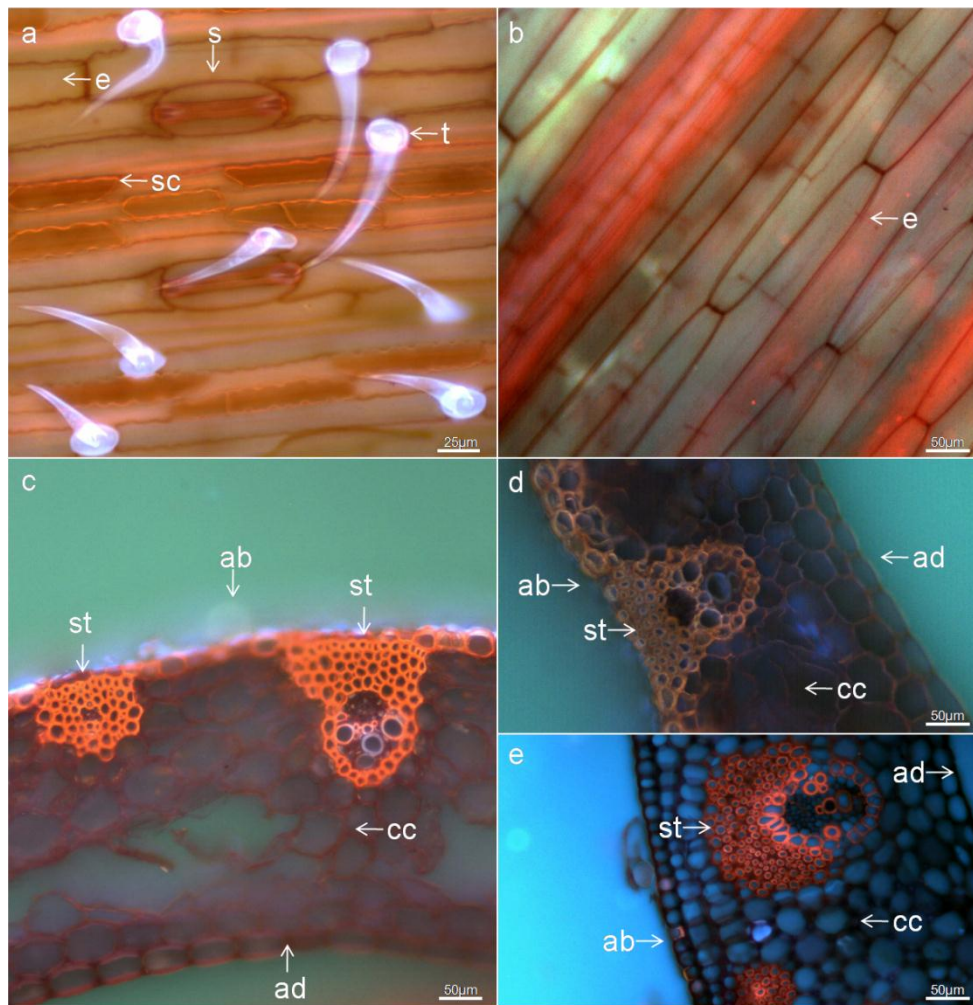


Figure 4.11. Cereal leaf sheath tissue anatomy. a, The abaxial surface of leaf sheaths had several types of epidermal cells (SV). Unspecialised epidermal cells (e), stomata (s) (with guard cells), trichomes (t) and sinuous silica cells (sc). b, The adaxial surface had unspecialised epidermal cells and few stomata (SV). No silica cells or trichomes are present. c and d, Vascular tissue in the leaf sheath was joined to the abaxial (ab) epidermis by a stereome (st) (TS). The abaxial epidermis and vascular tissues were heavily lignified, while the cortical cells (cc) and adaxial (ad) epidermis had low lignification. e, At the base of leaf sheaths, particularly where they had just differentiated from a node, the stereome was not directly linked to the epidermis (TS).

4.3.5.4.1 Abaxial surface

The abaxial surface of wheat LSs includes several kinds of specialised epidermal cells, such as guard cells, trichomes and sinuous silica cells (Figure 4.11a). Initial interactions between guard cells/trichomes and hyphae have been described, however, as colonisation progressed subsequent interactions with specific structures occurred.

After colonisation of epidermal and cortical parenchyma cells, hyphae re-emerged from the stomata (Figure 4.12a, b, c, d, e, f, g, h). These predominantly spread across the surface of the LS during favourable environmental conditions (Figure 4.13a, b, c). In Puseas, masses of conidia occasionally formed on top of stomata at the base of heavily infected leaf sheaths (Figure 4.14). During heavy infection hyphae were occasionally observed in the bases of broken trichomes or growing inside whole trichomes (Figure 4.15a, b, c). It appeared that if coleoptile or LS tissues were not colonised before senescence (LS senescence being characterised by leaf blade death) then hyphal spread was limited (Figure 4.15d, e).

On the abaxial LS surface hyphae rapidly penetrated through stomata into the epidermal cells. Surface growth of hyphae was generally limited, perhaps due to exposure to lower humidity and higher light levels than the adaxial surface. Hyphae readily extended through the epidermal cells located between the parallel vascular bundles. However, the vascular bundle and associated stereome (Percival, 1921) frequently restricted lateral hyphal growth (Figure 4.16a, b, c, d). On the abaxial surface the vascular bundles are covered by a single layer of epidermal cells connected by a stereome directly to the bundle sheath cells. Unspecialised epidermal cells were regularly interspaced with silica cells. These silica cells were typically most common near vascular bundles. In order to continue lateral growth hyphae either grew across the surface of the leaf sheath, when environmental conditions were favourable, or grew through the epidermal cells. When growing through the epidermal cells adjacent to the bundle sheath the hyphae were observed to grow only in the unspecialised epidermal cells between the silica cells, forming a network across this layer (Figure 4.17a, b, c, d, e, f, g). This suggests that the silica cells have wall properties which enable them to resist hyphal penetration. No difference in silica cell characteristics was observed between Puseas, 2-49, Wylie or Gregory.

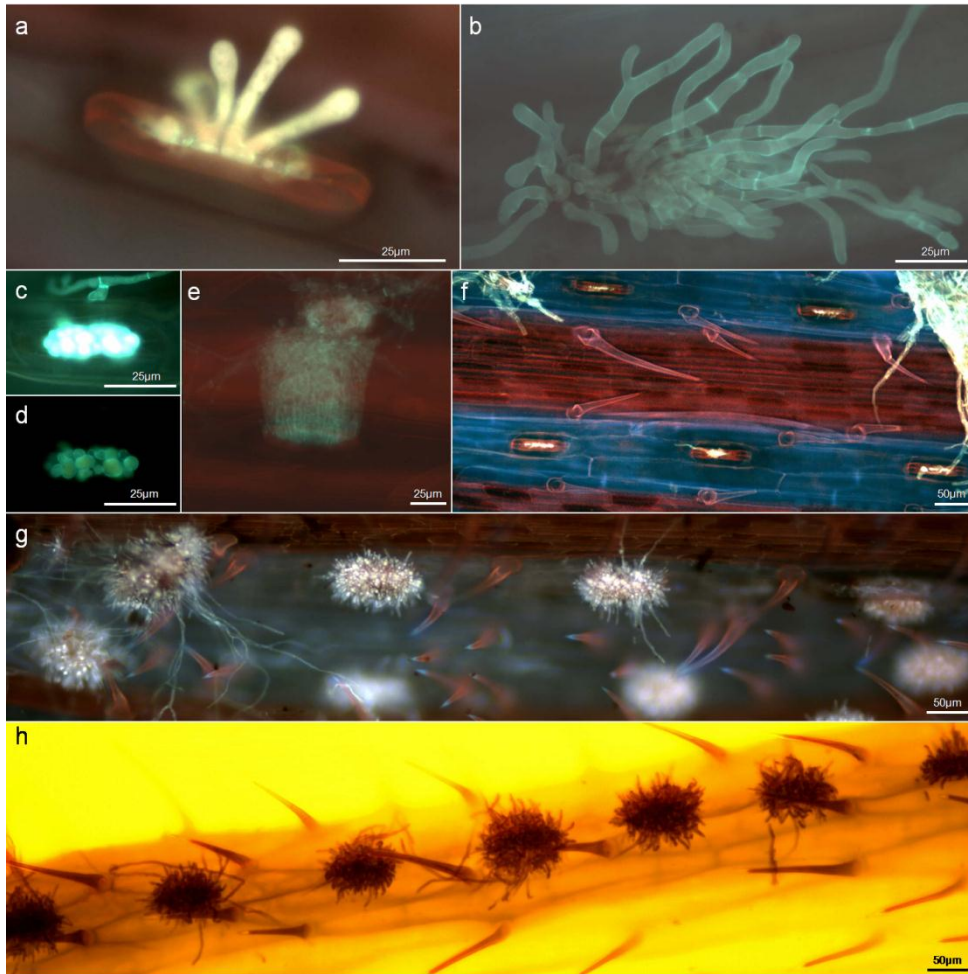


Figure 4.12. Re-emergence of *Fp* hyphae from stomata on the abaxial surface of cereal leaf sheath tissue (SV). a and b, Hyphae emerging from stomata after internal colonisation, 26 and 14 dai, respectively (2-49 and Puseas, respectively). c and d, Both images are of the same stomata at different camera exposure times, 14 dai (L). An appressoria is penetrating a cell adjacent to the stomata while hyphae are multiplying and beginning to emerge from the stoma. e, Mycelium erupting from a stomata en mass, 9 dai (W). f, Multiple stomata with hyphae beginning to emerge, 14 dai (P). g, Over time the number of hyphae emerging from the stomata increases, 10 dai (P). h, Tissue was observed under fluorescent filter B-2A. A row of stomata exhibiting prominent growth of hyphae out of the leaf sheath tissue (P). Surface growth of hyphae is limited.

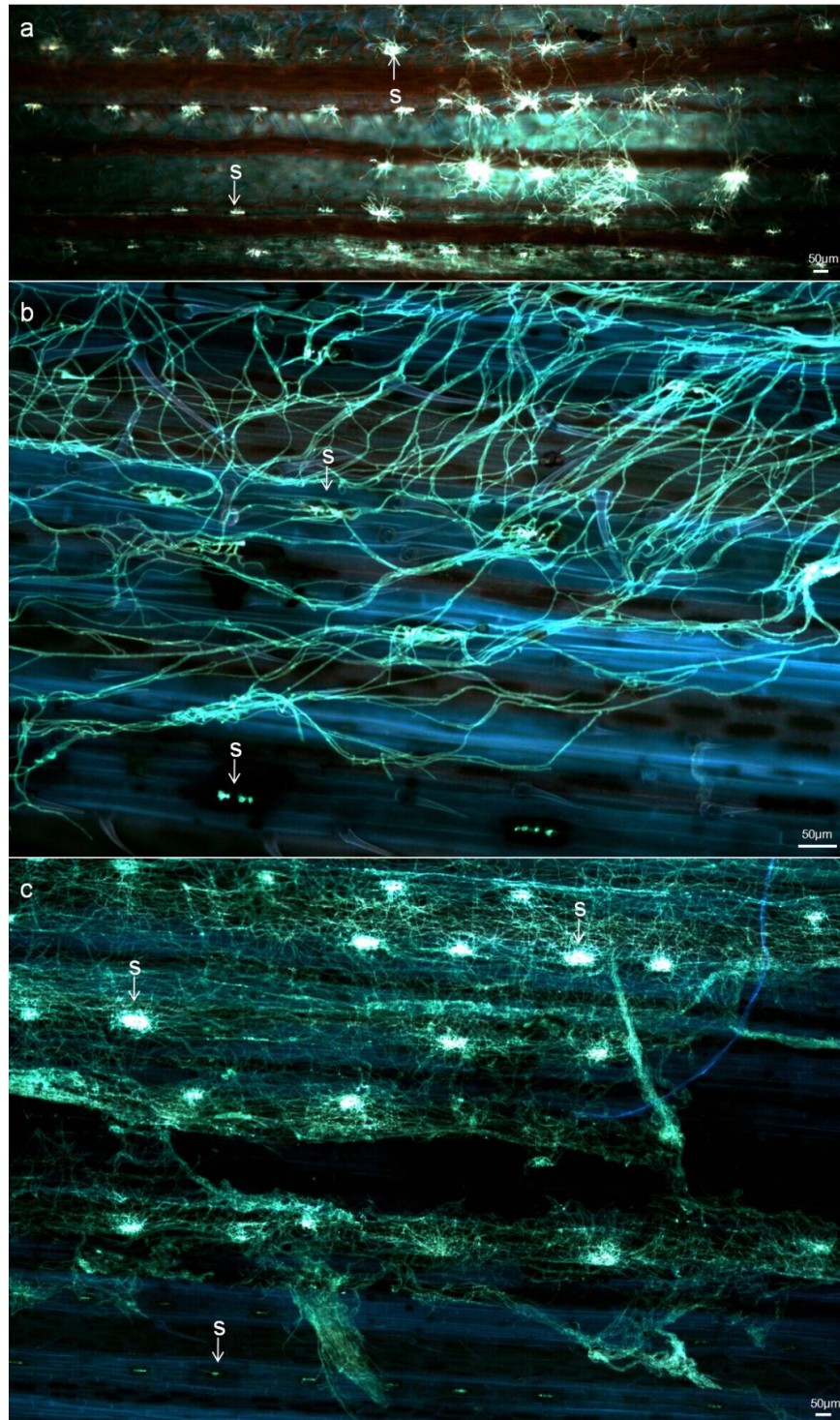


Figure 4.13. Heavy colonisation of the abaxial surface of leaf sheath tissue by *Fp* (SV). a, A heavily colonised leaf sheath with large amounts of hyphae emerging from stomata (s), 14 dai (P). b, Surface growth of hyphae across the leaf sheath surface, 14 dai (P). Hyphae are growing around trichomes and also emerging from stomata. c, Mycelial mat formed over the surface of the leaf sheath, 14 dai (P). The bright areas in the mat are due to dense growth of hyphae out of the stomata. The lower section of the image displays hyphae beginning to emerge from stomata.

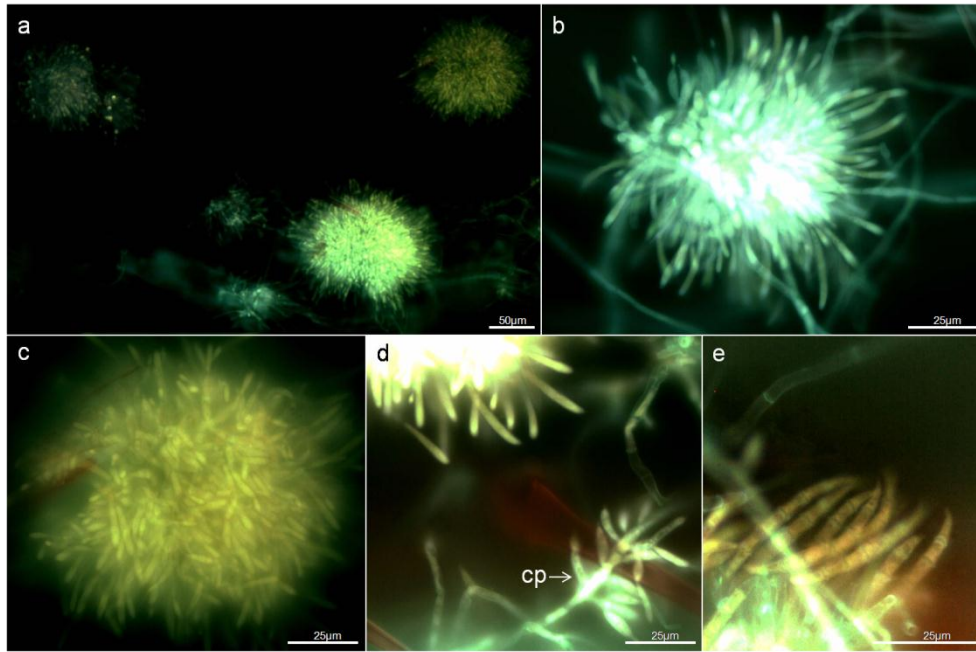


Figure 4.14. Masses of *Fp* conidia forming over stomata on the abaxial surface of leaf sheath 1 tissue of the wheat Puseas, 14 dai (SV). a, Multiple affected stomata. b and c, Forming conidia. d, Immature conidia on a conidiophore (cp). e, Conidia nearing maturity.

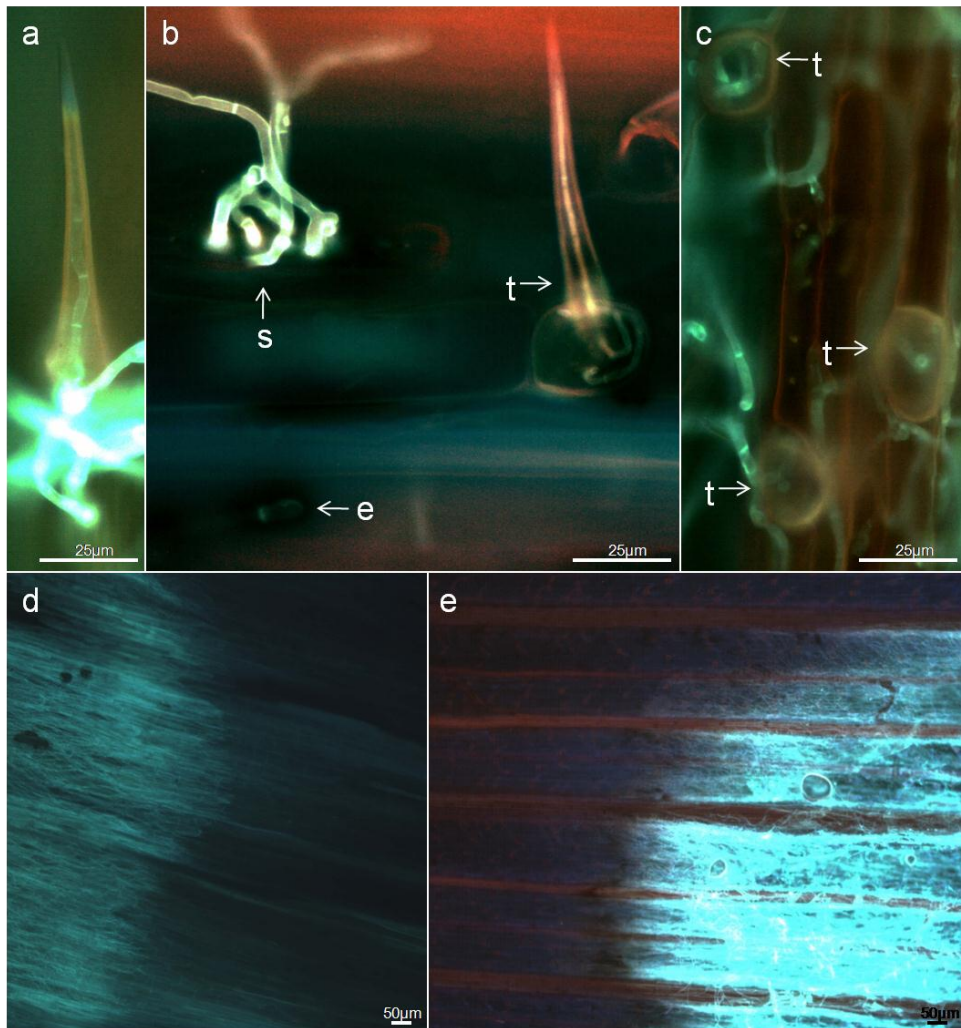


Figure 4.15. Growth of *Fp* hyphae occurred in trichomes during heavy infection, while colonisation of senescent tissue appeared decreased (SV). a, Hyphae growing at the base of a trichome and growing up inside the trichome, 14 dai (P). b, Hyphae growing in a stomate (s), inside a trichome (t) and penetrating the surface of an epidermal cell (e), 14 dai (P). c, Hyphae growing in the base of broken trichomes, 14 dai (P). d, Edge of hyphal growth in a senescent coleoptile, 9 dai (G). e, Edge of hyphal growth in a leaf sheath of a senescent leaf, 26 dai (W).

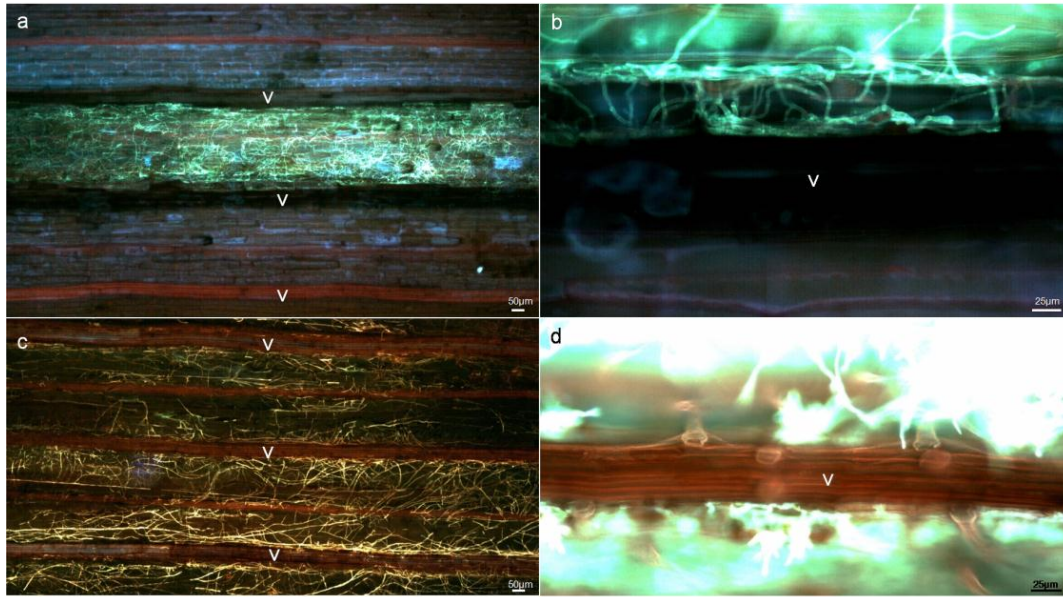


Figure 4.16. Restriction of *Fp* hyphal growth by vascular bundles (v) and associated stereome tissues, 14 dai (SV). a, Hyphal growth bordered by vascular tissues (P). b, Edge of hyphal growth where penetration is restricted (P). c, Heavy colonisation of cells between vascular tissues, while the surface of the vascular tissues has much less hyphal growth (2-49). d, Vascular tissue free from colonisation yet surrounded by hyphal growth (P).

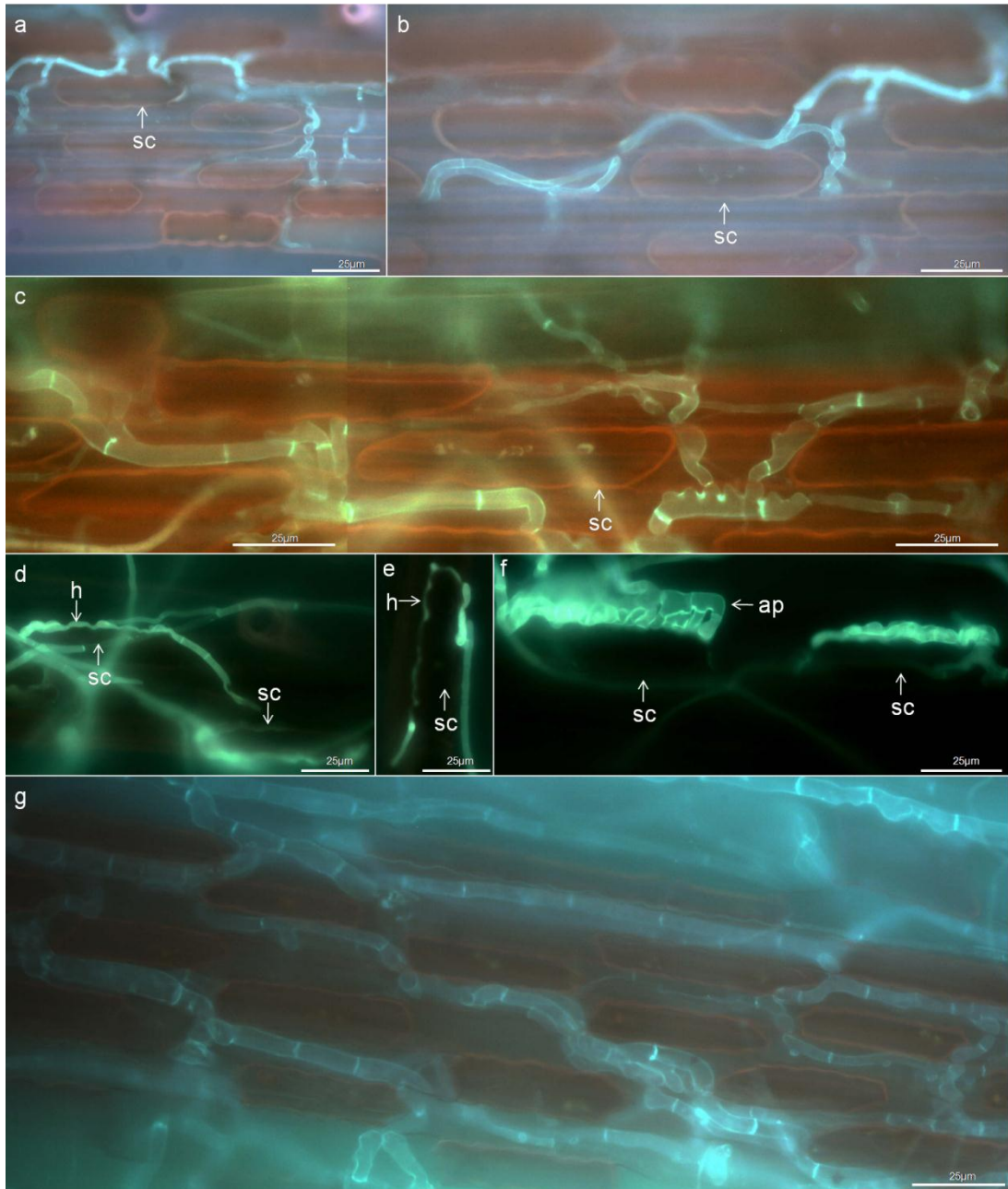


Figure 4.17. Sinuous silica cells (sc), present only on the abaxial surface and which were most common in epidermal tissue adjacent to vascular tissues, displayed properties enabling them to resist *Fp* hyphal penetration (SV). a and b, Hyphae growing through epidermal tissues while growing around silica cells. c, Hyphae growing between silica cells. Light coloured substance in the silica cell is stored silicic acid (P). d and e, Hyphae (h) growing appressed to silica cell walls were observed to form a sinuous pattern (P). f, Multiple appressoria (ap) formed against the wall of a silica cell but not successfully penetrating (P). g, Hyphae formed a network while growing in epidermal cells surrounding silica cells on the abaxial surface (SV, W).

4.3.5.4.2 Adaxial Surface

The adaxial epidermis included no trichome or silica cells and few guard cells. This cell layer supported dense growth of *F. pseudograminearum* mycelium, both internally and on the surface. It was difficult to discern if hyphae penetrated through from the abaxial to the adaxial surface or grew around the LS edge from the abaxial surface. The LS adaxial surface was typically facing the abaxial surface of the younger leaf blade and sheath furled within it. This more humid and sheltered location may be the reason for the formation of the observed mycelial mats. While these mats were observed less frequently on 2-49, their occurrence on all host genotypes was dependent on the severity of and time after infection. As with the abaxial surface, cells adjacent to the vascular bundles affected the hyphal growth. The adaxial surface adjacent to a vascular bundle included epidermal cells and typically two layers of cortical parenchyma cells, which were directly adjacent to the bundle sheath. Hyphae were observed to grow laterally through epidermal cells until encountering cells adjacent to a vascular bundle. At this point hyphae either grew across the surface, under favourable conditions, or produced large quantities of very thick hyphae, with obvious swellings, which facilitated crossing of the cell walls (Figure 4.18a, b, c, d, e, f, g). Hyphae penetrating across a cell frequently appeared curved. In some cases a foot like appressorial structure was obvious, however, in some cases hyphae appeared as swollen oblong shapes. These thickened hyphae were frequently appressed against each other, filling the cell cavity, and produced multiple cell wall crossing events. It could not be determined using the described methods if these hyphae had penetrated the cell membrane or whether penetrated cells were alive or dead.

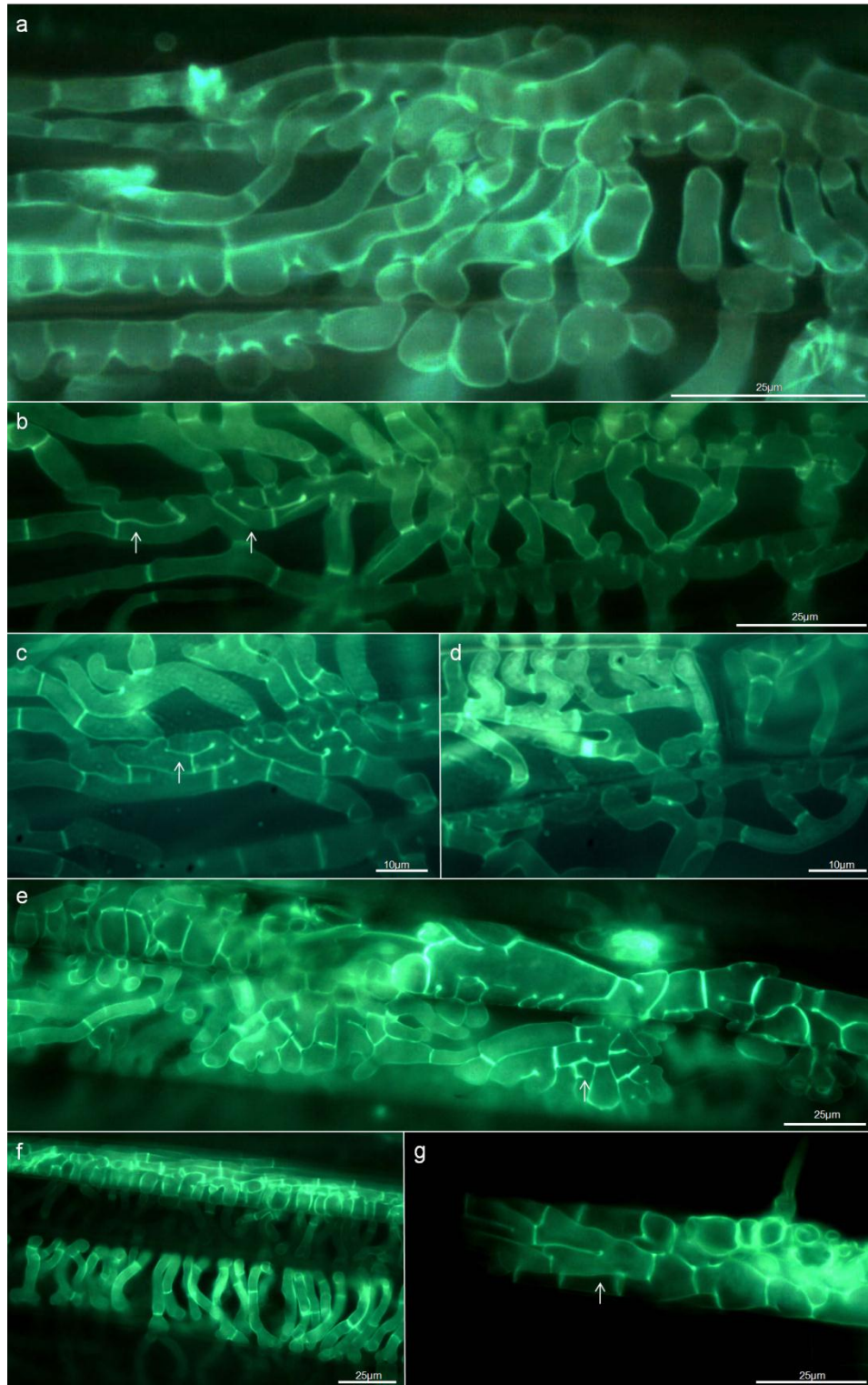


Figure 4.18. a and b, *Fp* hyphae within epidermal tissue adjacent to vascular bundles on the adaxial surface of a wheat leaf sheath frequently formed thickened hyphae (SV, P). These hyphae appeared to facilitate cell wall crossing in the same manner as appressoria. The hyphae frequently grew appressed to each other (arrows). c and d, Hyphae growing appressed to each other and frequently crossing cells walls (P). e, Very thick hyphae forming within cells (P). f, Hyphae filling a cell (top) while when hyphae were not closely packed within cells hyphal curvature was observed (bottom) (P). g, Thickened hyphae forming within an epidermal cell are limited by the cell walls (P). The cell walls are not visible as the fluorescent intensity of the hyphae required a shortened camera exposure time, which limited cell wall fluorescence to a non-visible level.

4.3.5.5 Description of Growth in Different Genotypes

Measurements of hyphal width indicated that hyphae growing in Puseas 2-49, Wylie and Gregory had a similar range of widths (Table 4.2). The maximum hyphal width observed growing in Puseas was greater than those observed in the other genotypes however, hyphae with this increased width were rare. The width of hyphae germinating from conidia was approximately 1 μm . Surface hyphae did not appear to become as wide as hyphae growing within tissues. During pathogenesis of the LS hyphae of *F. pseudograminearum* were of three sizes. These were thin (1 to 4 μm width), thick hyphae penetrating cells, typically adjacent to vascular bundles (4 – 8 μm width) and very thick hyphae occurring infrequently but only over cells adjacent to a vascular bundle (9 – 20 μm width).

Table 4.2. Mean and range of hyphal widths observed across leaf sheaths 1 to 4 of four wheat genotypes at 14 dai. For the purpose of the mean and standard error (SE) n = 26. No significant differences were reported using the Tukey multiple comparison test.

Genotype	Hyphal Width (μm)		
	Mean	SE	Range
2-49	4.4	0.6	1.4 – 12.2
Wylie	5.1	0.4	2.7 – 11.0
Gregory	5	0.6	2.3 – 11.6
Puseas	5.2	0.6	2.1 – 20.5

In the trial comparing 2-49, Gregory and Puseas at 14 days after inoculation more hyphae were visible on Puseas LS1 compared to 2-49 and Gregory. On LS2 of 2-49 hyphae were observed only on the abaxial surface and penetrating into stomatal apertures. In contrast, on LS2 of Gregory and Puseas hyphae were present on both surfaces with significant quantities of hyphae penetrating through their internal tissues. Tissues of Puseas frequently contained areas of more intense growth than Gregory. At this time no hyphae were present on LS3 of 2-49, while LS3 of Gregory bore small quantities of hyphae on the abaxial surface. LS3 of Puseas varied in infection intensity between individual plants, with small amounts of surface hyphae on some LS3 samples while on others mycelial mats were forming accompanied by significant internal growth in the adaxial epidermal cells. Hyphae were never observed on the tissues of control seedlings.

Preliminary comparisons of barley (Lindwall) and oat (Riverina Racehorse Oats) seedlings inoculated with *F. pseudograminearum* indicated hyphal growth

patterns in barley similar to those observed on Gregory at 14 dai (LS2 moderately colonised). Fewer hyphae (small quantities of hyphae on LS1) were observed on oats at this stage of infection than on 2-49. No stomatal penetration was observed on the oat leaf sheaths. Both oats and barley develop shorter, wider trichomes than wheat, however, no other obvious anatomical differences in leaf sheath structure were observed between the three species.

A direct comparison between genotypes is difficult due to significant variation in growth patterns between different plants. Infection of coleoptiles, LSs, INs and nodes is frequently more severe on one side of the tissue. The most consistent patterns of fungal growth are hyphal proliferation in stomata, hyphal growth between silica cells and thickened hyphae forming in cells adjacent to vascular bundles. No morphological differences affecting resistance are present between resistant and susceptible genotypes. Similarly, major differences between fungal growth in the partially resistant 2-49 and the susceptible Puseas were absent.

4.3.6 Initial penetration and growth in culms

4.3.6.1 Culm morphology

Culm tissues possess a wide range of cell types (Figure 4.19a, b). Epidermal cells encased the culm tissue and had moderately thickened cell walls. Stomata were present in this layer and typically had lacunae beneath (Figure 4.20a, b). Depending on the specific IN, if parenchymatous hypoderm was present the cell walls were moderately thin and there were only small intercellular spaces. The parenchymatous hypoderm frequently became smaller or absent in higher tissues of the culm. The sclerenchymatous hypoderm was composed of a layer of thick walled cells with very few to no intercellular spaces. This layer frequently had small vascular bundles within it. Vascular parenchyma cells were generally larger thin-walled cells surrounding large vascular bundles (Figure 4.20c, d). Pith parenchyma cells were generally very thin walled with large intercellular spaces, with the exception of IN1 and node bases, where pith cell walls were thicker.

The safranin stain was useful for identifying different cell types in the INs due to differences in lignification. Parenchymatous hypoderm and pith parenchyma had low fluorescence, typically of a purple colour. The more lignified tissues of the vascular parenchyma and particularly of the sclerenchymatous hypoderm were a

bright red/orange. The bundle sheath and xylem of the vascular bundles were of a similar colour. Large xylem and sclerenchyma cells sometimes appeared blue/white. Phloem cells and tracheids were a deep red.

Nodes were typically heavily sclerified and around the level of formation of the pith plexus the anastomosing vascular bundles were horizontally elongated and had multiple smaller diameter xylem vessels (Figure 4.21a, b, c, d, e, f). Around and within these bundles cells frequently stained a deep red, except for the xylem cells which were slightly brighter. The bundle sheath also produced some fluorescence. In some cases, particularly in more mature nodes and/or during infection, nodal tissues were much darker, with fluorescence nearly absent. This decrease in fluorescence occurred in both control and infected tissues; the reason for it is not known.

Visible structural differences between the plant genotypes and species were few and could not be linked to susceptibility to infection.

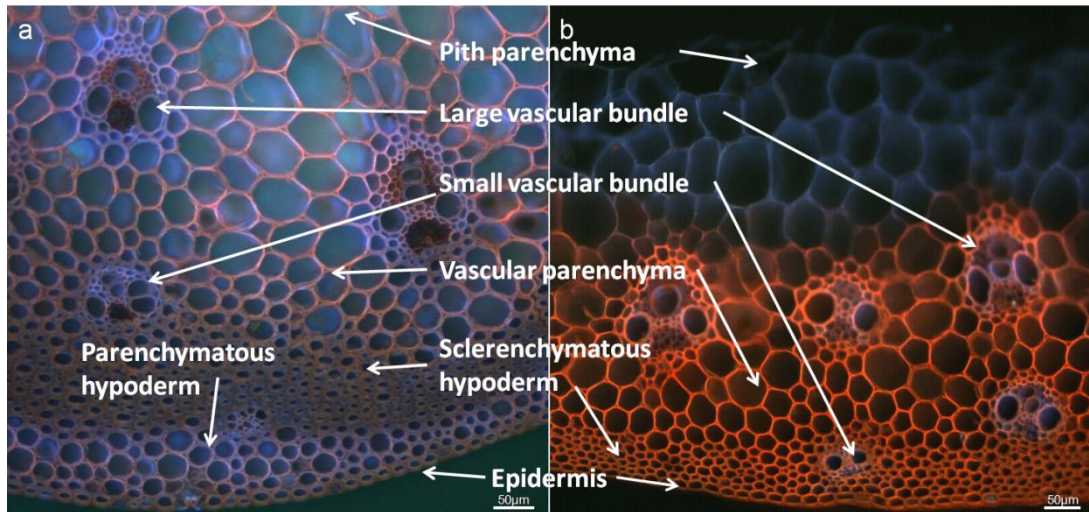


Figure 4.19. Cell types in cereal culm internode tissues (TS). a, Internodes near the base of a culm frequently had a parenchymatous hypoderm. b, Further up the culm the parenchymatous hypoderm was not present, instead only the sclerenchymatous hypoderm was present.

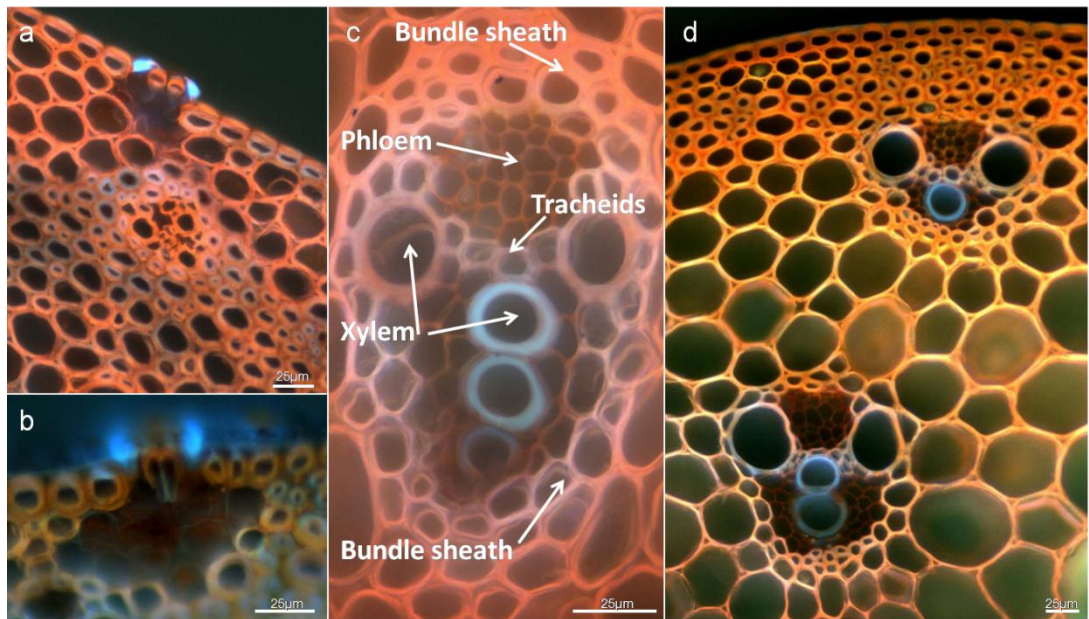


Figure 4.20. Stomata and vascular bundles in cereal internode tissues (TS). a and b, Stomata with lacunae beneath. c, Cell types in a typical internodal vascular bundle. d, Position of vascular bundles within internodal tissues.

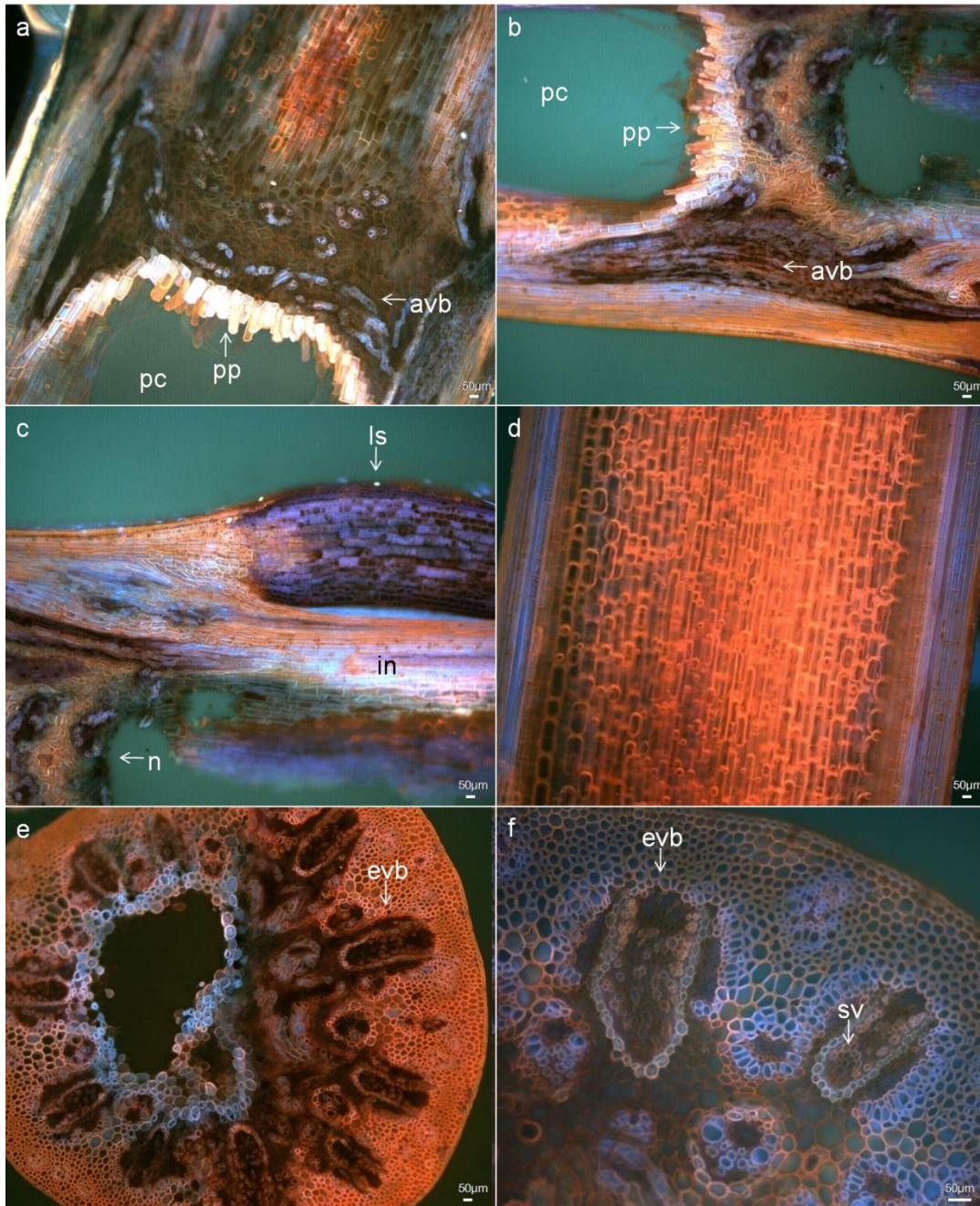


Figure 4.21. General anatomy of cereal nodal tissue. a and b, Formation of the pith plexus (pp) above the pith cavity (pc) allows anastomosing vascular bundles (avb) to form into the next internode and leaf sheath tissues (LSn). c, Above the node (n) the next internode (in) and leaf sheath (ls) tissue become fully formed (LSn). d, Internode tissue (LSn). The anatomy is much simpler than nodal tissue. e and f, Elongated vascular bundles (evb) form during node formation, while the pith cavity becomes solid pith tissue (TS). Cell tissues in the vascular layer of the node also became much darker. Vascular bundles do not keep the typical anatomy of internodal vascular bundles, with large xylem vessels becoming multiple smaller vessels (sv), distinguishable from phloem by their more intense fluorescence.

4.3.6.2 Culm Infection

Initial penetration appeared to occur around the level of the crown and secondary root traces. This was generally penetration of the epidermis. Actual penetration events were not clearly observed, however, it is believed that penetration was effected by appressoria-like swellings of hyphal tips, as described for LS tissue. In some cases, particularly for the field grown wheat, infection may have occurred at a lower level, perhaps through the SCI as hyphae were observed inside the pith but not in the outer cortex. Hyphal proliferation was frequently observed around emerging secondary roots. Further up the culm, as in LS material, initial lesion formation was also observed to occur at stomata (Figure 4.22a, b, c, d, e). This is not considered the main method of penetration, however, when infected LSs remained in close contact with the culm, lateral penetration did occur.

Infection of the different cell layers and types was recorded for multiple culms (Table 4.3). A summary of the presence of hyphae is displayed in Figure 4.23, Figure 4.24, Figure 4.25, Figure 4.26 and Figure 4.27.

Table 4.3. Number of culms sectioned for microscopic assessment.

Weeks after planting	Number of Culms Sectioned		
	10	16	22
2-49	2	15	2
Puseas	3	18	2
Grimmett	4	3	2
Bellaroi	3	3	2
Sunland	-	4	-
Vasco	-	6	-

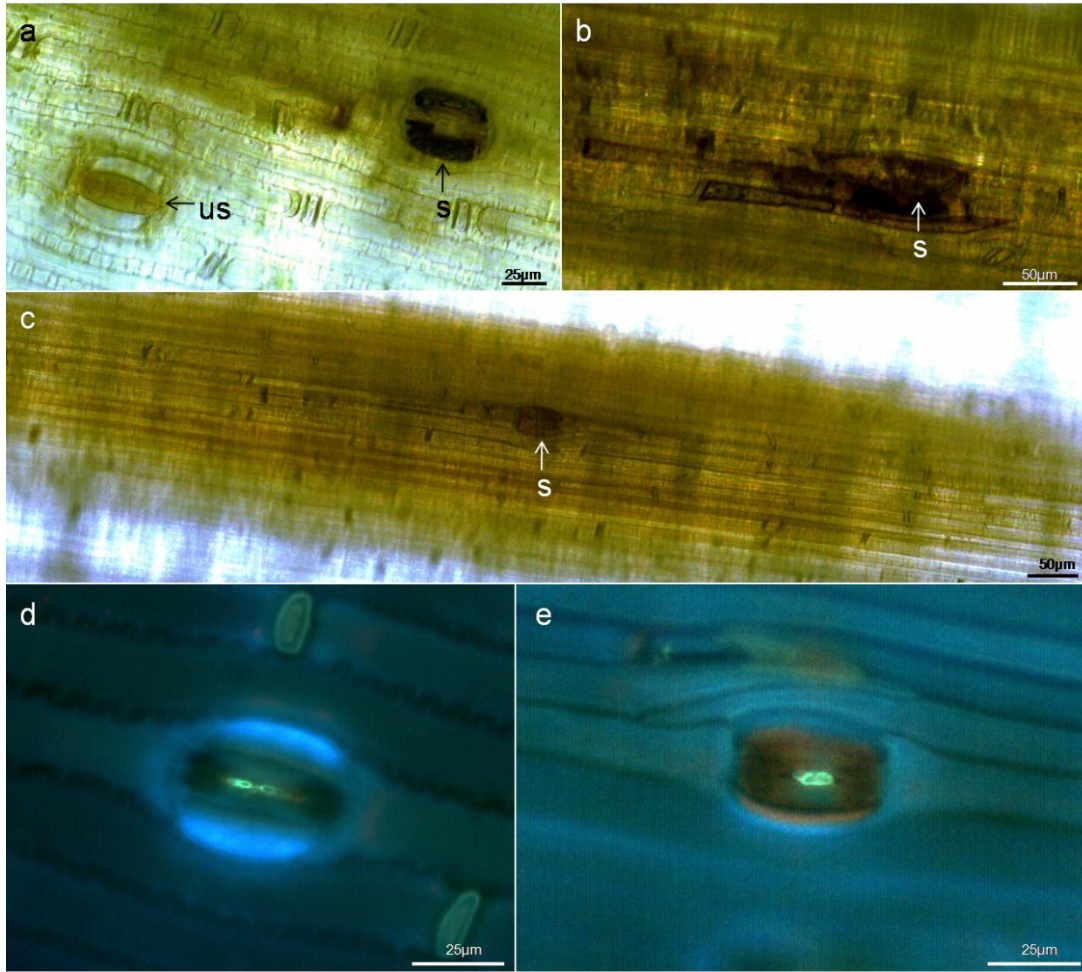


Figure 4.22. Initial lesions formation of internodal tissue could occur at stomata (SV). The affected stomata had been penetrated by *Fp* hyphae. a, b and c, Lesions initiating at stomata (s) (Sun). Unaffected stomata (us) did not have discoloration. a, b and c were viewed directly under bright field microscopy. d and e, Discoloured stomata were associated with hyphae (Sun).

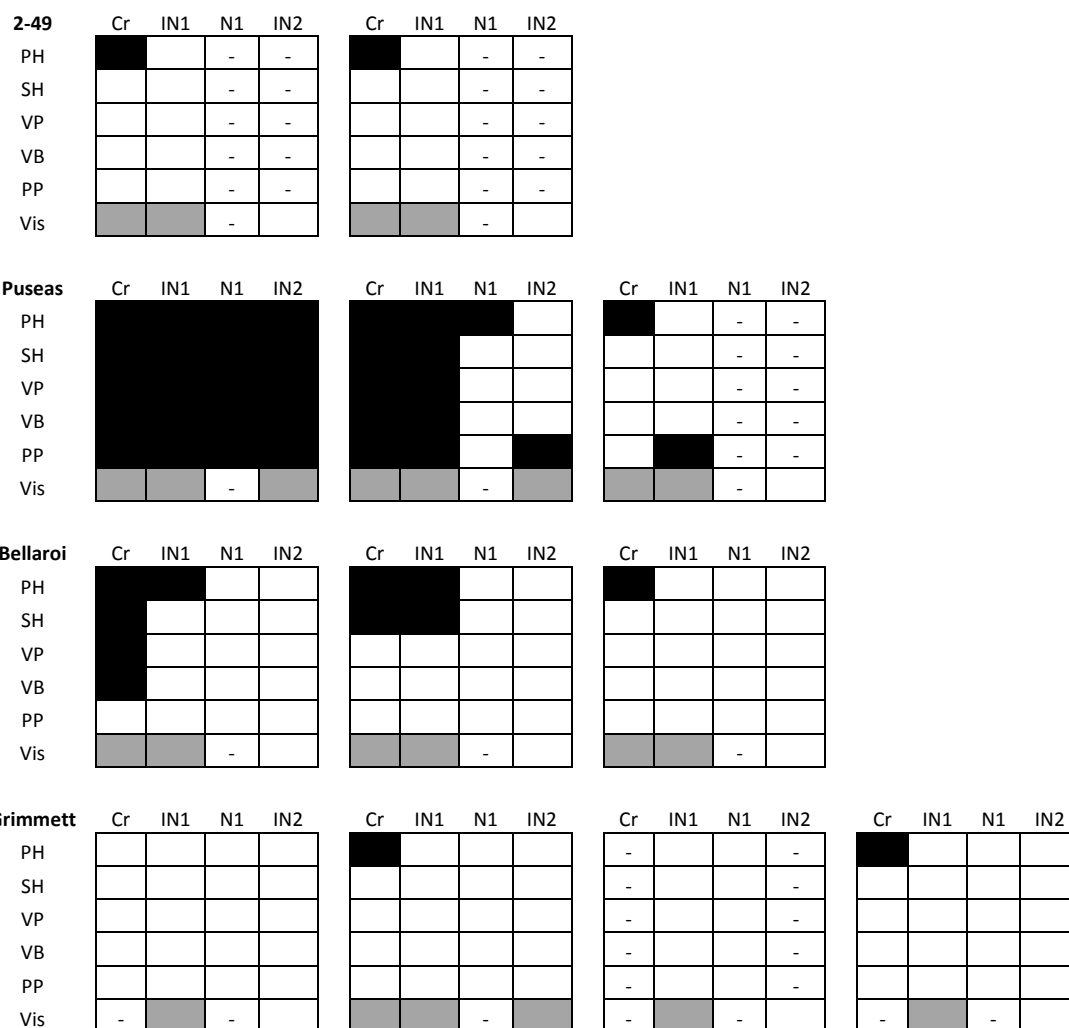


Figure 4.23. Summary of culm infection by *Fp* at 10 WAP in four cereal genotypes. Each individual box represents the primary culm of an infected plant. Black indicates hyphae were observed; grey indicates brown discoloration was observed visually before sectioning; white indicates absence of hyphae or discoloration. A dash indicates this tissue was either not observed or absent. Tissues assessed were parenchymatous hypoderm (PH), sclerenchymatous hypoderm (SH), vascular parenchyma, (VP), vascular bundle (VB), pith parenchyma (PP) and visual discoloration (Vis).

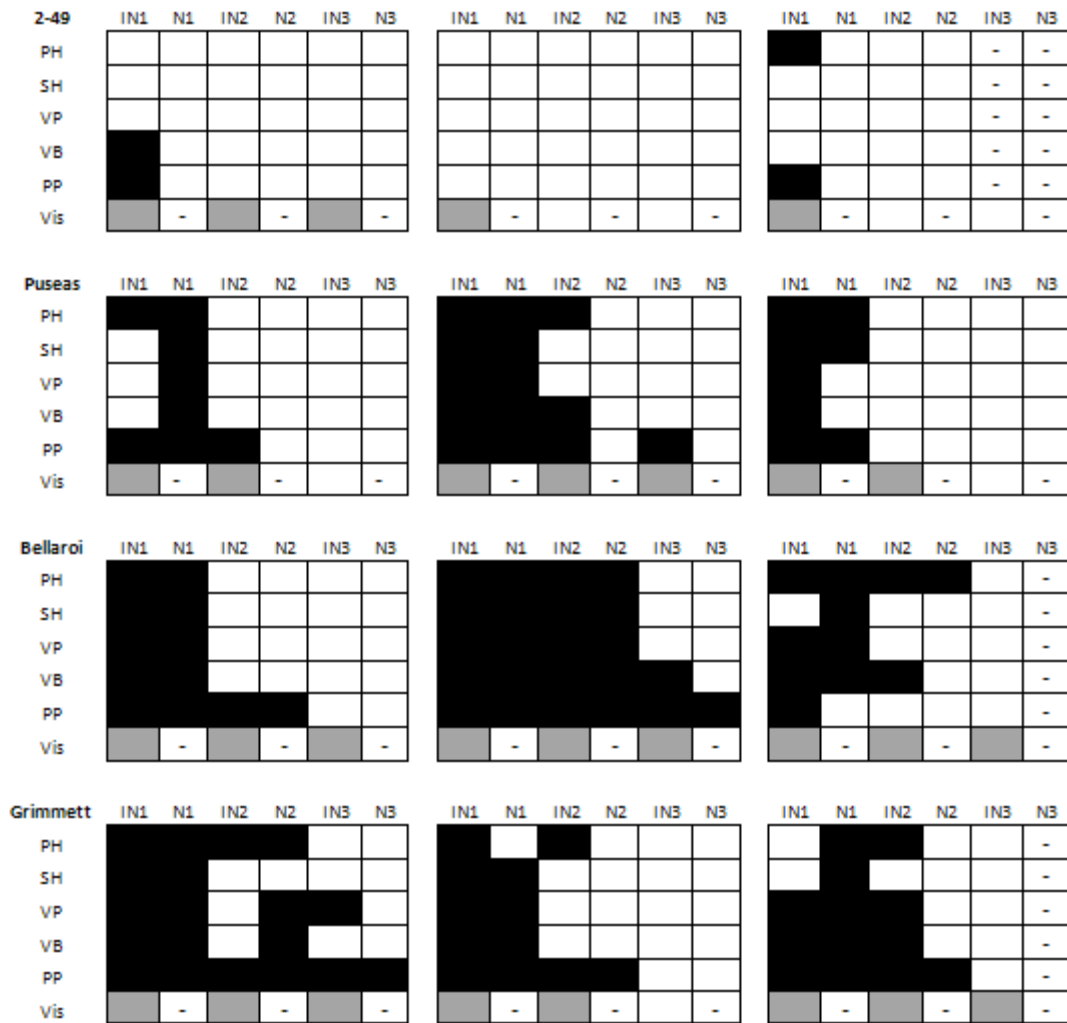


Figure 4.24. Summary of culm infection by *Fp* at 16 WAP in four cereal genotypes. Each individual box represents the primary culm of an infected plant. Black indicates hyphae were observed; grey indicates brown discoloration was observed visually before sectioning; white indicates absence of hyphae or discoloration. A dash indicates this tissue was either not observed or absent. Tissues assessed were parenchymatous hypoderm (PH), sclerenchymatous hypoderm (SH), vascular parenchyma, (VP), vascular bundle (VB), pith parenchyma (PP) and visual discoloration (Vis).

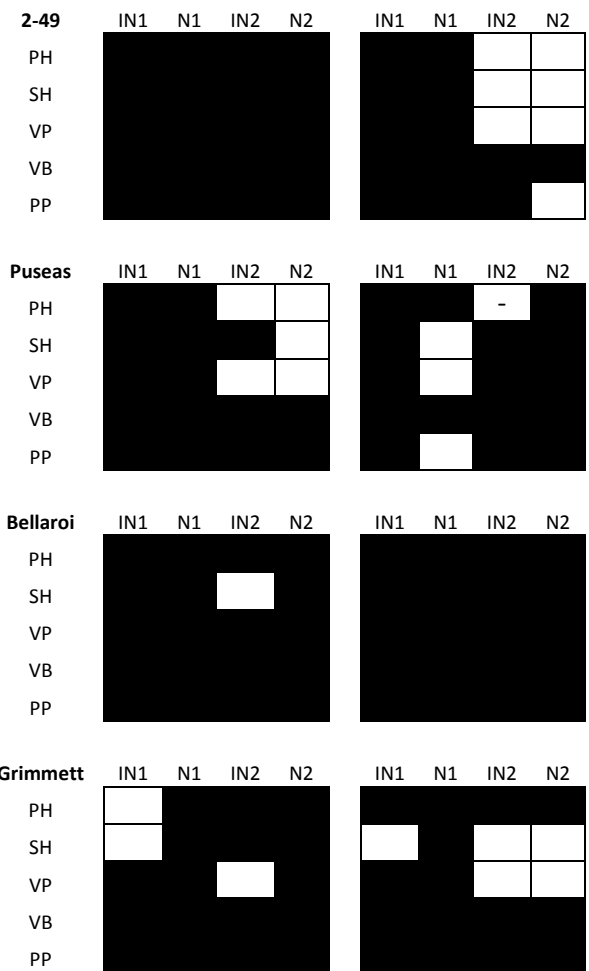


Figure 4.25. Summary of culm infection by *Fp* at 22 WAP in four cereal genotypes. Each individual box represents the primary culm of an infected plant. Black indicates hyphae were observed; grey indicates brown discoloration was observed visually before sectioning; white indicates absence of hyphae or discoloration. A dash indicates this tissue was either not observed or absent. Tissues assessed were parenchymatous hypoderm (PH), sclerenchymatous hypoderm (SH), vascular parenchyma, (VP), vascular bundle (VB), pith parenchyma (PP) and visual discoloration (Vis).

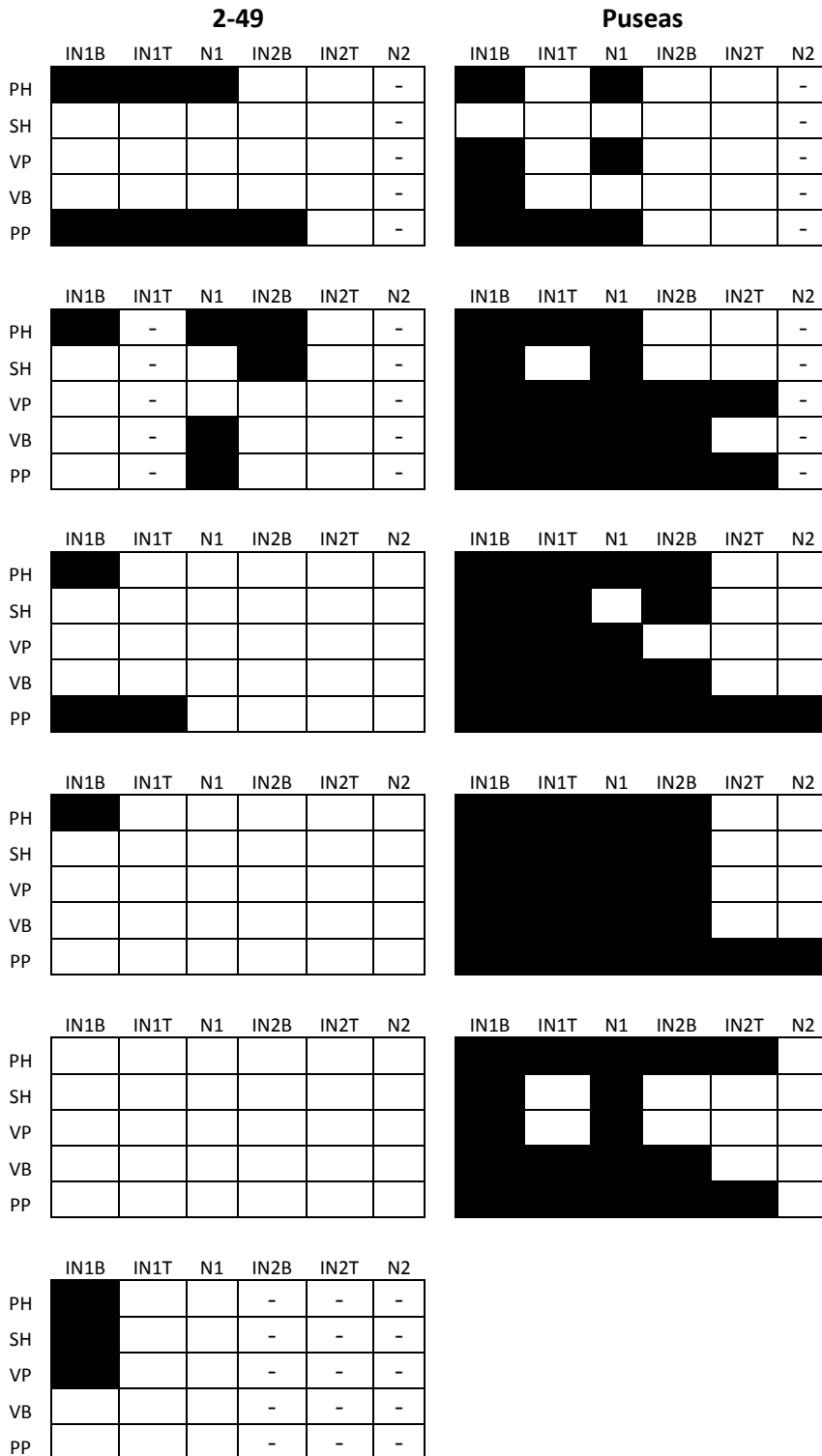


Figure 4.26. Summary of culm infection by *Fp* at 16 WAP of 2-49 and Puseas grown at the LRC. Each individual box represents the primary culm of an infected plant. Black indicates hyphae were observed; grey indicates brown discoloration was observed visually before sectioning; white indicates absence of hyphae or discoloration. A dash indicates this tissue was either not observed or absent. Where a B or T follows the tissue type, e.g. IN1B or IN1T, these letters indicate either the bottom (B) or top (T) third of the tissue. Tissues assessed were parenchymatous hypoderm (PH), sclerenchymatous hypoderm (SH), vascular parenchyma, (VP), vascular bundle (VB), pith parenchyma (PP) and visual discoloration (Vis).

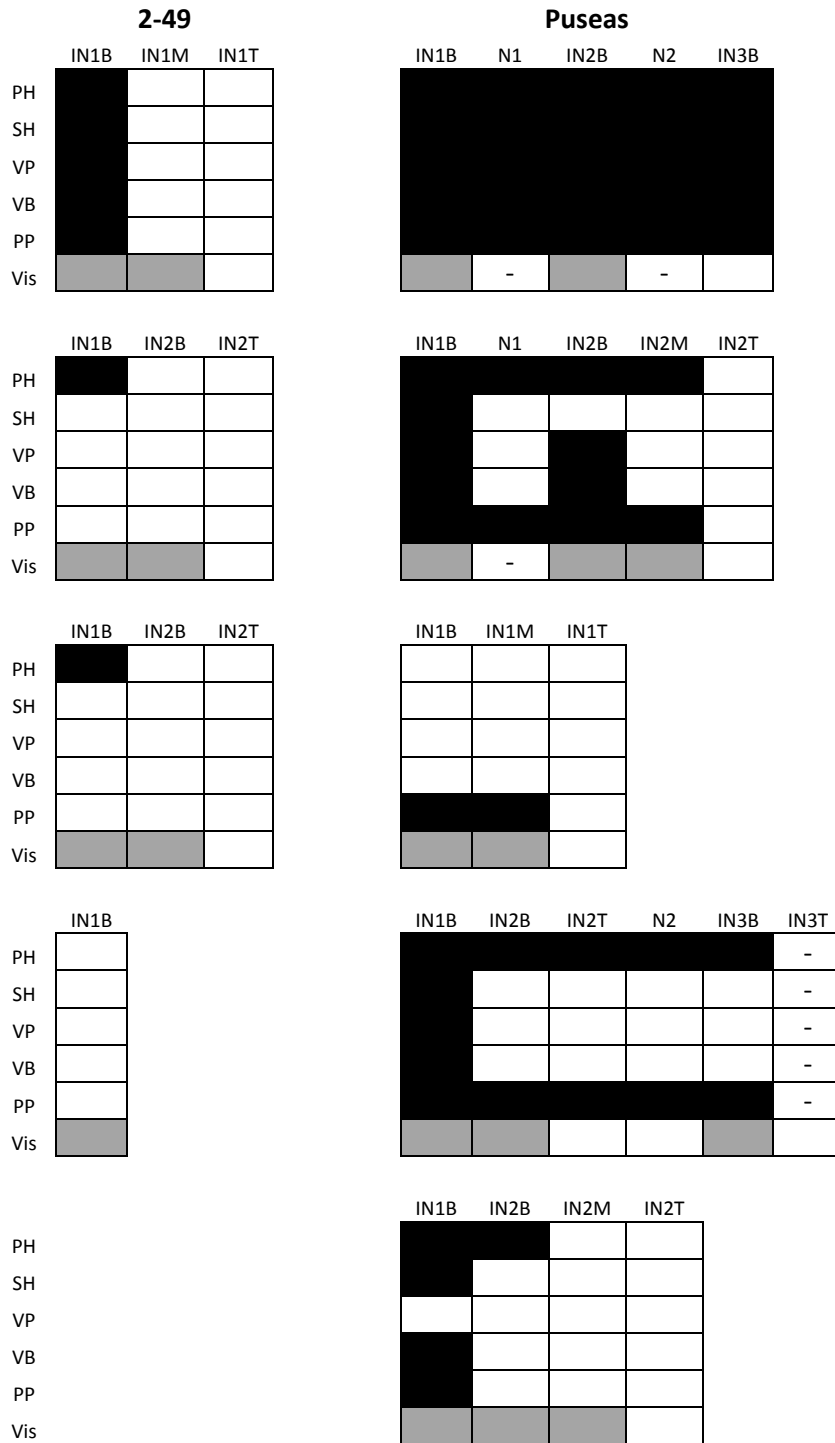


Figure 4.27. Summary of culm infection by *Fp* at 16 WAP of 2-49 and Puseas grown in the greenhouse. Each individual box represents the primary culm of an infected plant. Black indicates hyphae were observed; grey indicates brown discoloration was observed visually before sectioning; white indicates absence of hyphae or discoloration. A dash indicates this tissue was either not observed or absent. Where a B, M or T follows the tissue type, e.g. IN1B or IN1T, these letters indicate either the bottom (B), middle (M) or top (T) third of the tissue. Tissues assessed were parenchymatous hypoderm (PH), sclerenchymatous hypoderm (SH), vascular parenchyma, (VP), vascular bundle (VB), pith parenchyma (PP) and visual discoloration (Vis).

4.3.6.2.1 Summary of Observations

Few clear patterns of infection were observed. However, some events did occur frequently. All cell types within a wheat plant could be penetrated and colonised, which depended on the severity of infection rather than the host genotype. Certain cells, such as those of the sclerenchymatous hypoderm, became colonised much later in the infection process than parenchymatous cells.

Epidermal cells were predominantly intracellularly colonised (Figure 4.28a, b, c). This was typically more prevalent in the lower parts of the culm, that is, IN1 and 2. Hyphae were also frequently observed to be under the epidermis but not in the epidermal tissues (Figure 4.28d). Hyphae were infrequently observed on the surface of epidermal cells.

Cells of the parenchymatous hypoderm were colonised predominantly by intracellular hyphae, with these cells typically appearing distorted and discoloured when colonised (Figure 4.29a, b, c, d). Hyphae were frequently observed to proliferate in discoloured parenchyma cells surrounding secondary root traces. Sub-stomatal lacunae and lacunae in the parenchymatous hypoderm commonly supported hyphal growth (Figure 4.29e, f, g, h). It was observed that cells of the parenchymatous hypoderm rapidly became discoloured and it is believed that the visible brown discolouration used for visual rating for resistance is due to discolouration of this cell layer. Initial discolouration of cells, particularly of the parenchymatous hypoderm, was not always associated with visible hyphae in or adjacent to these cells. Visual rating of the 10 and 16 week old plants demonstrated that discolouration could precede hyphal infection of the hypoderm. In some cases the hypoderm was rated as slightly discoloured but hyphae were only present in the pith.

The sclerenchymatous hypoderm was frequently observed to be absent of hyphae during initial stages of infection and sometimes appeared to act as a barrier to lateral growth between the epidermis and the vascular layer or pith (Figure 4.30a). When hyphae, which were only intracellular, were observed in the sclerenchymatous hypoderm the cells did not appear to become significantly discoloured (Figure 4.30b, c, d).

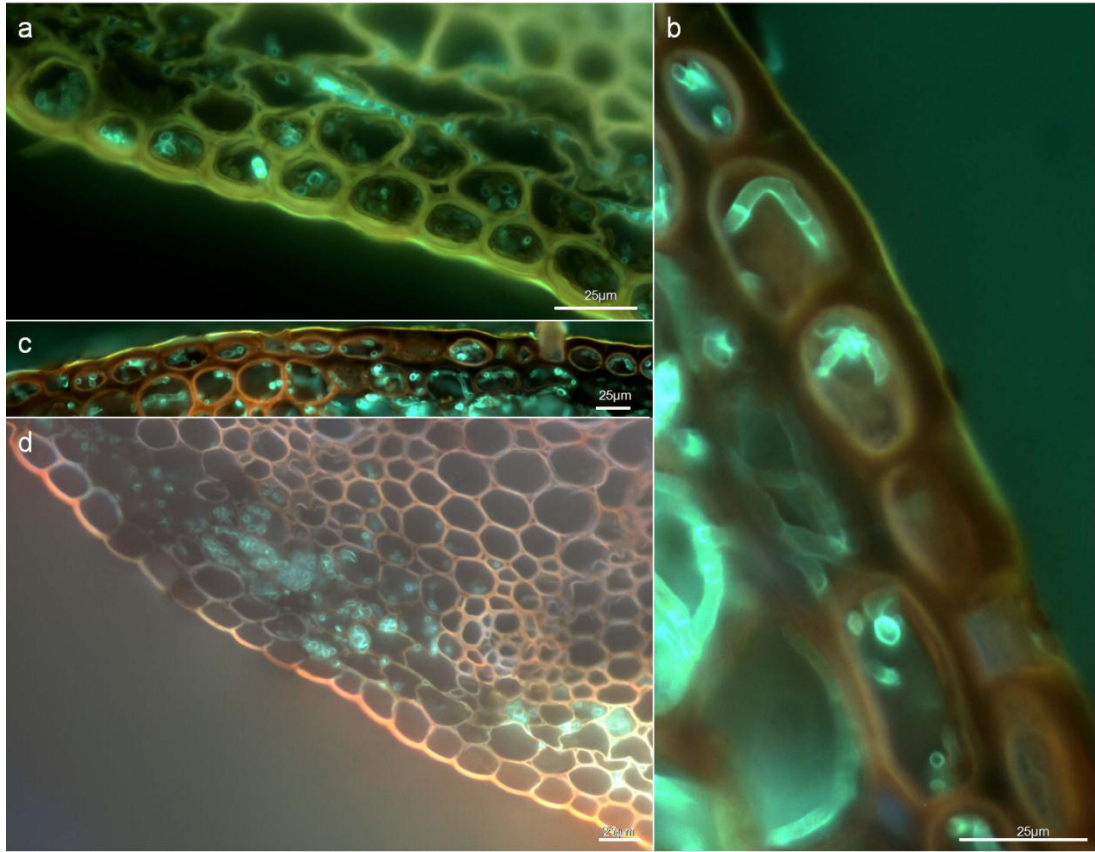


Figure 4.28. *Fp* hyphae intracellularly colonised epidermal tissues (TS). a, b and c, Intracellular hyphae in epidermal tissue and in the parenchymatous hypoderm (Sun). d, Hyphae colonising the parenchymatous hypoderm but not the epidermis (P).

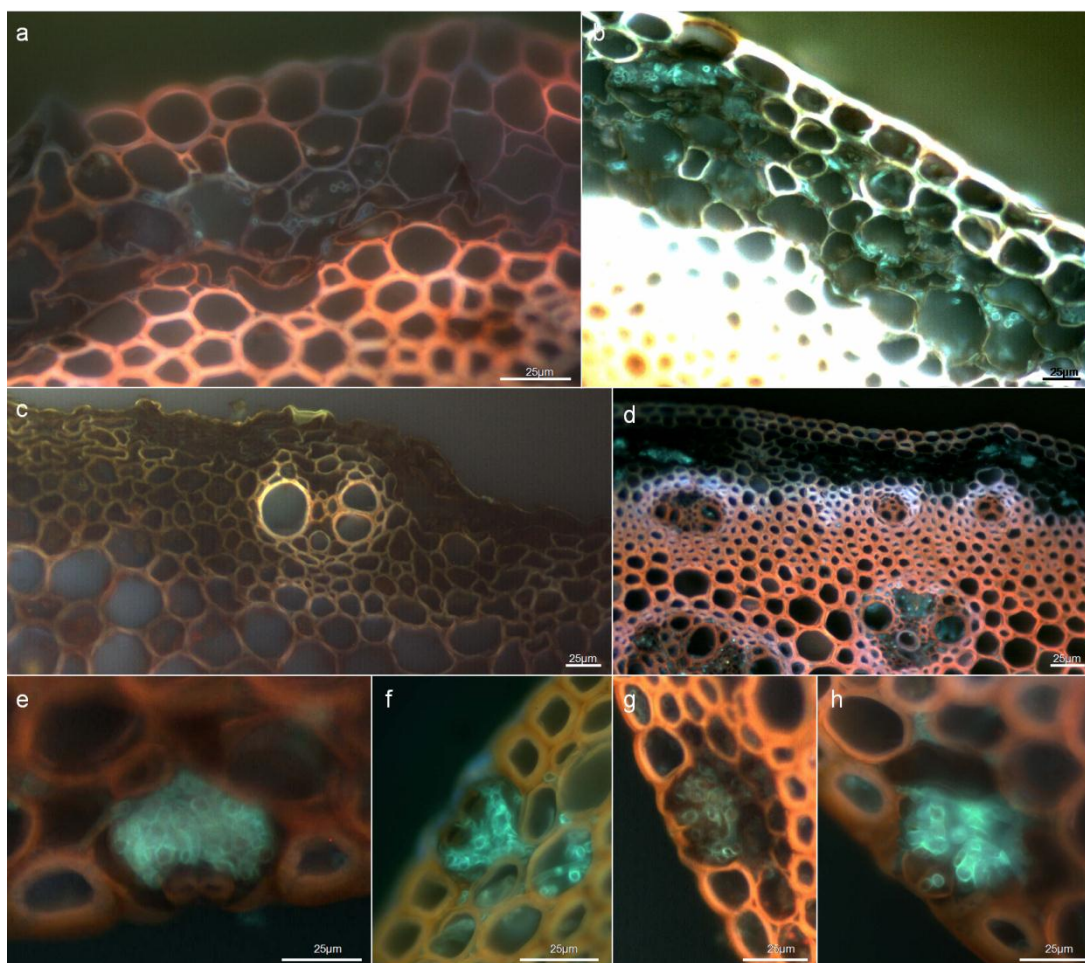


Figure 4.29. Parenchymatous hypoderm was colonised by intracellular *Fp* hyphae (TS). These cells frequently appeared distorted and discoloured during colonisation. a and b, Colonised parenchymatous hypoderm displaying distorted and discoloured cells (2-49 and P, respectively). c, discoloured and distorted cells in the parenchymatous hypoderm above the infection edge (P). d, Colonised parenchymatous hypoderm displaying a great level of discoloration compared to the sclerenchymatous hypoderm and vascular parenchyma (P). e-h, Colonisation of stomata and associated lacunae (P, Sun, P, and P, respectively).

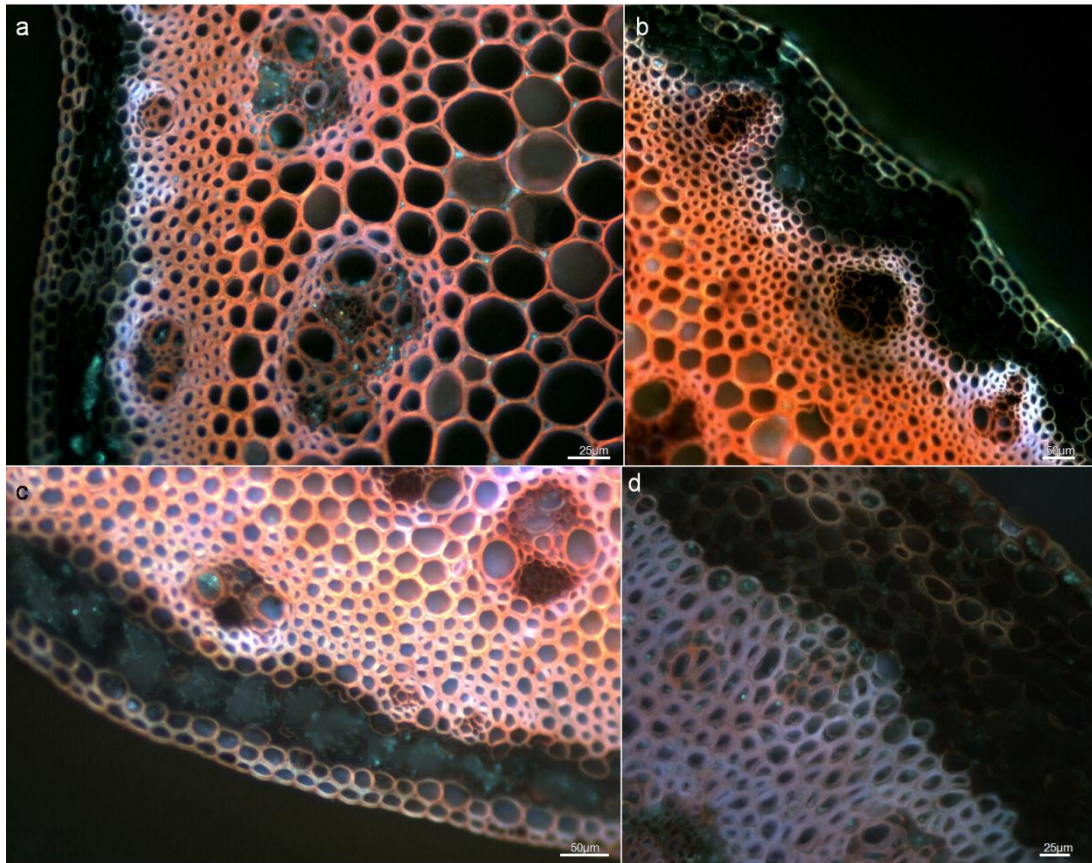


Figure 4.30. Colonisation of the sclerenchymatous hypoderm by *Fp* (TS). a and b, Colonisation occurring through two separate areas, the parenchymatous hypoderm and pith/vascular parenchyma (P). The sclerenchymatous hypoderm has not been colonised (P). c and d, Hyphae have colonised the sclerenchymatous hypoderm however the cells have not become discoloured or distorted. (P and B, respectively).

By 16 WAP vascular bundles were frequently colonised for all genotypes except 2-49. Colonisation differed between vascular bundles, with xylem, phloem and tracheids all potentially being colonised (Figure 4.31a, b, c, d and Figure 4.32). No preference for one cell type was observed, however, the phloem sometimes became colonised more obviously than the xylem and tracheids. Large xylem vessels infrequently became occluded by hyphae (Figure 4.31e). Infected cells of the vascular bundles did not appear discoloured. The parenchyma cells surrounding the large vascular bundles were both inter- and intracellularly colonised and could become discoloured. At maturity the phloem cells appeared to have disintegrated in some culms (Figure 4.31f).

Initial infection of the pith was by intercellular hyphae, which later became intracellular (Figure 4.33a, b, c, d, e, f, g). During infection these cells frequently became distorted and discoloured. The pith cavity supported large growths of hyphae, which were particularly obvious in the INs of culms with deadheads, where the pith cavity could be a solid mycelial mass (Figure 4.34).

Nodal tissue showed variable colonisation (Figure 4.35a, b, c, d, e, f and Figure 4.36a, b, c, d). The pith plexus, where pith becomes solid at node base up to node top, included various pith cell types. At the node base the pith region formed very thick walled cells whereas typical pith cells were present towards the top of the node (Figure 4.37a, b, c, d, e, f and Figure 4.38a, b, c, d, e, f, g). These thick walled pith cells appeared to be resistant to penetration, however the layer of more typical pith cells above it could be colonised, perhaps by lateral growth of hyphae from the vascular layer. Vascular bundles were frequently colonised. The anatomy of nodal tissue was extremely complicated and made tracing of hyphae through the tissues difficult.

A frequent observation was of intense patches of infection on one side of a culm, sometimes extending from the crown to IN2. These patches could have hyphae in all cell types, while the other side of the culm could be free of hyphae. As colonisation decreased either towards one side of the culm or upwards in the culm, it was observed that infection was predominantly spreading from two separate areas, the pith and the hypoderm. At higher points on the culm the pith was most frequently the tissue initially colonised.

Hyphae predominantly grew vertically. Horizontal growth was more frequent in parenchyma cells during intense infection and penetration of cells walls was

facilitated by hyphal swellings and appressoria-like structures, followed by penetration through the cell wall via a penetration peg (Figure 4.39a, b). No difference in hyphal widths was observed in culm tissues between genotypes (Table 4.4).

Table 4.4. Minimum and maximum hyphal widths observed within the culm tissue of four cereal genotypes. For the purpose of the mean and standard error (SE) n = 12. No significant differences were reported using the Tukey multiple comparison test.

Genotype	Hyphal Width (μm)		
	Mean	SE	Range
2-49	4.0	0.4	2.2 – 7.2
Puseas	3.9	0.3	2.2 – 7.2
Grimmett	3.8	0.5	2.1 – 6.7
Bellaroi	4.3	0.3	2.8 – 5.0

Plants harvested at 10, 16 and 22 WAP demonstrated a general increase in infection over time. Puseas was most infected, followed by Bellaroi, Grimmett and 2-49. Intensity of infection of each individual culm was the greatest variable. In plants harvested at 22 WAP hyphae displaying no fluorescence were observed, these were believed to be dead hyphae (Figure 4.31f). Vascular parenchyma and xylem vessels were infrequently observed to be filled with a dense black mass at 22 WAP, which had no obvious structure (Figure 4.39c, d). This was observed in all genotypes except 2-49. Hyphae were frequently observed to colonise the leaf trace forming from node 1 and occasionally in the leaf trace from node 2 (Figure 4.40a, b, c, d). The colonisation of this material depended on the colonisation of the hypoderm in tissues below, as this is where the cells of the leaf trace originated. Colonisation was most frequently in the cortical cells of the leaf trace but vascular bundles were able to be colonised during severe infection.

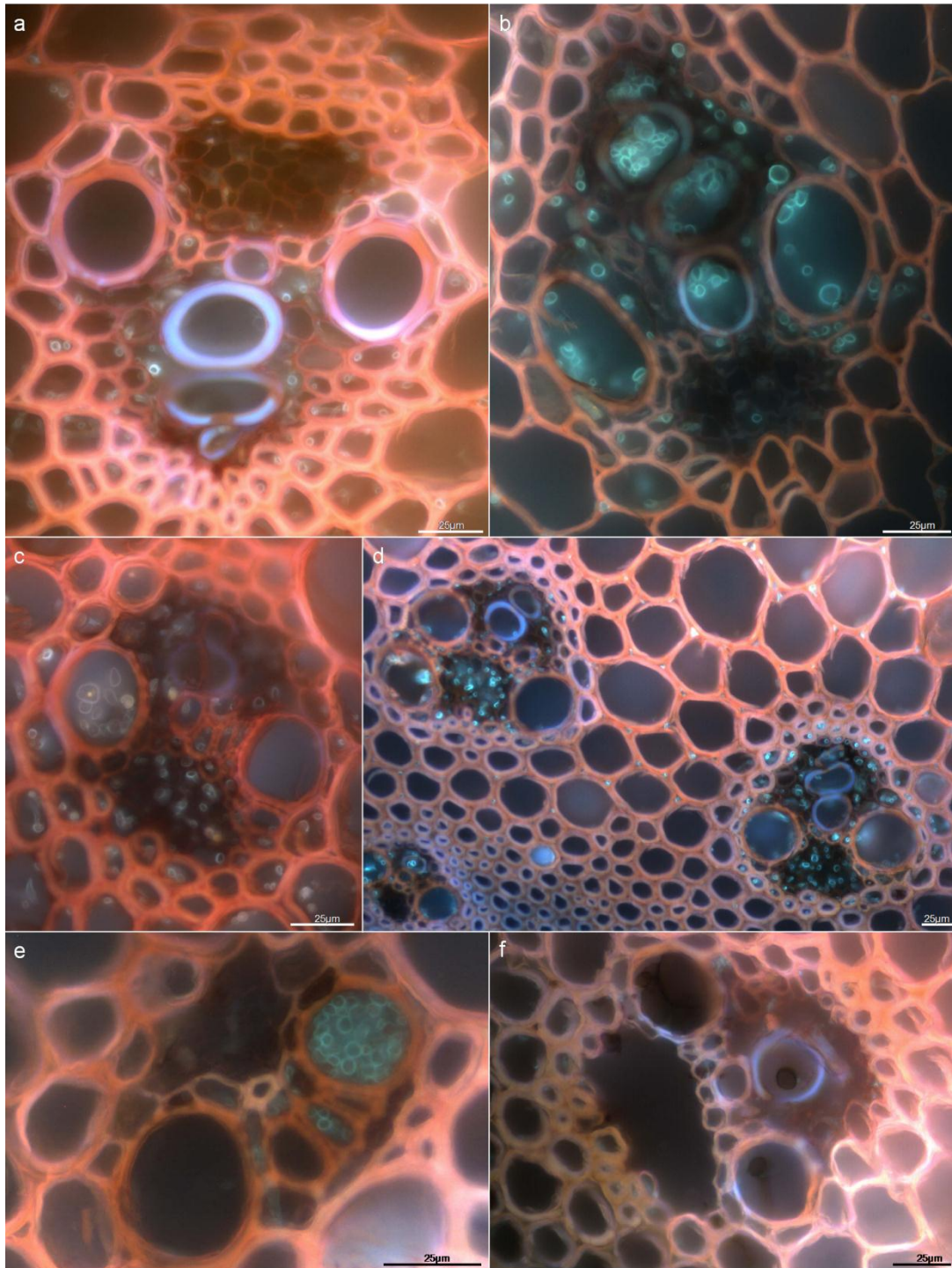


Figure 4.31. *Fp* colonisation of vascular tissues occurred in all cell types (TS). a-d, Colonisation of vascular tissues (P). e, Large xylem vessels infrequently became occluded by hyphae (P). f, Disintegrated phloem cells in a vascular bundle of a mature culm (P). The dark hyphae are dead.

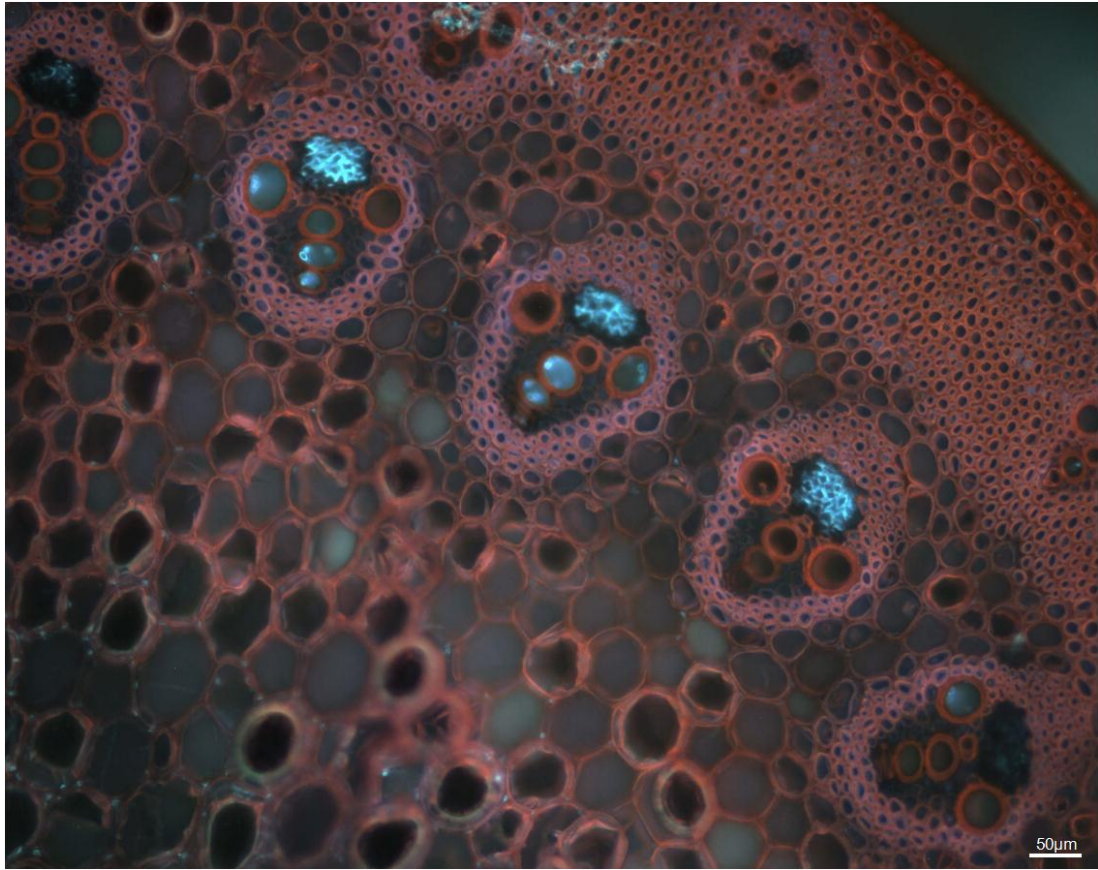


Figure 4.32. Colonisation of phloem vessels by *Fp* in internode tissue (TS, B).

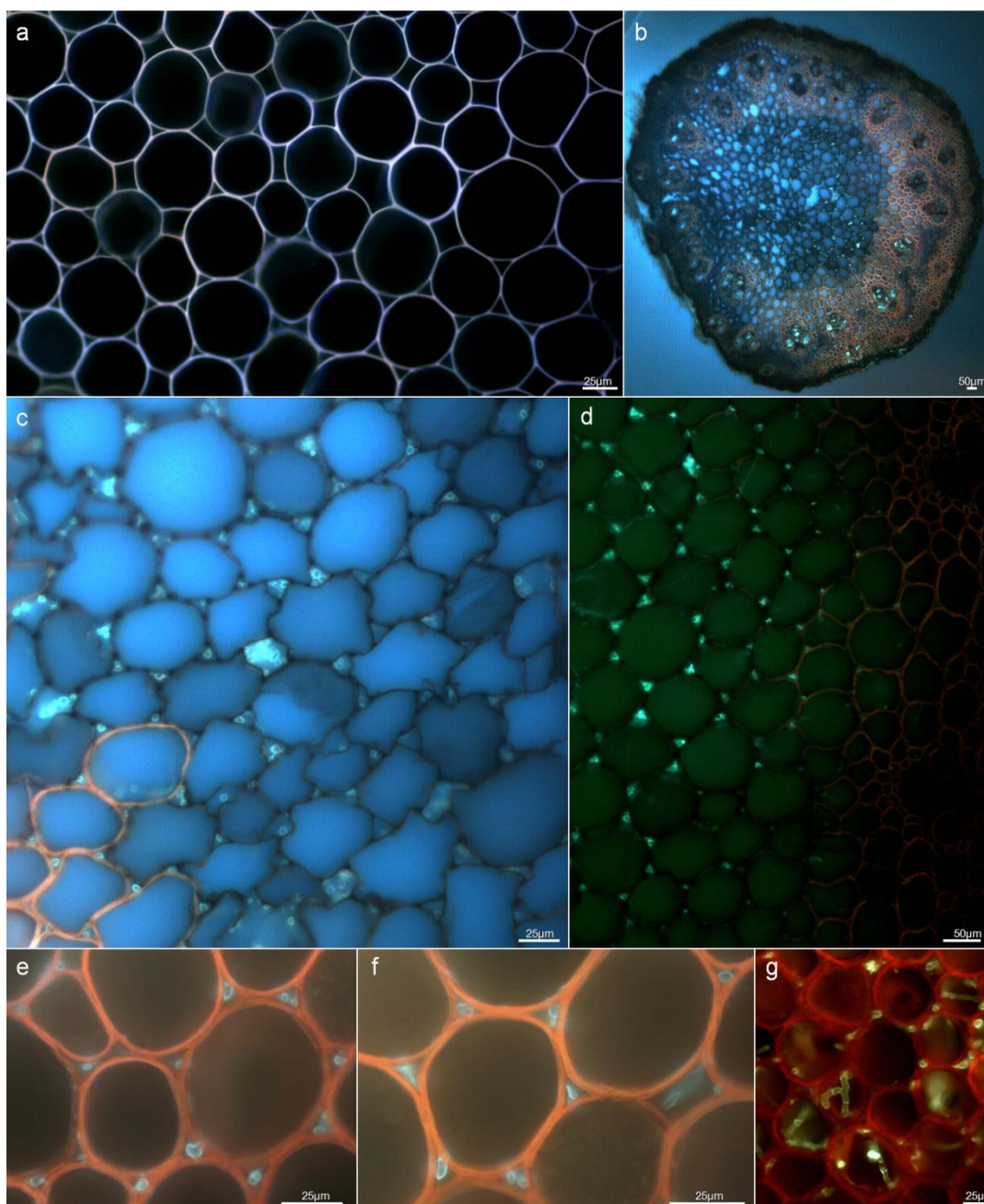


Figure 4.33. Infection of pith cells by *Fp* (TS). a, Uninfected pith parenchyma (V). b, Colonisation of a culm base (P). The pith cells are greatly discoloured. c and d, Colonisation of pith parenchyma was initially intercellular (P). The cells became greatly distorted and discoloured. e and f, Intercellular colonisation of pith parenchyma (P). g, Inter- and intracellular colonisation of pith parenchyma (Sun).

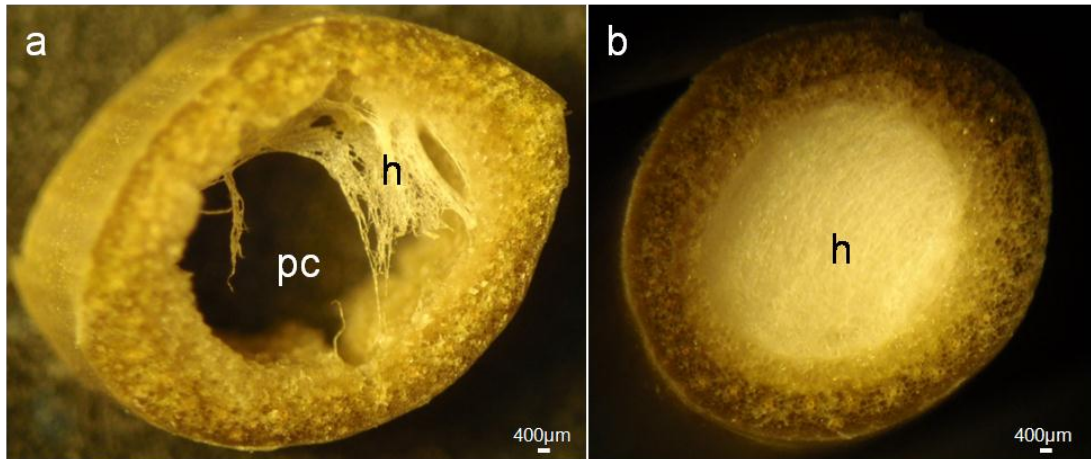


Figure 4.34. Colonisation of the pith cavity by *Fp* (TS). a, Hyphae (h) grew across the pith cavity (pc) (V). b, The entire pith cavity could be occluded by hyphae, particularly in dead culms (V). Images were captured using an Olympus μ 1020 digital camera.

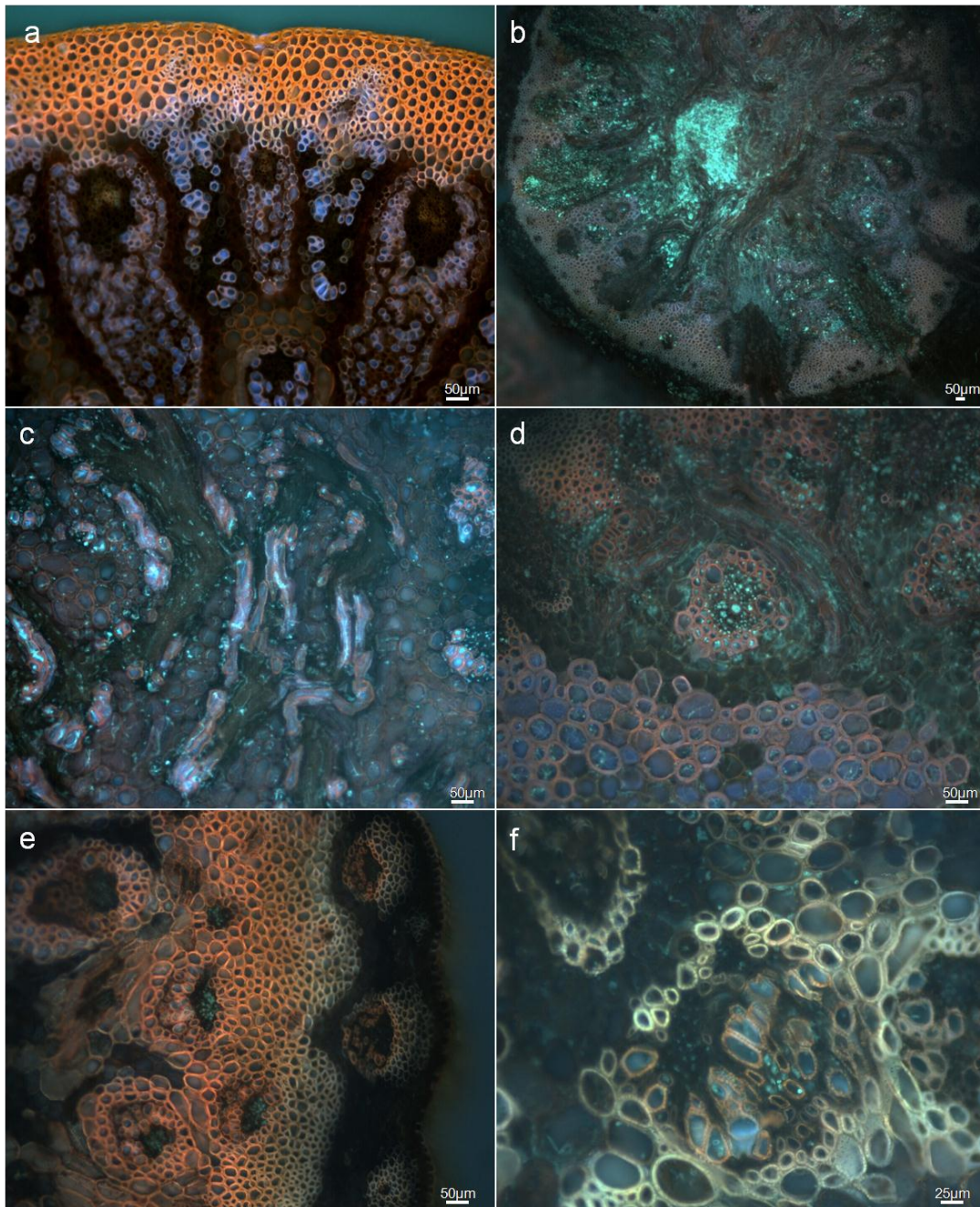


Figure 4.35. Colonisation of nodal tissue by *Fp* (TS). a, Uninfected nodal section (V). Blue colouration of some cells is an artefact of chemical changes occurring in vascular elements during node formation. b, Heavily colonised nodal tissue, with a great density of hyphae in the pith parenchyma (Gr). c, Pith parenchyma tissue was integrated with anastomosing vascular bundles (V). Colonisation occurred throughout the tissue. d, Hyphae colonising all cell types in nodal tissue (Gr). e, Hyphae predominantly colonising the phloem of vascular bundles (Gr). f, Colonisation of vascular tissues in the node (B).

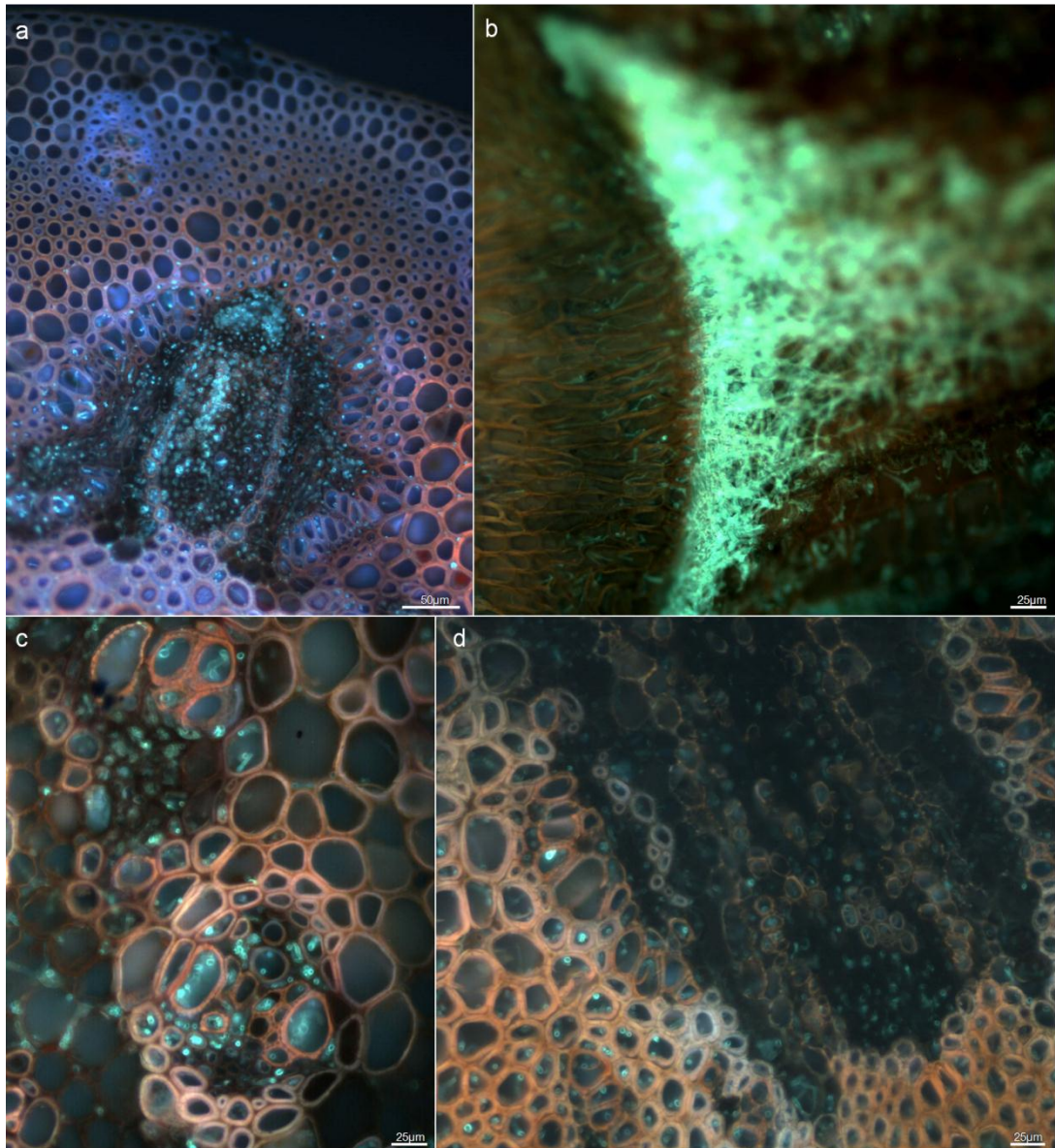


Figure 4.36. Colonisation of cereal nodal tissues by *Fp*. a, Heavy colonisation of an elongated vascular bundle (TS, P). b, Growth of hyphae in the pith cavity below a nodal pith plexus (right) (LSn, Sun). c, Colonised vascular bundles (TS, P). d, Colonised elongated vascular bundle (TS, B). The cells of an elongated vascular bundle frequently had low fluorescence.

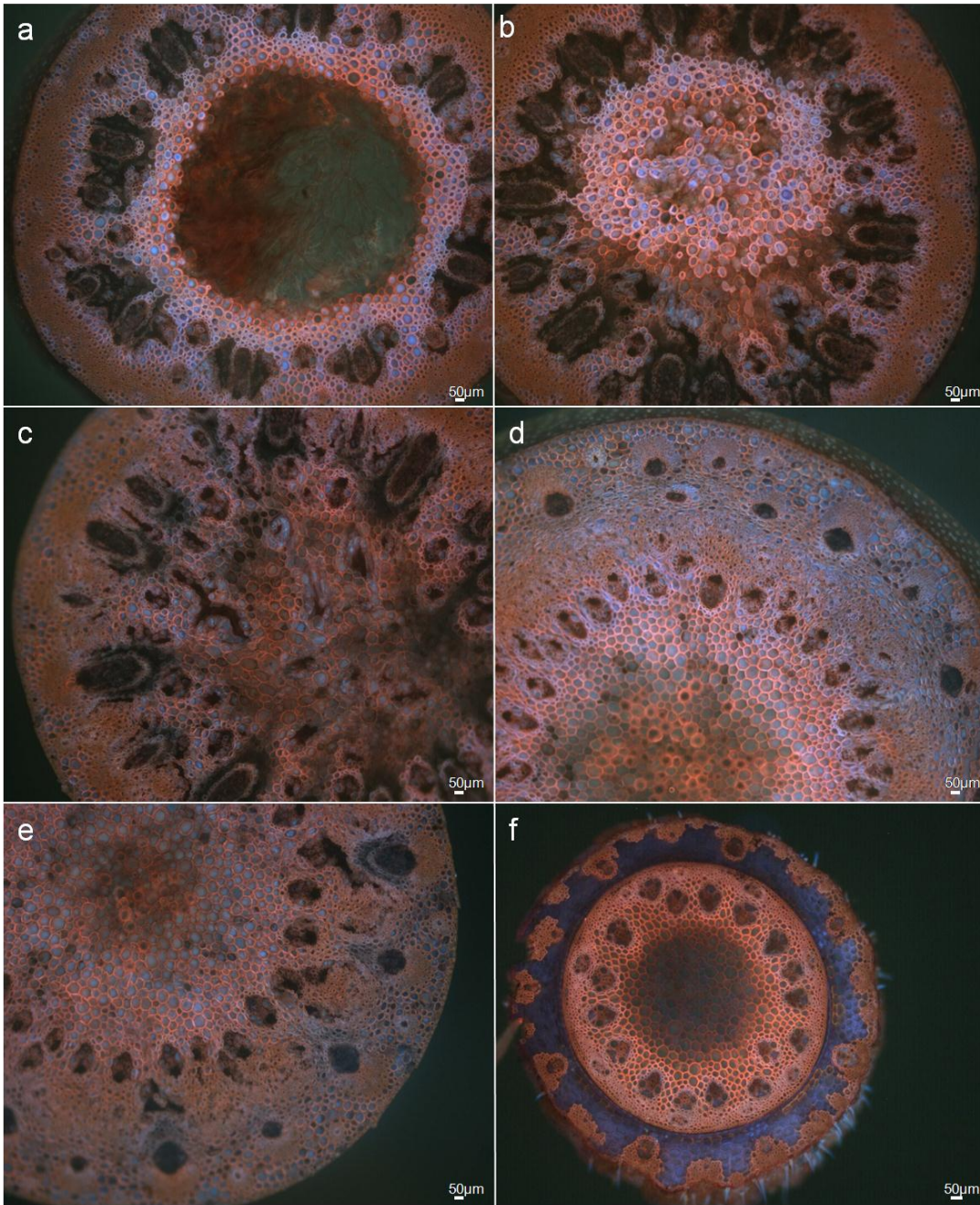


Figure 4.37. Series of sections rising through a lightly infected cereal node (TS). a, Formation of elongated vascular bundles and thick walled pith cells. b, Formation of the pith plexus. c, Formation of anastomosing vascular bundles. d, Beginning of differentiation of the leaf sheath and internodal tissues. e, Further differentiation of leaf sheath and internodal tissues. Leaf trace bundles are obvious. f, Fully formed leaf sheath and internodal tissues.

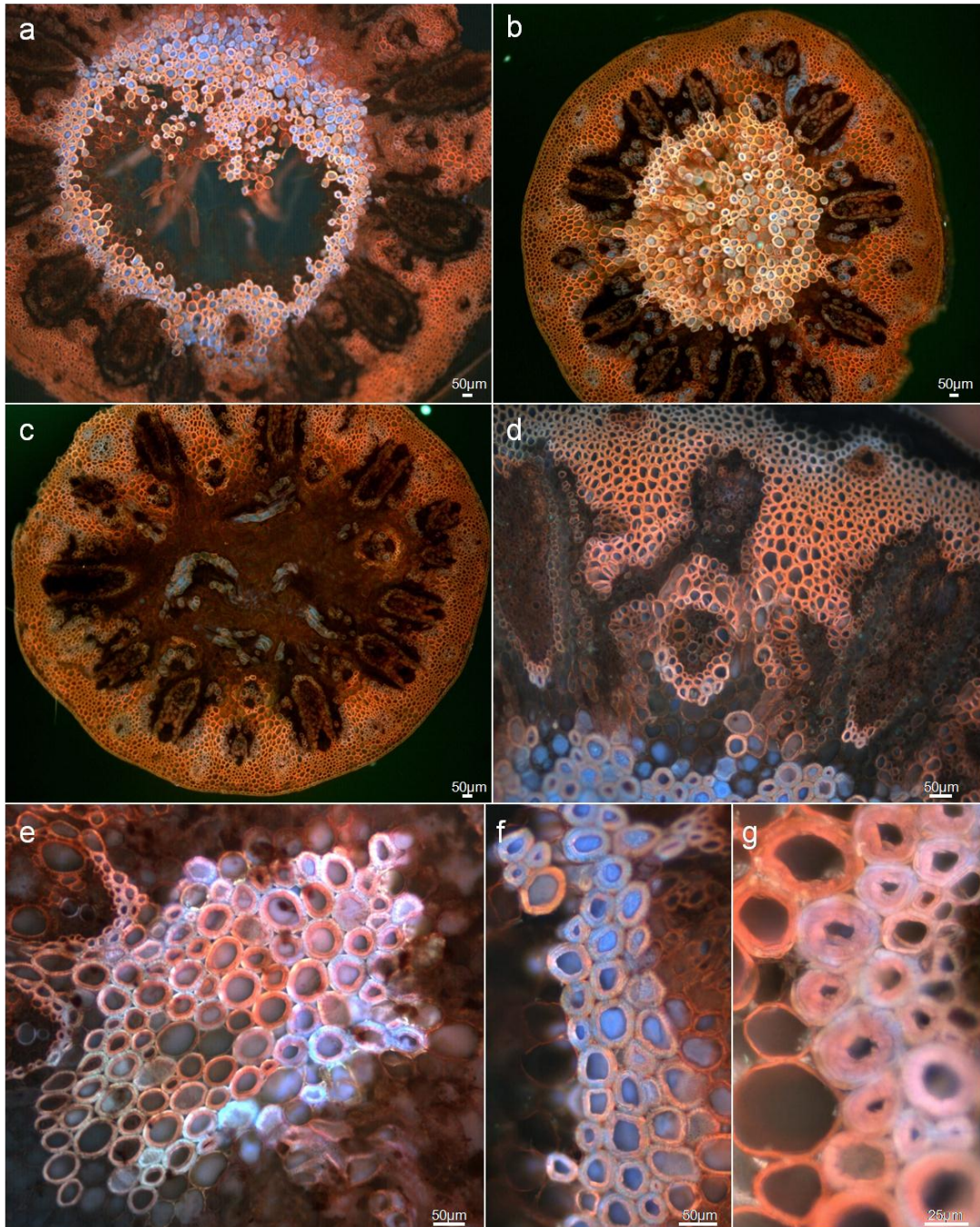


Figure 4.38. Thick walled pith cells (TS). a and b, The thick walled cells have intense fluorescence (Gr and V, respectively). They are located at the base of a node where the pith plexus initiates. c, The thick walled cells are generally only one layer thick and immediately above them anastomosing vascular bundles form (V). d, The thickness and fluorescence of the cell walls of the pith cells are much greater than the other cell types (Gr). e, f and g, Various forms of thick walled pith cells (B, Gr and V, respectively).

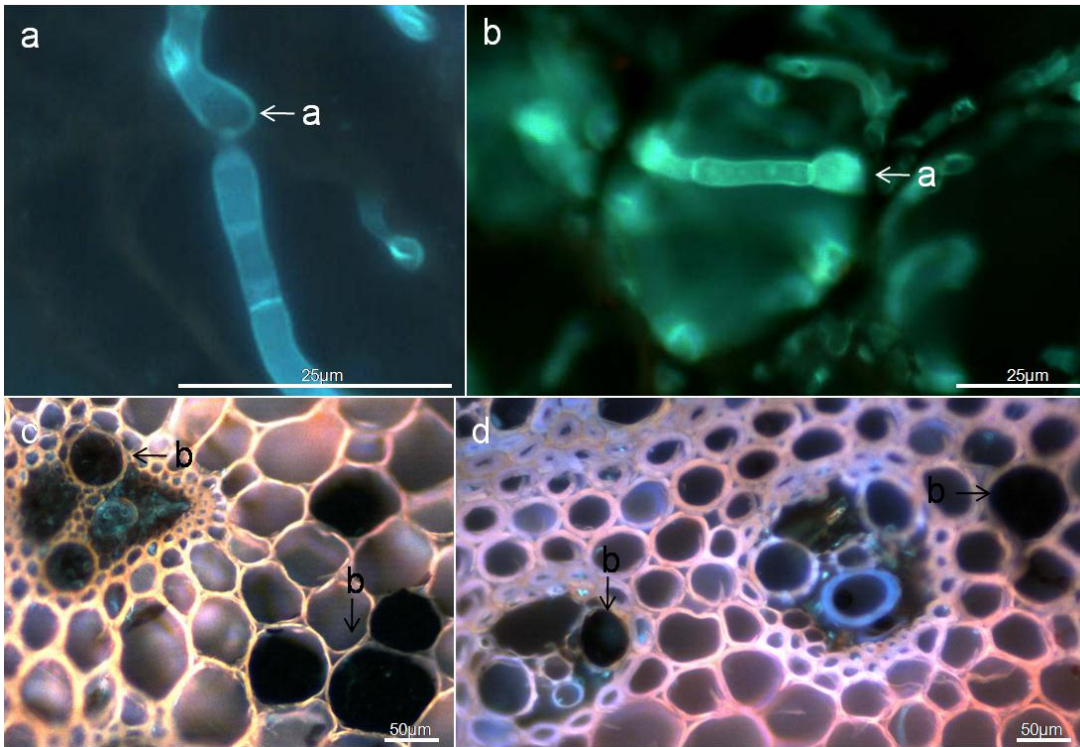


Figure 4.39. a and b, Penetration of cell walls by *Fp* was facilitated by appressoria (a) appearing as swollen hyphal tips (TS, P and Sun, respectively). c and d, Dense black substance (b) filling cells (TS, B and Gr, respectively).

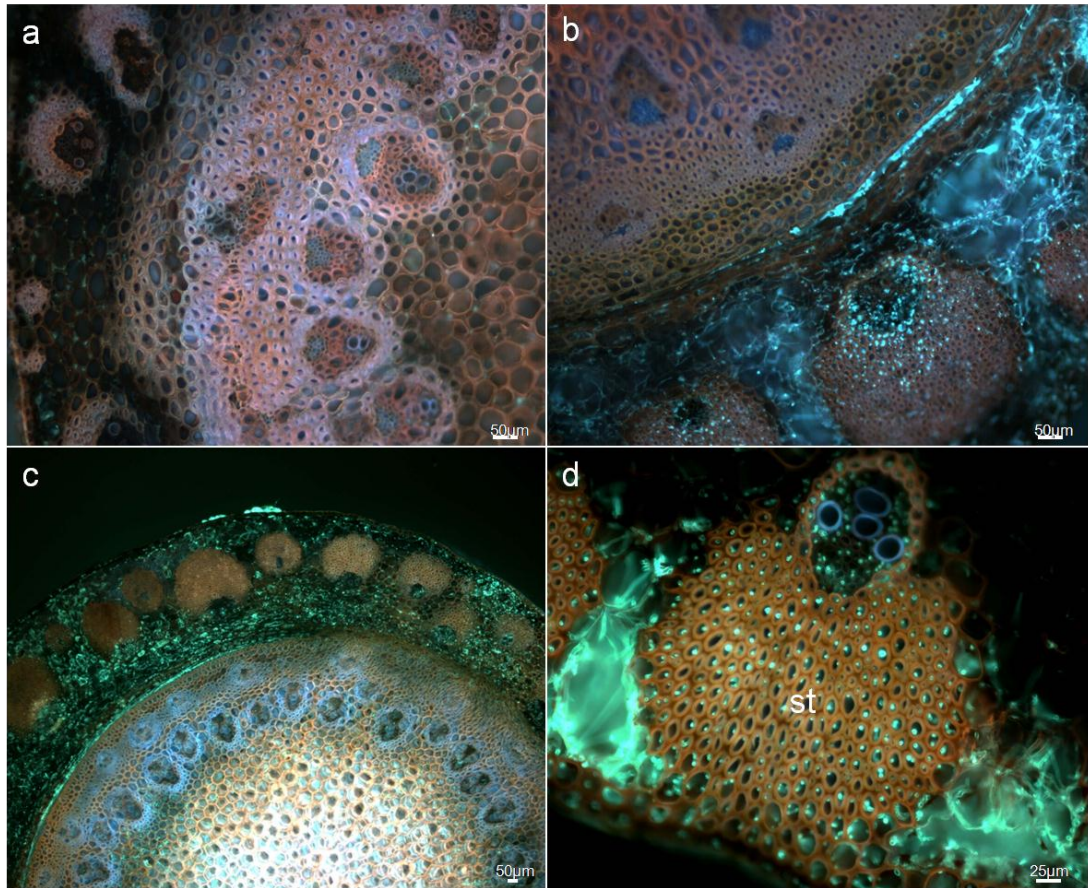


Figure 4.40. Colonisation of leaf trace tissues by *Fp* (TS). a, Hyphal colonisation of the pith and forming leaf sheath tissue (P). The vascular layer is not colonised. b and c, Heavily colonised leaf traces (Gr and Sun, respectively). Internode tissues are also colonised, however, the dark cortical cells of the leaf trace result in a strong contrast between plant and hyphal cells. d, Colonised leaf trace bundle (Sun). Vascular tissues and associated stereome (st) tissues are all colonised.

4.3.6.2.2 Comparison of Fungal Growth in Culms with White (Dead) and Green Heads

A comparison was performed, within selected wheat plants, between culms of similar size having a green or dead head (entire culm exhibited premature senescence) (Figure 4.41 and Figure 4.42). Infection of the dead culm involved much lateral growth of hyphae and frequent colonisation of vascular bundles (Figure 4.43a, b, c, d, e, f and Figure 4.44a, b, c, d, e). In some cases large xylem vessels were completely occluded by hyphae. Small vascular bundles in the sclerenchymatous hypoderm were sometimes observed to be areas of intense hyphal growth, with sclerenchyma cells between the bundles being relatively free of hyphae. Hyphae were not observed above IN4. In colonised sections the hyphae had penetrated into the majority of the tissue, except for the infection edge which varied in the extent of colonisation.

Hyphae observed in the green culms were frequently in the vascular bundles and in some cases colonised up to node 2 (Figure 4.45a, b), however the density of hyphae generally appeared less than that in dead culms. It is interesting to note that culms harvested at 22 WAP (maturity) did not have a similar spread or intensity of hyphal growth as culms with dead heads.

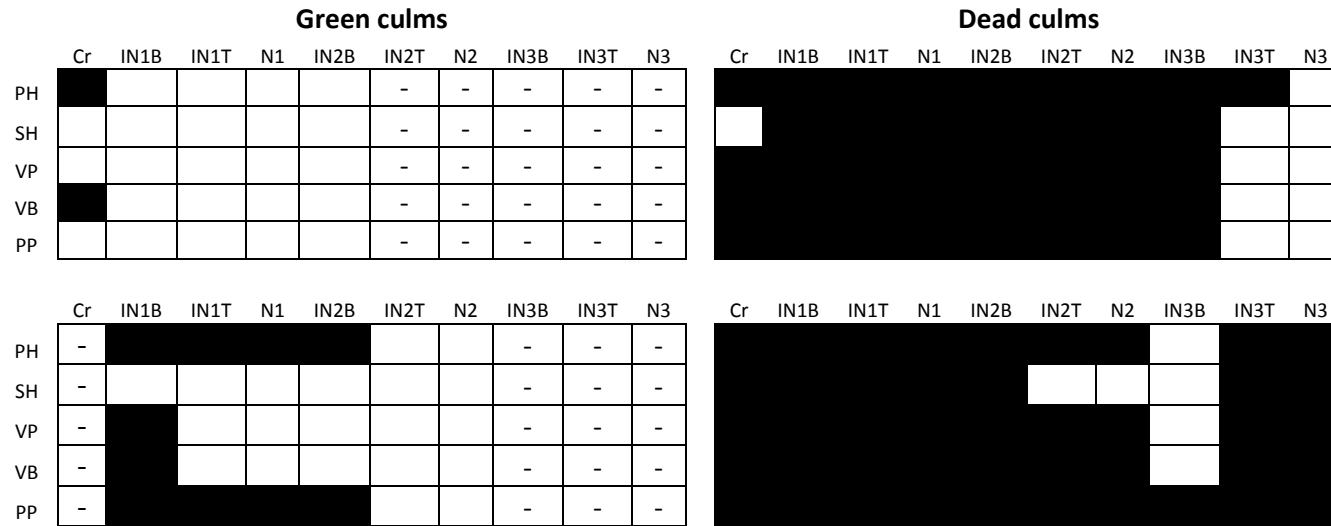


Figure 4.41. Summary of culm infection by *Fp* of green culms and dead culms at 16 WAP of the wheat genotype Sunland. Each individual box represents the primary culm of an infected plant. Black indicates hyphae were observed; grey indicates brown discoloration was observed visually before sectioning; white indicates absence of hyphae or discoloration. A dash indicates this tissue was either not observed or absent. Where a B or T follows the tissue type, e.g. IN1B or IN1T, these letters indicate either the bottom (B) or top (T) third of the tissue. Tissues assessed were parenchymatous hypoderm (PH), sclerenchymatous hypoderm (SH), vascular parenchyma, (VP), vascular bundle (VB), pith parenchyma (PP) and visual discoloration (Vis).

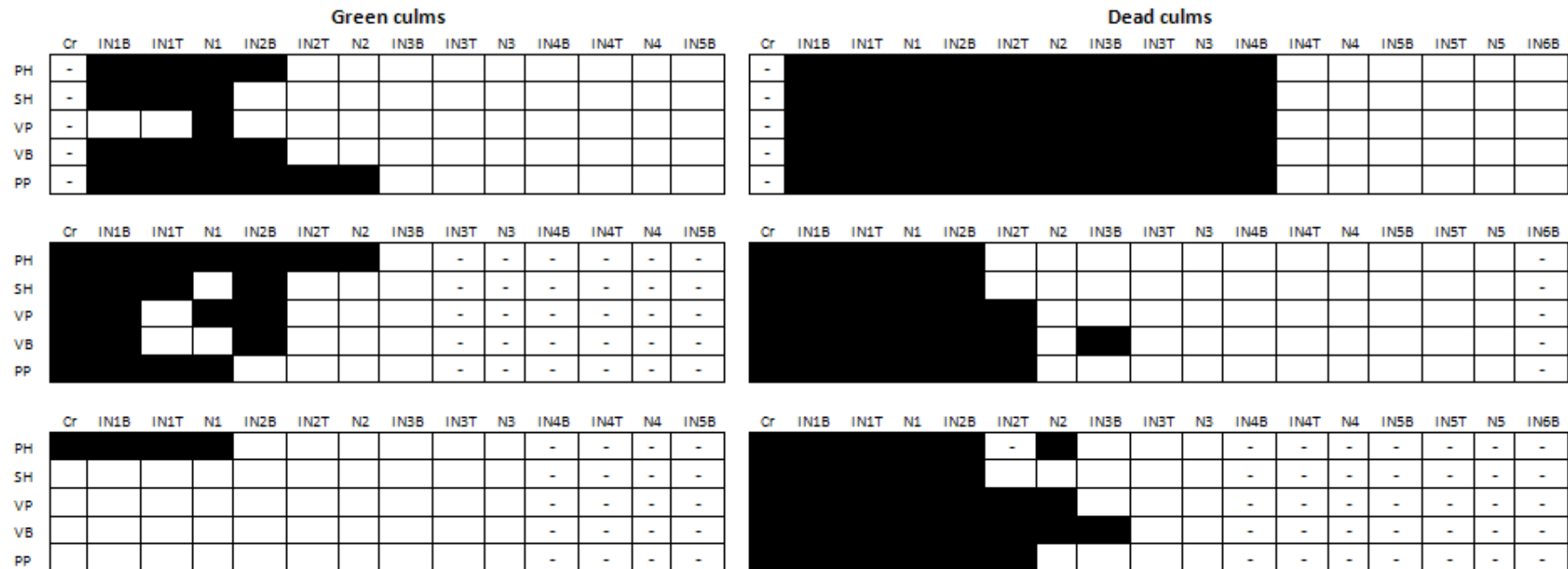


Figure 4.42. Summary of culm infection by *Fp* of green culms and dead culms at 16 WAP of the wheat genotype Vasco. Each individual box represents the primary culm of an infected plant. Black indicates hyphae were observed; grey indicates brown discoloration was observed visually before sectioning; white indicates absence of hyphae or discoloration. A dash indicates this tissue was either not observed or absent. Where a B or T follows the tissue type, e.g. IN1B or IN1T, these letters indicate either the bottom (B) or top (T) third of the tissue. Tissues assessed were parenchymatous hypoderm (PH), sclerenchymatous hypoderm (SH), vascular parenchyma, (VP), vascular bundle (VB), pith parenchyma (PP) and visual discoloration (Vis).

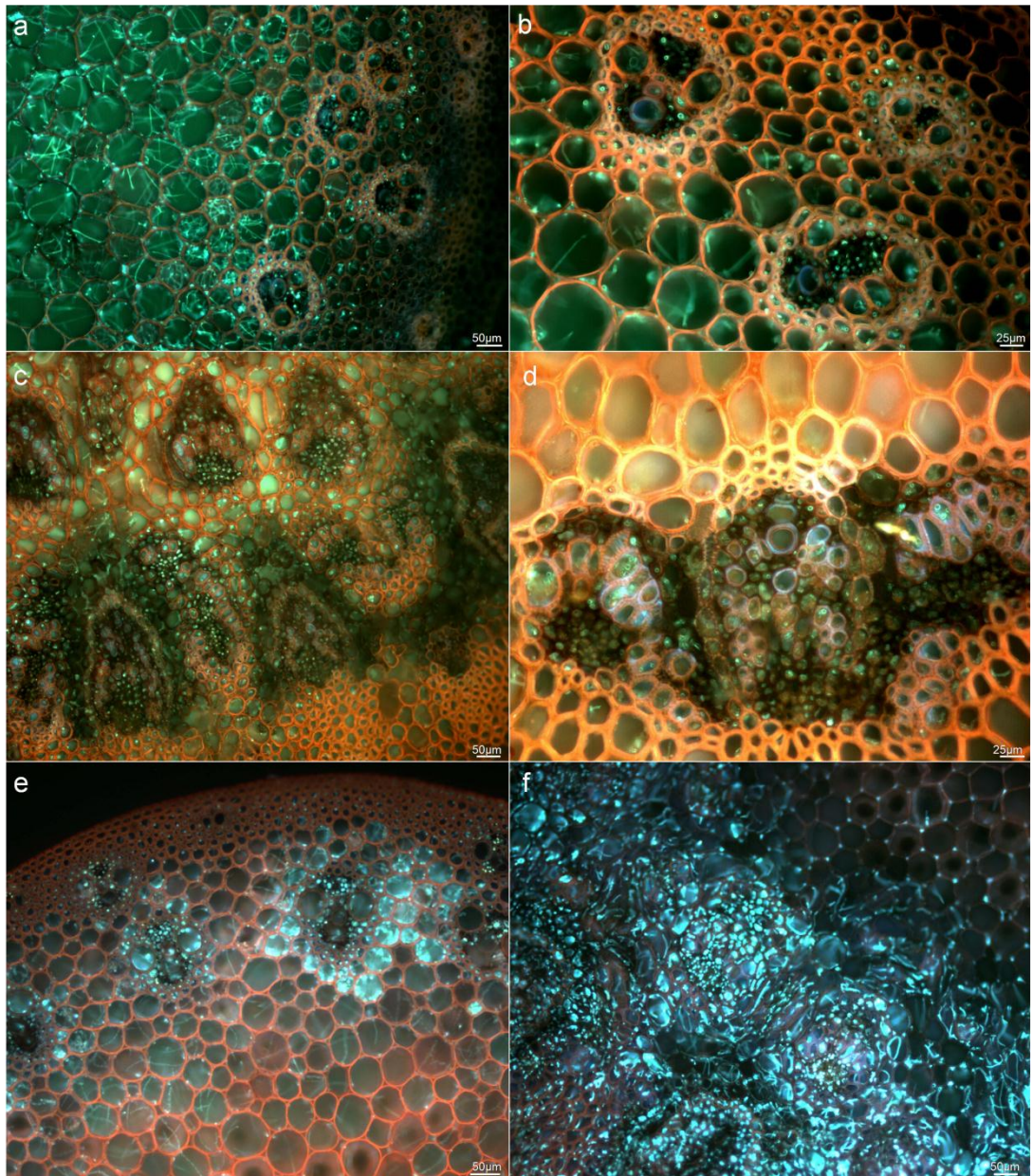


Figure 4.43. Colonisation of dead culm tissues by *Fp* (TS). a, Extensive colonisation of all tissues within a culm base (Sun). b, Lateral hyphal penetration (Sun). Even during heavy infection this is only prominent in parenchymatous tissues. c and d, Nodal tissue colonisation (Sun). All cell types are colonised, however, the vascular bundles have the most dense colonisation. e, Dense colonisation occurring around and within vascular bundles (P). f, Dense colonisation of anastomosing vascular bundles in nodal tissue (V).

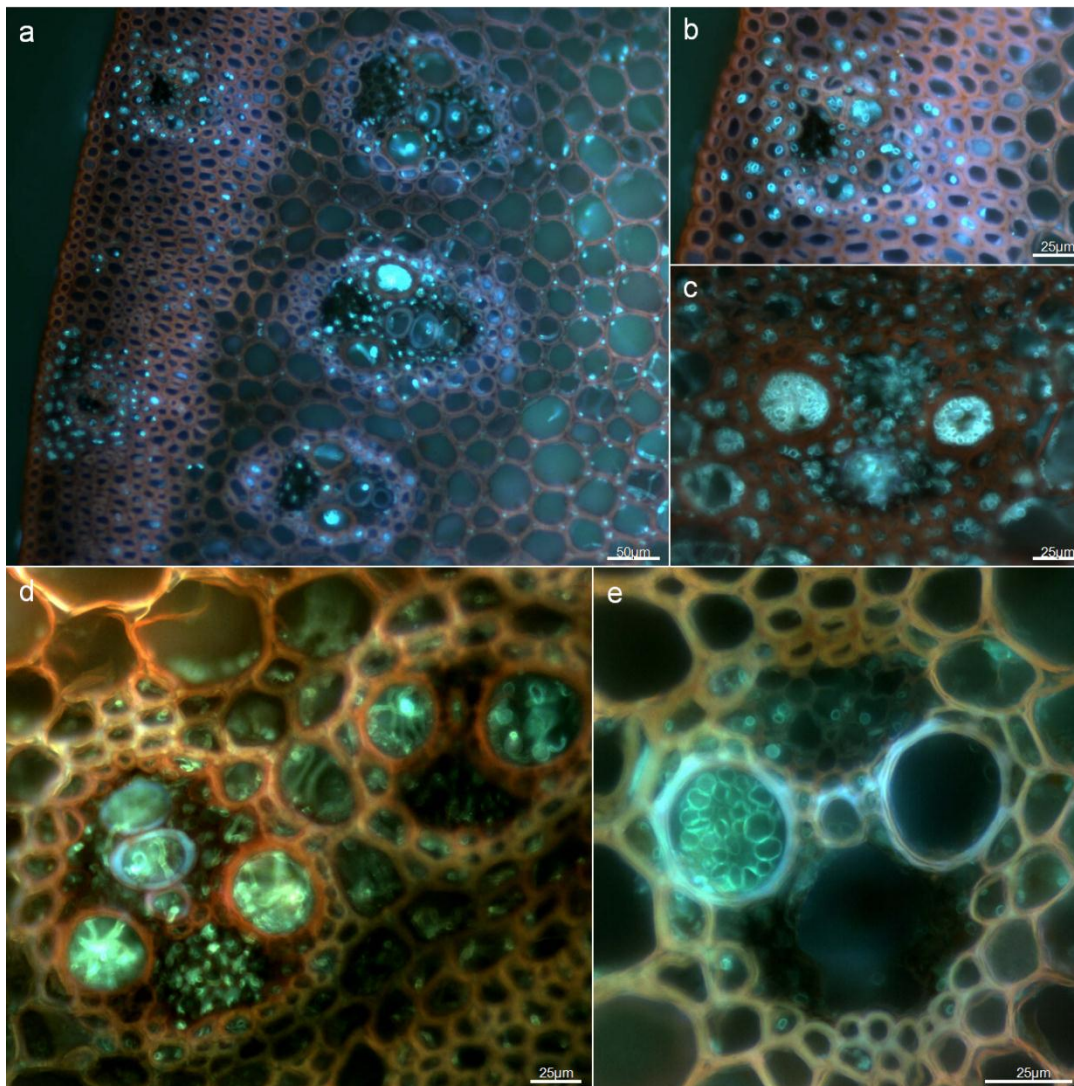


Figure 4.44. Colonisation of vascular tissues by *Fp* in dead culms (TS). a and b, Dense hyphal colonisation around and within vascular tissues (V). c, d and e, Large xylems vessels occluded by hyphae (V). Phloem cells are also heavily colonised.

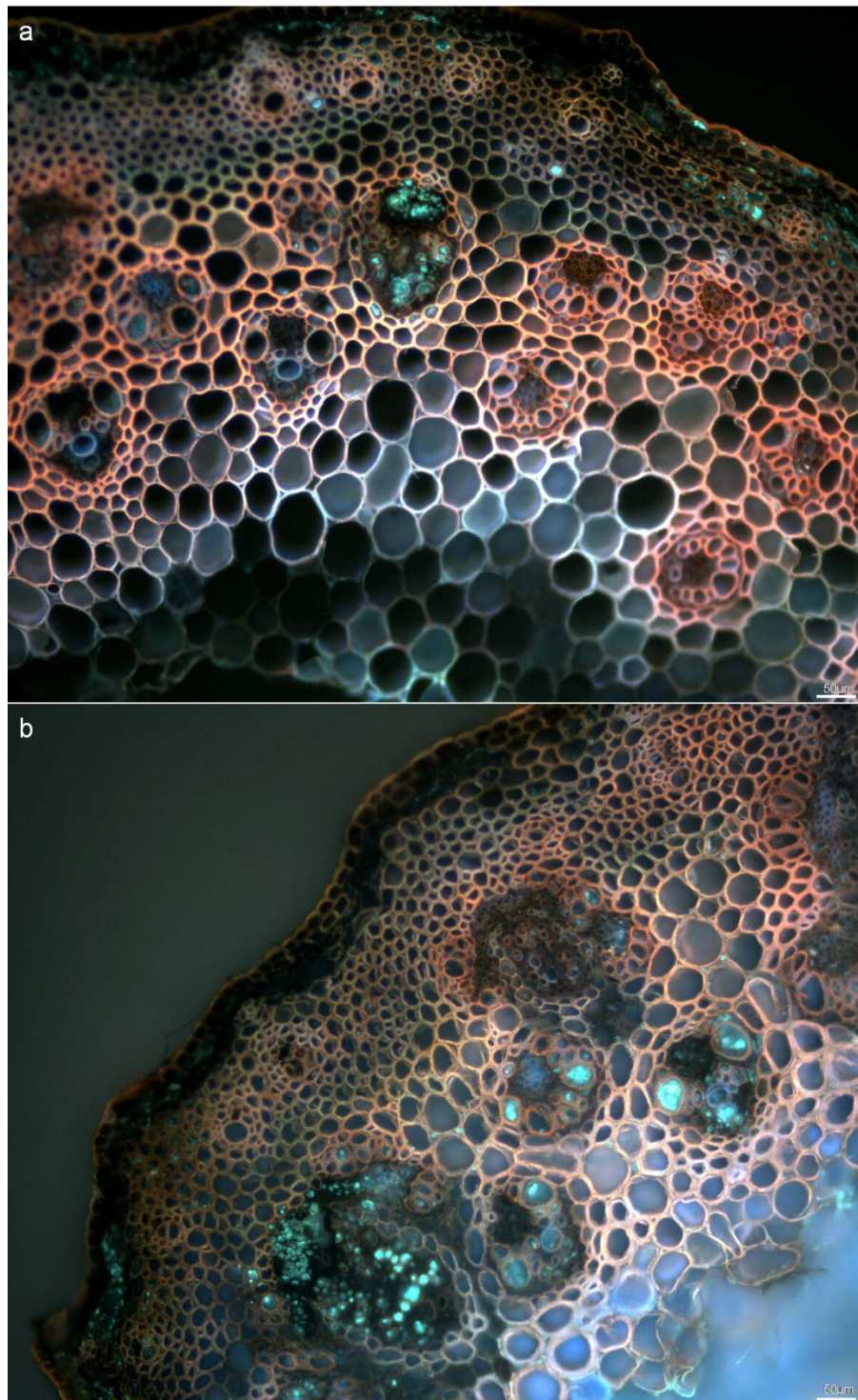


Figure 4.45. Colonisation of green culm tissues by *Fp* (TS). a, Colonised internodal tissue (V). Colonisation has occurred in the parenchymatous hypoderm and in vascular bundles. Only one vascular bundle is heavily colonised. b, Colonised nodal tissue (V). Colonisation has occurred in the parenchymatous hypoderm, pith and in several vascular bundles. Several large xylem vessels have been occluded by hyphae.

4.3.7 Staining of Lignin, Suberin and Callose

This method of staining gave a similar range of fluorescence of cell types as the safranin, just at a greater intensity. Berberine resulted in a vivid green staining of lignified cell walls. Phloem appeared yellow or blue/black and thin-walled parenchyma cells were blue. The results were not in direct agreement with what was reported to occur by Brundrett *et al.* (1988). The bright staining of lignin was the only certain result, with no suberin or callose identified.

A comparison of control and infected tissues is presented in Figure 4.46. During experimentation tissues from six infected and six control culms of 2-49 and Puseas were compared. In control tissues nearly all cell types had intense green fluorescence, with that of the vascular tissues equal to the surrounding parenchyma and sclerenchyma cells. It is noted, however, that in a LS only the abaxial surface and vascular bundles fluoresced green, while the adaxial surface and cortical cells had almost no fluorescence.

Sections of infected culms exhibited much less fluorescence than the controls for all cell types, except for the sclerenchymatous hypoderm. This was particularly obvious for the vascular parenchyma which became a dull blue-green in colour. At levels in the infected culm where colonisation had not occurred the fluorescence was similar to that in the control culms.

The decrease in fluorescence following infection was most noticeable in the parenchymatous hypoderm. When the vascular parenchyma lost fluorescence the vascular bundles remained relatively bright. Sclerenchyma tissues typically had the least fluorescence loss. In cases of severe infection fluorescence of the vascular layer and pith was observed but both the hypoderm layers were not visible. The decrease in fluorescence did not appear to be dependent on infection of each cell, but on the presence of the fungus within at least some tissues of the whole section.

Extent of fluorescence decrease was related to the extent of infection, with Puseas appearing to have a greater amount of fluorescence decrease than 2-49 (Figure 4.46). No definite difference could be determined between controls of 2-49 and Puseas; however, it is possible that 2-49 controls had a slightly less intensity of fluorescence than Puseas.

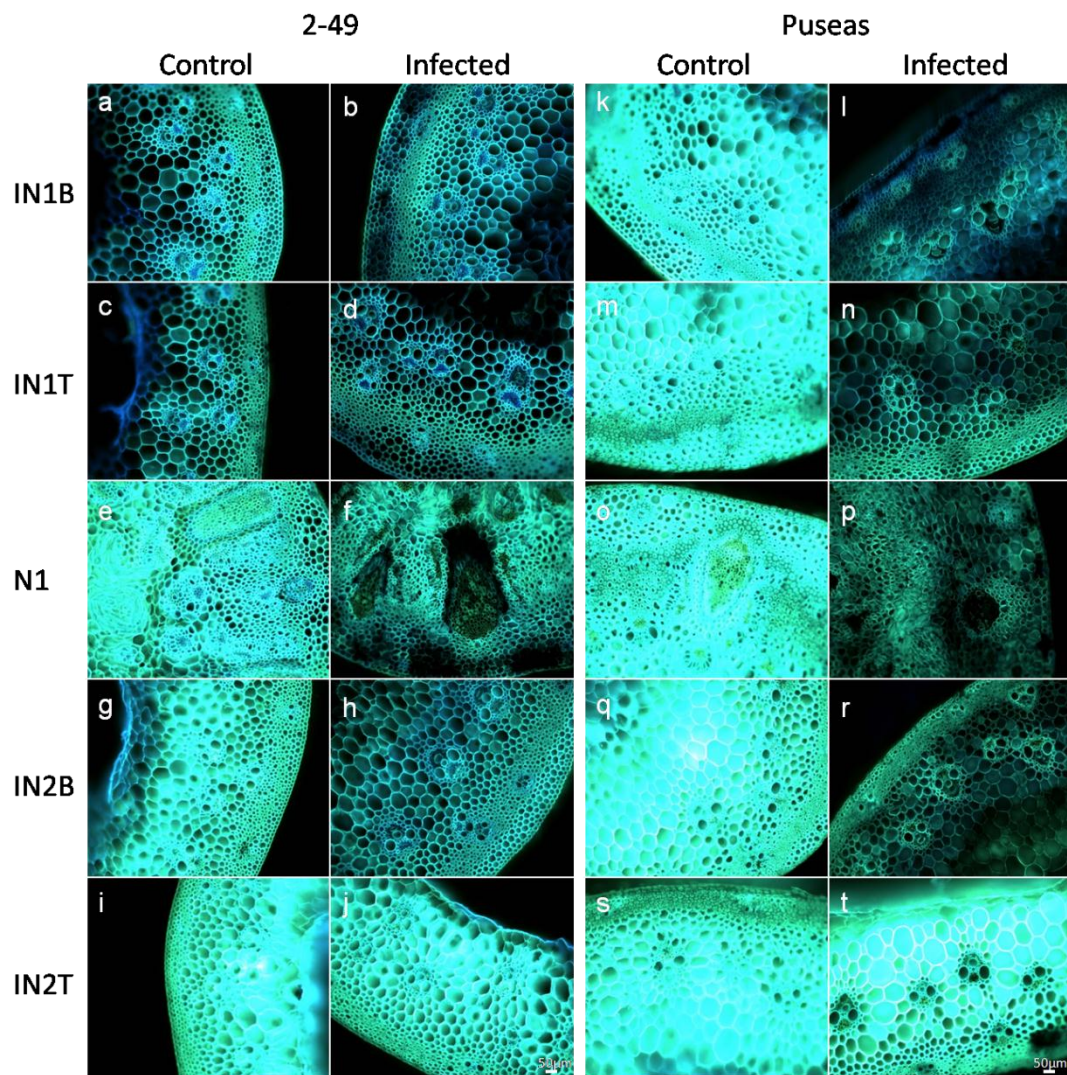


Figure 4.46. Control and infected culm tissues of 2-49 (a-j) and Puseas (k-t) at 16 wap. a-h/k-r, The fluorescence of the infected tissues was much less than the control tissues. i and j/s and t, Above the infection edge the fluorescence of the infected tissues was similar to the control tissues Transverse culm sections were stained with berberine hemi-sulphate and aniline blue and viewed under fluorescence using filter UV-2A. The image capturing conditions were 200ms exposure, 1800 gain and 850 offset. IN is internode, N is node, B is base and T is top.

4.4 Discussion

4.4.1 Fluorescent Staining

Solophenyl flavine 7GFE has previously been reported to stain cell walls of many fungal species, including *Saccharomyces cerevisiae*, *Sclerotinia sclerotiorum*, *Alternaria brassicicola*, *Thielaviopsis basicola*, *Phyllosticta ampellicida*, *Colletotrichum graminicola*, *Colletotrichum higginsianum* and the oomycetes *Pythium irregulare*, *Pythium debaryanum* and *Phytophthora infestans* (Hoch *et al.*, 2005, Oliver *et al.*, 2009, Takahara *et al.*, 2009). However the study by Oliver *et al.* (2009) of *Pythium* infections in a moss host (*Physcomitrella patens*) is, to date, the only report of hyphal staining inside host tissues using this dye.

Solophenyl flavine 7GFE stains fungal cell walls and septa in a similar manner to calcofluor white M2R, however, solophenyl flavine 7GFE does not fade as quickly when exposed to light of selected wavelengths (Hoch *et al.*, 2005, Anderson *et al.*, 2010). Hoch *et al.* (2005) reported that oomycetes with cellulosic wall components generally fluoresced more intensely than fungal species with chitinous walls, however there was sufficient fluorescence for observation from both wall types. Anderson *et al.* (2010) characterised solophenyl flavine 7GFE during a study on plant cell walls, determining that it is selective for polysaccharides containing β -1,4 linkages. Molecules containing this linkage type are common to both plant and fungal cell walls (Bartnicki-Garcia, 1968), explaining why staining with solophenyl flavine 7GFE alone distinguishes poorly between plant cells and fungal hyphae. By including an additional staining step using a dye such as safranin, which binds to components predominantly found in plant cell walls, such as lignin, suberin and cutin (Ruzin, 1999, Lodish *et al.*, 2000), a clear distinction between plant and fungal cell walls is observed.

The novel method of sequential staining with both safranin and solophenyl flavine 7GFE, resulting in strong differentiation between fungal and plant cell walls, demonstrates that using a combination of stains can enhance the ability to visualise hyphae in relation to plant cell structures, while also highlighting differences between plant cell types. Apart from the rapid and simple nature of this method, one of the benefits is that the stained specimens retain significant fluorescence for a period of at least two months. This methodology has been applied in an extensive study of *F. pseudograminearum* infections in bread wheats, durum and barley. The

ability of solophenyl flavine 7GFE to stain walls of multiple fungal species in culture (Hoch *et al.*, 2005) indicates that this method may have applications in the study of many other plant-pathogen relationships.

4.4.2 Histopathology of Crown Rot

The results presented in this Chapter represent the most comprehensive microscopic investigation of *F. pseudograminearum* crown rot yet performed. The findings were based predominantly on direct observation of colonisation events rather than reporting statistically relevant results which are notoriously difficult to produce using microscopy. This project was the first to microscopically compare partially resistant and susceptible bread wheat genotypes, as well as genotypes of durum wheat and barley, during crown rot disease. Differences in infection pathways and patterns between bread wheat, durum wheat and barley were not detected and as such the following discussion on infection is similarly relevant to each species. Differences between the cereal genotypes were related to the timing and extent of infection, which was generally in relation to their partial resistance or susceptibility. Neither partial resistance nor susceptibility appears to be due to either constitutive or induced visible structural differences. The results support other studies which have simply reported that fungal growth is slower in more resistant tissues (Purss, 1966, Malligan, 2008). Smith and Walker (1930) similarly reported that infection sites in cabbage plants resistant or susceptible to *F. conglutinans* did not show associated morphological differences.

Taylor (1983) reported the only previous microscopic assessment of infection of wheat plants by *F. pseudograminearum*. In Taylor's study the penetration and colonisation of the coleoptile, SCI, scutellum and culm tissues at seedling stages (7, 14 and 56 dai) through to maturity were described in detail. Unfortunately the findings detailed in this Masters dissertation have never been more widely published in the journal literature.

4.4.2.1 Initial Plant-Fungi Interactions

Initial hyphal growth on LS tissues was observed to occur in loops around trichomes, frequently with multiple hyphae growing around a single trichome (Figure 4.4). This is a potential method by which the fungus could attach itself to the host surface.

Initial lesion formation could also occur at trichomes on the LS surface (Figure 4.5). Growth around the trichome involved close contact of the hyphae to the trichome base. Penetration was not clearly observed but it appears that penetration hyphae can form over the union of vertical cell walls at the trichome base. It is possible that the observed hyphal looping around trichomes was an artefact of the clearing, fixation and staining procedures. However, hyphal wrapping around trichomes and penetration of trichomes has also been reported for *F. solani* f. sp. *phaseoli*, *F. lini* and *F. graminearum* (Nair and Kommedahl, 1957, Mulligan *et al.*, 1990, Stephens *et al.*, 2008).

Stomatal penetration by hyphae was frequently observed in LS tissue. Stomata were most frequently the cells where initial penetration and lesion formation occurred on LS tissue (Figure 4.3 and Figure 4.5). This method of penetration was not as important during infection of the coleoptile. It is also believed that penetration of internodes above ground level was predominantly via stomata, with penetration hyphae growing from infected LSs. Not only was stomatal penetration by *F. pseudograminearum* observed but re-emergence from stomata by multiple hyphae was also a common occurrence (Figure 4.12). The stomata were the pathway of least resistance to penetration and re-emergence, and appeared to act as gateways for hyphae to grow out to seek further sites for infection. Stomata also allowed production of conidia on the LS surface, where greater distribution through the environment could occur via wind or rain splash (Figure 4.14). The fact that this event was only observed on the susceptible Puseas demonstrates how susceptibility may aid rapid fungal reproduction.

The ability of *F. pseudograminearum* to penetrate through stomata was not observed by Taylor (1983), however this phenomenon has been reported for other *Fusarium* phytopathogens. Initial flecks of discolouration reported during *F. solani* infection of pea plants were frequently caused by hyphae penetrating the stomata (Bywater, 1959, Christou and Snyder, 1962). Both *F. culmorum* and *F. nivale* (*Microdochium nivale*) have been reported to penetrate coleoptiles of cereals via stomata (Malalasekera *et al.*, 1973), while *F. nivale* has also been observed to penetrate stomata of rye leaves (Malan 1969 as cited in Malalasekera *et al.*, 1973). Recently, Prats *et al.* (2010) reported that a hypersensitive response against *Blumeria graminis* f. sp. *hordei* infection in barley was associated with stomata “lockup” (where stomata become unable to close), leading to increased leaf water

conductance. An assessment of the effects of stomatal penetration by *F. pseudograminearum* may reveal the potential for crown rot to similarly affect water conductance. It is uncertain whether effects of the two pathogens would be similar as, in contrast to *F. pseudograminearum*, *Blumeria graminis* is a known biotroph. Nevertheless, such an experiment would yield valuable information regarding water transport during crown rot infection.

Granulation of host cytoplasm around penetration sites in epidermal tissues observed during this study has similarly been reported by Pearson (1931) and Taylor (1983). Pearson (1931) suggested that these responses in the cytoplasm may precede or accompany some physicochemical changes which result in the secretion of materials into the intercellular space or their accumulation in the cell walls. This effect may have been observed as the production of a 'halo' around penetration sites of stomata and trichomes of the LSs. 'Halo' effects around fungal penetration sites have frequently been reported (Young, 1926, Pearson, 1931, Ghemawat, 1977, Taylor, 1983). Further investigation of this response is required.

The ability of the cell walls of silica cells in LSs to resist penetration provides the only evidence of durable resistance to penetration by *F. pseudograminearum* observed in this study (Figure 4.17). Silicification in grasses is a normal feature of development; it has been demonstrated that silicon may be present, in the form of silica gel ($\text{SiO}_2 \cdot n\text{H}_2\text{O}$), as a component of the cell wall, where it is strongly bound to cellulose or lignin and as an infilling of the cell lumen in the form of solid bodies in silica cells (Lewin and Reimann, 1969, Schwarz, 1973, Ponzi and Pizzolongo, 2003). A useful review on the role of silicon in plant physiology was provided by Epstein (1994). Ample evidence was presented that silicon plays a large role in plant growth, mineral nutrition, mechanical strength and resistance to fungal diseases and herbivory. However, these studies were generally based on systemic silica rather than the silica cells in particular.

The specific role of silica cells has not been deduced (Kaufman *et al.*, 1985), however silica itself has been reported to confer greater resistance to attack by pathogenic fungi. Increased resistance in rice to rice blast disease caused by *Pyricularia oryzae* has been observed when silica was applied to rice plants (Kawashima, 1927, Miyake and Ikeda, 1932). Rice leaves suffering from disease had less silica present in them than healthy leaves and blast resistant cultivars had higher silica contents than those exhibiting susceptibility. Evidence of silica increasing

resistance to fungal attack has also been reported for various diseases of different plants, including leaf spot disease (*Helminthosporium oryzae*) of rice (Jones and Handreck, 1967), bean rust (*Uromyces phaseoli var. typical*) of French bean (Heath, 1981) and spot blotch (*Bipolaris sorokiniana*) of wheat (Domiciano *et al.*, 2010). Infections of wheat, barley, cucumber and morning glory by different fungi resulted in silicon accumulating in the leaves of these plants at fungal penetration sites (Kunoh and Ishizaki, 1975). It has been suggested that silicon can play an active role in resistance, such as mediating some defence responses functionally similar to systemic acquired resistance, rather than simply forming a physical barrier to impede fungal penetration (Fawe *et al.*, 2001).

In young wheat leaves the abaxial epidermal cells are important sites of silica deposition, but in older leaves silica is also deposited in the adaxial epidermis (Kaufman *et al.*, 1985, Hodson and Sangster, 1988). Little information can be found for the relationships between silica cells in the LS epidermis and fungal hyphae. Guenther and Trail (2005) reported that perithecium formation by *Gibberella zeae* (anamorph *F. graminearum*) was initiated in association with stomata and silica cells. Perithecia formed from epidermal cells adjacent to silica cells in nodes, but hyphae did not colonise silica cells. The inability of the hyphae to colonise silica cells was also observed in this study. While differences in silica cells between resistant and susceptible genotypes were not observed the properties of these cells to resist penetration are impressive. This may be indicative of the ability of silica to confer resistance to penetration in cell walls. As silica binds to cells walls it may have been at higher levels in walls of the silica storing cells, but other cell walls also allow this binding. It is a possibility that a resistant genotype, exhibiting slower hyphal growth, may be more silicon-efficient and have higher amounts of silica present in its cell walls. A study into the effect of available silica and quantitation of silica in crown rot resistant and susceptible wheat genotypes is required.

4.4.2.2 Colonisation

During colonisation hyphae of *F. pseudograminearum* were of varying widths, which appeared to change in relation to the cell type being colonised. LS tissue had a large range of hyphal widths (Table 4.2), with hyphae at their greatest width in the susceptible Puseas. Hyphae in culm tissues did not display great

variation in width (Table 4.4). The infrequent formation of hyphae with very large widths and the relative similarity in the formation of hyphae between partially resistant and susceptible tissues suggest that this is not related to resistance. No report discussing such a range in widths of hyphae during plant infection has been discovered.

It is interesting that no leaf sheath, internode or node cell type, excluding silica cells, was resistant to penetration, with hyphae able to grow inter- and intracellularly throughout the tissues. *F. pseudograminearum* initially invaded the intercellular spaces and only developed intracellularly where cells were closely packed together and there were no intercellular spaces. Growth upwards in the culm was more rapid in the pith, most likely because of the large intercellular spaces and the presence of the pith cavity. Intracellular growth generally occurred later in the infection process. Lateral penetration in the vascular and sclerenchyma cells was infrequent until culm senescence, which suggests that *F. pseudograminearum* opportunistically enters cells through any available opening until host metabolism alters during senescence. It is possible that *F. pseudograminearum* has ligninolytic properties or that it is able to penetrate cells via small openings, such as plasmodesmata (Taylor, 1983) or pits in the cell walls (Malalasekera *et al.*, 1973). Ligninolytic properties have been described for the *Fusarium* species *F. proliferatum*, *F. oxysporum* and *F. solani* (Rodriguez *et al.*, 1996, Mönkemann *et al.*, 1997, Regalado *et al.*, 1997). Pearson (1931) reported that wall composition in host plants may play an important role in determining how walls are penetrated. She goes on to say that greatly thickened walls may not offer as much resistance as supposed and chemical action of these walls may result in them offering no more resistance than thinner walls. The current study suggests that thickened cell walls in culms did initially provide greater resistance to penetration by *F. pseudograminearum* than thinner walls, however, penetration of thick walls still occurred later in the colonisation process.

Penetration of cell walls was most likely a mechanical process due the production of swollen hyphae and the observation of cell wall indentions under some of these swollen hyphae (Figure 4.10). These swollen hyphae are described as appressoria due to their being thick-walled structures delimited by septa (Emmett and Parbery, 1975). The appressoria were frequently appressed to the cell wall and enlarged prior to constriction, as though exerting a pressure. The appressoria usually

became greatly constricted at the point of penetration; a fine filament (penetration peg) passed through the wall and immediately swelled to its original diameter upon emerging into the opposite cell cavity. Enlargement of the appressorial swellings appeared to be relative to the strength of the cell wall. This was most conspicuous in epidermal cells adjacent to the vascular tissue in LS tissue, which are strengthened stereome tissues. During growth through these cells hyphae appeared bent. Hyphal bending has been reported to occur when a hypha extends across a cell cavity and in attempting to penetrate the opposite wall meets with resistance (Hawkins and Harvey, 1919, Leach, 1923). The author agrees with a statement by Pearson (1931), that penetration of cell walls is not either by mechanical or chemical processes, but a combination of both which result in the passage of the fungus through the cell walls of the host. A greater understanding of the events leading to cell wall penetration by *F. pseudograminearum* is needed.

Nodes represent an interesting region of the grass culm, for they lack the comparative uniformity of the INs (Chrysler, 1906). Nodes appeared to delay growth of the hyphae up the stem; however, this was only due to the formation of the pith plexus, which interrupted the hollow pith cavity, and thicker-walled parenchyma cells. There was no difference between partially resistant and susceptible genotypes for this effect. Nodes were able to be colonised to a similar level as the INs, with vascular bundles sometimes exhibiting even greater colonisation than their IN counterparts. Nodes may be an area which when infected result in systemic effects through the culm. It was also observed that as the infected parenchymatous hypoderm of the lower IN becomes parenchyma of the LS at the node above (Percival, 1921), this transition can channel hyphae into the LS and away from the hypoderm of the IN above. This does not appear to play a role in resistance.

Frequently culms showed asymmetric infections in which one side of the stem was densely colonised, while the opposite side showed sparse or no colonisation. This could be due to the orientation of the culm, as infection may be enhanced by environmental effects, or it could be a random event based on where the culm encountered inoculum.

A conspicuous change in the culm tissues was a marked decrease in stain uptake, of both safranin and berberine, during infection compared to control tissues (Figure 4.46). As both these stains are reported to bind lignin (Brundrett *et al.*, 1988, Ruzin, 1999) it might suggest that the properties of cell wall components in infected

cells, particularly parenchyma cells, are altered during infection. Pearson (1931) reported a similar diminished affinity for stains in extensively invaded maize tissues.

4.4.2.2.1 Colonisation and Visual Symptoms

Spread of the fungus, or more accurately its disease symptoms, has been a major focus of crown rot research, with visual ratings for resistance based on the distance the disease symptoms have spread up the culm (Wildermuth and McNamara, 1994, Wallwork *et al.*, 2004, Malligan, 2008). The brown discolouration characteristic of crown rot infection is predominantly due to infection of the parenchymatous hypoderm. This layer of cells decreased in fluorescent emissions and became distorted during colonisation (Figure 4.29), with discolouration sometimes appearing to be ahead of hyphal colonisation. It is possible that variation in the thickness of this layer may affect visual ratings used to classify disease, as the sclerenchymatous hypoderm, which may be present instead, does not become discoloured as readily. Parenchymatous cells of the pith also become discoloured and distorted during infection. Distortion of parenchyma cells and visual symptoms beyond the limits of hyphal penetration have also been reported by Pearson (1931), Taylor (1983) and Xi *et al.* (2008). Pearson (1931) provides a detailed discussion of studies concerned with production of a substance, such as an enzyme or fungal metabolite, which diffuses into tissues just ahead of hyphal penetration and weakens cell walls/membranes. During some plant-pathogen interactions this occurs, e.g. *Gibberella saubinetii* infection of maize plants (Pearson, 1931), and it is possible that *F. pseudograminearum* can produce this effect using toxins such as deoxynivalenol, which has been reported to have an effect on colonisation of wheat culms (Mudge *et al.*, 2006). The strong correlations between visual discolouration and fungal biomass reported in Chapter 2 and 3 and the limited spread of symptoms away from direct fungal colonisation suggest that any metabolite released by *F. pseudograminearum* has short ranged effects.

It may be that the importance of visual rating relies on the extent of symptom development up the culm correlating with lateral spread of the fungus through the culm, particularly in the lower portions. Based on the observations in this study, the author suggests that spread of the hyphae through the cells of the culm base,

particularly the vascular bundles of the first IN and node, determines the severity of infection, rather than spread up the culm.

4.4.2.2.2 Inoculation and Hyphal Spread

Slight differences between the current study and that of Taylor (1983) were predominantly due to the method of inoculation. Taylor used a layer of inoculum under the soil and while the current study did use a similar method for adult plants it also used conidial suspensions placed on above ground portions of the coleoptile of seedlings. This resulted in the fungus infecting and colonising plant tissues by potentially different routes. Banded inoculum in the pot simulates contact of the wheat plant with field inoculum below the soil surface, leading to initial infection of the coleoptile, SCI and scutellum. The conidial suspension on above ground tissues simulates infection due to contact with inoculum above ground, such as surface or standing stubble. Purss (1966) described the importance of above ground infection of LSs, as he stated that if LS bases were heavily infected then the hyphae could spread to the culm base. This is precisely what was observed to occur in this study.

Spread from infected tissues below ground was just as important as infection of above ground tissues, as it appeared that the below ground tissues were frequently the region of initial penetration into cells beyond the hypoderm. This penetration occurred at the coleoptile, SCI and at emerging secondary roots (Cook, 1980, Taylor, 1983). Taylor (1983) described colonisation of these tissues, particularly the vascular tissues of the scutellum and SCI and reported that spread of the hyphae occurred through the vascular bundles up into the crown and culm tissues. The current study supports the idea that initial colonisation frequently occurs below ground, however, initial spread of the fungus via the vascular tissues was not observed. Xi *et al.* (2008) reported similar findings using *F. pseudograminearum* and *F. graminearum*. Initial infection and spread more frequently occurred through the pith parenchyma cells and pith cavity. A separate region of infection spread was frequently observed in the parenchymatous hypoderm, which was separated from the pith and vascular layer by the sclerenchymatous hypoderm. This is in contrast to Taylor (1983) who reported that hyphae appeared to move up the stems through the xylem vessels and to a lesser extent through the hollow pith cavity in the culm INs.

While initial spread of the fungus was not via the vascular bundles, they were an area of intense colonisation in culm tissues. In contrast to Taylor, vascular colonisation was not common in LS tissue. Colonised vascular bundles in LSs were only observed when the node of the phytomer linked to that LS had been colonised. This suggests that vascular colonisation may only be initiated following disruption of subtending crown and nodal tissues.

4.4.2.2.3 Vascular Tissue Colonisation

Colonisation of the vascular bundles has the potential to be the most debilitating effect of *F. pseudograminearum* infection. In the current study colonisation of both the phloem and xylem occurred, with no obvious preference (Figure 4.31). Susceptible genotypes had colonisation of the vascular bundles earlier and to a greater extent than the partially resistant genotype 2-49. At maturity differences between partially resistant and susceptible genotypes became less obvious in the lower INs. While xylem vessels were rarely occluded before culm senescence, it is feasible that their colonisation by hyphae limited their water transporting potential. Furthermore, colonisation of the phloem may have exacerbated this effect by limiting sugar transport to the roots, resulting in lower water uptake. This is supported by a report by Purss (1966) stating that a feature of the roots in plants with severely affected crowns was their complete collapse. Taylor (1983) did not describe differential infection of xylem and phloem in vascular bundle tissue but merely stated that xylem were frequently colonised and at maturity could be occluded by hyphae. He reported that penetration from xylem vessel to xylem vessel appeared to occur via the pits in the vessel walls.

4.4.2.2.4 Colonisation of Culms Exhibiting Green and Dead Heads

The comparison of green and prematurely dead culms revealed intense colonisation in the three lower INs of the dead culms, with frequent hyphal occlusions of xylem vessels and phloem tubes (Figure 4.43 and Figure 4.44). Dead heads may represent culms in which multiple infection events have occurred around the culm base, leading to early colonisation of a greater number of vascular bundles. As these culms were dead it was difficult to determine if the intense hyphal growth preceded or followed the death of the culm. It is possible that water stress in the culm

stimulates *F. pseudograminearum* to aggressively colonise culm tissues, as it has been demonstrated that maximal growth by *F. pseudograminearum* requires progressively drier conditions (Wearing and Burgess, 1979, Beddis and Burgess, 1992). Green culms had moderate vascular colonisation along a shorter length of the culm which demonstrates that vascular colonisation in itself does not cause culm senescence. It is possible that vascular transport becomes significantly decreased when a longer portion and/or a greater proportion of the vascular tissue is colonised, potentially resulting in culm death.

F. pseudograminearum does not cause a classical vascular wilt (Dimond, 1970), as spread of hyphae is not by xylem vessels alone and infection does not become systemic in the sense of propagule spread in the vasculature (Xi *et al.*, 2008). Similar to Malligan (2008) and Xi *et al.* (2008), hyphae were predominantly in the lower three INs and were never observed in the IN on which the grain head formed.

These results encompass the first comprehensive microscopic study of crown rot infections of partially resistant and susceptible cereals. The observations recorded represent progress in understanding *F. pseudograminearum* infection processes and patterns during crown rot of cereals; they also indicate that further investigation is required. In particular further studies are required to address the ability of *F. pseudograminearum* to interfere with vascular systems and cause the effects of crown rot. Information on the chemical and metabolic characteristics of susceptible and partially resistant cereals may also identify the role of specific nutrients during disease reactions. This may enable more efficient selection of genotypes better able to resist and/or tolerate infection.

Chapter 5: General Discussion and Conclusions

Two major methodological approaches were developed and then applied to the research objectives of this study. Firstly, a multiplex real time quantitative PCR assay able to accurately quantify both *F. pseudograminearum* and wheat DNA extracted from infected host tissues was established. Secondly, a fluorescent staining technique which differentially stained *F. pseudograminearum* hyphae and cereal tissues was developed, allowing rapid processing and microscopic observation of infected host tissues.

Specifically this study has:

- Examined crown rot infected seedlings (of a range of crown rot resistances) from 1 to 35 dai using both visual discolouration and qPCR rating methods. (Chapter 2)
- Examined crown rot infected adult plants (of a range of crown rot resistances) from 10 to 22 WAP using both visual discoloration and qPCR rating methods. (Chapter 3)
- Correlated *F. pseudograminearum* DNA content to visual discolouration ratings in seedling and field tests. (Chapters 2 and 3)
- Determined the most discriminating time points after infection in relation to assessing crown rot resistance. (Chapters 2 and 3)
- Investigated the ability of host plants to tolerate *F. pseudograminearum* colonisation. (Chapters 2, 3 and 4)
- Observed colonisation of seedling and adult cereal tissues by *F. pseudograminearum* using fluorescence microscopy. (Chapter 4)

The sensitivity of the qPCR assay allowed greater differentiation between partially resistant and susceptible genotypes than visual assessment. However, the strong correlations between visual discolouration ratings and qPCR data support the use of visual discolouration as a useful indicator of the presence of the crown rot pathogen in host tissue.

While qPCR data is more sensitive than visual rating, the time required for sample preparation, laboratory costs and requirement for sophisticated laboratory

facilities suggest that it is unlikely to replace visual rating techniques for large-scale field screening of breeding populations. The sensitivity of qPCR may prove most useful for studies targeting specific host-pathogen interactions. For example, qPCR may be used to enhance the identification of quantitative trait loci in segregating populations. In addition, after initial selection of resistant lines from new populations using visual symptom data, qPCR could be applied as a method for accurately classifying new resistant genotypes. A qPCR rating system may be useful as a method for classifying disease reactions in released cultivars, as it will provide the most useful information to the farmer.

qPCR may also prove useful for describing crown rot infection in the field, in relation to not only crown rot severity but also to grain yield. Hogg *et al.* (2007) analysed relationships between crown rot infection and grain yield, reporting that yields for two spring wheat genotypes were negatively correlated with *Fusarium* DNA quantities. Both visual and qPCR measurements were comparable in predicting yield reduction. Variation in infection between experiments greatly altered the correlations. Further studies comparing grain yield and *F. pseudograminearum* DNA quantities in both seedling and adult tissues under Australian conditions are warranted.

The strength of the correlations between qPCR and visual rating, and the ability of each method to discriminate between genotypes of differing susceptibility, is dependent on the time of rating after infection. Later times, such as 35 dai for seedlings or 22 WAP for adult plants, provide poor discrimination between partially resistant and susceptible genotypes. Similar studies, such as Wildermuth and McNamara (1994) and Percy (2008), have also highlighted the benefits of rating crown rot symptoms relatively early in the process of disease development, for example 14 dai for seedlings and 16 WAP for adult plants. However, several recent reports seek to apply different visual rating methods at varying observation times (Mitter *et al.*, 2006, Li *et al.*, 2008).

A variety of visual rating methods have been described for crown rot disease in seedling and adult cereal tissues (Wildermuth and McNamara, 1994, Wallwork *et al.*, 2004, Mitter *et al.*, 2006, Li *et al.*, 2008, Poole *et al.*, 2009). The variation between these methods makes comparisons between projects difficult and limits the potential usefulness of the reported results. A GRDC-funded investigation is currently in progress comparing multiple crown rot rating methods across the

country. The new project involves comparing qPCR (using the methodology developed in this project), visual ratings and yield losses based on a comparison of inoculated and uninoculated plots of a range of genotypes. The ability of each method to adequately describe crown rot disease reactions will be determined, with the aim of identifying the method/s which most consistently and accurately report crown rot infections and predict yield loss.

The strong correlation between visual discolouration and qPCR values, along with microscopic observations, also indicates localised symptom development in relation to the presence of *F. pseudograminearum*. This suggests that potential elicitors of discolouration, such as the mycotoxin deoxynivalenol (Desmond *et al.*, 2008), do not readily diffuse away from the sites of infection in host tissues. The apparent need to have *F. pseudograminearum* physically close for symptom development is in contrast to Mudge *et al.* (2006), where asymptomatic infections by *F. graminearum* and *F. pseudograminearum* were reported. It is possible that infection of the pith tissues occurred, rather than the parenchymatous hypoderm, making visible symptoms difficult to recognise. In the selection of cereal genotypes assessed no tolerance to the crown rot organism was detected, as presence of the fungus was always associated with tissue discolouration.

Microscopic assessment of *F. pseudograminearum* colonisation revealed the aggressive nature and extensive growth of the fungus in host tissue. This detailed study is the first to report important growth characteristics of *F. pseudograminearum*, such as the ability to initiate colonisation through stomata, the failure to penetrate silica cells and the ability to colonise both xylem and phloem cells of the vascular bundles. The inability to relate resistance to a visible structural adaptation in cereal tissues is disappointing, yet not surprising. This study is only the second to have ever microscopically described *F. pseudograminearum* growth *in planta*, but the first to comprehensively compare partially resistant and susceptible genotypes and it is hoped that this information may provide the first step in targeting tissues and physiological responses which may be involved in crown rot resistance.

5.1 Future Directions

1. Due to the common, yet unsubstantiated, belief that plant water conductance is reduced under *F. pseudograminearum* infection, an investigation to measure this process in partially resistant and susceptible genotypes during infection is warranted. In the current study vascular occlusion was rare in non-senescent tissues, however vascular tissues were frequently colonised.

The effect of colonisation of both the phloem and xylem appears to represent two important aspects of crown rot development. While water translocation could be limited due to colonisation of xylem, sugar and nutrient transport could be altered due to colonisation of the phloem. The effect of this colonisation on water conductance, transpiration, sugar transport, disease severity, grain fill and yield loss during crown rot disease is worthy of investigation.

2. Observation of an increase in infected LS weight compared to control tissues, not caused by hyphal weight, suggests that a biochemical analysis of infected and colonised LS tissues may reveal the identity of the biomolecules responsible for this increase in mass. In particular, assays of silicon and lignin should be conducted since these structural materials are likely candidates for being part of a host response to *F. pseudograminearum* infection.

As no biological explanation for resistance has been described, novel studies designed to elucidate processes related to resistance will provide much needed information. The identification of resistance mechanisms will assist the selection of cereal genotypes which carry these characteristics.

3. Identification of DNA markers for quantitative trait loci linked to fungal growth, as indicated by qPCR. A comparison between quantitative trait loci identified by visual and, particularly, qPCR methods may allow new quantitative trait loci or at least more accurate mapping of currently known quantitative trait loci to be achieved. Comparative assessment of large wheat populations using visual and qPCR ratings would also further indicate the relationship between fungal DNA content and visible symptoms in a range of host tissues.

4. qPCR could also be used to determine the aggressiveness of different *F. pseudograminearum* isolates across a differential set. This may provide a more sensitive assessment than the methods used by Malligan (2008).
5. Assessment of the effect of photosynthetic capacity to inhibit colonisation by *F. pseudograminearum*, such as in seedling leaf blades, would indicate whether active photosynthesis may have a negative effect on *F. pseudograminearum* growth. Inoculation experiments using seedlings grown under no light conditions, with limited photosynthetic capacity, may reveal if non-photosynthetic leaf blade tissue can be colonised in a similar manner to LS tissue.
6. The distinction between resistance and tolerance to crown rot is still unclear. This project found no evidence for tolerance, however a comprehensive study assessing yield and tissue discolouration or qPCR data across a wide range of genotypes and cereals would more adequately address the ability of plants to tolerate *F. pseudograminearum* colonisation.

Further evaluation of the variation in intensity of symptoms of plants under a range of stress conditions could indicate whether tolerance may be more apparent under particular environmental conditions. It could also identify situations under which resistance may be more or less effective.

During the sixty years since the first official report of crown rot in Queensland a large body of research has been performed, from characterising the pathogen to applying crop management practices to identifying new resistance sources. However the challenge posed by crown rot is increasing, with it now causing approximately \$79 million and \$18 million worth of lost yield of wheat and barley, respectively, in Australia every year (Murray and Brennan, 2009b, Murray and Brennan, 2009a). Modern farming practices such as minimum till are becoming ever more popular due to the increase in soil moisture retention, however this also limits stubble and inoculum breakdown. Integrated approaches are required, utilising crop rotations with minimum tillage in order to decrease pathogen inoculum before planting another host crop. These practices are implemented in close consultation with an

agronomist and require careful planning to maximise revenue. The particular difficulty of dealing with crown rot for growers and researchers is the absence of any genotypes exhibiting complete, or even strong, resistance. At best only moderately resistant cultivars have been released for commercial production, however these cultivars are not always the farmers first choice as other quality traits desired by the market place are frequently associated with susceptible varieties. This is the challenge for researchers and breeders, to identify and combine strong crown rot resistance with desirable quality traits in adapted cereal varieties.

Modern technologies, such as marker assisted selection (MAS), may reduce the time needed to identify genotypes containing genetic regions associated with crown rot resistance, however this relies on genetic markers strongly linked to resistance. The sensitivity of qPCR may allow more accurate mapping of quantitative trait loci used for MAS and thus increase the potential for identifying more resistant genotypes. qPCR may also be used for fine comparisons between limited numbers of select genotypes, leading to the identification of novel or stronger resistance or more accurate characterisation of resistance.

The immediate effect of the microscopic assessment is less obvious than that of the qPCR. While the qPCR has proven to be very useful for describing fungal load the microscopy delves more into the biology of the disease. It has begun to address how *F. pseudograminearum* causes the effects observed during crown rot disease and patterns of infection. Numerous avenues of further investigation have been identified, from studying biochemical responses/characteristics in cell wall structure to monitoring the effect of vascular tissue colonisation on disease severity. The current project and its future directions aim to build a greater understanding of the crown rot disease complex by firstly understanding how the pathogen causes disease and secondly by characterising the responses of the host tissues. These are all performed with the final aim of producing new varieties with greater crown rot resistance, enabling growers to increase yields and provide food to an ever increasing human population.

References

- Agrios, G. N. (2005) *Plant Pathology*, Academic Press.
- Akinsanmi, O. A., Backhouse, D., Simpfendorfer, S. & Chakraborty, S. (2006) Genetic diversity of Australian *Fusarium graminearum* and *F. pseudograminearum*. *Plant Pathology*, 55, 494-504.
- Akinsanmi, O. A., Mitter, V., Simpfendorfer, S., Backhouse, D. & Chakraborty, S. (2004) Identity and pathogenicity of *Fusarium* spp. isolated from wheat fields in Queensland and northern New South Wales. *Australian Journal of Agricultural Research*, 55, 97-107.
- Alexopoulos, C. J., Mims, C. W. & Blackwell, M. (1996) *Introductory mycology*, New York, John Wiley & Sons Inc.
- Anderson, C. T., Carroll, A., Akhmetova, L. & Somerville, C. (2010) Real-time imaging of cellulose reorientation during cell wall expansion in *Arabidopsis* roots. *Plant Physiology*, 152, 787-796.
- Aoki, T. & O'Donnell, K. (1999a) Morphological and molecular characterisation of *Fusarium pseudograminearum* sp. nov., formerly recognised as the Group 1 population of *F. graminearum*. *Mycologia*, 91, 597-609.
- Aoki, T. & O'Donnell, K. (1999b) Morphological characterization of *Gibberella coronicola* sp. nov., obtained through mating experiments of *Fusarium pseudograminearum*. *Mycoscience*, 40, 443-453.
- Apoga, D. & Jansson, H. (2001) Adhesion of conidia and germlings of the plant pathogenic fungus *Bipolaris sorokiniana* to solid surfaces. *Mycological Research*, 105, 1251-1260.
- Atanasoff, D. (1920) *Fusarium*-blight (scab) of wheat and other cereals. *Journal of Agricultural Research*, 20, 1-32.
- Australian-Bureau-of-Statistics (2009) Historical Selected Agriculture Commodities, by State (1861 to Present).
- Australian-Government-Bureau-of-Meteorology (2009) Annual Australian Climate Statement 2008.
- AWB (2004) *Investor fact book*, Melbourne, Australian Wheat Board.
- Backhouse, D., Abubakar, A. A., Burgess, L. W., Dennis, J. I., Hollaway, G. J., Wildermuth, G. B., Wallwork, H. & Henry, F. J. (2004) Survey of *Fusarium* species associated with crown rot of wheat and barley in eastern Australia. *Australasian Plant Pathology*, 33, 255-261.
- Backhouse, D. & Burgess, L. W. (2002) Climatic analysis of the distribution of *Fusarium graminearum*, *F. pseudograminearum* and *F. culmorum* on cereals in Australia. *Australasian Plant Pathology*, 31, 321-327.
- Backhouse, D., Burgess, L. W., Swan, L. J. & Esdaile, R. J. (1997) Crown rot of cereals in conservation farming systems. *Proceedings of the Farming Systems Conference*. Moree.
- Balmas, V. (1994) Root rot of wheat in Italy caused by *Fusarium graminearum* Group 1. *Plant Disease*, 78, 317.
- Bartnicki-Garcia, S. (1968) Cell wall chemistry, morphogenesis, and taxonomy of fungi. *Annual Review of Microbiology*, 22, 87-108.
- Bateman, G. L., Edwards, S. G., Marshall, J., Morgan, L. W., Nicholson, P., Nuttall, M., Parry, D. W., Scrancher, M. & Turner, A. S. (2000) Effects of cultivar and fungicides on stem-base pathogens, determined by quantitative PCR, and on diseases and yield of wheat. *Annals of Applied Biology*, 137, 213-221.

- Beddis, A. L. & Burgess, L. W. (1992) The influence of plant water stress on infection and colonisation of wheat seedlings by *Fusarium graminearum* Group 1. *Phytopathology*, 82, 78-83.
- Bent, A. F. (1996) Plant disease resistance genes: Function meets structure. *Plant Cell*, 8, 1757-1771.
- Bentley, A. R. (2007) Genetic variation in field populations of the crown rot fungus *Fusarium pseudograminearum*. Thesis. The University of Sydney,
- Bentley, A. R., Cromeey, M. G., Farrokhi-Nejad, R., Leslie, J. F., Summerell, B. A. & Burgess, L. W. (2006) *Fusarium* crown and root rot pathogens associated with wheat and grass stem bases on the South Island of New Zealand. *Australasian Plant Pathology*, 35, 495-502.
- Bentley, A. R., Leslie, J. F., Liew, E. C. Y., Burgess, L. W. & Summerell, B. A. (2008) Genetic structure of *Fusarium pseudograminearum* populations from the Australian grain belt. *Phytopathology*, 98, 250-255.
- Bentley, A. R., Milgroom, M. G., Leslie, J. F., Summerell, B. A. & Burgess, L. W. (2009) Spatial aggregation in *Fusarium pseudograminearum* populations from the Australian grain belt. *Plant Pathology*, 58, 23-32.
- Benyon, F. H. L., Burgess, L. W. & Sharp, P. J. (2000) Molecular genetic investigations and reclassification of *Fusarium* species in sections *Fusarium* and *Roseum*. *Mycological Research*, 104, 1164-1174.
- Bovill, W., Horne, M., Herde, D., Davis, M., Wildermuth, G. & Sutherland, M. (2010) Pyramiding QTL increases seedling resistance to crown rot (*Fusarium pseudograminearum*) of wheat (*Triticum aestivum*). *Theoretical and Applied Genetics*, 121, 127-136.
- Bovill, W. D., Ma, W., Ritter, K., Collard, B. C. Y., Davis, M., Wildermuth, G. B. & Sutherland, M. W. (2006) Identification of novel QTL for resistance to crown rot in the doubled haploid wheat population 'W21MMT70' x 'Mendos'. *Plant Breeding*, 125, 538-543.
- Brennan, J. P. & Murray, G. M. (1998) *Economic importance of wheat diseases in Australia*, Wagga Wagga, NSW, NSW Agriculture.
- Briske, D. D. (1991) Developmental morphology and physiology of grasses. IN HEITSCHMIDT, R. K. & STUTH, J. W. (Eds.) *Grazing management: An ecological perspective*. Portland, Oregon, Timber Press, Incorporated
- Brundrett, M. C., Enstone, D. E. & Peterson, C. A. (1988) A berberine-aniline blue fluorescent staining procedure for suberin, lignin, and callose in plant tissue. *Protoplasma*, 146, 133-142
- Burgess, L. W. (1967) Ecology of some fungi causing root and crown rots of wheat. Thesis. The University of Sydney,
- Burgess, L. W., Backhouse, D., Summerell, B. A. & Swan, L. J. (2001) Crown rot of wheat. IN SUMMERELL, B., LESLIE, J., BACKHOUSE, D., BRYDEN, W. & BURGESS, L. (Eds.) *Fusarium: Paul E. Nelson Memorial Symposium*. St. Paul, Minnesota, USA, APS Press.
- Burgess, L. W., Backhouse, D., Swan, L. J. & Esdaile, R. J. (1996) Control of *Fusarium* crown rot of wheat by late stubble burning and rotation with sorghum. *Australasian Plant Pathology*, 25, 229-233.
- Burgess, L. W., Dodman, R. L., Pont, W. & Mayers, P. (1981) *Fusarium* diseases of wheat, maize and grain sorghum in eastern Australia. IN NELSON, P. E., TOUSSOUN, T. A. & COOK, R. J. (Eds.) *Fusarium: Diseases, biology and taxonomy*. Pennsylvania State University Press.

- Burgess, L. W., Klein, T. A., Bryden, W. L. & Tobin, N. F. (1987) Head blight of wheat caused by *Fusarium graminearum* group 1 in New South Wales in 1983. *Australasian Plant Pathology*, 16, 72-78.
- Burgess, L. W., Wearing, A. H. & Toussoun, T. A. (1975) Surveys of Fusaria associated with crown rot of wheat in eastern Australia. *Australian Journal of Agricultural Research*, 26, 791-799.
- Butler, F. C. (1961) Root and foot rot diseases of wheat. *Science Bulletin*, 77, 1-98.
- Bywater, J. (1959) Infection of peas by *Fusarium solani* var *Martii* forma 2 and the spread of the pathogen. *Transactions of the British Mycological Society*, 42, 201-212.
- Carranza, T. M. (1961) Root decay and blight of cereals in Argentina caused by *Gibberella zeae* (*Fusarium graminearum*). *Revista Facultad Agronomic (3rd Ser.) La Plata Univ.*, 37, 35-38.
- Carver, B. F. (Ed.) (2009) *Wheat: Science and Trade*, Ames, Iowa, USA, Wiley-Blackwell.
- Chamberlain, J. S., Gibbs, R. A., Rainer, J. E., Nguyen, P. N. & Thomas, C. (1988) Deletion screening of the Duchenne muscular dystrophy locus via multiplex DNA amplification. *Nucl. Acids Res.*, 16, 11141-11156.
- Christou, T. & Snyder, W. C. (1962) Penetration and host-parasite relationships of *Fusarium solani* f. sp. *phaseoli* in the bean plant. *Phytopathology*, 52, 219-226.
- Chrysler, M. A. (1906) The nodes of grasses. *Botanical Gazette*, 41, 1-16.
- Clement, J. A. & Parry, D. W. (1998) Stem-base disease and fungal colonisation of winter wheat grown in compost inoculated with *Fusarium culmorum*, *F. graminearum* and *Microdochium nivale*. *European Journal of Plant Pathology*, 104, 323-330.
- Colhoun, J. (1973) Effects of environmental factors on plant disease. *Annual Review of Phytopathology*, 11, 343-364.
- Colhoun, J. & Park, D. (1964) *Fusarium* diseases of cereals I. Infection of wheat plants, with particular reference to the effects of soil moisture and temperature on seedling infection. *Transactions of the British Mycological Society*, 47, 559-572.
- Collard, B. C. Y., Grams, R. A., Bovill, W. D., Percy, C. D., Jolley, R., Lehmensiek, A., Wildermuth, G. & Sutherland, M. W. (2005) Development of molecular markers for crown rot resistance in wheat: mapping of QTLs for seedling resistance in a '2-49' & 'Janz' population. *Plant Breeding*, 124, 532-537.
- Collard, B. C. Y., Jolley, R., Bovill, W. D., Grams, R. A., Wildermuth, G. B. & Sutherland, M. W. (2006) Confirmation of QTL mapping and marker validation for partial seedling resistance to crown rot in wheat line '2-49'. *Australian Journal of Agricultural Research*, 57, 967-973.
- Cook, R. (1980) *Fusarium* foot rot of wheat and its control in the Pacific northwest. *Plant Disease*, 64, 1061-1066.
- Cook, R. & Papendick, R. (1970) Soil water potential as a factor in the ecology of *Fusarium roseum* f. sp. *cerealis* 'Culmorum'. *Plant and Soil*, 32, 131-145.
- Cook, R. J. (1968) *Fusarium* root and foot rot of cereals in the Pacific Northwest. *Phytopathology*, 58, 127-131.
- Cook, R. J. (1973) Influence of low plant and soil water potentials on diseases caused by soilborne fungi. *Phytopathology*, 63, 451-458.
- Cook, R. J. & Christen, A. A. (1976) Growth of cereal root-rot fungi as affected by temperature-water potential interactions. *Phytopathology*, 66, 193-197.

- Cooke, M. C. (1892) *Handbook of Australian Fungi*, London, Williams and Norgate.
- Cornell, H. J. & Hoveling, A. W. (1998) *Wheat: chemistry and utilization*, Lancaster, Pennsylvania, Technomic.
- Curtis, B. C., Rajaram, S. & Gómez Macpherson, H. (Eds.) (2002) *Bread Wheat: Improvement and Production*, Rome, Food and Agriculture Organisation of the United Nations.
- Darken, M. A. (1961) Applications of fluorescent brighteners in biological techniques. *Science*, 133, 1704-1705.
- Desjardins, A. E. (2006) *Fusarium mycotoxins: chemistry, genetics and biology*, St. Paul, Minnesota The American Phytopathological Society.
- Desmond, O. J., Manners, J. M., Stephens, A. E., Maclean, D. J., Schenk, P. M., Gardiner, D. M., Munn, A. L. & Kazan, K. (2008) The *Fusarium* mycotoxin deoxynivalenol elicits hydrogen peroxide production, programmed cell death and defence responses in wheat. *Molecular Plant Pathology*, 9, 435-445.
- Dickson, J. G. (1923) Influence of soil temperature and moisture on the development of the seedling blight of wheat and corn caused by *Gibberella saubinetii*. *Journal of Agricultural Research*, 23, 837-870.
- Dickson, J. G., Eckerson, S. H. & Link, K. P. (1923) The nature of resistance to seedling blight of cereals. *Proceedings of the National Academy of Sciences of the United States of America*, 9, 434-439.
- Didenko, V. (2001) DNA probes using fluorescence resonance energy transfer (FRET): designs and applications. *Biotechniques*, 31, 1106-1121.
- Dimond, A. E. (1970) Biophysics and biochemistry of the vascular wilt syndrome. *Annual Review of Phytopathology*, 8, 301-322.
- Dodman, R. L. & Reinke, J. R. (1982) A selective medium for determining the population of viable conidia of *Cochliobolus sativus* in soil. *Australian Journal of Agricultural Research*, 33, 287-291.
- Dodman, R. L. & Wildermuth, G. B. (1987) Inoculation methods for assessing resistance in wheat to crown rot caused by *Fusarium graminearum* Group 1. *Australian Journal of Agricultural Research*, 38, 473-486.
- Domiciano, G. P., Rodrigues, F. A., Vale, F. X. R., Filha, M. S. X., Moreira, W. R., Andrade, C. C. L. & Pereira, S. C. (2010) Wheat resistance to spot blotch potentiated by silicon. *Journal of Phytopathology*, 158, 334-343.
- Duckett, J. G. & Read, D. J. (1991) The use of the fluorescent dye, 3,3'-dihexyloxycarbocyanine iodide, for selective staining of ascomycete fungi associated with liverwort rhizoids and ericoid mycorrhizal roots. *New Phytologist*, 118, 259-272.
- Ellis, J., Dodds, P. & Pryor, T. (2000) Structure, function and evolution of plant disease resistance genes. *Current Opinion in Plant Biology*, 3, 278-284.
- Emmett, R. W. & Parbery, D. G. (1975) Appressoria. *Annual Review of Phytopathology*, 13, 147-165.
- Epstein, E. (1994) The anomaly of silicon in plant biology. *Proceedings of the National Academy of Sciences of the United States of America*, 91, 11-17.
- Evans, M. L., Hollaway, G. J., Dennis, J. I., Correll, R. & Wallwork, H. (2010) Crop sequence as a tool for managing populations of *Fusarium pseudograminearum* and *F. culmorum* in south-eastern Australia. *Australasian Plant Pathology*, 39, 376-382.
- FAOSTAT (2010). Food and Agriculture Organisation of the United Nations.

- Fauteux, F., Rémus-Borel, W., Menzies, J. G. & Bélanger, R. R. (2005) Silicon and plant disease resistance against pathogenic fungi. *FEMS Microbiology Letters*, 249, 1-6.
- Fawe, A., Menzies, J. G., Chérif, M., Bélanger, R. R., L.E. Datnoff, G. H. S. & Korndörfer, G. H. (2001) Chapter 9 Silicon and disease resistance in dicotyledons. *Studies in Plant Science*. Elsevier.
- Felton, W., Marcellos, H., Alston, C., Martin, R., Backhouse, D., Burgess, L. & Herridge, D. (1998) Chickpea in wheat-based cropping systems of northern New South Wales II. Influence on biomass, grain yield, and crown rot in the following wheat crop. *Australian Journal of Agricultural Research*, 49, 401-407.
- Fineblum, W. L. & Rausher, M. D. (1995) Tradeoff between resistance and tolerance to herbivore damage in a morning glory. *Nature*, 377, 517-520.
- Fowler, J., Cohen, L. & Jarvis, P. (1998) *Practical Statistics for Field Biology*, Chichester, John Wiley and Sons.
- Francis, R. G. & Burgess, L. W. (1977) Characteristics of two populations of *Fusarium roseum* 'Graminearum' in eastern Australia. *Transactions of the British Mycological Society*, 68, 421-427.
- Frey, M., Chomet, P., Glawischnig, E., Stettner, C., Grun, S., Winklmaier, A., Eisenreich, W., Bacher, A., Meeley, R. B., Briggs, S. P., Simcox, K. & Gierl, A. (1997) Analysis of a chemical plant defense mechanism in grasses. *Science*, 277, 696-699.
- Frohlich, M. W. (1984) Freehand sectioning with Parafilm. *Stain Technology*, 59, 61-62.
- Gargouri, S., Hamza, S. & Hajlaoui, M. R. (2006) AFLP analysis of the genetic variability and population structure of the wheat crown rot fungus *Fusarium pseudograminearum* in Tunisia. *Tunisian Journal of Plant Protection*, 1, 93-104.
- Gäumann, E. (1950) *Principles of plant infection*, London, Crosby Lockwood & Son Ltd.
- Ghemawat, M. S. (1977) Polychromatic staining with toluidine blue O for studying the host-parasite relationships in wheat leaves of *Erysiphe graminis* f. sp. *tritici*. *Physiological Plant Pathology*, 11, 251-253.
- GRDC (2009) Crown rot in cereals fact sheet. Barton, Grains Research and Development Corporation.
- Grewal, H., Graham, R. & Rengel, Z. (1996) Genotypic variation in zinc efficiency and resistance to crown rot disease (*Fusarium graminearum* Schw. Group 1) in wheat. *Plant and Soil*, 186, 219-226.
- Guenther, J. C. & Trail, F. (2005) The development and differentiation of *Gibberella zeae* (anamorph: *Fusarium graminearum*) during colonization of wheat. *Mycologia*, 97, 229-237.
- Güldener, U., Seong, K.-Y., Boddu, J., Cho, S., Trail, F., Xu, J.-R., Adam, G., Mewes, H.-W., Muehlbauer, G. J. & Kistler, H. C. (2006) Development of a *Fusarium graminearum* Affymetrix GeneChip for profiling fungal gene expression in vitro and in planta. *Fungal Genetics and Biology*, 43, 316-325.
- Guo, J.-R., Schnieder, F. & Verreet, J.-A. (2006) Presymptomatic and quantitative detection of *Mycosphaerella graminicola* development in wheat using a real-time PCR assay. *FEMS Microbiology Letters*, 262, 223-229.

- Hawkins, L. A. & Harvey, R. B. (1919) Physiological study of the parasitism of *Pythium debaryanum* Hesse on the potato tuber. *Journal of Agricultural Research*, 18, 275-297.
- Heath, M. C. (1981) The suppression of the development of silicon-containing deposits in French bean leaves during growth of the bean rust fungus and extracts from bean rust infected tissue. *Physiological Plant Pathology*, 18, 149-155.
- Heid, C. A., Stevens, J., Livak, K. J. & Williams, P. M. (1996) Real time quantitative PCR. *Genome Research*, 6, 986-994.
- Hietala, A. M., Eikenes, M., Kvaalen, H., Solheim, H. & Fossdal, C. G. (2003) Multiplex real-time PCR for monitoring *Heterobasidion annosum* colonization in Norway spruce clones that differ in disease resistance. *Applied and Environmental Microbiology*, 69, 4413-4420.
- Hill, J. P. (1984) Quantitative disease assessment of wheat seedling leaves inoculated with *Fusarium roseum* 'Culmorum'. *Phytopathology*, 74, 665-667.
- Hoch, H. C., Galvani, C. D., Szarowski, D. H. & Turner, J. N. (2005) Two new fluorescent dyes applicable for visualization of fungal cell walls. *Mycologia*, 97, 580-588.
- Hodson, M. J. & Sangster, A. G. (1988) Observations on the distribution of mineral elements in the leaf of wheat (*Triticum aestivum* L.), with particular reference to silicon. *Annals of Botany*, 62, 463-471.
- Hogg, A. C., Johnston, R. H. & Dyer, A. T. (2007) Applying real-time quantitative PCR to *Fusarium* crown rot of wheat. *Plant Disease*, 91, 1021-1028.
- Hollaway, G. J. & Exell, G. K. (2010) Survey of wheat crops for white heads caused by crown rot in Victoria, 1997-2009. *Australasian Plant Pathology*, 39, 363-367.
- Hood, M. E. & Shew, H. D. (1996) Applications of KOH-aniline blue fluorescence in the study of plant-fungal interactions. *Phytopathology*, 86, 704-708.
- Howard, R. J., Bourett, T. M. & Czymmek, K. J. (2004) Essential microscopy-based technology for studies of fungal pathogen-plant host interactions. *Microscopy and Microanalysis*, 10, 218-219.
- Hückelhoven, R. & Kogel, K.-H. (1998) Tissue-specific superoxide generation at interaction sites in resistant and susceptible near-isogenic barley lines attacked by the powdery mildew fungus (*Erysiphe graminis* f. sp. *hordei*). *Molecular Plant Microbe Interactions*, 11, 292-300.
- Hynes, H. J. (1924) On the occurrence in New South Wales of *Gibberella saubinetii*, the organism causing scab of wheat and other cereals. *Journal and Proceedings of the Royal Society of New South Wales*, 57, 337-348.
- Jackson, E. W., Avant, J. B., Overturf, K. E. & Bonman, J. M. (2006) A quantitative assay of *Puccinia coronata* f. sp. *avenae* DNA in *Avena sativa*. *Plant Disease*, 90, 629-636.
- Jansen, C., von Wettstein, D., Schafer, W., Kogel, K.-H., Felk, A. & Maier, F. J. (2005) Infection patterns in barley and wheat spikes inoculated with wild-type and trichodiene synthase gene disrupted *Fusarium graminearum*. *Proceedings of the National Academy of Sciences*, 102, 16892-16897.
- Johansen, D. A. (1940) *Plant microtechnique*, New York, McGraw-Hill.
- Jones, L. H. P. & Handreck, K. A. (1967) Silica in soils, plants and animals. *Advances in Agronomy*, 19, 107-149.

- Kaufman, P. B., Dayanandan, P., Franklin, C. I. & Takeoka, Y. (1985) Structure and function of silica bodies in the epidermal system of grass shoots. *Annals of Botany*, 55, 487-507.
- Kawashima, R. (1927) Influence of silica on rice blast disease. *Japanese Journal of Soil Science and Plant Nutrition*, 1, 86-91.
- Kirkegaard, J., Holland, J., Moore, K., Simpfendorfer, S., Bambach, R., Marcroft, S. & Hollaway, G. (2003) Effect of previous crops on crown rot infection and yield of wheat. *Proceedings of the 11th Australian Agronomy Conference*. Geelong.
- Kirkegaard, J. A., Simpfendorfer, S., Holland, J., Bambach, R., Moore, K. J. & Rebetzke, G. J. (2004) Effect of previous crops on crown rot and yield of durum and bread wheat in northern NSW. *Australian Journal of Agricultural Research*, 55, 321-334.
- Klaasen, J., Matthee, F., Marasas, W. & Van Schalkwyk, D. (1991) Comparative isolation of *Fusarium* species from plant debris in soil and wheat stubble and crowns at different locations in the southern and western Cape. . *Phytophylactica*, 23, 299-307.
- Klein, T. A., Burgess, L. W. & Ellison, F. W. (1989) The incidence of crown rot in wheat, barley and triticale when sown on two dates. *Australian Journal of Experimental Agriculture*, 29, 559-563.
- Klein, T. A., Burgess, L. W. & Ellison, F. W. (1990) Survey of the incidence of whiteheads in wheat crops grown in northern New South Wales, 1976-1981. *Australian Journal of Experimental Agriculture*, 30, 621-7.
- Klein, T. A., Burgess, L. W. & Ellison, F. W. (1991) The incidence and spatial patterns of wheat plants infected by *Fusarium graminearum* Group 1 and the effect of crown rot on yield. *Australian Journal of Agricultural Research*, 42, 399-407.
- Klein, T. A., Liddell, C. M., Burgess, L. W. & Ellison, F. W. (1985) Glasshouse testing for tolerance of wheat to crown rot caused by *Fusarium graminearum* Group 1. IN PARKER, C. A., ROVIRA, A. D., MOORE, K. J., WONG, P. T. W. & KOLLMORGEN, J. F. (Eds.) *Ecology and management of soilborne plant pathogens*. Minnesota, U.S.A., American Phytopathological Society.
- Knight, N. L., Platz, G. J., Lehmensiek, A. & Sutherland, M. W. (2010) An investigation of genetic variation among Australian isolates of *Bipolaris sorokiniana* from different cereal tissues and comparison of their abilities to cause spot blotch on barley. *Australasian Plant Pathology*, 39, 207-216.
- Knight, R. & Quirk, J. P. (1994) Colin Malcolm Donald 1910-1985. *Historical Records of Australian Science*, 10, 51-60.
- Kunoh, H. & Ishizaki, H. (1975) Silicon levels near penetration sites of fungi on wheat, barley, cucumber and morning glory leaves. *Physiological Plant Pathology*, 5, 283-287
- Laday, M., Bagi, F., Mesterhazy, A. & Szecsi, A. (2000) Isozyme evidence for two groups of *Fusarium graminearum*. *Mycological Research*, 104, 788-793.
- Lagopodi, A. L., Ram, A. F. J., Lamers, G. E. M., Punt, P. J., Van den Hondel, C. A. M. J. J., Lugtenberg, B. J. J. & Bloemberg, G. V. (2002) Novel aspects of tomato root colonization and infection by *Fusarium oxysporum* f. sp. *radicis-lycopersici* revealed by confocal laser scanning microscopic analysis using the green fluorescent protein as a marker. *Molecular Plant-Microbe Interactions*, 15, 172-179.

- Lamprecht, S. C., Marasas, W. F. O., Knox-Davies, P. S. & Calitz, F. J. (1990) Seed treatment and cultivar reaction of annual *Medicago* species and wheat to *Fusarium avenaceum* and *Fusarium graminearum* Gr. 1. *Phytophylactica*, 22, 201-208.
- Larsen, R. C., Vandemark, G. J., Hughes, T. J. & Grau, C. R. (2006) Development of a real-time polymerase chain reaction assay for quantifying *Verticillium albo-atrum* DNA in resistant and susceptible Alfalfa. *Phytopathology*, 97, 1519-1525.
- Leach, J. G. (1923) The parasitism of *Colletotrichum lindemuthianum*. *University of Minnesota Agricultural Experiment Station Technical Bulletin*, 14, 41p.
- Leslie, J. F. & Summerell, B. A. (2006) *The Fusarium Laboratory Manual*, Carlton, Blackwell Publishing.
- Lev-Yadun, S., Gopher, A. & Abbo, S. (2000) The Cradle of Agriculture. *Science*, 288, 1602-1603.
- Lewin, J. & Reimann, B. E. F. (1969) Silicon and plant growth. *Annual Review of Plant Physiology*, 20, 289-304.
- Li, X., Liu, C., Chakraborty, S., Manners, J. M. & Kazan, K. (2008) A simple method for the assessment of crown rot disease severity in wheat seedlings inoculated with *Fusarium pseudograminearum*. *Journal of Phytopathology*, Online.
- Li, Y. H., Windham, M. T., Trigiano, R. N., Fare, D. C., Spiers, J. M. & Copes, W. E. (2005) Spore germination, infection structure formation, and colony development of *Erysiphe pulchra* on dogwood leaves and glass slides. *Plant Disease*, 89, 1301-1304.
- Li, Z., Hansen, J. L., Liu, Y., Zemetra, R. S. & Berger, P. H. (2004) Using real-time PCR to determine transgene copy number in wheat. *Plant Molecular Biology Reporter*, 22, 179-188.
- Liddell, C. M. (1985) The comparative pathogenicity of *Fusarium graminearum* group 1, *Fusarium culmorum* and *Fusarium crookwellense* as crown, foot and root rot pathogens of wheat. *Australasian Plant Pathology*, 14, 29-31.
- Liddell, C. M. & Burgess, L. W. (1985) Wax layers for partitioning soil moisture zones to study the infection of wheat seedlings by *Fusarium graminearum*. IN PARKER, C. A., ROVIRA, A. D., MOORE, K. J. & WONG, P. T. W. (Eds.) *Ecology and management of soilborne plant pathogens*. Minnesota, U.S.A., American Phytopathological Society.
- Liddell, C. M. & Burgess, L. W. (1988) Wax partitioned soil columns to study the influence of soil moisture potential on the infection of wheat by *Fusarium graminearum* Group 1. *Phytopathology*, 78, 185-189.
- Liddell, C. M., Burgess, L. W. & Taylor, P. W. J. (1986) Reproduction of crown rot of wheat caused by *Fusarium graminearum* Group 1 in the greenhouse. *Plant Disease*, 70, 632-635.
- Lodish, H., Berk, A., Zipursky, S. L., Matsudaira, P., Baltimore, D. & Darnell, J. (2000) *Molecular Cell Biology*, New York, W. H. Freeman.
- Lorang, J. M., Tuori, R. P., Martinez, J. P., Sawyer, T. L., Redman, R. S., Rollins, J. A., Wolpert, T. J., Johnson, K. B., Rodriguez, R. J., Dickman, M. B. & Ciuffetti, L. M. (2001) Green fluorescent protein is lighting up fungal biology. *Applied Environmental Microbiology*, 67, 1987-1994.
- Lu, Z., Gaudet, D. A., Frick, M., Puchalski, B., Genswein, B. & Laroche, A. (2005) Identification and characterization of genes differentially expressed in the

- resistance reaction in wheat infected with *Tilletia tritici*, the common bunt pathogen. *Journal of Biochemistry and Molecular Biology*, 38, 420-431.
- Malalasekera, R. A. P. & Colhoun, J. (1968) *Fusarium* diseases of cereals III. Water relations and infection of wheat seedlings by *Fusarium culmorum*. *Transactions of the British Mycological Society*, 51, 711-720.
- Malalasekera, R. A. P., Sanderson, F. R. & Colhoun, J. (1973) *Fusarium* diseases of cereals IX. Penetration and invasion of wheat seedlings by *Fusarium culmorum* and *F. nivale*. *Transactions of the British Mycological Society*, 60, 453-462.
- Malligan, C. D. (2008) Crown rot (*Fusarium pseudograminearum*) symptom development and pathogen spread in wheat genotypes with varying disease resistance. PhD Thesis. University of Southern Queensland, Toowoomba.
- McAlpine, D. (1896) Australian fungi. *Agricultural Gazette of NSW*, 7, 299-306.
- McKnight, T. & Hart, J. (1966) Some field observations on crown rot disease of wheat caused by *Fusarium graminearum*. *Queensland Journal of Agricultural and Animal Sciences*, 23, 373-378.
- McRae, F. J., McCaffery, D. W. & Matthews, P. W. (2010) *Winter crop variety sowing guide*, Industry and Investment NSW.
- Meldrum, S. I., Platz, G. J. & Ogle, H. J. (2004) Pathotypes of *Cochliobolus sativus* on barley in Australia. *Australasian Plant Pathology*, 33, 109-114.
- Mesterházy, Á., Barto, P., Goyeau, H., Niks, R. E. & Csösz, M. (2000) European virulence survey for leaf rust in wheat. *Agronomie*, 20, 793-804.
- Meyberg, M. (1988) Selective staining of fungal hyphae in parasitic and symbiotic plant-fungus associations. *Histochemistry*, 88, 197-199.
- Miedaner, T. (1988) The development of a host-pathogen system for evaluating *Fusarium* resistance in early growth stages of wheat. *Journal of Phytopathology*, 121, 150-158.
- Mishra, P. K., Tewari, J. P., Clear, R. M. & Turkington, T. K. (2006) Genetic diversity and recombination within populations of *Fusarium pseudograminearum* from western Canada. *International Microbiology*, 9, 65-68.
- Mitter, V., Zhang, M. C., Liu, C. J., Ghosh, R., Ghosh, M. & Chakraborty, S. (2006) A high-throughput glasshouse bioassay to detect crown rot resistance in wheat germplasm. *Plant Pathology*, 55, 433-441.
- Miyake, K. & Ikeda, M. (1932) Influence of silica application on rice blast. *Japanese Journal of Soil Science and Plant Nutrition*, 6, 53-76.
- Moldenhauer, J., Pretorius, Z. A., Moerschbacher, B. M., Prins, R. & Van Der Westuizen, A. J. (2008) Histopathology and PR-protein markers provide insight into adult plant resistance to stripe rust of wheat. *Molecular Plant Pathology*, 9, 137-145.
- Monds, R. D., Cromey, M. G., Lauren, D. R., Menna, M. & Marshall, J. (2005) *Fusarium graminearum*, *F. cortaderiae* and *F. pseudograminearum* in New Zealand: molecular phylogenetic analysis, mycotoxin chemotypes and co-existence of species. *Mycological Research*, 109, 410-420.
- Mönkemann, H., Hölker, U. & Höfer, M. (1997) Components of the ligninolytic system of *Fusarium oxysporum* and *Trichoderma atroviride*. *Fuel Processing Technology*, 52, 73-77.
- Morrissey, J. P. & Osbourn, A. E. (1999) Fungal resistance to plant antibiotics as a mechanism of pathogenesis. *Microbiology and Molecular Biology Reviews*, 63, 708-724.

- Mudge, A. M., Dill-Macky, R., Dong, Y., Gardiner, D. M., White, R. G. & Manners, J. M. (2006) A role for the mycotoxin deoxynivalenol in stem colonisation during crown rot disease of wheat caused by *Fusarium graminearum* and *Fusarium pseudograminearum*. *Physiological and Molecular Plant Pathology*, 69, 73-85.
- Mulligan, M. F., Safir, G. R. & Klomparens, K. L. (1990) Association of *Fusarium solani* f.sp. *phaseoli* with trichomes of *Phaseolus vulgaris*. *Mycological Research*, 94, 409-411.
- Mullis, K. (1987) Process for amplifying nucleic acid sequences. *United States Patent No. 4 683 202*.
- Murray, G. M. & Brennan, J. P. (2009a) *The current and potential costs from diseases of barley in Australia*, Barton, ACT, Grains Research and Development Corporation.
- Murray, G. M. & Brennan, J. P. (2009b) *The current and potential costs from diseases of wheat in Australia*, Barton, ACT, Grains Research and Development Corporation.
- Murray, G. M. & Brown, J. F. (1987) The incidence and relative importance of wheat diseases in Australia. *Australasian Plant Pathology*, 16, 34-37.
- Nair, P. N. & Kommedahl, T. (1957) The establishment and growth of *Fusarium lini* in flax tissues. *Phytopathology*, 47, 25.
- Nelson, K. E. & Burgess, L. W. (1994) Reaction of Australian cultivars of oats and barley to infection by *Fusarium graminearum* Group 1 *Australian Journal of Experimental Agriculture*, 34, 655-658.
- Nelson, K. E. & Burgess, L. W. (1995) Effect of rotation with barley and oats on crown rot of wheat in the northern wheat belt of New South Wales. *Australian Journal of Experimental Agriculture*, 35, 765-770.
- Nicholson, P., Simpson, D. R., Weston, G., Rezanoor, H. N., Lees, A. K., Parry, D. W. & Joyce, D. (1998) Detection and quantification of *Fusarium culmorum* and *Fusarium graminearum* in cereals using PCR assays. *Physiological and Molecular Plant Pathology*, 53, 17-37.
- Nicol, J., Bagci, S. A., Hekimhan, H., Tunali, B., Bolat, N., Braun, H. J. & Trethowan, R. (2004) Strategy for the identification and breeding of resistance to dryland root rot complex for International spring and winter wheat breeding programs. *Proceedings of the 4th International Crop Science Congress*. Brisbane.
- Nirenberg, H. I. (1976) Untersuchungen über die morphologische Differenzierung in der *Fusarium* Sektion *Liseola*. *Mitteilungen aus der Biologischen Bundesanstalt Für Land- und Forstwirtschaft (Berlin-Dahlem)*, 169, 1-117.
- O'Donnell, K., Cigelnik, E. & Casper, H. H. (1998) Molecular phylogenetic, morphological, and mycotoxin data support reidentification of the Quorn mycoprotein fungus as *Fusarium venenatum*. *Fungal Genetics and Biology*, 23, 57-67.
- Oliver, J., Castro, A., Gaggero, C., Cascón, T., Schmelz, E., Castresana, C. & Ponce de León, I. (2009) *Pythium* infection activates conserved plant defense responses in mosses. *Planta*, 230, 569-579.
- Ophel-Keller, K., McKay, A., Hartley, D., Herdina & Curran, J. (2008) Development of a routine DNA-based testing service for soilborne diseases in Australia. *Australasian Plant Pathology*, 37, 243-253.
- Osborn, A. E. (2001) Plant mechanisms that give defence against soilborne diseases. *Australasian Plant Pathology*, 30, 99-102.

- Ouellet, T. & Seifert, K. A. (1993) Genetic characterization of *Fusarium graminearum* strains using RAPD and PCR amplification *Phytopathology*, 83, 1003-1007.
- Papendick, R. I. & Cook, R. J. (1974) Plant water stress and development of *Fusarium* foot rot in wheat subjected to different cultural practices. *Phytopathology*, 64, 358-363.
- Pearson, N. (1931) Parasitism of *Gibberella saubineti* on corn seedlings. *Journal of Agricultural Research*, 43, 569-596.
- Percival, J. (1921) *The wheat plant: a monograph*, London, Duckworth and Co.
- Petrisko, J. E. & Windes, J. M. (2006) Quantification of *Fusarium culmorum* in crown rot resistant and susceptible wheat varieties using a tri5 gene-based real-time PCR assay. *Phytopathology*, 96, S92.
- Ponzi, R. & Pizzolongo, E. (2003) Morphology and distribution of epidermal phytoliths in *Triticum aestivum* L. *Plant Biosystems*, 137, 3-10.
- Poole, G., Paulitz, T. C., Nicol, J., Erginbas, G., Campbell, K. & Smiley, R. R. (2009) Evaluation of inoculation methods to assay wheat for resistance to *Fusarium* crown rot. *Phytopathology* 99, S103
- Prats, E., Gay, A. P., Roberts, P. C., Thomas, B. J., Sanderson, R., Paveley, N., Lyngkjær, M. F., Carver, T. L. W. & Mur, L. A. J. (2010) *Blumeria graminis* interactions with barley conditioned by different single R genes demonstrate a temporal and spatial relationship between stomatal dysfunction and cell death. *Phytopathology*, 100, 21-32.
- Purss, G. S. (1966) Studies of varietal resistance to crown rot of wheat caused by *Fusarium graminearum* Schw. *Queensland Journal of Agricultural and Animal Sciences*, 23, 475-498.
- Purss, G. S. (1969) The relationship between strains of *Fusarium graminearum* Schwabe causing crown rot of various gramineous hosts and stalk rot of maize in Queensland. *Australian Journal of Agricultural Research*, 20, 257-264.
- Purss, G. S. (1971) Effect of planting time on the incidence of crown rot (*Gibberella zeae*) in wheat. *Australian Journal of Experimental Agriculture and Animal Husbandry*, 11, 85-89.
- Quazi, S. A. J., Burgess, L. W. & Smith-White, J. (2009) Sorghum is a suitable break crop to minimise *Fusarium pseudograminearum* in any location regardless of climatic differences, whereas *Gibberella zeae* is location and climate specific. *Australasian Plant Pathology*, 38, 91-99.
- Raberg, L., Sim, D. & Read, A. F. (2007) Disentangling genetic variation for resistance and tolerance to infectious diseases in animals. *Science*, 318, 812-814.
- Read, N. D. & Beckett, A. (1996) Ascus and ascospore morphogenesis. *Mycological Research* 100, 1281-1314.
- Regalado, V., Rodriguez, A., Perestelo, F., Carnicero, A., De La Fuente, G. & Falcon, M. (1997) Lignin degradation and modification by the soil-inhabiting fungus *Fusarium proliferatum*. *Applied and Environmental Microbiology*, 63, 3716-3718.
- Rodriguez, A., Perestelo, F., Carnicero, A., Regalado, V., Perez, R., De la Fuente, G. & Falcon, M. A. (1996) Degradation of natural lignins and lignocellulosic substrates by soil-inhabiting fungi imperfecti. *FEMS Microbiology Ecology*, 21, 213-219.

- Rozen, S. & Skaletsky, H. J. (2000) Primer3 on the WWW for general users and for biologist programmers. IN S, K. & S, M. (Eds.) *Bioinformatics methods and protocols: Methods in molecular biology*. Totowa, NJ, Humana Press.
- Ruzin, S. E. (1999) *Plant microtechnique and microscopy*, Oxford, Oxford University Press.
- Ryerson, D. E. & Heath, M. C. (1996) Cleavage of nuclear DNA into oligonucleosomal fragments during cell death induced by fungal infection or by abiotic treatments. *The Plant Cell*, 8.
- Saha, D. C., Jackson, M. A. & Johnson-Cicalese, J. M. (1988) A rapid staining method for detection of endophytic fungi in turf and forage grasses. *Phytopathology*, 78, 237-239.
- Saremi, H., Ammarellou, A. & Jafary, H. (2007) Incidence of crown rot of wheat caused by *Fusarium pseudograminearum* as a new soil born fungal species in North West Iran. *Pakistan Journal of Biological Sciences*, 10, 3606-3612.
- Schaad, N. W. & Frederick, R. D. (2002) Real-time PCR and its application for rapid plant disease diagnostics. *Canadian Journal of Plant Pathology*, 24, 250-258.
- Schäfer, P., Hüchelhoven, R. & Kogel, K.-H. (2004) The white barley mutant *Albostrians* shows a supersusceptible but symptomless interaction phenotype with the hemibiotrophic fungus *Bipolaris sorokiniana*. *Molecular Plant Microbe Interactions*, 17, 366-373.
- Schena, L., Nigro, F., Ippolito, A. & Gallitelli, D. (2004) Real-time quantitative PCR: a new technology to detect and study phytopathogenic and antagonistic fungi. *European Journal of Plant Pathology*, 110, 893-908.
- Schilling, A. G., Möller, E. M. & Geiger, H. H. (1996) Polymerase chain reaction-based assays for species-specific detection of *Fusarium culmorum*, *F. graminearum*, and *F. avenaceum* *Phytopathology*, 86, 515-522.
- Schwarz, K. (1973) A bound form of silicon in glycosaminoglycans and polyuronides. *Proceedings of the National Academy of Sciences of the United States of America*, 70, 1608-1612.
- Scott, J., Akinsanmi, O., Mitter, V., Simpfendorfer, S., Dill-Macky, R. & Chakraborty, S. (2004) Prevalence of *Fusarium* crown rot pathogens of wheat in southern Queensland and northern New South Wales. *Proceedings of the 4th International Crop Science Congress*. Brisbane.
- Scott, J. B. & Chakraborty, S. (2006) Multilocus sequence analysis of *Fusarium pseudograminearum* reveals a single phylogenetic species. *Mycological Research*, 110, 1413-1425.
- Scott, J. B. & Chakraborty, S. (2007) Identification of 11 polymorphic simple sequence repeat loci in the phytopathogenic fungus *Fusarium pseudograminearum* as a tool for genetic studies. *Molecular Ecology Notes Online*.
- Simmonds, J. H. (1966) *Host Index of Plant Diseases in Queensland*, Brisbane, Queensland Department of Primary Industries.
- Simmonds, P. M. (1941) Root rots of cereals. *Botanical Review*, 7, 308-332.
- Simmons, S. R., Oelke, E. A. & Anderson, P. M. (1995) Growth and development guide for spring wheat. University of Minnesota.
- Skerman, P. J. (1990) Soutter, Richard Ernest (1878 - 1955). *Australian Dictionary of Biography* Melbourne, Melbourne University Press.
- Smiley, R. W. (2009) Water and temperature parameters associated with winter wheat diseases caused by soilborne pathogens. *Plant Disease*, 93, 73-80.

- Smiley, R. W., Gourlie, J. A., Easley, S. A., Patterson, L.-M. & Whittaker, R. G. (2005) Crop damage estimates for crown rot of wheat and barley in the Pacific Northwest. *Plant Disease*, 89, 595-604.
- Smith, R. S. & Walker, J. C. (1930) A cytological study of cabbage plants in strains susceptible or resistant to yellows. *Journal of Agricultural Research*, 41, 17-35.
- Sparrow, D. & Graham, R. (1988) Susceptibility of zinc-deficient wheat plants to colonization by *Fusarium graminearum* Schw. Group 1. *Plant and Soil*, 112, 261-266.
- Spear, R. N., Cullen, D. & Andrews, J. H. (1999) Fluorescent labels, confocal microscopy, and quantitative image analysis in study of fungal biology. *Methods in Enzymology*, 307, 607-623.
- Stephens, A. E., Gardiner, D. M., White, R. G., Munn, A. L. & Manners, J. M. (2008) Phases of infection and gene expression of *Fusarium graminearum* during crown rot disease of wheat. *Molecular Plant Microbe Interactions*, 21, 1571-1581.
- Strausbaugh, C. A., Overturf, K. & Koehn, A. C. (2005) Pathogenicity and real-time PCR detection of *Fusarium* spp. in wheat and barley roots. *Canadian Journal of Plant Pathology*, 27, 430-438.
- Summerell, B. A., Burgess, L. W., Backhouse, D., Bullock, S. & Swan, L. J. (2001) Natural occurrence of perithecia of *Gibberella coronicola* on wheat plants with crown rot in Australia. *Australasian Plant Pathology*, 30, 353-356.
- Summerell, B. A., Burgess, L. W. & Klein, T. A. (1989) The impact of stubble management on the incidence of crown rot of wheat. *Australian Journal of Experimental Agriculture*, 29, 91-98.
- Swan, L. J., Backhouse, D. & Burgess, L. W. (2000) Surface soil moisture and stubble management practice effects on the progress of infection of wheat by *Fusarium pseudograminearum*. *Australian Journal of Experimental Agriculture*, 40, 693-698.
- Takahara, H., Dolf, A., Endl, E. & O'Connell, R. (2009) Flow cytometric purification of *Colletotrichum higginsianum* biotrophic hyphae from *Arabidopsis* leaves for stage-specific transcriptome analysis. *The Plant Journal*, 59, 672-683.
- Tan, M.-K. & Niessen, L. M. (2003) Analysis of rDNA ITS sequences to determine genetic relationships among, and provide a basis for simplified diagnosis of, *Fusarium* species causing crown rot and head blight of cereals. *Mycological Research*, 107, 811-821.
- Taylor, P. W. J. (1983) The influence of soil moisture on infection and colonisation of wheat by *Fusarium graminearum* Group 1. Master's Thesis. The University of Sydney.
- Terzi, V., Malnati, M., Barbanera, M., Stanca, A. M. & Faccioli, P. (2003) Development of analytical systems based on real-time PCR for *Triticum* species-specific detection and quantitation of bread wheat contamination in semolina and pasta. *Journal of Cereal Science*, 38, 87-94.
- Thelwell, N., Millington, S., Solinas, A., Booth, J. & Brown, T. (2000) Mode of action and application of Scorpion primers to mutation detection. *Nucl. Acids Res.*, 28, 3752-3761.
- Trewin, D. (2006) *Year Book Australia 2006, Catalogue No. 1301.0*, Canberra, Australian Bureau of Statistics.
- Tunali, B., Nicol, J. M., Hodson, D., Uçkun, Z., Büyük, O., Erdurmuş, D., Hekimhan, H., Aktaş, H., Akbudak, M. A. & Bağcı, S. A. (2008) Root and

- crown rot fungi associated with spring, facultative, and winter wheat in Turkey. *Plant Disease*, 92, 1299-1306.
- Turner, A. S., Nicholson, P., Edwards, S. G., Bateman, G. L., Morgan, L. W., Todd, A. D., Parry, D. W., Marshall, J. & Nuttall, M. (2002) Relationship between brown foot rot and DNA of *Microdochium nivale*, determined by quantitative PCR, in stem bases of winter wheat. *Plant Pathology*, 51, 464-471.
- Van der Plank, J. E. (1975) *Principles of plant infection*, New York, Academic Press.
- Van Wyk, P., Los, O., Pauer, G. & Marasas, W. (1987) Geographic distribution and pathogenicity of *Fusarium* species associated with crown rot of wheat in the Orange Free State, South Africa. *Phytophylactica*, 19, 271-274.
- Vance, C. P., Kirk, T. K. & Sherwood, R. T. (1980) Lignification as a mechanism of disease resistance. *Annual Review of Phytopathology*, 18, 259-288.
- Vandemark, G. J. & Ariss, J. J. (2007) Examining interactions between legumes and *Aphanomyces euteiches* with real-time PCR. *Australasian Plant Pathology*, 36, 102-108.
- Veseth, R. (1987) Pacific North West Conservation Tillage Handbook.
- Waalwijk, C., van der Heide, R., de Vries, I., van der Lee, T., Schoen, C., Costrel-de Corainville, G., Häuser-Hahn, I., Kastelein, P., Köhl, J., Lonnet, P., Demarquet, T. & Kema, G. (2004) Quantitative detection of *Fusarium* species in wheat using TaqMan. *European Journal of Plant Pathology*, 110, 481-494.
- Wallwork, H. (2000) *Cereal root and crown diseases*, Kingston, ACT, Grains Research and Development Corporation.
- Wallwork, H., Butt, M., Cheong, J. P. E. & Williams, K. J. (2004) Resistance to crown rot in wheat identified through an improved method for screening adult plants. *Australasian Plant Pathology*, 33, 1-7.
- Wearing, A. H. & Burgess, L. W. (1979) Water potential and the saprophytic growth of *Fusarium roseum* "Graminearum". *Soil Biology and Biochemistry*, 11, 661-667.
- Wildermuth, G. B., McNamara, K. B., Sparks, T. & Davis, M. (1999) Sources and types of resistance to crown rot in wheat. *Proceedings of the Ninth Assembly of the Wheat Breeding Society of Australia*. Toowoomba.
- Wildermuth, G. B. & McNamara, R. B. (1994) Testing wheat seedlings for resistance to crown rot caused by *Fusarium graminearum* Group 1. *Plant Disease*, 78, 949-953.
- Wildermuth, G. B., McNamara, R. B. & Quick, J. S. (2001) Crown depth and susceptibility to crown rot in wheat. *Euphytica*, V122, 397-405.
- Wildermuth, G. B. & Morgan, J. M. (2004) Genotypic differences in partial resistance to crown rot caused by *Fusarium pseudograminearum* in relation to an osmoregulation gene in wheat. *Australasian Plant Pathology*, 33, 121-123.
- Wildermuth, G. B. & Purss, G. S. (1971) Further sources of field resistance to crown rot (*Gibberella zeae*) of cereals in Queensland. *Australian Journal of Experimental Agriculture*, 11, 455-459.
- Wildermuth, G. B., Thomas, G. A., Radford, B. J., McNamara, R. B. & Kelly, A. (1997) Crown rot and common root rot in wheat grown under different tillage and stubble treatments in southern Queensland, Australia. *Soil and Tillage Research*, 44, 211-224.
- Wilhelm, W. W. & McMaster, G. S. (1995) Importance of the phyllochron in studying development and growth in grasses. *Crop Science*, 35, 1-3.

- Winton, L. M., Stone, J. K., Watrud, L. S. & Hansen, E. M. (2002) Simultaneous one-tube quantification of host and pathogen DNA with real-time polymerase chain reaction. *Phytopathology*, 92, 112-116.
- Xi, K., Turkington, T. K. & Chen, M. H. (2008) Systemic stem infection by *Fusarium* species in barley and wheat. *Canadian Journal of Plant Pathology*, 30, 588-594.
- Young, P. A. (1926) Penetration phenomena and facultative parasitism in *Alternaria*, *Diplodia* and other fungi. *Botanical Gazette*, 81, 258-279.
- Zohary, D. & Hopf, M. (2000) *Domestication of plants in the old world*, Oxford, UK, Clarendon Press.